siRNA DEPLETION OF ENDOCYTIC PROTEINS AND PATHWAYS FOR ANALYSING THE CELLULAR UPTAKE OF CELL PENETRATING PEPTIDES AS VECTORS FOR DRUG DELIVERY

Submitted by:

Monerah Alsoraj

A Thesis submitted to the faculty for degree of

PHILOSOPHIAE DOCTOR

The Welsh School of Pharmacy

Cardiff University

April 2011

ProQuest LLC
789 East Eisenhower Parkway
P.O. Box 1346
Ann Arbor, MI 48106-1346

Abstract:

Cell-penetrating peptides (CPPs) have the potential to deliver a host of macromolecular therapeutics into cells including peptides, proteins, and nucleotides. The mechanism by which they are internalised has been hotly-disputed but is important if improvements are to be made in their delivering capacities. Endocytosis is thought to be of significant importance but identifying the exact uptake mechanism has been difficult due predominantly to a lack of specific tools. Multiple pathways have been reported to contribute to uptake, including macropinocytosis and those regulated by clathrin and cavaeolin-1.

The aim of this thesis was to utilise siRNA-depletion to develop cell models with defects in specific endocytic proteins and pathways that could then be utilised to study the uptake of drug delivery vectors such as CPPs. Targeted pathways were those regulated by clathrin heavy chain, dynamin-2, caveolin-1, flotillin-1 and P21-activated kinase (PAK-1). Significant variation between cell lines emerged in the expression of these proteins and the ease with which they could be depleted. Single siRNA sequences were, however, discovered that effectively depleted these proteins and using a variety of endocytic probes the effects of depletion could be determined. Eventually, model cell lines were generated that were measurably defective in at least one of the five different endocytic pathways and these were tested to determine routes utilised by two well characterised CPPs, HIV-Tat and octaarginine. Only cells depleted of pak-1 protein and thus macropinocytosis were defective in CPP uptake. Further analysis revealed defective actin organisation in these cells that could have caused the effects and support data presented here and elsewhere on actin disruption with cytochalasin D. With comparative studies using pharmacological inhibitors of endocytic pathways these methods provide new tools to study drug delivery systems as shown here for CPPs and also for polyplexes through a collaboration with the University of Ghent, Belgium.

To My Family

Acknowledgement:

I would like to express my deep and sincere gratitude to my supervisor, Dr. Arwyn Jones. His wide knowledge and his logical way of thinking have been of great value for me. His understanding, encouraging and personal guidance have provided a good basis for the present thesis. The joy and enthusiasm he has for his research was contagious and motivational for me, even during tough times during my studies. I could not have imagined having a better advisor and mentor for my PhD study.

I have had the pleasure to work with or alongside with my colleagues Dr. Catherine Watkins, Edward Sayers and Dr. Helene Bruyere for whom I have great regards, they helped and supported me a lot during my lab work. In my later work of purifying His_6-EGFP-R8, I am particularly indebted to Anja Schermann, who set up the basic protocols for expression and purification.

I wish to extend my warmest thanks to all those who have helped me with my work in Cardiff University, Dr. Peter Watson (Cardiff School of Biosciences), Laurence Pearce, who helped me with Flow Cytometry at Heath Hospital, Dr Rossen Donev who kindly gave me with the anti-CD59 antibody, and Dr Jon Lane for providing me with the A431 cells.

I have very much appreciated the collaboration we have had with the University of Ghent and the help given to me by Dries Vercauteren, Professors. Stefaan De Smedt and Dr. Kevin Braechmans

I'm also gratefully acknowledged the financial support of the Kuwait University and Kuwait Government.

I owe my loving thanks to my beloved mother Mrs. Nahed Salem, who has given me huge support and helped me a lot in taking care of my daughter during my research.. I thank my great husband Dr. Ahmad Salem, who always stood by me with love and support, and my lovely daughter Noor, who has filled my life with happiness and joy. I also would like to deeply thank my brother Khaled and my sister Bothaina, for their continuous support and encouragement. Without this and their understanding it would have been impossible for me to finish this work. A special gratitude I send out to Mr. Salah Waheedi's family, especially his wife and my best friend Mrs. Manal Alhazeem. They were always besides me during happy and sad times and they provided me with much happiness in Cardiff.

Last but not least, I would like to dedicate my thesis to my FATHER'S SOUL, God bless him. He was my first spiritual teacher and this guidance will stay with me for the rest of my life.

Monerah Alsoraj

Index

Chapter 1: General Introduction

Chapter 5: Evaluation of the role of Macropinocytosis in the cellular uptake of CPPs Tat and R8

List of Abbreviations:

ACN	-acetonitrile
APS	- ammonium persulphate
BCA	-bicinhoninic acid
Blebb	-Blebbistatin
BSA	-bovine serum albumin
CAV-1	- caveolin-1 protein
CHC	-clathrin heavy chain
CME	-clathrin mediated endocytosis
CytD	-cytochalasin D
DMSO	-dimethyl sulohoxide
DNM2	-dynamin 2 protein
DTT	-dithiothreitol
ECL	-enhanced chemiluminescence
EGF	-epidermal growth factor
EGFP	-enhanced green fluorescent protein
EIPA	-5-(N-ethyl-N-isopropyl) amiloride
FBS	-foetal bovine serum
Flot-1	-flotillin-1 protein
GFP	-green fluorescent protein
HPLC	-high performance liquid chromatography
PAK-1	-p21-activated kinase 1
PBS	-phosphate buffered saline
PFA	-paraformaldehyde
RISC	-RNA indudced silencing complex
R8	-octaarginine (L isomer)
siRNA	-small interfering RNA
Tat	-trans –activator of transcription
Tf	-Transferrin

Chapter 1: General Introduction

1.1. The drug delivery challenge

Recently, we have observed a remarkable increase in the interest surrounding the potential of using large therapeutic molecules, such as proteins, peptides and nucleic acid as therapeutics. This stems in part from an increased understanding of the molecular causes of diseases such as cancer and inherited genetic diseases. However, progress in this field is restricted by a lack of efficient drug delivery systems for these new therapeutics. Problems include poor stability *in vivo*, insufficient cellular uptake and the difficulty in reaching a specific molecular target. This is in addition to a requirement for high doses in order to reach the effective potency but at the same time avoiding the risks of side effects. Therefore, there is a real requirement for new and more efficient drug delivery systems. To solve this problem there are some issues that need to be considered in order to establish potential new delivery systems, including (i) delivery or uptake efficiency in different tissues; (ii) rapid endosomal escape; (iii) ability to reach a specific target; (iv) efficiency at low doses; (v) lack of toxicity; and (vi) affordability for mass production (Sahay et al. 2010).

A number of different strategies have been attempted to improve drug delivery efficiency (de Fougerolles et al. 2007; Jarver and Langel 2004; Kong and Mooney 2007; Torchilin 2005b), including non-viral approaches using for example liposomes, polycationic polymers, nanoparticles and peptide-based strategies (Jarver and Langel 2004; Morris et al. 2000; Torchilin 2005b).

Cell-penetrating peptides (CPPs) is a term used to describe short peptides that are typically < 30 residues in length. Today CPPs are still considered to be one of the most promising strategies to overcome the limitations of delivering

various bioactive molecules such as plasmid DNA, oligonucleotide, siRNA, peptide-nucleic acid (PNA), peptides and proteins into cells. As described below CPPs come in many different forms but the fact that they are called CPPs is due to the fact that they have some kind of mechanism for overcoming at least one biological barrier and most importantly a number have also demonstrated a further capacity to act as delivery vectors for cargo that may be several orders of magnitude larger that the peptides themselves (Derossi et al. 1994; Meade and Dowdy 2007; Morris et al. 2008; Pooga et al. 1998). Importantly this also includes cargo with therapeutic potential such as those described above (Johnson et al. 2011).

1.2. Membrane active, to cell penetrating peptides

Cellular membranes such as the plasma membrane and endosomal membranes serve as the major barriers to drug delivery for many therapeutic agents thus limiting their prospects of ever reaching the clinic. The search is therefore always on for agents that can interact with membranes and aid in the delivery of a bioactive molecule to the interior of the cell. This may be directly across the plasma membrane but more likely the strategy would depend on uptake of the vector and carrier into the cell interior by one of several endocytic pathways that cells have (Jones 2008). Peptide sequences that have affinities for biological membranes have been described for decades and in the main focus was given to antimicrobial peptides or those that were toxic to mammalian cells such as mastoporan (Bernheimer and Rudy 1986). There was also interest in pH sensitive peptides such as GALA, a 30 residue synthetic peptide that partitioned into membranes (Parente et al. 1990). However, at the

very end of the last century, peptide sequences were discovered that were membrane active without necessarily being membrane damaging and thus cytotoxic. The first one to be highlighted was transcription-transactivating (Tat) protein of HIV-1(Frankel and Pabo 1988) followed closely by Drosophila Antennapedia (Derossi et al. 1994). Initially they were called protein transduction domains as they formed the domains of larger proteins, such as the 100 residue HIV-Tat protein, but this terminology has now largely been replaced with cell penetrating peptides or CPPs. Since then hundreds of different sequences have been described that fall into this classification and some older peptides such as mastoparan have since fallen into this category. It is often asked whether CPP is a good terminology for these entities over membrane active or translocating peptides.

CPPs are generally composed of small (<30 amino acid) peptides and several classes have been described that compose a variety of sequences and electrostatic charges (Fischer et al. 2005; Foerg and Merkle 2008). In addition to their ability to penetrate the plasma membrane, they have the ability to deliver a wide variety of otherwise membrane impermeable macromolecules including fluorophores, peptide nucleic acids, proteins, oligonucleotides, and plasmids (Aoki et al. 2010; Jarver and Langel 2006; Johnson et al. 2011; Morris et al. 2008).

1.3. CPPs Classification

Several attempts have been made to classify CPPs depending on, for example, the basis of their primary sequences, or whether they are natural peptides, synthetic or chimeras. Recently, André Ziegle introduced another classification system for CPPs, which stands on studies carried out on model membranes. This classification grouped CPPs into sub-classes according to their physical properties in the presence of membranes of different compositions (Ziegler 2008). The system highlighted in Figure 1.1 is based on a number of factors (Fischer et al. 2005) but highlights the most common variants. This formed the basis for organisation of the sequences shown in Table 1.1 that classifies them into three main groups:

1.3.1. Antimicrobial peptides

They were first isolated from blood leukocytes and lymphatic tissue 100 years ago. They have antimicrobial activity against Gram positive and Gram negative bacteria (Skarnes and Watson 1957). Examples include: buforin, magainin and LL-37 (Sandgren et al. 2004; Takeshima et al. 2003).

1.3.2. Protein derived CPPs

They are usually known as protein transduction domains PTDs, and are composed of minimal effective sequence of the parent protein, which is responsible for the translocation activity. For example, Penetratin, pVEC, and Tat are derived from the third helix of the Drosophila antennapedia transcription factor, the murine vascular endothelial cadherin and HIV-1 Tat

protein, respectively (Derossi et al. 1994; Elmquist et al. 2001; Vives et al. 1997).

1.3.3. Designed CPPs

They can be subdivided to:

- Amphiphilic : MAP (Oehlke et al. 1998).
- Chimeric: Transportan and MPG (Morris et al. 1997; Pooga et al. 1998).
- Homing peptides: Lyp-1 and F3 (Laakkonen and Vuorinen 2010).
- Synthetic: Pep-1 and oligoarginines (Arg_n where n is usually 7-20 residues) (Futaki et al. 2001; Morris et al. 2001).

At physiological pH, most CPPs have net positive charge and most often have only negative charge at the C terminus when that terminus is amidated. That negative charge does not prevent the penetration of CPPs, an example given by VT5 peptide that carries five positive charges and four negative charges and internalised efficiently (Oehlke et al. 1997). It should be noted that a number of the sequences described in Table 1.1 have been synthesised in the D form as this will significantly reduce proteolysis (Gammon et al. 2003).

	Origin	Sequence	Reference
Antimicrobial peptides (MAPs)			
Buforin	Stomach of the Asian toad *Bufo bufo gargarizans*	TRSSRAGLQFPVGRVHRLLRK	(Takeshima et al. 2003)
Magainin	skin of the African clawed frog Xenopus laevis	GIGKFLHSAKKFGKAFVGEIMNS	(Takeshima et al. 2003)
LL-37	Induced from Bacterial infections epithelial surfaces interaction	LLGDFFRKSKEKIGKEFKRIVQRIK DFLRNLVPRTES-C-amide	(Sandgren et al. 2004)
SynB Peptides	protegrin 1, an antimicrobial peptide	RGGRLSYSRRRFSTSTGR, RRLSYSRRRF	(Drin et al. 2003)
Protein derived CPPs			
Tat	HIV TAT	GRKKRRQRRRPPQ	(Gump et al. 2010; Vives et al. 1997)
Penetratin (pAntp)	Drosophila Antennapedia Homeodomain	RQIKIWFQNRRMKWKK	(Derossi et al. 1994)
pVEC	Vascular endothelial Cadherin	LLIILRRRIRKQAHAHSK-amide	(Elmquist et al. 2001)
Designed CPPs			
MAP	Model amphipathic peptide	KLALKLALKALKAALKLA-amide	(Oehlke et al. 1998)
Transportan	Galanin(1-12)-Lys-Mastoparan, desigened as GalR ligand.	GWTLNSAGYLLGKINLKALAALA KKIL-amide	(Pooga et al. 1998)
MPG	Cationic NLS + Hydrophobic tail	GALFLGWLGAAGSTMGAPKKKR KV-cysteamide	(Morris et al. 1997)
Pep-1	Cationic NLS + hydrophobic tail	KETWWETWWTEWSQPKKKRKV-cysteamide	(Morris et al. 2001)
Polyarginines	Synthetic	(R)n	(Futaki et al. 2001; Rothbard et al. 2000)

Table 1.1. A three classification system for the more common CPPs.

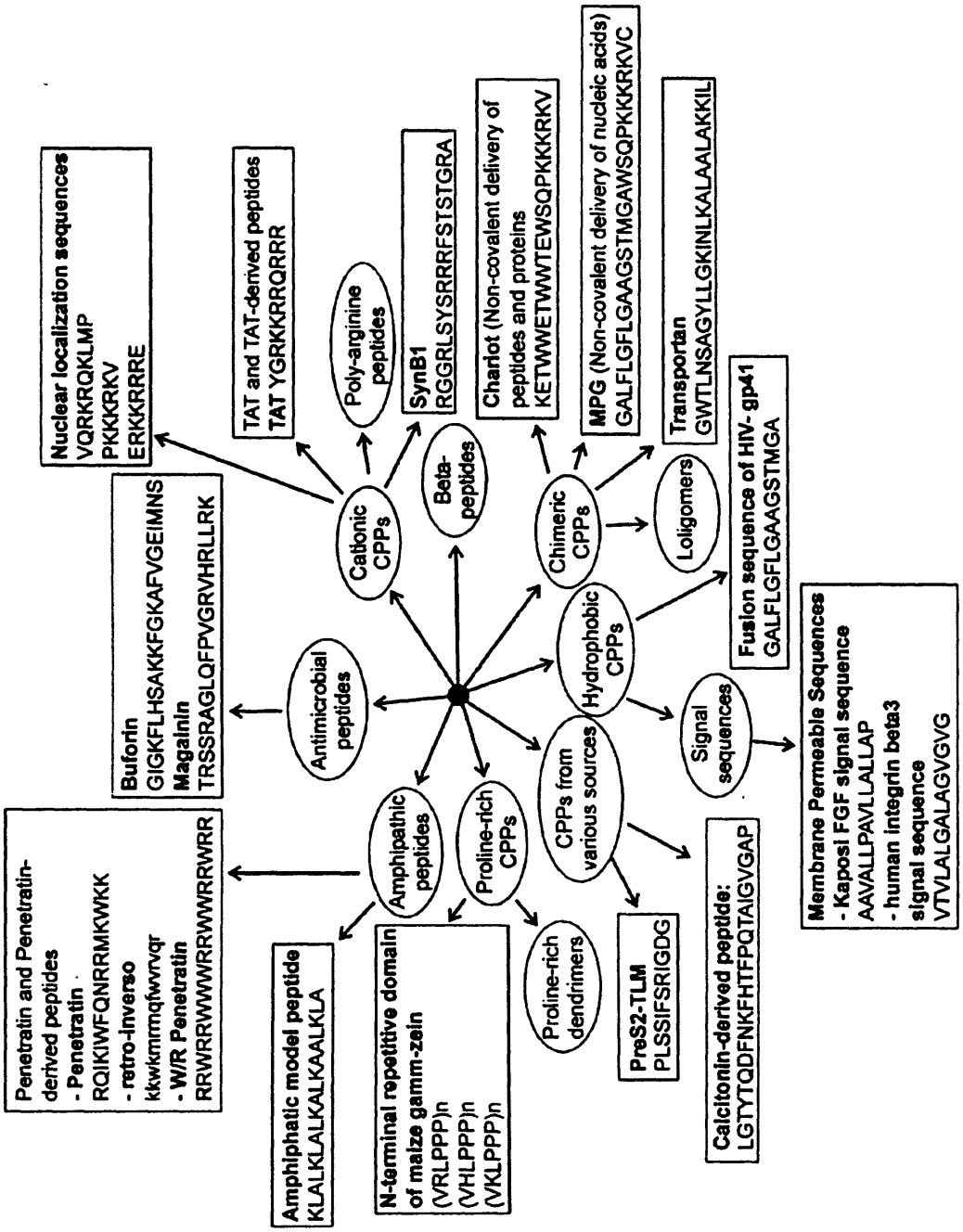

Figure 1.1. A family tree of cell penetrating peptides(Fischer et al. 2005)

1.4. CPPs and the delivery of therapeutic molecules

Although the mechanisms of uptake of CPPs alone or with cargo is largely undetermined they have been shown to successfully deliver a wide range of interesting pharmacological molecules into different cell-lines (Foerg and Merkle 2008; Gupta et al. 2005; Johnson et al. 2011; Temsamani and Vidal 2004). The following sections show the main applications of CPPs in the drug delivery field emphasising the nature of the cargo.

1.4.1. Peptide delivery

Rather than using full-length proteins to modify cellular physiology in a disease state, it is preferable to use a specific peptide sequence that can have protein-specific biological activity. One of the main reasons for this is that peptides are easier to manufacture and to deliver. Many studies have been done on different CPP conjugated peptides but relatively few studies have been described where their mechanism of uptake has been scrutinized at the same time as measuring their bioactivities. The fact that CPPs can enter most cell types offers some advantages and disadvantages but for cancer it is often required that some form of specific cell targeting is needed and this has also been shown for CPPs. For example, conjugating DV3, the ligand for chemokine receptor 4 (CXCR4) that is over-expressed in more than 20 types of cancer, to a CPP enhanced the delivery of CPPs specifically to cancer cells (Snyder et al. 2005). Recently, two interesting studies were performed using a sequence derived from the C-terminus of p53-derived linked to the N-terminus of penetratin (p53p–Ant) (Li et al. 2005b; Senatus et al. 2006). They first showed that p53p–Ant induced cell death selectively only in pre-malignant or

malignant cells, and avoided normal cells or p53 null cells (Li et al. 2005b). The second study showed that the same chimeric peptide promoted apoptosis in human and rat glioma cells both in vitro and in vivo (Senatus et al. 2006). Now hundereds of manuscripts are published describing the use of CPPs for the delivery of bioactive peptides, and these show great potential for treating cancer, ischemia and heart disease, inflammation, diabetes and many other diseases.

It is however important to note that the sequence itself may have effects on the ability of CPPs to enter cells. Work from our lab on the proapoptotic peptide $(KLAKLAK)_2$ (PAD) showed that attaching this to R8 led to the manufacture of a highly necrotic peptide but that cells incubated with a combination of R8 and PAD were unaffected (Watkins et al. 2009a). Here charge is a major factor as the PAD sequence is also highly positive, and also helical. But this highlights that peptide cargo and CPP together could produce non-specific effects (Watkins et al. 2009a).

1.4.2. Protein Delivery

Entire proteins do however offer exciting alternatives to peptides as therapeutic molecules but here the problem of delivery is higher as they are larger and there is a need to maintain their three-dimensional structure (Tan et al. 2009). Furthermore, another obstacle for using proteins as therapeutics (to function inside cells) is their stability, which depends on weak non-covalent interactions between their secondary, tertiary and quaternary structures. Thus, these molecules have short in vivo half-lives and poor bioavailability. Accordingly,

they require vectors that efficiently deliver them into cells both in vitro and in vivo (Morris et al. 2001; Tan et al. 2009; Wadia and Dowdy 2005).

Different types of delivery vectors based, for example, on lipids and polymer have been used for protein delivery, including liposomes, microparticles and nanoparticles, but unfortunately most of them show relatively poor efficiency (Tan et al. 2009).

On the other hand, CPPs have been shown to be able to promote the delivery of several different types of proteins and importantly this maintained biological activity. In fact it was the demonstration that a CPP (HIV TAT) coupled to β-galactosidase could deliver the enzyme into several mouse tissues following IV injection that sparked initial interest in this field and significantly raised the profile of CPPs as potential delivery vectors (Fawell et al. 1994; Schwarze et al. 1999). Other studies have used β- galactosidase as a delivery model and other proteins that have been shown to be successfully delivered by CPPs are eGFP (Caron et al. 2001), Bcl-xL (Cao et al. 2002; Embury et al. 2001), human catalase (Jin et al. 2001), and human glutamate dehydrogenase (Yoon et al. 2002). Most of CPPs are coupled to proteins via either covalent bonds, avidin-biotin affinity or via fusion constructs (Deshayes et al. 2008; Gros et al. 2006; Jones 2010; Patel et al. 2007). These studies demonstrate that CPPs can be considered as effective tools to mediate protein-based therapeutics for curing many diseases, such as cancer, inflammatory diseases, diabetes and brain injury.

1.4.3. Delivery of low molecular weight drugs

A main obstacle for successful cancer treatment is clinical resistance highlighted by the ability of cancer cells to develop resistance initially to one or two types of drugs but to then evolve to be multidrug resistance (Szakacs et al. 2006). Thus, many studies have been done to enhance the uptake of anticancer agents and to overcome clinical resistance. An example of low molecular weight drug or small molecule that has been commonly studied in drug delivery applications is the anthracycline doxorubicin, which is commonly used as anticancer agent; but also as a model drug for multidrug resistance. Studies have been published whereby doxorubicin has, via one form or other, been associated with CPPs in an attempt to overcome resistance mechanisms. Two studies have assessed the uptake of a doxorubicin-SynB conjugate into the brain of mice and rats following in vivo cerebral perfusion (Rousselle et al. 2000; Rousselle et al. 2001). The SynB peptide (Table 1.1) was conjugated to doxorubicin and an in situ brain perfusion technique was applied. This method is a simple and sensitive method in which the BBB is exposed for a short time (15 to 90 s) to a drug under infusion conditions where the fluid composition and the rate of infusion are controlled. The studies highlighted that SynB vectors enhanced brain uptake of doxorubicin without affecting blood brain barrier integrity and the same results were obtained when doxorubicin was administered intravenously (Rousselle et al. 2000). Cardiac levels of doxorubicin-SynB conjugate were very low, and this is important as cardiac complications are one of the main side effects of doxorubicin treatment. D- penetratin has also been conjugated to this drug (DOX-D-penetratin) using in vivo brain perfusion, which has been mentioned previously

(Rousselle et al. 2000). The results show that even at low concentration of DOX-D-penetratin shows a fivefold to sevenfold improvement in delivery, compared with free doxorubicin (Bolton et al. 2000).

Antibiotics have also been linked to CPPs in an attempt to deliver them into the brain and these include benzyl-penicillin (Rousselle et al. 2002). These types of antibiotics required for CNS infection are characterized by poor brain permeability, which reduce their therapeutic efficacy. Benzyl-penicillin was conjugated to SynB1 vector through glycolamidic ester linker and its uptake into brain was evaluated via in situ brain perfusion. Uptake increased eightfold, compared with free B-Pc (Rousselle et al. 2002).

1.4.4. DNA delivery

There is also a wealth of literature on the use of CPPs for delivering DNA and other nucleotide based compounds. One major advantage of cationic CPPs is that they have high affinity for negatively charged phosphates on nucleotides and this allows the formation of complexes similar to those of cationic polymer or lipids with nucleotides. For example a series of synthesized complexes containing 1-8 Tat moieties and plasmid DNA, in different cell lines have been evaluated (Tung et al. 2002). The study reveals that high transfection ability was only found with complexes, containing eight molecules of Tat peptide per DNA molecule. Liposomes, are widely used to deliver genes for gene therapy but their poor cellular penetration decreases the bioactivity of their cargo. Researchers have examined the potential for improving cellular penetration, and nucleotide delivery of liposomes when they are further conjugated with different CPPs. For example, penetratin and Tat peptides when conjugated to

liposomes enhanced cellular delivery and transfection capacity (Console et al. 2003; Torchilin et al. 2001; Tseng et al. 2002). The Torchilin group have also shown how a polyethylene glycol masked liposome can be constructed that hides the CPP Tat until low pH, that is typically seen in the tumour environment, cleaves the mask to reveal the CPP that then mediates uptake of the liposome into cells and presumably aids in endosomal escape (Torchilin 2005a)

1.4.5. Delivery of oligonucleotides (ONs)

The discovery of short sequences of mRNA, typically 21-27 residues in length could potentially silence the expression of any protein in the genome was a new opportunity for drug delivery research. These are however membrane impermeable and like plasmid DNA they require a delivery vector (Meade and Dowdy 2007). These have largely overtaken the use of antisense systems that at one time were also of considerable interest and other examples of ONs are locked nucleic acids (LNAs) and phosphorodiamidate morpholino oligomers (PMOs), decoy-ONs and plasmids, and their analogues such as peptide nucleic acids (PNAs) (Saleh et al. 2010). Again there are several examples of the use of CPPs for delivering these short nucleotide sequences to modify cell physiology (Eguchi and Dowdy 2010; Palm-Apergi et al. 2011; Saleh et al. 2010)

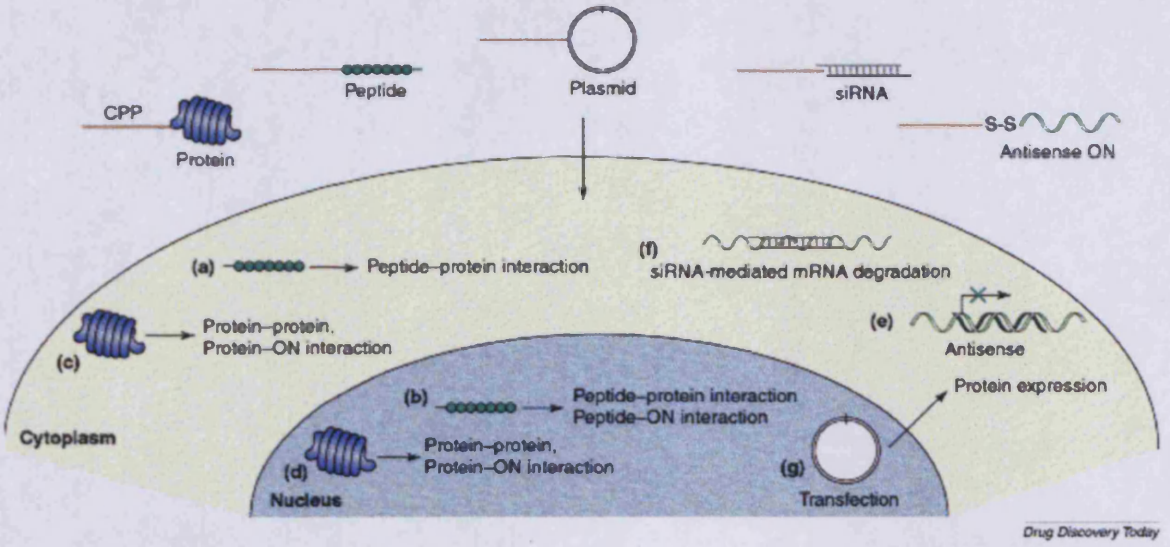

Figure 1.2. (Jarver and Langel 2004). Various possible applications for cell penetrating peptides.

(a) Peptide–protein interaction in the cytoplasm. **(b)** Peptide–protein and peptide–ON interaction in the nucleus. **(c)** Protein–protein interaction in the cytoplasm. **(d)** Protein–protein and protein–ON interaction in the nucleus. **(e)** Antisense ON–mRNA hybridization. **(f)** siRNA-mediated mRNA degradation. **(g)** Transfected plasmid and protein expression.

1.5. Cellular Uptake of CPPs

Despite the wide use of CPPs for delivery purposes, the exact mechanisms underlying their cellular uptake remain unclear and are still debatable. It is often claimed that CPP internalisation is highly efficient and non-toxic to the cells, without causing membrane destabilization and loss of cellular integrity. But there is also plenty of evidences to suggest that even at low micro-molar concentrations (5-50) that even the most commonly studied are not without effects on cells. There are reports of leakage out of cellular material at 20-50 μM and also leakage in of normally membrane impermeable probes such as propidium iodide (El-Andaloussi et al. 2007; Tunnemann et al. 2008)

It is important to note here, as shown in Table 1.1, the high degree of heterogeneity in amino acid sequences between one class of peptides called CPP and this complicates matters when a single pathway or mechanism is searched for to answer questions regarding uptake. It is now appreciated that a single mechanism is unlikely to emerge but there remains a need to study their uptake further in order to understand how this can be improved for drug delivery purposes.

Initially, CPP internalisation was reported to occur even at low temperatures, excluding endocytotic pathways as the main mechanism responsible for the uptake of these peptides. This suggested the existence of an energy-independent internalisation mechanisms, not requiring the involvement of membrane receptors or any active process (Derossi et al. 1996). In fixed cells using microscopy, peptides such as HIV-Tat and R9 were shown to enter cells efficiently and then move to the nucleus. Later two independent studies showed that both CPP protein delivery to the nucleus and CPP-fluorophore

delivery to the same organelle was a product of fixation artefact (Lundberg et al. 2003; Vives et al. 2003). This required a complete reassessment of the mechanisms involved in CPP internalisation.

The data, which has been obtained from these reassessment studies, were performed in live cells, and overall they highlight that in addition to the previously described endocytosis-independent mechanisms, uptake of CPPs could involve several endocytic pathways, such as caveolae-mediated endocytosis (Ferrari et al. 1998; Fittipaldi et al. 2003), macropinocytosis (Kaplan et al. 2005; Wadia et al. 2004) and clathrin-mediated endocytosis (Richard et al. 2005). Additionally, variations were observed between the internalisation of unconjugated (small fluorophore) and conjugated CPPs, suggesting different internalisation mechanisms for the same peptide, depending on the presence or absence of cargo and the size of the cargo. Moreover, it has been shown that cell surface heparan sulphate proteoglycans (HSPG) play an important role in the CPPs uptake process (Belting 2003) especially with cationic peptides that are likely to have high affinity for negatively charged sugars that reside on these molecules. Figure 1.3 illustrates different proposed mechanisms to explain the internalisation of free or cargo-conjugated CPPs.

CPP attached to fluorophores and cargo have been shown to be enriched in endocytic organelles thus clearly demonstrating the roles for some kind of internalisation pathway but as mentioned a cell has many different kinds of endocytic pathways. Endocytosis is discussed in the following section, which deals with this process itself breaking it down into several pathways and describing proteins that regulate specific events and routes and some that

regulate multiple pathways. Characterising the roles of these proteins and pathways in the uptake of CPPs was a major focus of the thesis.

1.6. Endocytosis

The plasma membrane acts as a highly effective barrier between the inside and outside of cells and this is necessary to maintain and control the intracellular microenvironment. Only few compounds can pass this barrier and this depends mostly on their molecular size, net charge and polarity. Essential amino acids and ions such as sodium and potassium cross the plasma membrane via specific proteins pumps and ion channels, while large molecules enter via endocytosis. During this process, the plasma membrane is invaginated and converted into a vesicle, for example a clathrin coated vesicle, which then detaches from the plasma membrane and migrates into the cell. This then fuses with some sort of sorting endosome that regulates further delivery to many different organelles or back to the cell surface (Conner and Schmid 2003; Doherty and McMahon 2009; Johannes and Lamaze 2002). Endocytosis plays key roles in allowing entry of nutrients for the cell and in regulating many intracellular signaling cascades. As mentioned, several types of endocytic pathways have now been described and a number of reviews have been written to describe these and but it is highly unlikely that the list is complete. (Doherty and McMahon 2009). The most characterised pathways and mechanisms are described below and shown in Figure 1.3.

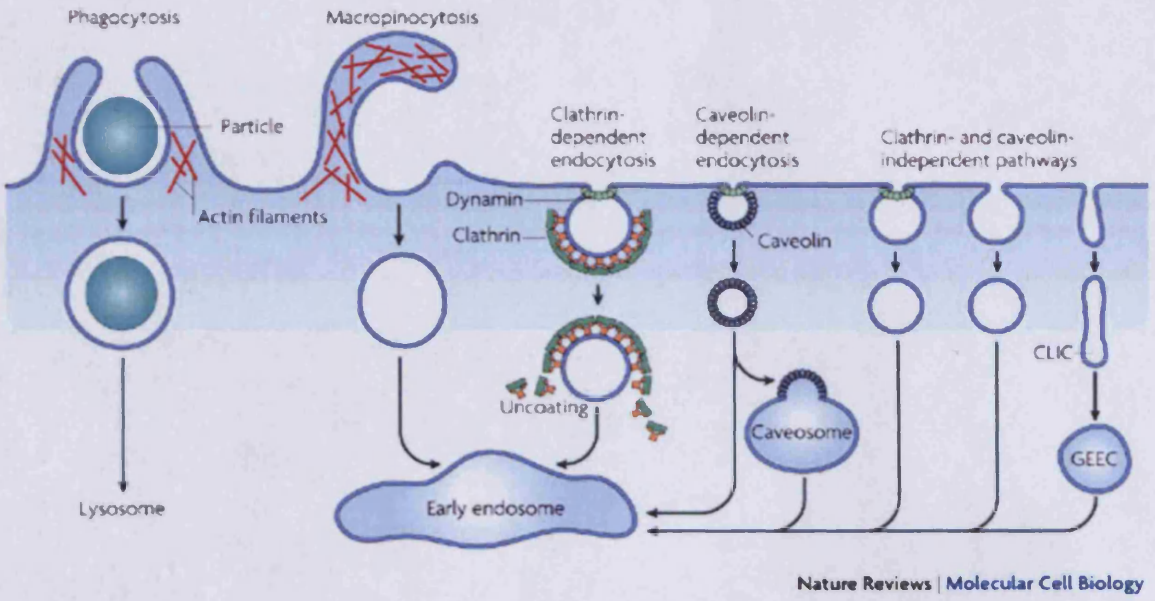

Figure 1.3. Defined Endocytic pathways (Mayor and Pagano 2007)

*Clathrin- and dynamin-Independent Carriers (CLICs)

*Glycosyl phosphatidylinositol-anchored protein enriched Early Endosomal Compartments (GEEC)

1.6.1. Endocytic pathways

1.6.1.1.Clathrin-mediated endocytosis (CME)

CME is by far the most studied endocytic pathway and takes place in several mammalian cell lines, and plays an important role in the uptake of a number of receptor ligands such as transferrin (Tf), and low-density lipoprotein (LDL). CME is also crucial for essential for tissues and organ development as it is required for intracellular communication and to control transduction of signals by mediating or down-regulating activated signaling receptors (Brodsky et al. 2001; Conner and Schmid 2003; Di Fiore and De Camilli 2001; Johannes and b Lamaze 2002; Schmid 1997). Furthermore, CME also plays an important role in regulating membrane pumps that control the uptake of small molecules, ions (Conner and Schmid 2003) and in controlling the strength of synaptic transmission, as well as in efficient recycling of synaptic vesicle membrane proteins after neurotransmission (Beattie et al. 2000; De Camilli and Takei 1996; Royle and Lagnado 2010).

Three different types of coat proteins have been described in cells and these organise themselves usually on the cytosolic portion of transmembrane proteins to initiate the budding process whether this be on the plasma membrane for endocytosis or on other locations such as the *trans*-Golgi network or endoplasmic reticulum for secretion. These three types are known as coat protein-I (COP-I), coat protein-II (COP-II), and clathrin. Their organisation on membranes is involved with cargo selection and usually the coat consists of several different proteins. COP-I coats are responsible for transfer of material from the Golgi apparatus and the endoplasmic reticulum (ER), whereas, COP-II coats are associated with vesicles that transferred from

ER to Golgi apparatus (Alberts 2002; Johannes and b Lamaze 2002). However COPII has also been implicated in mediating traffic from early to late endosomes (Aniento et al. 1996).

Clathrin is the major protein component of clathrin coated vesicles (CCV). Clathrin associates as a triskelia consisting of three clathrin light chains (CLC, 25 kD), and three much larger proteins called clathrin heavy chains (CHC, 190 KDa) (Alberts 2002; Marsh and McMahon 1999). The clathrin triskelions form hexagons and pentagons to organise the classical basketlike frameworks that by electron microscopy can be seen as coated pits on the cytosolic surface of the plasma membrane (Figure 1.4).

Other members of the clathrin coat proteins family are the adaptor proteins (APs); multi-subunit complexes, which are necessary to attach the clathrin coat to the membrane. Furthermore, they are required to pack or cluster specific membrane proteins (i.e. cargo receptors) and proteins that interact with them into each newly made CCV (Alberts 2002). Clathrin is known to function not only on the plasma membrane but also on sorting endosomes for recycling and the *trans*-Golgi network for secretion of proteins from this organelle (Harasaki et al. 2005). Specificity for these membrane trafficking systems comes in part from the fact that four different types of adaptor complexes have now been identified and are termed AP1, AP2, AP3, and AP4. Each is required for a specific set of cargo receptors but importantly only AP2 is associated in CCV formation at the plasma membrane (Conner and Schmid 2003; Motley et al. 2003). AP2 is composed of four sub-units called α-adaptins and β2-adaptins, μ2, and σ2 sub-units Figure 1.5.

Another important regulator of endocytosis via clathrin is the GTPase Dynamin. This acts as a scissor to separate the CCV from the plasma membrane. It assembles as a ring around each CCV neck and it is considered as regulatory GTPase in CME (Alberts 2002; Conner and Schmid 2003). Activation of dynamin occurs when it goes through GTP-hydrolysis-driven conformational change (Song and Schmid 2003). Many studies show that over-expression of dominant-negative GTPase domain mutants of dynamin can inhibit receptor-mediated endocytosis (Damke et al. 1994; Damke et al. 2001). There are two major isoforms of this protein termed Dynamin I and Dynamin II. Dynamin I is neuron specific but Dynamin II is ubiquitously expressed and also occurs as several different splice variants and each may have a different role to play in endocytosis (Cao et al. 2007). CME is a dynamic network of protein-protein and protein-lipid interactions and several other proteins such as Epsin, AP180, amphiphysin are involved in regulating this process then in stripping the coat off the CCV through to fusion of this vesicle with the sorting endosome.

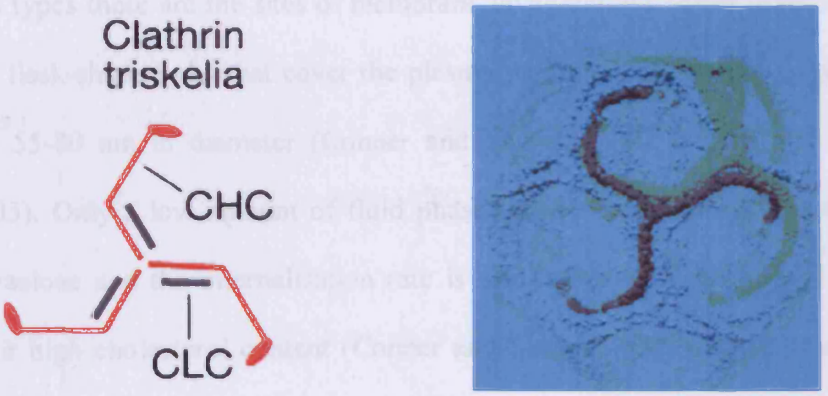

Figure 1.4. The structure of the clathrin coat (Alberts 2002; Conner and Schmid 2003).

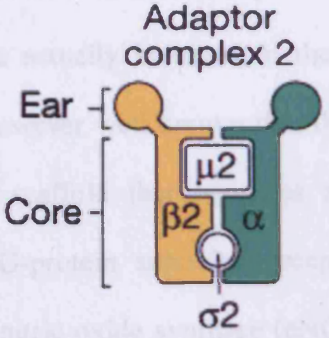

Figure 1.5 The organisation of the AP2 adaptor protein complex (Conner and Schmid 2003).

1.6.1.2.Caveolae-dependent endocytosis

Lipid rafts are major sites for non-clathrin coated invaginations and in many cell types these are the sites of membrane invaginations called caveolae. They are flask-shaped pits that cover the plasma membrane of many cell types, and are 55-80 nm in diameter (Conner and Schmid 2003; Parton and Richards 2003). Only a low amount of fluid phase uptake is thought to occur through cavaeloae and the internalisation rate is also low due to their small size and their high cholesterol content (Conner and Schmid 2003; Mayor et al. 1998). The most notable protein in cavaeolae is caveolin of which there are three types, Caveolin 1, 2 and 3. Caveolin 1 and 2 are expressed in many different tissues but caveolin 3 is specific for muscle. Cells lacking caveolins do not have caveolae but it is still unclear exactly how caveolin organizes caveolae or whether caveolin are actually involved in the invagination of caveolae into caveosomes. It is however well known that the cytosolic portion of caveolin acts as a signaling scaffold that regulates a number of different cellular processes such as G-protein subunits, receptor and non-receptor tyrosine kinases, endothelial nitric oxide synthase (eNOS), and small GTPases (Couet et al. 2001; Frank et al. 2003). Caveolin-1 is a 21 KDa integral membrane protein that strongly binds to cholesterol (Anderson 1998; Furuchi and Anderson 1998; Parton and Richards 2003), and caveolin dependent uptake also has a requirement for active dynamin and the actin cytoskeleton (Nichols 2002; Thomsen et al. 2002). Different types of cargo such as; lipids, proteins and lipid-anchored proteins are internalised by caveolae (Doherty and McMahon 2009; Mayor and Pagano 2007). Caveolin mediated endocytosis results in the formation of caveosomes, which are then able to fuse with early

endosomes. Only a few proteins are thought to be involved in the invagination process but one example is PTRF-Cavin (Hill et al. 2008). To study and to investigate the involvement of caveolin dependent endocytosis in the uptake of different cargo researchers have used cholesterol sequesters/binders methyl-ß-cyclodextrin (MβCD), filipin and nystatin; thus the effects are not directly on caveolin but on the entire plasma membrane. Overexpression of dominant-negative caveolin mutants, and genetic knockout of caveolin genes, have also been used to inhibit caveolin dependent uptake (Drab et al. 2001; Razani et al. 2002). Despite the fact that much is known about caveolins, relatively little knowledge is available on the regulation of endocytosis by this pathway. It is also important to note that cells of the haematopoietic system do not express caveolin (Fra et al. 1994, 1995) and these can be a good models to study the absolute requirement of caveolae in uptake of any particular cargo.

Several attempts have been made to identify a protein or cargo that is specifically internalised by caveolae and not through other pathways. An initial candidate was cholera toxin B that enters cells via the GM1 ganglioside receptor. This probe is available commercially as a fluorescent conjugate but more recent studies have shown that the protein can also enter cells through CME (Hansen et al. 2005). The group of Pagano demonstrated that the glycosphingolipid (GSL) LacCer (lactosylceramide) enters cells through caveolae and several studies have used this probe as a marker for caveolae endocytosis. This was shown by Pagano's group via a detailed study of GSL analog internalisation in multiple cell types, such as HeLa, CHO-K1, Calu-1, and Calu-6, and they have compared those results to parallel studies using fluorescent Cholera toxin B. Their data has provided strong evidence that

fluorescent GSL analogs of widely varying structure are internalised primarily by a Cav-1 dependent process (Singh et al. 2003). a new role for caveolae has been proposed by Sinha B et al, where caveolin acts as a physiological membrane reservoir that quickly accommodates sudden and acute mechanical stresses such as osmotic swelling, shear stress, or mechanical stretching (Sinha et al. 2011).

1.6.1.3.Clathrin and Caveolin independent endocytosis (Flotillin-dependent endocytosis

It has been shown that different types of cargo and receptor molecules are internalised into cells by vesicular carriers that are formed without the requirement for clathrin and caveolin. Recently, a new pathway was described that is regulated by flotillin-1 and 2, also known as Reggie-2 and 1, respectively. These have been reported to be expressed as integral membrane proteins in cholesterol rich membrane microdomains. Although they have similar topology to caveolin-1 and generate structures that look like caveolae, it has been shown that flotillin-1 is not colocalized with caveolin (Frick et al. 2007; Glebov et al. 2006; Solis et al. 2007; Stuermer et al. 2001). Flotillin and caveolin share same characteristics as both of them bind to Src-family kinases and any mutation in specific tyrosine residues cause an alteration in their subcellular distribution (Neumann-Giesen et al. 2007). Lately, flotillin dependent uptake was described as a new clathrin and caveolin independent pathway (Glebov et al. 2006). Beside flotillin itself, there are no well-characterised probes available for labelling this pathway inside cells. It has however been shown that depleting flotillin-1, reduces the uptake rate of an

antibody recognising CD59 (protectin) (Glebov et al. 2006). This was demonstrated through siRNA depletion of flotillin-1 that reduced the uptake of anti-CD59 antibody but it should be noted that inhibition was only 25-30 % suggesting it may also enter via a different mechanism. CD59 is a glycophosphatidyinositol (GPI) linked protein that protects cells form self damage by the complement system but may have other functions (Kimberley et al. 2007). For demonstrating the role of flotillin-1 in CD59 uptake a commercial FITC-anti-CD59 was used, but this is no longer available. The group of Professor Paul Morgan at the University of Wales Hospital in Cardiff has studied CD59 in detail and has published on different antibodies recognizing distinct regions of the molecule (Bodian et al. 1997). To use an antibody for live uptake studies, it is important that it recognizes the extracellular domain of the protein and one such example is A35 that was used for this thesis- see section 2.3.5.2. Interestingly uptake of the cationic polymer and vector polyethylenimine was also shown to be inhibited in siRNA-flotillin silenced cells (Payne et al. 2007) and as CPPs studied here are also cationic it is interesting to discover if they also enter through this pathway. One of the problems of using siRNA to deplete endocytic proteins and pathways is that there may be effects on other pathways and depleting flotillin-1 was shown to significantly decrease caveolin-1 expression but the effect was not observed after down-regulation of flotillin-2 (Vassilieva et al. 2009). This effect was reversed after cell exposure to lysosomal inhibitor, but not proteosomal inhibitor.

1.6.1.4.Macropinocytosis

Macropinocytosis is a form of endocytosis that is associated with cell surface ruffling in which a large amount of extracellular fluid and other components are internalised (Doherty and McMahon 2009; Jones 2007a). The so formed macropinocytic vesicles or macropinosomes are heterogeneous in size and can be up to 10 μm in diameter. There are different forms of ruffles, such as planner folds, cup-shaped, and circular extensions of cytoplasm and the extent of ruffling is different from one cell type to another, therefore the rate of macropinocytosis may varying between cell types. It is still debatable whether all cell types can mediate this pathway and also whether this can be a constitutive process or one that will only proceed in an activated cell. Ruffles occur due to actin polymerization near the plasma membrane, which cause an extension of the cell surface (Swanson and Watts 1995). The ruffling process can therefore be inhibited by cytochalasin D, which disrupts the actin cytoskeleton (Grassme et al. 1996). In addition, it has been shown that actin-based mechanochemical enzymes such as myosin II, which are required for ruffling, can be inhibited using a drug called blebbistatin (Mercer and Helenius 2008). It is a small molecule inhibitor discovered in a screen for inhibitors of nonmuscle myosin IIA and its effects are reversible upon washout of the drug (Limouze et al. 2004). Moreover, it has been shown that macropinocytosis is inhibited by amiloride, which is a guanidinium-containing pyrazine derivative and inhibitor of the Na^+/H^+ exchanger; more recently it has also been shown to also affect intracellular and endosomal pH (Koivusalo et al. 2010). This amiloride effect has been used as an identification tag for macropinocytosis, however the exact mechanism of inhibiting macropinocytosis by this drug is

still unclear (Meier et al. 2002; Veithen et al. 1996). Studies from our laboratory have however shown that the drug and the more commonly used amiloride analogue 5-(N-Ethyl-N-isopropyl) (EIPA) also has large effects on the distribution of endocytic organelles.

Once inside the cell the ruffle is invaginated as a macropinosome and studies have shown that these can then be delivered to lysosomes in some cells types or be recycled in others (Jones 2007). They have also been shown to contain classical early endosomal markers such as EEA1 and Rab5 (Schnatwinkel et al. 2004).

Although, there is no specific endocytic marker for macropinocytosis, growth factor induced ruffling results in a rapid increase in fluid phase endocytosis of endocytic probes/markers such as dextrans and horseradish peroxidase and it is the uptake of these that is measured to show that macropinocytosis is occurring. For example it has been shown that treatment of skin epithelia A431 cells with epidermal growth factor (EGF) results in extensive membrane ruffling and this is associated with an extremely rapid increase in dextran uptake (Haigler et al. 1979; Liberali et al. 2008). It has been reported that many pathogens utilize this mode of endocytosis to invade eukaryotic cells and these include ebola virus, HIV, vaccinia viris and adenovirus (Marechal et al. 2001; Meier and Greber 2004; Mercer and Helenius 2008; Saeed et al. 2010).

It is now established that P21-activated kinase (PAK-1) plays an important role in macropinocytosis. This protein is characterized by its capacity to bind activated Rho, GTPases, Cdc42, and Rac1 (Parrini et al. 2005) and its function is to coordinate extracellular signals with the reorganization of the actin cytoskeleton and focal adhesions (Hofmann et al. 2004). It was shown that

endogenous PAK-1, in Swiss 3T3 fibroblasts, localized to pinocytic vesicles (Dharmawardhane et al. 1997) and they also revealed that PAK-1 can induce the formation of circular dorsal ruffles, which can be associated with the macropinocytic uptake process. In another study from the same group, the inhibition of endogenous PAK activity using a PAK-specific autoinhibitory domain inhibits growth factor-induced macropinocytosis, proving that PAK activity is required for normal macropinocytosis (Dharmawardhane et al. 2000). The roles of PAK-1 and PAK-2 in breast carcinoma cell invasion was studied by targeting these proteins with siRNA sequences (Coniglio et al. 2008). The depletion of PAK-1, compared with PAK-2 had a stronger inhibitory effect on lamellipodial protrusion, and highlighted the importance of this protein in regulating the actin cytoskeleton during cell motility and invasion

1.6.1.5.Other endocytic pathways and proteins

The best characterized endocytic pathways have been described but this list is incomplete as others have also been discovered. But they are still new and there is no real agreement on the types of proteins that act as regulators or the types of probes that should be used to mark them. Examples include pathways regulated by ARF-6 and GRAF-1. ARF-6 is a member of the ADP ribosylation factor family of GTP-binding proteins and has been shown to be required for a number of different endocytic processes (D'Souza-Schorey and Chavrier 2006; Schweitzer et al. 2010). GRAF-1 (GTPase regulator associated with focal adhesion kinase-1) has been shown to be involved in the internalisation GPI (glycosylphosphatidylinositol)-anchored proteins, bacterial toxins and large

amounts of extracellular fluid and is thought to mediate the formation of Clathrin-Independent Carriers (CLICs) and GPI- Enriched Endocytic Compartments (GEECs) (Fig 1.3) (Doherty and Lundmark 2009).

1.6.2. Tools to study different endocytic pathways

Cell biologists studying endocytic proteins, lipids and pathways and drug delivery researchers interested in intracellular transport need tools to be able to selectively target different endocytic pathways. A number of approaches have been investigated but the three main methods are : (i) Using pharmacological inhibitors (ii) Depleting a key regulatory endocytic protein using a siRNA sequence and (iii) transfecting cells with a mutated or truncated from of an endocytic protein. The following section will cover the first two methods and will highlight the advantages and disadvantages of each.

1.6.2.1.Chemical Inhibitors

It is essential to have simple, reliable, and affordable methods that can be used to investigate different endocytic pathways. By far the most common, especially in drug delivery studies, employ the use of pharmacological or chemical inhibitors. There are several advantages of these inhibitors over the more sophisticated molecular biological tools. First, they equally affect all cells in a population, and these effects can be easily quantified. Second, the incubation period of cells with these drugs are usually short, and thus exclude the development of delayed side effects or compensation machinery. Third, pharmacological inhibitors still considered as the tools of choice for in vitro studies. In addition, they are relatively cheap to purchase and experiments

using these is technologically less demanding then other methods. On the whole, however, they suffer enourmously from lack of specificity (Ivanov 2008; Vercauteren et al. 2010). Table 1.2 shows the most common endocytic pharmacological inhibitors, their mechanism of action and the pathways that they effect. An in depth analysis of their lack of specificity is not given here but for example MßCD is commonly used as a drug affecting lipid rafts and uptake through cavaeolae but in some cell types it inhibits CME (Rodal et al. 1999). Cytochalasin D is also used to inhibit macropinocytosis and phagocytosis but chlopromazine has been shown to be be a strong inhibitor of CME in many cell types (Fujimoto et al. 2000). It is also important to consider their toxicity, even at short time points, and this was noted recently for chlorpromazine through work with our collaborators in Ghent (Vercauteren et al. 2010).

1.6.2.2.siRNA depletion of endocytic proteins to modify endocytic pathways

Today there is documentation in thousands of manuscripts studies describing RNA interference for silencing the expression of specific proteins in eukaryotic cells. It is an experimental process in which a small synthetic RNA fragment binds to its complementary sequences of mRNA target and consequently blocks the expression of this mRNA and thus the expression of one protein is depleted or silenced altogether. These RNA fragments are so called siRNAs Figure 1.6 and siRNA mediated gene silencing provides a reliable way to characterize a gene knockdown phenotype *in* vitro. The method is however not without its own problems such as the need for transfection and the possibility of affecting other protein targets beyond the one selected for study.

The application of RNAi technology is widely used now in different research areas; for instance, it has been shown that RNAi tools was used to inhibit the replication of HIV-1 in established cell lines as well as in primary peripheral blood lymphocytes (Jacque et al. 2002). For neurodegenerative diseases, siRNA was used to suppress the toxic gain-of-function gene mutation for amyotrophic lateral sclerosis (Ding et al. 2003) and Huntington's disease (Harper et al. 2005). In addition, the RNAi-mediated gene-silencing machinery is also used to study cancer (Billy et al. 2001), and different studies have studied knockdown phenotypes of oncogenes using siRNA (Wilda et al. 2002). There is also very active research into the use of siRNA as therapeutic entities (Walton et al. 2010).

Furthermore, siRNA depletion has also been utilized to evaluate and investigate different endocytic pathways and Table 1.3 highlights some of these studies. This allows for one single protein to be depleted and then one can study the effects of this depletion on one or more endocytic pathways.

siRNA has the capacity to be highly specific but there are also reports of the siRNA target depleting more than one protein, and the possibility that by depleting one protein you are affecting a relationship between one protein and another and so the loss of activity of one protein could increase or decrease the activity of another. Some proteins are also critical for survival and thus depletion leads to lack of viability; this was shown for long term (72 hrs) depletion of clathrin heavy chain (Motley et al. 2003). The method also depends on having the available reagents to transfect the cells with the siRNAs and also measure the loss of depletion using PCR or immunolabelling; not all cells are equally easy to transfect. For endocytosis studies it is also critical that

the loss of a protein can be functionally assayed with an endocytic probe such as measuring the reduced uptake of transferrin in CHC depleted cells (Table 1.3). For some of the more recent and less well characterised endocytic proteins and pathways this is not so easy.

Inhibitor	Mode of action	Affected endocytic pathways	References
Chlorpromazine	Prevents assembly of clathrin-coated pits at the plasma membrane	Clathrin-Mediated Encocytosis	(Marina-Garcia et al. 2009)
Dynasore	Dynamin GTPase inhibitor	Dynamin-dependent endocytosis	(Kirchhausen et al. 2008)
MâCD	Disrupts rafts by its ability to extract cholesterol from the membrane	Caveolin dependent and lipid raft endocytosis	(Duchardt et al. 2007)
Filipin	Disrupt raft and caveolae function by precipitating cholesterol in the plane of the host cell plasma membrane.	Caveolin dependent and lipid raft endocytosis	(Ruter et al. 2010)
Nystatin	Disrupt raft and caveolae function by precipitating cholesterol in the plane of the host cell plasma membrane	Caveolin dependent and lipid raft endocytosis	(Rothe et al. 2010)
CytoD	Blocks actin polymerisation by occupying fast growing end of filament	Macropinocytosis	(Kalin et al. 2010)
EIPA	Na^+/H^+ ion exchange inhibitor	Macropinocytosis	(Mercer and Helenius 2008)
Blebbistatin	Myosin II inhibitor, prevents membrane blebbing	Macropinocytosis	(Mercer and Helenius 2008)
Wortmannin	PI-3 kinase inhibitor	Macropinocytosis	(Elmquist et al. 2006)

Table 1.2. Chemical inhibitors for different endocytic pathways.

Endocytic proteins	siRNA	Endocytic Probe(s)	Reference
CHC	Single sequence	Transferrin	(Huang et al. 2004) (Motley et al. 2003)
DNM2	Pooled mixture of siRNA duplexes	Transferrin dextran	(Cao et al. 2007)
Flot-1	Single sequence	CD59 antibody	(Glebov et al. 2006)
Cav-1	Pooled mixture of siRNA duplexes	BODIPY-LacCer	(Trushina et al. 2006)
PAK-1	Single sequence	70-kD Dextran	(Mercer and Helenius 2008)

Table 1.3. Different endocytic proteins that have been depleted using siRNA targeting.

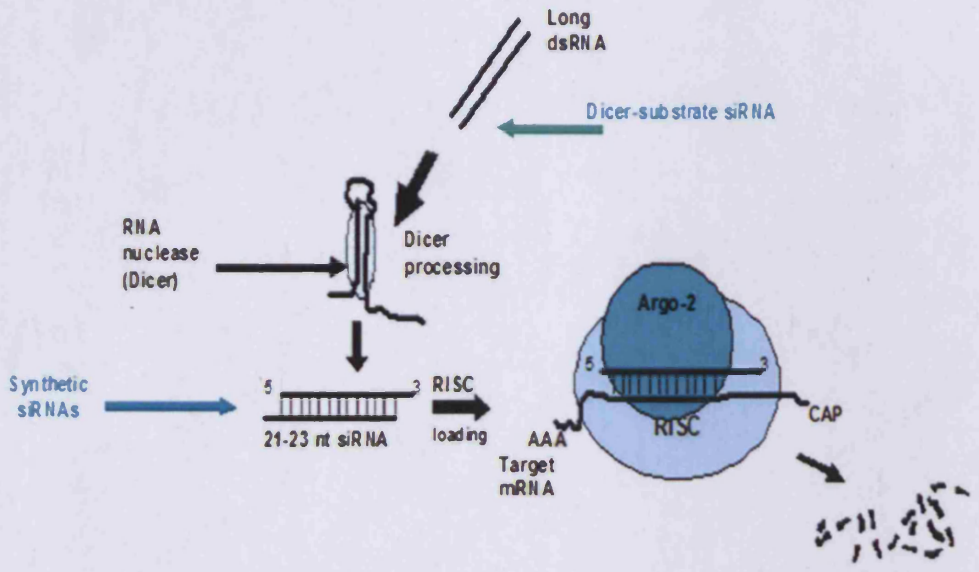

Figure 1.6. The mechanism of RNA interference

1.6.3. Endocytosis and CPP entry

There is good evidence to support the fact that fractions of most CPPs enter cells via endocytosis, but there is little agreement on the type of pathway(s) that is used by each variant and whether there is any commonality between them. It was believed for a long period in the history of CPPs research that uptake was independent of endocytosis and energy. The problems of fixation has already been described and since this period endocytosis gained popularity as a mechanism of uptake. Lebleu and co-workers originally presented a revised cellular uptake mechanism for CPPs, which was deemed to be dependent on CME (Richard et al. 2003) but there has been little agreement since then . It is important here to distinguish here between studies investigating CPP uptake when attached to small cargo such as fluorescent probes over other studies looking at entry when CPPs are attached to larger cargo such as proteins. It is likely that the mechanism will be different. Also important is that the term CPP relates to hundereds of different sequences and sequence is also a vital factor. In the main, in this section, focus will be given to CPP attached to small cargo and cationic sequences such as HIV-TAT and oligoarginines.

Most of the studies have based their interpretation on the visualization of CPPs inside cells using fluorescently labelled CPPs and either microscopy or flow cytometry. More recently, radiolabelled peptides and mass spectrometry have been used together as an alternative mechanism that also allows for analysis of peptide degradation (Aubry et al. 2010)

Overall, several endocytic routes of entry have been suggested, but there continues to be reports of the capacity of the cationic forms to directly cross

membranes without the need for endocytosis (Fretz et al. 2007; Jiao et al. 2009; Rothbard et al. 2004; Thoren et al. 2003; Watkins et al. 2009b)

Although it remains difficult to establish a general proposal for a CPP uptake mechanism, there is an agreement that the first interaction between the cationic CPPs and the cell surface occur via electrostatic interactions with proteoglycans. Proteoglycans play an essential role in the regulation of cell surface microdomains, and it has been reported that there is a direct relationships between cytoskeletal organization and activation of small GTPases (Conner and Schmid 2003). Heparan sulfate proteoglycans and syndecans are the major elements of the extracellular matrix, and their aggregation stimulates cytoskeletal remodelling upon activation of protein kinase C and Rho/Rac GTPases (Beauvais and Rapraeger 2004).

The initial CPPs and cell surface interaction occur through electrostatic binding with cell surface proteoglycans called glycosaminoglycans (GAGs), followed by a remodelling of the actin network and then an activation of the small GTPase Rho A or Rac1 (Duchardt et al. 2007). It is suggested that actin remodeling, affecting membrane fluidity influences R8, penetratin and Tat uptake via macropinocytosis or clathrin-dependent endocytosis (Nakase et al. 2009; Nakase et al. 2007; Richard et al. 2005) or for MPG via membrane perturbation (Gerbal-Chaloin et al. 2007). CPPs interaction with extracellular matrix is suggested to stimulate the uptake through an energy-dependent endocytotic process and this has been shown for Tat (Console et al. 2003; Murriel and Dowdy 2006), polyarginine and penetratin (Nakase et al. 2004; Nakase et al. 2007). Macropinocytosis has been reported as the main route of internalisation of cationic CPPs (Kaplan et al. 2005), however other

endocytotic pathways such as clathrin-and caveolin-dependent endocytosis has also been reported (Richard et al. 2005; Ziegler et al. 2005).

The uptake mechanisms of cationic CPPs and other variants have been studied in detail and some consensus is emerging regarding the possibility of both endocytosis and direct translocation being involved. For translocation there is only the plasma membrane to overcome and then the peptide and its cargo -low molecular weight- will emerge in the cytosol. However if the cargo is large then it probably needs endocytosis for uptake and then there is the problem of breaking across the membrane(s) of the endolysosomal system. Very little is known regarding this step though some elegant studies have been attempted using fluorescent proteins (Lee et al. 2008). Only small fraction of CPPs is probably able to escape from endosomes and it is likely that a major fraction is sent to lysosomes and degraded (Al-Taei et al. 2006) . It has been shown that internalised CPPs may be degraded upon delivery to late endosomes and lysosomes or inside the cytoplasm and it has been demonstrated that a large fraction of internalised TAT and penetratin peptides is degraded after a 2 hrs of incubation (Fischer et al. 2004). There is also the possibility that much degradation occurs outside the cells, i.e. during the incubation, especially when full serum containing medium is used (Aubry et al. 2010; Palm-Apergi et al. 2011).

1.7. Arginine-rich cell penetrating peptides

Arginine-rich cell-penetrating peptides have been the most extensively studied among all cell-penetrating peptides (El-Sayed et al. 2009; Wender et al. 2008). The most well characterized examples are peptide from HIV transactivator

protein Tat, penetratin, a 16 amino acid domain from the antennapedia protein of Drosophila (Derossi et al. 1994), and oligoarginines (El-Sayed et al. 2009; Wadia and Dowdy 2005). Arginine rich CPPs have been successfully employed to deliver various macromolecular cargos, including proteins, oligonucleotides, plasmid DNA, and liposomes into mammalian cells (Dietz and Bahr 2004). Despite the fact that arginine rich CPPs can be successfully to deliver various macromolecules, their mechanism of uptake remains undetermined.

1.7.1. Challenges for studying cellular uptake of cationic CPPs

It is clear that methodological issues has hindered progress in our understanding of the mechanisms of uptake of cationic CPPs. As mentioned, the most common experimental techniques, used to study arginine rich CPPs, are fluorescence microscopy and flow cytometry. Unfortunately, they are subject to the artifacts that relate to the highly cationic nature of these entities. Initially their cationic nature attract them to negative surfaces such as the plasma membrane of cells and cell culture plastic (Chico et al. 2003). The normal simple washes with buffer such as PBS is not efficient to remove the fraction bound to the plasma membrane (Richard et al. 2003). Common methods that have been introduced many studies for efficient removal of surface-bound CPP are (i) protease digestion (Richard et al. 2005; Wadia et al. 2004), washing with negatively charged compounds such as heparin and a combination of both (Kaplan et al. 2005). Another major problem facing the researcher when studying the uptake of cationic CPPs using microscopy is that the cells cannot be fixed. Therefore, live-cell imaging is preferred and when the extracellular concentration of peptides R8 and HIV-TAT, is low (1-2μM)

then the peptide is predominantly observed in cytoplasmic vesicles. But increasing the concentration above 5μM highlights that the cytosol itself is also labeled suggesting strongly that the peptides are leaking through the plasma membrane (Fretz et al. 2007; Watkins et al. 2009b). The concentration of peptide that allow this to occur will be much lower if experiments are performed in the presence of serum free medium compared to full medium (Kosuge et al. 2008). Thus when studying these peptides one has to consider at least two entry mechanism. There may also be a third as studies have suggested that zones on the plasma membrane allow for initial entry of the peptide into the cytoplasm at a distinct site and that the peptide then spreads across the cytoplasm (Duchardt et al. 2007).

1.7.2. Internalisation of arginine rich CPPs via endocytic pathways

For endocytosis the data is confusing but at low concentrations (<5μM) both live-cell microscopy and flow cytometry show efficient inhibition of cellular uptake of different cationic CPPs at 4 °C or using ATP depletion with various metabolic inhibitors (Ferrari et al. 1998; Fretz et al. 2004; Letoha et al. 2003; Watkins et al. 2009b). For fluorophores and other cargoes, endocytic pathways suggested to be involved are CME (Drin et al. 2003; Richard et al. 2005; Saalik et al. 2004), caveolin-dependent endocytosis (Ferrari et al. 1998; Fittipaldi et al. 2003; Saalik et al. 2004) and macropinocytosis (Kaplan et al. 2005; Potocky et al. 2003; Wadia et al. 2004). The uptake of TAT has been shown to occur via clathrin dependent endocytosis in cell lines such as HeLa, CHO and HepG2 (Potocky et al. 2003; Richard et al. 2005). Many studies employed chemical inhibitors to study CPPs uptake. Clathrin-dependent

endocytosis inhibitors such as chlorpromazine, competently inhibited the uptake of TAT in HeLa and CHO cell lines. Moreover, nystatin, an inhibitor of raft dependent endocytosis, has a weak inhibition effect on the internalisation of TAT in the same cell lines (Richard et al. 2005). On the other hand, caveolin dependent uptake and macropinocytosis were suggested to be involved in the uptake of TAT in Namalwa cells using MßCD and CytD (Kaplan et al. 2005). Similarly, macropinocytosis has been suggested to be involved the uptake of R8 in HeLa cells and of TAT-Cre protein in T cells (Nakase et al. 2004; Wadia et al. 2004). The later study used cells expressing dynamin K44A mutant as an addition to inhibitors. Moreover, there was no evidence of colocalization with transferrin or caveolin-1, indicating that a clathrin- and caveolin-dependent pathway may have limited contribution in the uptake of TAT-Cre in cells of these types. Involvement of the caveolin-dependent pathway is also proposed by the inhibition of GST-TAT-GFP uptake by MβCD treatment of HeLa cells (Fittipaldi et al. 2003), which is also inhibits the uptake of TAT-avidin and penetratin-avidin (Saalik et al. 2004). More recently the involvement of caveolin-1 and flotillin-1 in the uptake of a transportans-avidin complex was studied highlighting that transportan/avidin complex uptake is mediated via caveolin dependent rather than flotillin. Interestingly these experiments were performed by depleting flotillin-1 and caveolin-1 with siRNA (Saalik et al. 2009). Furthermore, arginine rich CPPs were reported to cause up-regulation of specific endocytic pathways. For example R8 stimulates F-actin polymerization in HeLa cells (Nakase et al. 2004), and TAT induces the uptake of 70-kDa neutral dextran, suggesting it is activating macropinocytosis (Wadia et al. 2004). More recently the capacity to increase the fluid phase uptake of

dextran was also proposed for penetratin, and its analogs PenArg and PenLys (Amand et al. 2008).

These studies highlight the fact that a number of entry pathways have been proposed to be involved in the uptake of unconjugated or cargo-conjugated arginine rich CPPs and other CPPs. So many factors could influence this but until suitable methods are in place to measure uptake and specifically inhibit distinct pathways then confusion is likely to continue.

1.8. Model cell lines for CPP study

Many different cell lines have been utilized to study CPPs and CPPs-cargo uptake, including non-mammalian cells such as yeasts and bacteria (Holm et al. 2005; Nekhotiaeva et al. 2004) as well as mammalian cultured cell lines, embryonic stem cells and primary cells (Manceur et al. 2007; Mueller et al. 2008; Simon et al. 2009b). In this thesis two adherent cell lines were employed to study the uptake of CPPs and the following section will describe their different features and characteristics.

1.8.1. HeLa Cells

HeLa cells are a human epithelial cervical cancer (cervical cancer), and was the first human permanent cell line established in culture. In 1951, surgeon Lawrence Wharton Jr. removed the tissue from the patient **He**nrietta **La**cks, a 31-year-old African American woman and thus the cell line called HeLa was originated, representing the first two letters from her name and surname. The tissue was passed along to Dr. George Gey, head of tissue culture research at Johns Hopkins, where they grew very quickly. The cells were from the carcinoma of the cervix and these cells have been widely used for many

research purposes throughout the world (Masters 2002). We have also used this cell lines for our studies with cationic CPPs (Al-Taei et al. 2006; Watkins et al. 2009a; Watkins et al. 2009b) and have also experience of careful analysis of the endocytic pathways of these cells (Simpson et al. 2004).

1.8.2. A431 Cells

A431 cells are a model epidermoid carcinoma cell line used in many biochemical researches. A431 cells were established from epidermoid carcinoma in the vulva of a 85 year old female patient. Since these cells express very high level of epidermal growth factor receptors (EGFR), they are usually used to study cell signaling pathways related to activation of this growth factor (Todaro et al. 1980). As EGF addition to cells stimulates macropinocytosis there have also been widely used to study this process (Araki et al. 2007; Liberali et al. 2008; West et al. 1989). This cell line was used in chapter 6 to study the uptake of CPPs via macropinocytosis.

1.9. Aims of the Thesis

Cell-penetrating peptides (CPPs) have the potential to deliver a host of therapeutic macromolecules into cells including peptides, proteins, and nucleic acids. Endocytosis is thought to be of significant importance for allowing cellular access under defined conditions. However, identifying the uptake mechanisms of different CPPs has remained problematic due in large part to a lack of suitable tools to perform accurate and specific analysis. Multiple pathways have been reported to contribute to CPP uptake, such as clathrin dependent uptake, cavaeolin and clathrin-independent routes and via

macropinocytosis. This work aims to enhance the use of cell penetrating peptides as drug delivery vectors by developing new tools to investigate cellular entry specifically through endocytosis. Almost exclusively the uptake of these molecules and other drug delivery vectors has been performed using chemical inhibitors of endocytosis but as described there are major problems with these and interpreting the data that is generated following their use. The main aim of this thesis was therefore to develop methods for siRNA targeted depletion of a number of different endocytic proteins. Once this was achieved an intention was to look at the cellular effects of this depletion on the uptake of specific probes thus generating cellular models of endocytosis. Finally it was hoped that thee models would allow for careful scrutiny of the uptake of fluorescent conjugates of CPPs HIV-TAT and R8 and that they could then be used for similar studies with other drug delivery vectors.

Chapter 2: Materials and Methods

2.1. Materials

2.1.1. General Chemicals

Triton X-100 [X100], Tricine (N-Tris [hydroxymethyl] methylglycine) and bovine serum albumin (BSA) [A2153] were purchased from Sigma-Aldrich (Gillingham, UK). Ethanol [E/0650/D17], Methanol (MeOH) [M/4056/17], Sodium Chloride (NaCl) [S/3120/53] and Potassium Chloride (KCl) [BPE360-500], Phosphate buffered saline tablets (PBS) [2810306], acetic acid [64-19-7] were purchased from Fischer Scientific laboratories (Leicestershire, UK).

2.1.2. *Tissue Culture*

Foetal Bovine Serum (FBS) [10270706] and D-MEM containing Glutamax [21885] were obtained from Invitrogen (Paisley, UK). Penicillin/Streptomycin [15070], Trypsin-EDTA (ethylenediamine tetraacetic acid) [25300], Trypan Blue [T8154] and dimethyl sulphoxide (DMSO) [D2650] were purchased from Sigma-Aldrich (Gillingham, UK). The cervical cancer HeLa cells [93021013] were from ECACC (Wiltshire, UK). A431 cells were a kind gift from Dr Jon Lane Bristol University.

2.1.3. *Conjugation of Alexa488 C5 maleimide to peptides*

Alexa Fluor® 488 C5 maleimide salt [A10254] was purchased from Invitrogen (Paisley, UK). R8 & Tat peptides were from American Peptide Company (California, USA).

2.1.4. *High pressure liquid chromatography (HPLC)*

Trifluoroacetic acid (TFA) [T/3258/PB05] and Acetonitrile (ACN) [A/0626/17] were purchased from Fisher Scientific Laboratories (Leicestershire, UK). Luna C18 100Å 5 µm, 250 x 10 mm, semi preparative column [OOG-4252-NO] and a Luna C18 100Å 5 µm, 150 x 4.6 mm, analytical column [OOF-4252-EO] were purchased from phenomenex (Macclesfield, UK).

2.1.5. *Flow cytometry*

Fluorescence assisted cell sorting (FACS) flow sheath fluid [342003], FACS rinse [340346] and FACS clean [340345] were purchased from Becton Dickinson (Oxford, UK). Heparin [H3149] was purchased from Sigma-Aldrich (Gillingham, UK).

2.1.6. *Fluorescence Microscopy*

Hoechst [861405] was purchased from Sigma (Dorset, UK). Microscope lens immersion oil [11513859] was from Leica Microsystems (Cambridge, UK). Imaging media (IM-RPMI 1640 without phenol red) [11835] was purchased from Invitrogen (Paisley, UK).

2.1.7. *Reagents*

Alexa Fluor488 transferrin (Alexa488-TF) [T13342], Alexa Fluor488 Dextran (Alexa488-Dextran) (10 KDa) [D22910], tetramethylrhodamine-Dextran (TMR-Dextran) (70 KDa) [D1819], and BODIPY® (4,4-difluoro-4-bora-3a,4 adiaza-s-indacene)–LacCer (lactosylceramide) (BODIPY-LacCer) [B34402]

were purchased from Invitrogen (Paisley, U.K). FITC-Dextran (40 KDa) [FD40S] and epidermal growth factor (EGF) [E9644] from Sigma–Aldrich (Dorset, UK) and FITC-Anti-CD59 antibodies (clones A35 and YTH53.1) were kindly provided by Dr Rossen Donev, School of Medicine, Cardiff University.

2.1.8. *Pharmacological inhibitors*

Dynasore [D7693], chlorpromazine (CPZ) [C8138], cytochalasin D (CytD) [C8273], Blebbistatin (Blebb) [B0560] and 5-ethylisopropyl amiloride (EIPA) [A3085] were obtained from Sigma–Aldrich (Dorset, UK).

2.1.9. *Cell Transfection*

Oligofectamine [12252-011] and Opit-MEM [51985] were purchased from Invitrogen (Paisley, UK). All siRNA sequences were purchased as desalted and at scale of 0.05μmol from Eurofins MWG Operon (Ebesburg, Germany) except for those sent by the University of Ghent. Details on each siRNA sequence is given in the appropriate chapter.

2.1.10. *Cell lysis*

Complete mini protease inhibitor cocktail tablets [11836153001] were from Roche Diagnostics (Mannheim, Germany).

2.1.11. *Protein determination*

Bicinchoninic acid (BCA) [B9643], copper sulphate [C2284] and bovine serum albumin (BSA) [B4287] were from Sigma-Aldrich (Gillingham, UK).

2.1.12. *Sodium Dodecyl Sulphate-Polyacrylamide Gel Electrophoresis (SDS-PAGE) and Immunoblotting*

Bis-acrylamide (40%) [A7168], Tween® 20 [P7949], ammonium persulphate (APS) [A3678], Dithiothreitol (DTT) [D9163] and Ponceau S [P7767] were purchased from Sigma-Aldrich (Gillingham, UK). N, N, N, N-tetramethylethylenediamine (TEMED) [161-0800], Coomassie Brilliant blue G-250 [161-0406] and sodium dodecyl sulphate (SDS) [160-0301] were from BioRad laboratories (Hertfordshire, UK). [tris(hydroxymethyl) aminomethane] (Tris-base) [BPE152-1], [tris(hydroxymethyl) hydrochloric acid] (Tris-HCl) [BPE153-1], glycerol [G/0600/08] and acetic acid [A/0400/PB17] were purchased from Fisher Scientific laboratories (Leicestershire, UK). Full range rainbow molecular weight marker [RPN800E] and Enhanced Chemiluminescence (ECL) hyperfilm [28906836] were from GE Healthcare Life Sciences (Buckinghamshire, UK). Marvel dried milk powder was from Tesco. Nitrocellulose paper [BRP-100-540T] was purchased from Schleicher & Schuell (Dassel, Germany). Super Signal Wesr Dura ECL Immunoblotting analysis system [37071] was from Pierce (Northumberland, UK).

2.1.13. *Antibodies*

HRP goat-anti-mouse [32430] and HRP goat-anti-rabbit [32460] were purchased from PIERCE (Northumberland, UK). Anti-∝-tubulin [T6199], anti-ARF6 [A5230], and anti-GRAF-1 [SAB2500488] were from Sigma (Dorset, UK). Anti-clathrin heavy chain [610499], anti-dynamin-2 [610263] and anti-flotillin-1 were from BD Transduction (Oxoford, UK). Anti-Caveolin-1 [3238]

was from Cell signalling (Hertfordshire, UK) and anti-PAK-1 [sc-882] was from Santa Cruz (Heidelberg, Germany). Anti-EGFR [MS-378] was from Thermo scientific (Cheshire, UK), and Anti-GFP [MMS-118P] was purchased from Covance (New Jersey, USA). Species and dilution information on these is provided in Table 2.5.

2.1.14. *Cell viability assays*

3-(4,5-dimethylthiazol-2-yl)-2,5-diphenyl-2H-tetrazolium bromide (MTT) [M5655 was from Sigma-Aldrich (Gillingham, UK).

2.2. Equipment

2.2.1. *General Laboratory Equipment*

Varifuge 3.0 RS centrifuge was obtained from Heraeus Instruments (Germany). Eppendorf centrifuge 5417R was from Eppendorf (Hamburg, Germany). Weighing scale Precisa 180A was purchased from Sartorius (Hanover, Germany). Sunrise multiwell plate absorbance reader was from Tecan (Austria).

2.2.2. *Cell Culture*

A Neaubauer haemocytometer was purchased from Weber Scientific (Sussex, UK). Tissue culture flasks (25 cm^2 and 75 cm^2) with vented lids, cryogenic vials, sterile 5, 10 and 25 ml pipettes and 39 ml universal tubes were purchased from corning, Fisher Scientific Laboratories (Leicestershire, UK). BD Plastipak syringes were from Becton Dickinson (Madrid, Spain). Ministart® 0.2 μM filters were from sartorious (Hanover, Germany).

2.2.3. *Fluorescence Microscopy*

2.2.3.1. Confocal Microscopy

Confocal microscopy was performed on a Leica TCS SP5 AOBS confocal inverted microscope equipped with an Ultraviolet 350 nm (UV), 405 nm, Argon 488 and HeNe 543 and 633 lasers and 20x, 40x, and 63x oil objectives (Cambridge, UK). In some cases live cell imaging dishes were placed on a temperature stage equilibrated to 37°C. Images were acquired using the Leica LCS Lite software and finally processed using Photoshop.

2.2.3.2. Wide-field Microscopy

Wide-field fluorescent images were obtained on a Leica DMIRB inverted fluorescence microscope equipped with a 63× oil-immersion objective and QImaging Retiga 1300 camera. The acquired images were processed with Improvision Openlab 5.0.2 software. 35mm imaging dishes [P35G-1.5-10-C] were from MatTek (Ashland, USA).

2.2.4. *Flow Cytometry*

A FACSCalibur® flow cytometer was purchased from Becton Dickinson (Oxford, UK).

2.2.5. *Sodium Dodecyl Sulphate-Polyacrylamide Gel Electrophoresis (SDS-PAGE)*

Mini PROTEAN® II gel electrophoresis tank with its accessories and the Powerpac 300 were purchased from BioRad Laboratories (Hertfordshire, UK).

2.3. Methods

2.3.1. *Tissue Culture*

2.3.1.1.General

All tissue culture procedures were carried out in a class II laminar flow hood following decontamination of all sterilised consumables with 70% v/v Ethanol solution. All cells were maintained at 37^0 C with 5% CO_2 in a humidified incubator.

2.3.1.2.Maintenance

HeLa and A431 cells were grown in DMEM-GlutaMAX-I media containing 10% FBS and 100 U/ml penicillin and 100µg/ml streptomycin (Complete Media (CM)). Cell passaging was done routinely three times per week and the whole procedure was done in a laminar flow cabinet. First, the media was aspirated from the flask ($75cm^3$) then the cells were washed once with PBS. The PBS was removed and 1ml of 0.05% Trypsin-EDTA was added and the cells were incubated in humidified incubator for 4min or until they were detached. 9ml of CM were added and the whole suspension was transferred to universal tube for centrifuging fro 5 min at 1000 x g. The supernatant was aspirated and the cell pallet was re-suspended in 10ml of CM. After counting the cells the required volume of cells suspension was taken and added to media in a $75cm^2$flaskThe flask was maintained under tissue culture conditions and passage number 5-40 were used for all experiments.

2.3.1.3.Cell storing (freezing)

2.3.1.3.1. HeLa cells

Cell stocks were maintained in liquid nitrogen. Freezing media consisted of 90% FCS (v/v), which was filtered and warmed at 37^0 C, and 10% DMSO (v/v). Cells were counted and centrifuged at 1000 x g for 1 min, and then the supernatant was aspirated. The cells were resuspended in freezing media with seeding density 2 x 10^6 cells/ml. 1ml aliquots of cell suspension were transferred to cryogenic vials and placed in -20^0 C freezer for 1hr. later, the vials were placed at -80^0 C overnight before being placed in liquid nitrogen.

2.3.1.3.2. A431 cells

Cell stocks were maintained in liquid nitrogen. Freezing media consisted of 95% FCS (v/v), which was filtered and warmed at 37^0 C, and 5% DMSO (v/v). Cells were counted and centrifuged at 1000 x g for 1 min, and then the supernatant was aspirated. The cells were resuspended in freezing media with seeding density 2 x 10^6 cells/ml. 1ml aliquots of cell suspension were transferred to cryogenic vials and placed in -20^0 C freezer for 1hr. later, the vials were placed at -80^0 C overnight before being placed in liquid nitrogen.

2.3.1.4.Cell recovery from frozen stock

The frozen vials were thawed in a water bath at 37^0 C for 5 min and cells were transferred to a 30 ml sterile universal sterilin. 5 ml of CM was then added, before centrifugation for 5 min at 1000 x g. The supernatant was aspirated and the cell pallet was re-suspended in 5ml of CM, and transferred to a sterile 25 cm^2 flask. The cells were then incubated until confluent (~2 days HeLa, and ~3

days A431) with the culture media being changed every 2 days. Once a confluent monolyer had formed they were seeded into 75 cm^2 flasks as described in 2.3.1.2.

2.3.2. *Conjugation of Alexa488 C5 maleimide salt to peptides*

2.3.2.1.HPLC

The peptides used in this study (Table 2.2) were synthesised with an extending GC at the C-terminus to allow conjugation to Alexa Fluor® 488 C5 maleimide salt. Labelling was performed with an excess of the peptide, at peptide:label molar ratio of 1:1.2. Peptides and Alexa488 were dissolved in MeOH at a concentration of 1 mg/ml, mixed together in a sterile 1.5 ml eppendorf and the reaction was allowed to proceed in the absence of light at room temperature. The reaction was monitored by HPLC every hour by taking 10 µl of reaction mixture and loading it on to an analytical C18 column. The reaction then was left for 4 hrs, and then the product was purified using a C18 5µ 100 Å semi-preparative column and the gradient shown in table 2.1. Fractions were collected, freeze dried, checked for purity on the semi-preparative column, and then analysed by mass spectrometry.

2.3.2.2.Mass Spectrometry

1 µl of α cyano matrix was loaded onto each well to be used then left to dry completely at room temperature. 1 µl of peptide sample (immediately following HPLC or following freeze drying and ressupension) was placed on the dried cyano matrix before analyzing by MALDI-TOF MS (Matrix-assisted laser desorption/ionisation-time of flight mass spectrometry) with a vacuum set

at 2 $^{e-6}$. This was performed under supervision of either Dr Catherine Watkins or Rob Smart in the School of Chemistry.

2.3.2.3.Calculation of Alexa488-Peptide concentration

An aliquot of the sample was used to determine the concentration based on the molar extinction coefficient of Alexa488- 71,000. The solution was then finally freeze dried and resuspended to a stock concentration of 1mM in distilled water. These were aliquoted and stored at -80°C. The final masses of R8-Alexa488 was determined by Dr Catherine Watkins and are shown in Table 2.2.

Peptide-Alexa488	Gradient	Peptide-Alexa488 Retention time (min)
R8	T0; 5% B T5; 20% B T25; 40% B T30; 95% B	11.5
Tat	T0; 5% B T5; 20% B T25; 40% B T30; 95% B	10.2

Table 2.1. HPLC ACN gradient used in the purification of Alexa488-R8 &-Tat

Peptide	Origin	Sequence	Mass unlabelled	Mass Alexa488 labelled (Precised)	Mass Alexa488 labelled (calculated)
R8	American Peptide company	RRRRRRRRGC	1427.7	2126.4	2125.3
Tat	American Peptide company	GRKKRRQRRRPPQ GC	1880.0	2578.9	2577.6

Table 2.2. Peptides used in this thesis

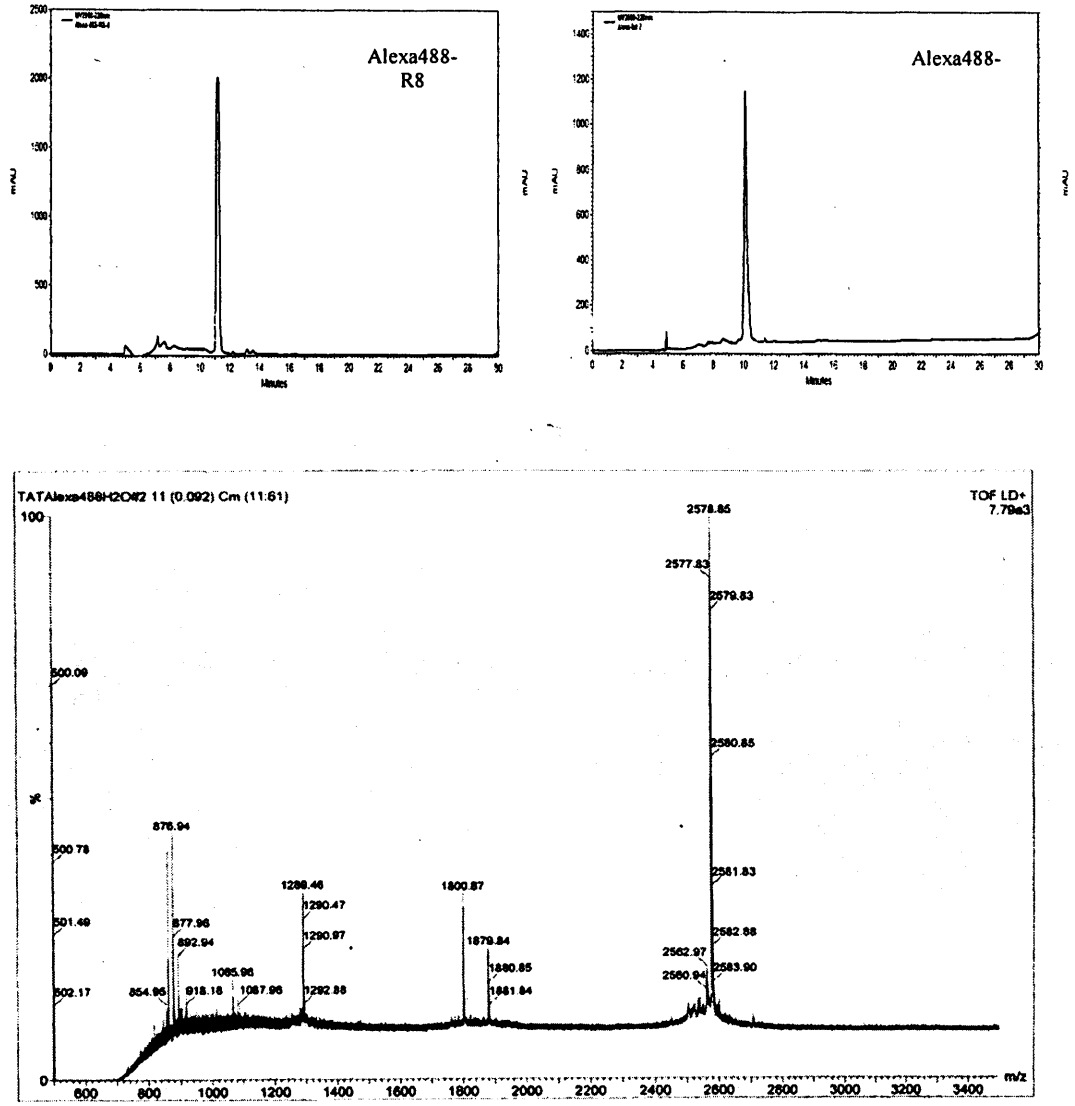

Figure 2.1. HPLC purity check for Alexa488-R8 and –Tat and Mass Spectrometry for Alexa488-Tat.

MALDI is know to cause some fragmentation including the breakage of the Alexa488-Cys linkage (I Nakase correspondence) resulting in these peaks that also correspond to different charged species (1289.46)

2.3.3. *Cells Transfection*

Transfection was curried out on HeLa and A431 cells in either 12 well or 6 well plates essentially as described the information provided with Oligofectamine. The cell confluency on the transfection day was 50-60% and different siRNA oligonucleotides were used based on the information given in Table 2.3. This describes the volumes required based on the relative surface area in proportion to the amount of oligonucleotide and oligofectamine that should be used.

The procedure was modified according to the above table depending on the plate type and the required oligonucleotide concentration. The following procedure was used for a final siRNA concentration of 50nM siRNA in a 6-well plate:

1μL of a 50μM stock oligonucleotide was diluted with 179μL of Opti-MEM I and mixed gently. In a separate tube 4μL of Oligofectaime was added to 16μl of Opti-MEM I and left at room temperature for 5-10 min. The two solutions were combined (total volume = 100 μL) and mixed gently, then incubated at room temperature for 15-20 min. From the 6 well plates, the growth medium (DMEM) was removed from the cells and they were washed once with Opti-MEM medium. 800μL of Opti-MEM medium was then added to each well prior to adding the Oligonucleotide/oligofectamine complex. The mixture on the cells was gently agitated and incubated with the cells under tissue culture conditions for 4 hours. Finally, 500μL of Opti-MEM containing 3X the normal concentration of serum was added **without** removing the transfection mixture and the cells were incubated for 48 hrs. The cells were then processed for further experiments as described later.

Oligo final Conc.	Culture Vessel	Relative Surf. Area vs.96-well	Oligo (µl of 50 µM stock) & dilution vol. (µl)	Oligofectamine (µl) & final dilution vol. (µl)	Plating medium vol.	Total vol. per well	Added vol. medium with 3X serum
50nM	6-well	25	1µl in 179µl	2-4 µl to 20µl	800 µl	1 ml	500 µl
50nM	12-well	10	0.5µl in 89.5µl	1-3µl to 10µl	400 µl	500 µl	250 µl
50nM	96-well	1	0.1 in 16µl	0.4-0.8µl to 3µl	80 µl	100 µl	50 µl

Table 2.3. Volumes of reagents used for preparing the transfection mixtures based on the surface area of the wells.

As many wells were treated for each experiments the volumes here were further scaled up as required. Oligo = Oligofectamine.

2.3.4. *Fluorescence Microscopy*

2.3.4.1.Transferrin internalisation in siRNA-transfected HeLa Cells

Cells growing on cover slips in 12-well plates were transfected with siRNA targeting CHC for 48hrs. On the day of experiment the growing media was removed and the cells were washed twice with serum free media (DMEM) containing 0.2% w/v BSA, pH7.3-7.4 (SFM/BSA) then incubated at 37^0 C in the incubator for 30 min in 2ml SFM/BSA. The cells were washed twice with PBS then 500 µl of 100nM Alexa-488 Tf (1/625 dilution in SFM/BSA) was added. The cells were incubated for 0, 4, 8, 16, or 32 min at 37^0 C. The media was then removed and the cells were incubated for 5 min in complete media. The plate was then placed on ice and the cells were washed three times for 1 min with ice cold PBS. The cells were fixed in 3% PFA (0.5ml) for 20 min at room temperature. After fixation, the cells were washed three times with PBS and incubated for 5 min in PBS/0.2% Triton-X followed by washing 2x with PBS. Finally, the cover slips were lifted and washed once in PBS followed by distilled water and then mounted on cover slides containing mounting oil.

2.3.4.2.Transferrin internalisation in dynasore treated HeLa Cells

Dynasore was stored as a 50mM stock solution in DMSO. Cells were grown on cover slips on 12-well plates until they were 80% confluent. The growing media was then removed and the cells were washed twice with PBS at room temperature and incubated at 37^0C and 5% CO_2 humidified incubator for 30 min in SFM/0.2%BSA containing 0 to 80µM Dynasore. Here and for all experiments with inhibitors a diluent control was used that is referred to as 0 µM or control. The medium was then removed and the cells were washed twice

with PBS at room temperature. 500 µl of 100nM Alexa-488 Tf in SFM/BSA is this right was then added in the continued presence of dynasore, and then the wells were incubated for 15 min at 37^0 C. The plate was then placed on ice and the cells were washed three times for 1 min with ice cold PBS. Prior to fixing as described above and processing for fluorescence microscopy.

2.3.4.3.PAK-1 immunolabelling in si-GFP vs. si-PAK-1 transfected A431 cells

Cells grown on cover slips in a 12-well plates were transfected with siRNA targeting PAK-1 or GFP as described in 2.3.3 and incubated for 48 hrs. The media was removed and the cells were washed 3x in PBS, then 3% PFA in PBS was added to each well left on the cells for 15 min prior to washing 3x with PBS. 50mM NH_4Cl/PBS was then added and left for 10 min, followed by 3x PBS washing. 0.2% w/v Triton X-100/PBS was then added and left for 10 min, followed by 3x PBS washing. The cells then were incubated with block solution (2% FBS, 2% BSA fraction V in PBS) for 30 min at room temperature. Then the blocking solution was removed and PAK-1 antibody in blocking buffer (1:50) was added and left for 30min, followed by 3x PBS/0.1% Triton washes and 1x PBS wash. Secondary Alexa488 chicken anti-rabbit in blocking buffer was then incubated with the cells (1:500) for 30 min. Finally, the cells were washed 3x PBS/0.1% Triton wash and 1x in PBS wash then processed for microscopy as described in 2.3.4.1.

2.3.4.4.Actin distribution in PAK-1 depleted A431 cells

Cells in 12-well plates were grown overnight on glass cover slips . They were transfected with siRNA against GFP or PAK-1 and incubated at 37^0 C and 5%

CO_2 for 48 hrs. Cells were then were washed 2x with PBS, followed by fixation with 3% PFA for 20 min at room temperature. Then cells were washed 3X with PBS and incubated for 5 min in PBS/0.2% Triton-X 100. Then they were washed 2X with PBS before incubation for 10 min with 2μg/ml rhodamine-phalloidin in PBS. The cells were washes 2X and then processed for fluorescence microscopy as described in 2.3.4.1.

2.3.4.5.Measuring the effect of Blebbistatin on actin distribution in EGF stimulated A431 cells

Cells in 12-well plates were grown overnight on glass cover slips. After 24 hrs they were washed 2x with PBS then were incubated in serum-free Ringer's buffer (155 mM NaCl, 5 mM KCl, 2 mM $CaCl_2$, 1 mM $MgCl_2$, 2 mM NaH_2PO_4, 10 mM HEPES, 10 mM glucose, and 0.5 mg/ml bovine serum albumin, pH 7.4) for 1hr prior to incubation with or without 100 μM Blebbistatin (Blebb) for 30 min at 37^0 C. The cells were then incubated in the presence or absence 50 nM EGF in absence or presence of Blebb. The cells were washed and then processed for labelling actin with rhodamine phalloidin as described in 2.3.4.4 and analysis by fluorescence microscopy.

2.3.4.6.Immunofluorescence of PAK-1 distribution after addition of cationic lipids, cationic polymers, EGF, and CPPs to A431 Cells

The complexes were formed first before starting the experiment. For Oligofectamine-siRNA complex, it was formed as mentioned in section 2.3.3 and also the same procedure was applied for lipofectamine/siRNA complex. Fugene-6/DNA complex was formed by diluting 3 μl of Fugene-6 [from

Roche, Mannheim, Germany] with 97 µl of DMEM media, followed by adding 1 µg of plasmid DNA, and then the solution was mixed and left for 30 min in room temperature before loading on to cells. PEI/DNA complex was formed by adding 2 µl of jetPEI™ transfection reagent (a linear polyethylenimine derivative from Polyplus transfections, Boulevard Sébastien Brant, France) to 1 µg of DNA plasmid and then the mixture was left for 15 min at room temperature before adding to cells. The cells in 12-well plates (1×10^5) were grown overnight on glass cover slips; for all experiments in 12-well dishes. After 24 hrs they were washed 2x with PBS prior to starvation for 1 hr in Ringer's buffer. The cells were then incubated with 50 nM EGF, oligofectamine-siRNA, lipofectamine-siRNA, Fugene-DNA or PEI-DNA (polyplexes) complexes or with 2µM unlabelled R8 or Tat for 10 min before washing with 2x with PBS and fixing with 3% PFA in PBS for 15 min. Then the cells were processed as mentioned in section 2.3.4.3 for immunodetection of PAK-1.

2.3.4.7.TMR-dextran internalisation in the presence of EGF and CPPs in A431 cells

A431 cells were seeded into glass-bottomed, 35 mm culture dishes and allowed to adhere for 24 h. The cells were then serum starved using Ringer's buffer for 1 hr before incubation for 1hr with 0.75 mg/ml TMR-dextran, 50 nM EGF, or 2µM of either unlabeled R8 or Tat. Then cells were washed 2x with ice cold PBS and 1x with ice cold acid wash (0.2M acetic acid, 0.2M NaCl, pH 2.0), followed by 3x PBS wash, then analyzed in imaging media (RPMI 1640 without phenol red) via confocal microscopy on the 37°C temperature stage.

2.3.4.8.Dextran internalisation in cytochalasin D pre-treated cells

A431 cells were seeded into glass-bottomed, 35 mm culture dishes and allowed to adhere for 24 h. The cells were washed 2x with PBS before incubating with 10 μM CytD in SFM/0.2%BSA for 15 min then incubated with SFM containing 5 mg/ml FITC-Dextran at 37 °C for 1 hr. The cells were washed with ice cold acid wash buffer followed by 3x PBS washes and then analysed in imaging media via confocal microscopy on the 37°C temperature stage.

2.3.4.9.Internalisation of Alexa488-CPPs in HeLa cells

HeLa cells were seeded into glass-bottomed, 35 mm culture dishes and allowed to adhere for 24 h. The cells were washed 2x with PBS before incubating with 2 μM Alexa488-R8 or Tat in SFM/0.2%BSA for 1 hr. The cells were then either directly imaged by confocal microscopy in the presence of the peptides or , washed 3x in PBS and analysed in imaging media via confocal microscopy on the 37°C temperature stage.

2.3.5. *Flow Cytometry*

In all flow cytometry experiments 10,000 gated cells were measured and all the data shown are an average of at least three independent experiments.

2.3.5.1.Measuring the effect of acid wash and temperature on Alexa488-Transferrin internalisation in HeLa cells

Cells were plated for 24 hrs on to 12-well plates and incubated at 4°C or 37°C with 100nM Alex488-Tf for 0-32 in as described section 2.3.4.1. The cells were then either washed 3x with ice cold PBS and then washed in either PBS

or acid wash solution for 1 min. The cells were then washed 3x with PBS prior to addition of 300µl trypsin/EDTA and incubation at room temperature for 2-3 min. The detached cells were then placed in a 1.5ml eppendorf tube containing 300µl ice cold PBS and centrifuged at 1500x g for 3 min. The pellet was then resuspended in 500µl PBS and the cells were centrifuge-washed again prior to resuspending the final pellet in 200µl of ice cold PBS. The cell suspension was then analysed by flow cytometry.

2.3.5.2.Internalisation of Alexa-488-Tf, FITC/Alexa488/TMR-Dextran, FITC - anti-CD59 antibody, and BODIPY-LacCer

Cells were plated for 24 hrs on to 12-well plates and transfected as described using siRNA sequences targeting CHC, DNM2, Flot-1, Cav-1, PAK-1 or GFP (control). After 48 or 72 hrs (only for DNM2), the cells were washed 2x with PBS at room temperature and then incubated for 30 min at 37^0 C in SFM containing 0.2% w/v BSA. The cells were then washed 2x with PBS at room temperature and incubated for various periods of time with SFM/BSA containing either 100 nM Alexa-488 Tf, 2µg/ml anti-CD59 antibody FITC-Dextran (40 KDa, 5.0mg/ml), Alexa488-Dextran (10KDa, 0.2 mg/ml) or TMR-Dextran (70KDa, 0.75 mg/ml). The plates were then placed on ice and washed 2x with ice cold PBS followed by a 1 min incubation in ice cold acid wash. The cells then were washed 3x with PBS at room temperature, prior to trypsinisation and processing fro flow cytometry as described.

For BODIPY-LacCer uptake cells were washed 2x with PBS at room temperature then incubated with 1 μM BODIPY-LacCer at 10°C for 30 min to load the plasma membrane with the lipid analog (Singh et al. 2003). The cells were then washed 3x times with SFM at 10°C, followed by incubation at 37° C for 15 min to allow endocytosis. Two methods were then used to remove the surface label. (1) Trypan Blue Method: the cells were rinsed 2x with ice-cold PBS and trypsinised at room temperature, followed by adding 0.33 mM trypan blue for 30 min to quench the extracellular fluorescence of BODIPY-LacCer. The cell suspension was washed with ice cold PBS, before measuring cell associated fluorescence by flow cytometry (2) Back exchange method. Following the endocytic step the cells were washed (6x 10 min) in PBS containing 5% fatty acid-free BSA at 4^0 C.

2.3.5.3.Cellular internalisation of Alexa488-CPPs in HeLa and A431 cells

Cells in 12 well plates cultured and transfected with the various siRNA sequences as described in Section 2.3.5.2. After 48 (72 hrs for siRNA-DNM2) of transfection, the cells were washed 2x with PBS at room temperature and then incubated for 30 min at 37^0 C in SFM containing 0.2% w/v BSA; this step was performed to keep consistency with the methods described above. The cells were then washed 2x with PBS at room temperature and incubated for various periods of time with SFM/BSA containing 2μM Alexa-488-R8 or Alexa-488-TAT for 0-80 min at 37^0 C. Cells were then placed on ice to stop endocytosis and washed 2x with ice cold PBS, 1x with PBS at room temperature, trypsinised as above and finally washed 2x with 14 μg/ml ice cold

heparin. The cell suspension was washed 2x with ice cold PBS and the internalised peptide was quantified by flow cytometry as previously described. In experiments investigating the effect of temperature on uptake of CPPs, the same procedure was carried out with non-transfected cells. The experiment was carried out 24 hrs after cells seeding and the uptake experiments were performed at 4^0 C and 37^0 C in parallel.

2.3.5.4.Endocytosis inhibitor studies

Cells were grown for 24 hrs on 12-well dishes. On the day of the experiment they were washed 2x with PBS at room temperature then preincubated with 10μM Cytochalasin D (CytD) for 15 min, 10μg/ml chlorpromazine (CPZ), 80μM dynasore, 100μM 5-ethylisopropyl amiloride (EIPA) or 100μM blebbestatin for 30 min at 37°C. The media was removed and fresh SFM/BSA media containing endocytic probe or Alexa488-CPP peptide as well as corresponding inhibitor was added and the cells were incubated for various periods of time (0-80 min). The cells were then processed as above for analysis of cell-associated fluorescence of either endocytic probe or Alexa488-CPP. For all inhibitor studies control cells were incubated with an equivalent volume of inhibitor diluent (DMSO or PBS).

2.3.5.5.EGF stimulation of macropinocytosis in A431 cells

Cells were grown for 24 hrs on 12-well dishes, washed 2x with PBS at room temperature and incubated in serum-free Ringer's buffer for 1hr. Then cells were incubated with Ringer's buffer containing 5mg/ml FITC-dextran or 0.75mg/ml TMR-dextran +/- 50nM EGF. The plates were then placed on ice

and washed 2x with ice cold PBS followed by a 1 min incubation in ice cold acid wash buffer. The cells were then washed 3x in PBS and processed for flow cytometry as described. In experiments employing blebbistatin the cells were pretreated with the drug 30 min before EGF stimulation and blebbistatin was present throughout the experiment. The effect of serum starvation was tested and in those experiment the cells are either serum starved, as mentioned above, or not, before measuring the effect of EGF stimulation on CPP and Dextran uptake.

2.3.5.6.Co-incubating CPPs with different molecular weight dextrans

Cells were grown for 24 hrs on 12-well dishes, washed 2x with PBS at room temperature and then incubated for 30 min at 37^0 C in SFM containing 0.2% w/v BSA. The cells were then washed 2x with PBS at room temperature and incubated for various periods of time with SFM/BSA containing either 5.0 mg/ml FITC-Dextran or 0.75 mg/ml TMR-Dextran +/- 2 μM unlabbeled R8 or Tat. The plates were then placed on ice to inhibit further uptake and washed 2x with ice cold PBS followed by a 1 min incubation in ice cold acid wash buffer. The cells then were washed 3x with PBS at room temperature, prior to trypsinisation and analysis by flow cytometry.

2.3.6. Bicinchonic Protein Assay (BCA)

This assay is used to measure the protein concentration in the cell lysates. The protein assay solution was prepared containing 49 parts BCA and 1 part Copper Sulphate. A calibration curve of BSA in lysis buffer (50 mM Tris-HCl, 150 mM NaCl, pH 8.0, 1% Triton X-100), was prepared by adding 20μl

volumes of different concentrations to the wells in addition to 20µl of the cell lysates. 250µl of protein assay solution then was added to each well that was incubated at 37 ^{0} C for 20min. the absorbance at 550nm was determined and the cell lysate concentration was extrapolated from the BSA calibration curve.

2.3.7. Sodium Dodecyl Sulphate-Polyacrylamide Gel (SDS-PAGE) Electrophoresis

Cells in 6-well plates were transfected with various siRNA sequences as described. 48 hours after transfection, the cells were washed three times in ice cold PBS prior adding 300 µl of ice-cold lysis buffer containing protease inhibitor cocktail. The plates then were placed on ice and then on a laboratory shaker for 5 min. The lysates were then transferred to eppendorf tubes and centrifuged at 13,000g for 10 min at 4^{0} C. The supernatant was collected and protein concentration determined. Aliquots corresponding to 20-50µg of protein was then added to 4x SDS sample buffer (40% Glycerol, 240 mM Tris/HCl pH 6.8, 8% SDS, 0.04% bromophenol blue, 5% beta-mercaptoethanol) containing dithiothreitol at a final concentration of 10mM and then either immediately processed for electrophoresis or stored at -20°C.

Stock Solution	10% separating gel TRIS 3M pH 8.8	11% separating gel TRIS 3M pH 8.8	4% stacking gel TRIS 1M pH 6.8
40% acry/Bis	5.0 ml	5.5 ml	1.0ml
Tris	2.5ml	2.5ml	1.3ml
10% SDS	0.2ml	0.2ml	0.1ml
dH_2O	12..3ml	11.8.ml	7.6ml
Temed	15µl	15µl	10µl
APS 10%	150µl	150µl	75µl
	20ml	20ml	10ml

Table.2.4. Solutions used for preparing running and stacking gels for SDS PAGE.

Depending on the percentage of the gel the solutions in table 2.4 were then used to prepare a running gel and stacking gel in the gel holders.

All protein samples were heated at 95^0 C for 5min, centrifuged at 1000 x g for 30 s and then loaded on to the gels; 10µl of multi colour molecular weight marker was loaded in the first well lane. The gel was run at 110 V until the dye-front reached the end of the gel. The gel was then removed from the cassette and immersed in PBS then incubated for 5-10 min in ice cold transfer buffer (150 mM Glycine, 20 mM Tris-base, MeOH (20% final), and completed to 2 L with dH_2O).

2.3.8. Western Blotting

Two pieces of sponge pads, filter papers, and one piece of nitrocellulose (NC) paper were cut to the size of the gel and pre-soaked in the transfer buffer. The pre-soaked sponge placed on the cassette, followed by filter paper, then the gel, NC paper and the surface was rolled to take out air bubbles. Another filter paper was layered on the NC paper followed by sponge pad then the cassette was closed carefully. For efficient transfer, an ice unit was placed in the tank to cool down the transfer system and a stirrer was placed in the tank to ensure uniform temperature during the transfer process. Transfer was for 90 min at 100 V thereafter the NC paper was removed and washed with dH_2O. Ponceau S solution was added to the NC paper for 1 min to ensure that effective transferred had occurred and this also allowed for cutting the paper for immunolabelling with different antibodies. The Ponceau S was then removed via successive washes with PBS and the paper was then stored in PBS.

2.3.8.1. Detection of Transferred Proteins after Western blotting

For immunolabelling the NC paper was soaked in a block solution 5% w/v milk powder dissolved in TBS (50 mM Tris-base pH 7.5, 150mM NaCl, 0.01% Tween made to 1 L with dH_2O) for 45 min to block non-specific protein binding sites. The paper was then washed with PBS and primary antibody solution in block solution was added and the container was placed on the laboratory shaker for gentle agitation for 1 hr. The dilutions of the antibodies used are shown in Table 2.5.

Following the primary antibody incubation, the paper was washed once in PBS/0.05% Tween for 5 min prior washing twice in PBS for 5min, then incubated for 1 hour in HRP goat anti-mouse/anti-rabbit secondary antibody solution [dilution 1:5000 in 5% milk/TBS]. The NC Paper was washed again, one in PBS 0.05% Tween for 5 min and twice in PBS for 5 min before developing. Initially, 1 ml of each of the ECL reagents were mixed and added to the NC paper and left for 1 min. The paper was gently shaken to remove any excess reagents, and placed inside the developer cassette, covered by cling film, and transferred to a dark room. The cassette was opened and the chemiluminescence film paper placed over the cling film. The cassette was then closed for the required exposure time and after the film was placed in the developer.

Primary antibody	Type	Dilution 5% Milk/PBS
Anti-∝-Tubulin	Mouse	1:1000
Anti-clathrin heavy chain	Mouse	1:500
Anti-DNM2	Mouse	1:250
Anti-Flot-1	Mouse	1:500
Anti-Cav-1	Rabbit	1:1000
Anti-PAK-1	Rabbit	1:200
Anti-GFP	Mouse	1:2000
Anti-EGFR	Mouse	1:500
Anti-Arf6	Mouse	1:1000
Anti-GRAF-1	Goat	1:500

Table 2.5. Antibodies and dilutions used for Immunolabelling NC papers

2.3.9 MTT Assay to determine cell viability

HeLa cells were seeded into 96 well plates at 8 x 10^3 cells/well 24 hrs prior to the experiment. On the day of the experiment the media was removed and cells were transfected as mentioned in section 2.3.3. 48 hrs after the transfection, an aliquot (20 µL) of a sterile, filtered solution of MTT in PBS (5mg/ml) was added to each well and the plate was then incubated for 5 h at 37 °C, 5 % CO_2. The media and MTT solution were aspirated and an aliquot (100 µL) of DMSO was added to each well to dissolve the resulted purple formazan crystals. After the plate had been incubated for 30 min at 37 °C, 5 % CO_2 the UV absorbance was measured at 550 nm (Sunrise, Tecan). Cell growth as % was determined relative to the control cells.

Reduction of yellow MTT to the purple formazan crystals is irreversible and is catalysed by enzymes located within the mitochondria and thus measures cell viability.

$$Cell Viability(\%) = \frac{\lambda_{550nm} treated cells}{\lambda_{550nm} untreated cells} x100$$

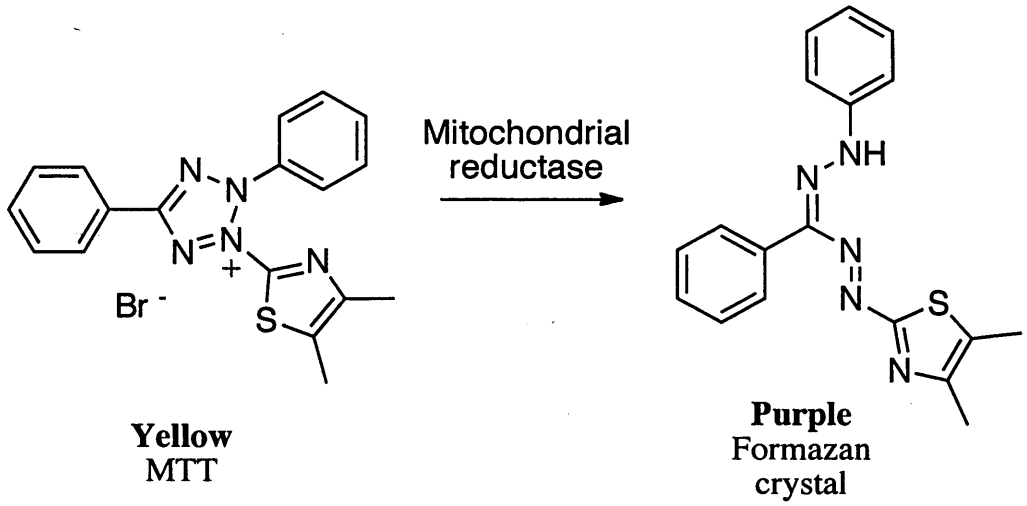

Figure 2.2 The reduction of MTT.

Chapter 3: Revaluation of the role of Clathrin Mediated Endocytosis in cellular uptake of CPPs Tat and R8

3.1. Introduction

Widespread studies on the internalisation mechanism of cell penetrating peptides have been performed with non-amphipathic peptides Tat (48–60) and oligoarginines, mostly as fluorescent conjugates. The uptake of pTat as well as pTat-PNA conjugates were reported to take place via an energy-dependent clathrin-mediated endocytosis (CME) (Richard et al. 2003). An alternative mechanism not involving endocytosis was proposed for polyarginine peptides that also suggested internalisation of when experiments were performed on ice (Kosuge et al. 2008; Maiolo et al. 2005; Zaro and Shen 2005). Three different studies show that at low concentrations (2 μM) polyarginine peptides were shown to be trapped in endosomal vesicles clearly indicating the involvement of an endocytosis process (Duchardt et al. 2007; Fretz et al. 2007; Potocky et al. 2003). At concentrations greater than 5μM there is strong evidence to show that these peptides can enter cells directly across the plasma membrane and this was especially noted in leukaemia cells (Watkins et al. 2009b).

In order to study CME, or any other endocytic pathway, and its involvement in CPP uptake, it is necessary to have knowledge of proteins that distinctly regulate the pathway such that they can then be modified (mutated) or depleted to generate a cellular model that is deficient in only this pathway. CME is by far the most well-characterized endocytotic pathway and is known to be regulated by many different proteins and lipids. This process initiates via the formation of well structured ligand-receptor complexes on the plasma membrane using clathrin assembly proteins such as adaptors working in conjunction with clathrin heavy and light chain. Consequently, these coated pits invaginate and pinch off from the plasma membrane to form intracellular

clathrin coated vesicles (Khalil et al. 2006). Within two minutes the vesicles loses its clathrin coat and the stripped vesicle then fuses with an early or sorting endosome. Fluorescent labelled HIV-Tat peptide, has been reported to colocalize with transferrin, which is considered as a classical CME marker (Potocky et al. 2003; Richard et al. 2003). Another study demonstrated that Tat uptake is inhibited by 50 % in chlopromazine treated HeLa cells(Richard et al. 2005). This drug is a well characterised CME inhibitor, and to support these findings incubation in potassium-free buffer, another inhibitor of CME, resulted in a 40% decrease in peptide uptake. Other studies, however, with fluorescently labeled polyarginine revealed very little colocalization with transferrin (Jones et al. 2005; Nakase et al. 2004) suggesting only a minor role for CME and the involvement of other pathways. Thus the actual involvement of CME remains to be fully determined.

In this chapter the role of CME was investigated using two approaches: The use of classical pharmacological inhibitors and the use of siRNA depletion of the CME regulator clathrin heavy chain (CHC). Transferrin is known to be a well-characterised probe for this pathway thus published methods and Alexa probes were available. The goal here was to develop the siRNA methods in the laboratory using this identifiable probe and then test the models for uptake of CPP Tat and R8 that formed our CPP models. The uptake of the fluid phase marker dextran was assessed using the same approach.

3.2. Methods

HeLa cells were used as a model cell-line to study CME pathway in this chapter. Different concentrations of Alexa-488 Tf were tested, 2 nM, 20 nM, and 100 nM and the requirement of energy/temperature on Tf uptake was analysed by carrying out the incubation at both 4 and 37^0 C as described in section 2.3.5.1. In addition, the effect of acid washing to remove the plasma membrane binding was also examined.

HeLa cells were transfected using different siRNA sequences as described in chapter 2.3.3. Alexa-488 Tf uptake was investigated in siRNA-Lamin A/C (+ve control) and CHC depleted cells. To optimize the transfection procedure, different siRNA concentrations and different incubation periods were tested. Cell associated fluorescence was measured by flow cytometry and by confocal microscopy as described in sections 2.3.4 and 2.3.5.

To study the role of CME in dextran internalisation, two different dextran conjugates, Alexa488-Dextran (10 kDa) and FITC-Dextran (40 kDa), were used. To characterize the involvement of CME pathway in Alexa-488 R8 and Tat uptake, 2 μM of CPPs was added to either CHC depleted HeLa cells or after pre-incubation with chlorpromazine (CME inhibitor) for different incubation period 0-80 prior to analysis by flow cytometry. For these peptide experiments an additional wash in Heparin was included to further remove surface bound peptide.

Finally, SDS-PAGE electrophoresis and Western blotting techniques were used to measure CHC depletion as described in sections 2.3.7 and 2.3.8

siRNA	Sequences	Ref.
Lamin A/C	CUGGACUUCCAGAAGAACAdTdT	(Schmid et al. 2007)
GFP	GGCUACGUCCAGGAGCGCAdTdT	Designed by MWG
CHC	UAAUCCAAUUCGAAGACCAAUdTdT	(Motley et al. 2003)

Table 3.1. siRNA sequences used as control or for targeting CHC.

3.3. Results

3.3.1. Effect of temperature and acid washing on Alexa488-Tf uptake

Alexa-488 Tf was used as a classic marker for CME and its cellular uptake was evaluated at two different temperatures 37^0 C and at 4^0 C (Figure 3.1.A). Alexa488-Tf internalisation was completely inhibited at 4^0 C, which confirms that CME is an energy dependant process. Here and in most experiments uptake was measured at different time points rather than at a single time point as is most often the case.

To investigate whether some of the cell associated fluorescence was probe on the plasma membrane further experiments were performed employing an acid wash step as described in chapter 2. The flow cytometry results show a significant reduction in Alexa488-Tf cell associated florescence in acid washed cells compared with non-acid washed (Figure 3.1.B) cells. Therefore, acid wash was applied as an essential step to exclude the fraction that was localised to the plasma membrane thus giving a more accurate value for the fraction that was intracellular.

3.3.2. Effect of depleting clathrin heavy chain (CHC) expression on Alexa488-Tf uptake

Initially, the siRNA concentration was optimized and evaluated to ensure that the general procedure was non-toxic to the cells prior to assessing the effectiveness of transfection. Many reasearchers use siRNA at concentration <100 nM and in this chapter different siRNA concentrations were tested 10 nm, 50 nM, 100 nM, and 250 nM (Figure 3.2.A). Using a single time point assay we observed a similar reduction in transferrin uptake at all siRNA

concentrations studied and marginally the highest reduction was observed at 50 nM. For siRNA controls in each experiment, we used either siRNA targeting Lamin A/C protein, which is required to form the nuclear lamina and has no role in CME or siRNA targeting green fluorescent protein (GFP) that is not normally expressed in these cells. Cells transfected with siRNA targeting Lamin had much higher Tf levels compared with cells targeted with siRNA against CHC (Figure 3.2.B) and fluorescence values in these siRNA Lamin cells were the same as non-transfected cells showing that the transfection procedure had no effect on transferrin uptake.

SDS-PAGE electrophoresis was then used as stated previously to detect the effectiveness of the siRNA method in depleting CHC. Figure 3.3 shows that there was effective though not complete depletion of clathrin in these cells (Figure 3.3A) but repeated experiments showed a consistent reduction of over 85%.

Following the development of these transfection protocols time course studies of Tf uptake was performed. Cells, 48 hrs after transfection, we incubated with 100nM Alexa-488-Tf for different incubation periods 0-32 min and processed as mentioned previously for flow cytometry studies. From the earliest time point there was a reduction in Tf uptake in siRNA CHC cells. This continued throughout the experiment though the percentage inhibition gradually decreased with increasing incubation time. (Figure 3.4.A).

In order to observe these findings using a different method, cells following transfection with siRNA targeting CHC or Lamin were plated on coverslips and incubated for different periods of time with Alexa488-Tf. The cells were

then washed in PBS and acid wash buffer prior to analysis by confocal microscopy. Data in (Figure 3.4.B) shows a reduction in cell associated fluorescence in siRNA CHC cells at all time points. In agreement with flow cytometry studies, there was some uptake of Tf in CHC targeted cells rather than a complete inhibition.

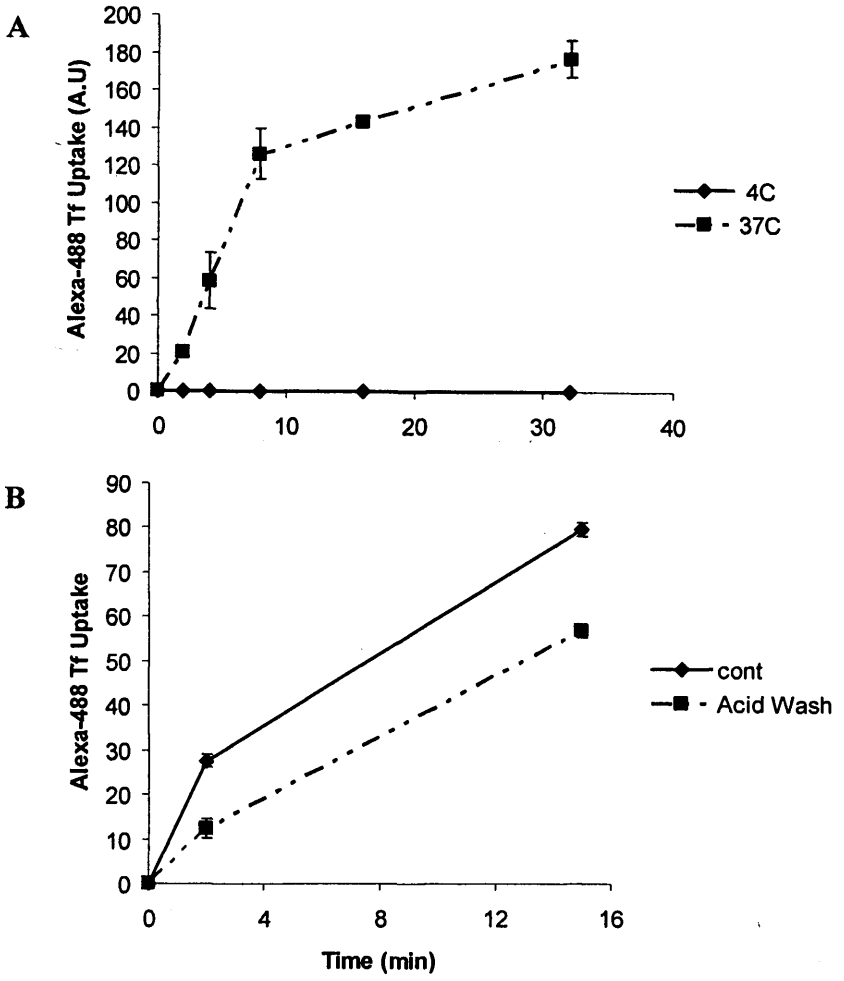

Figure 3.1. Effect of temperature and acid washing on cellular uptake of Alexa488-Tf.

(A) HeLa cells were incubated with 100 nM Alexa488-Tf at 37^0 C and at 4^0 C for 0-32 min prior to washing and analysis by flow cytometry (n=3). (B) Following Tf incubation, HeLa cells were either washed in PBS or acid wash buffer prior to trypsinisation and flow cytometry analysis (n=3).

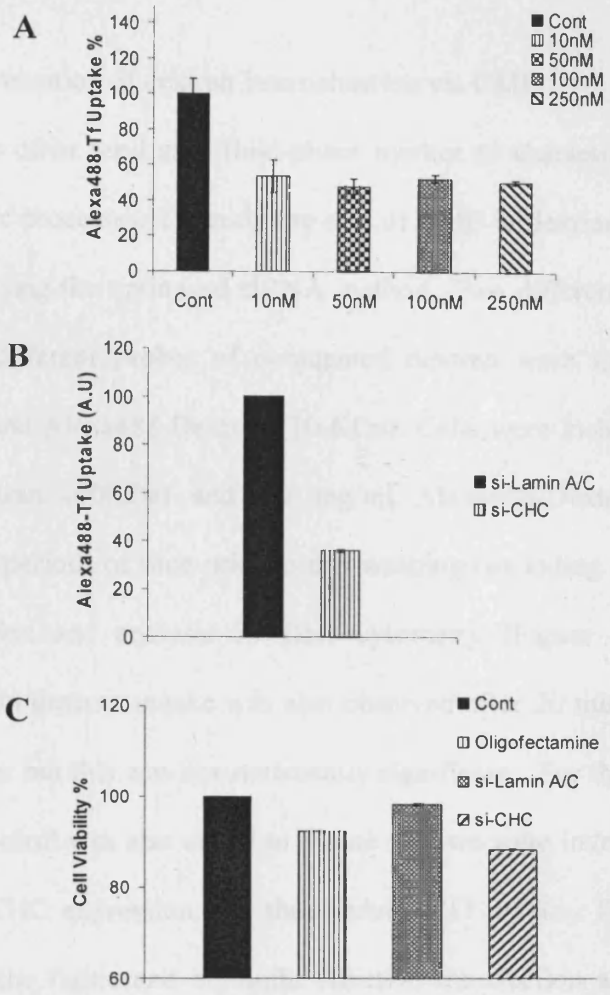

Figure 3.2. Effect of using siRNA transfections on cell viability and Alexa488-Tf uptake.

HeLa cells were transfected using different siRNA (CHC) concentrations for 48hr then incubated with 100 nM Alexa488-Tf at 37^0 C for 15 min prior to washing and analysis by flow cytometry (n=3). (B) Cells were transfected with 50nM si-Lamin A/C and si-CHC for 48hr then incubated with 100 nM Alexa488-Tf for 15 min prior to processing and analysis by flow cytometry (n=2). (C) MTT cell viability assays were performed on untreated cells, cells incubated with oligofectamine alone or cells transfected with siRNAs against CHC, Lamin. The assays were performed 48 hrs after transfection. The data representative of two independent experiments performed in triplicate.

3.3.3. Evaluation of dextran internalisation via CME

Dextran is often used as a fluid-phase marker to characterize endocytic and transcytotic processes. To study the role of CME in dextran uptake, CHC was depleted using the optimised siRNA method. Two different molecular weight and two different probes of conjugated dextran were used, FITC-Dextran (40KDa) and Alexa488-Dextran (10 KDa). Cells were incubated with 5mg/ml FITC-Dextran (40KDa) and 0.2 mg/ml Alexa488-Dextran (10 KDa) for increasing periods of time prior to cell washing (including acid wash) prior to trypsinisation and analysis by flow cytometry (Figure 3.5). A consistent inhibition in dextran uptake was also observed after 20 min of uptake and for both probes but this was not statistically significant. For these experiments an internal control was also added to ensure that we were investigating cells with depleted CHC expression and thus reduced Tf uptake. These are shown as inserts in the figure and highlight effective transfection and an effect on Tf uptake. This gave us confidence that the transfection was successful and this "Internal siRNA control" was included from here on in in most experiments.

3.3.4. Characterize the requirement of CME in Alexa488-R8 and -Tat uptake

Previous studies have suggested that CME route may be utilized by CPPs to cross plasma membrane. Thus, the uptake of both Alexa488-R_L8 and -Tat were investigated further using two methods: siRNA depletion and pharmacological inhibition. As CPPs have been shown to be internalised by both a temperature independent (translocation) and dependent method it was important to show that uptake was energy dependent and therefore most probably due to endocytosis. At 2μM extracellular peptide concentration in HeLa cells these

CPPs labels endocytic vesicles and no cytosolic labelling can be seen (Watkins et al. 2009b) This concentration also allows a sufficient signal to noise ratio for us to be able to monitor uptake by flow cytometry. The requirement for energy was therefore determined at this concentration. Hela cells were incubated for 15 min at either 37°C or 4°C prior to adding Alexa488-R8 or -Tat for various periods of time prior to washing trypsinisation and analysis by flow cytometry (Figure 3.6). The data shows that for all time points only approximately 15% of peptide associates with the cells when incubated at 4°C. Thus under these conditions only a very small fraction of the peptide enters cells in an energy independent manner.

Intially, Alexa488-R8 and -Tat were incubated in control HeLa cells for 1 hr, then washed (Figure 3.7.A) or unwashed (Figure 3.7.B) with PBS and imaging media before being processed immediately for life-cell imaging with confocal microscopy. The result in Figure 3.7 shows a clear internalisation of both Alexa488-R8 and -Tat and very well distributed inside the cells in a vesicular manner.

Alexa488-R8 and -Tat were then incubated in with siRNA CHC cells or those transfected with control (GFP/Lamin) siRNA. Under these conditions the internal siRNA control showed effective inhibition of transferrin uptake but there was no effect on internalisation of either CPP (Figure 3.8). Chlopromazine (CPZ) was then used as a CME inhibitor to further investigate CME in CPPs uptake. Cells were pre-equilibrated with the drug for 30 min and then incubated with either CPPs or Alexa488-Tf in the continued presence of the drug. High inhibition was shown for transferrin uptake, but again there was no evidence of a reduction in CPP uptake between 0 and 80 mins (Figure 3.9).

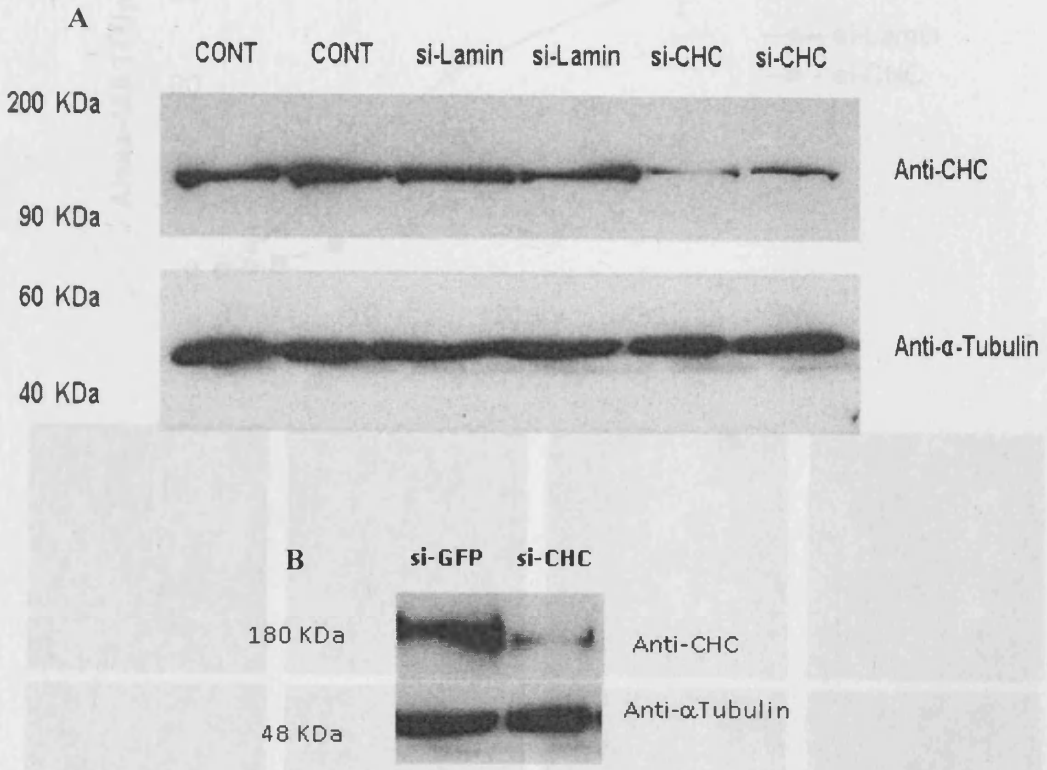

Figure 3.3. Analysis of CHC expression and depletion following siRNA-CHC targeting.

Following transfection of cells with different siRNAs, lysates were prepared and 20 or 25 µg protein were loaded on to 10 % SDS-PAGE gels, transferred to nitrocellulose papers, probed with antibodies against CHC, Lamin, GFP or α-tubulin that were then detected with HRP conjugated secondary antibodies. Control lanes are corresponding to non-transfected cells, while si-Lamin and si-GFP lanes are representing positive control. In (**A**) duplicate loading has been performed to assess reproducibility and in (**B**).

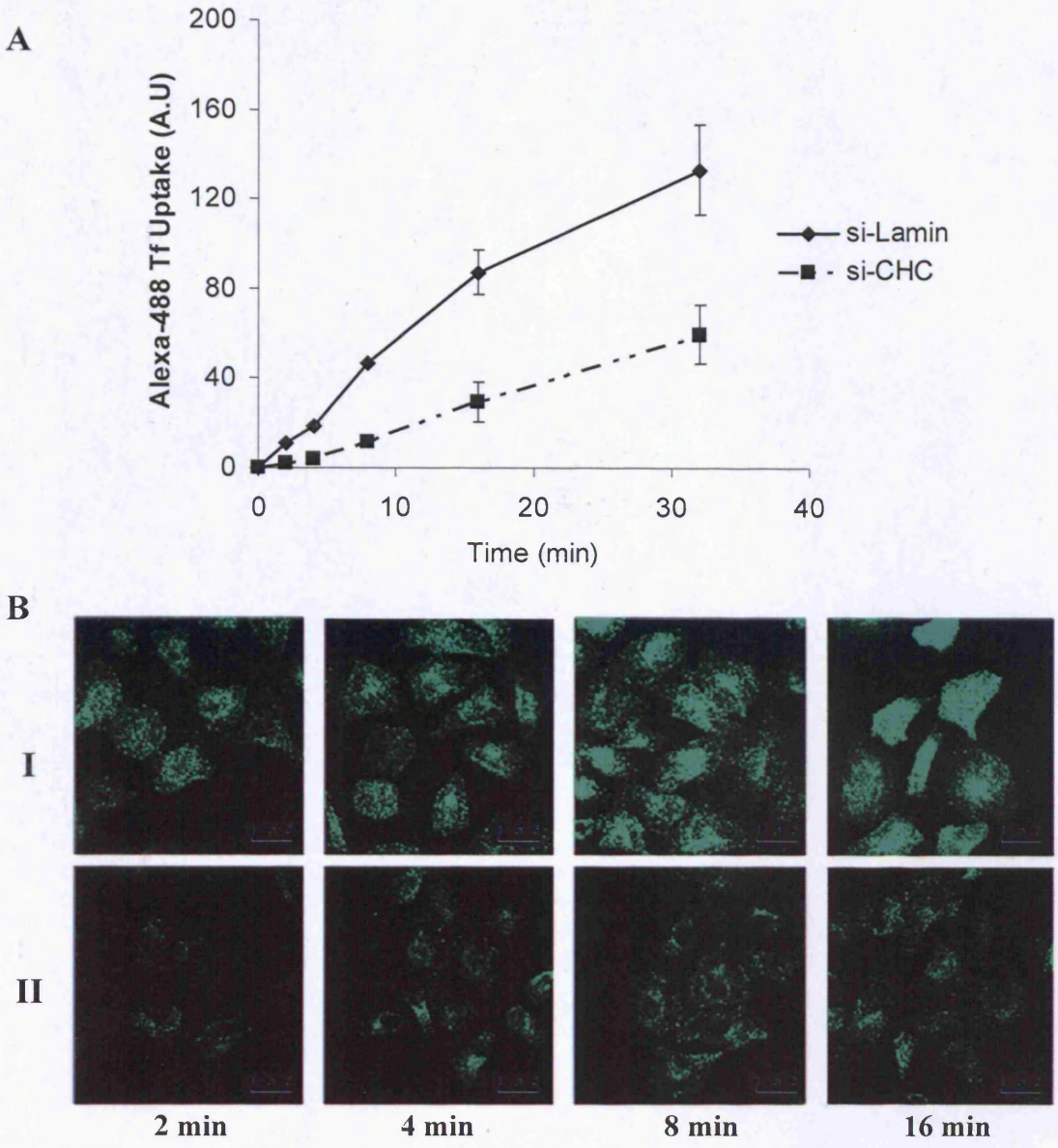

Figure 3.4. Uptake of Alexa488-Tf in si-Lamin A/C vs. si-CHC transfected HeLa cells.

HeLa cells were transfected with si-Lamin A/C **(I)** or with si-CHC **(II)** for 48hr, then incubated for the indicated time points with 100 nM Alexa488-Tf at 37^0 C before washing and analysis by either Flow cytometry (A) or confocal microscopy (B). Flow cytometry data represents cell associated fluorescence for three independent experiments (n=3). Confocal images represent maximum projection images. Scale bars = 25μm.

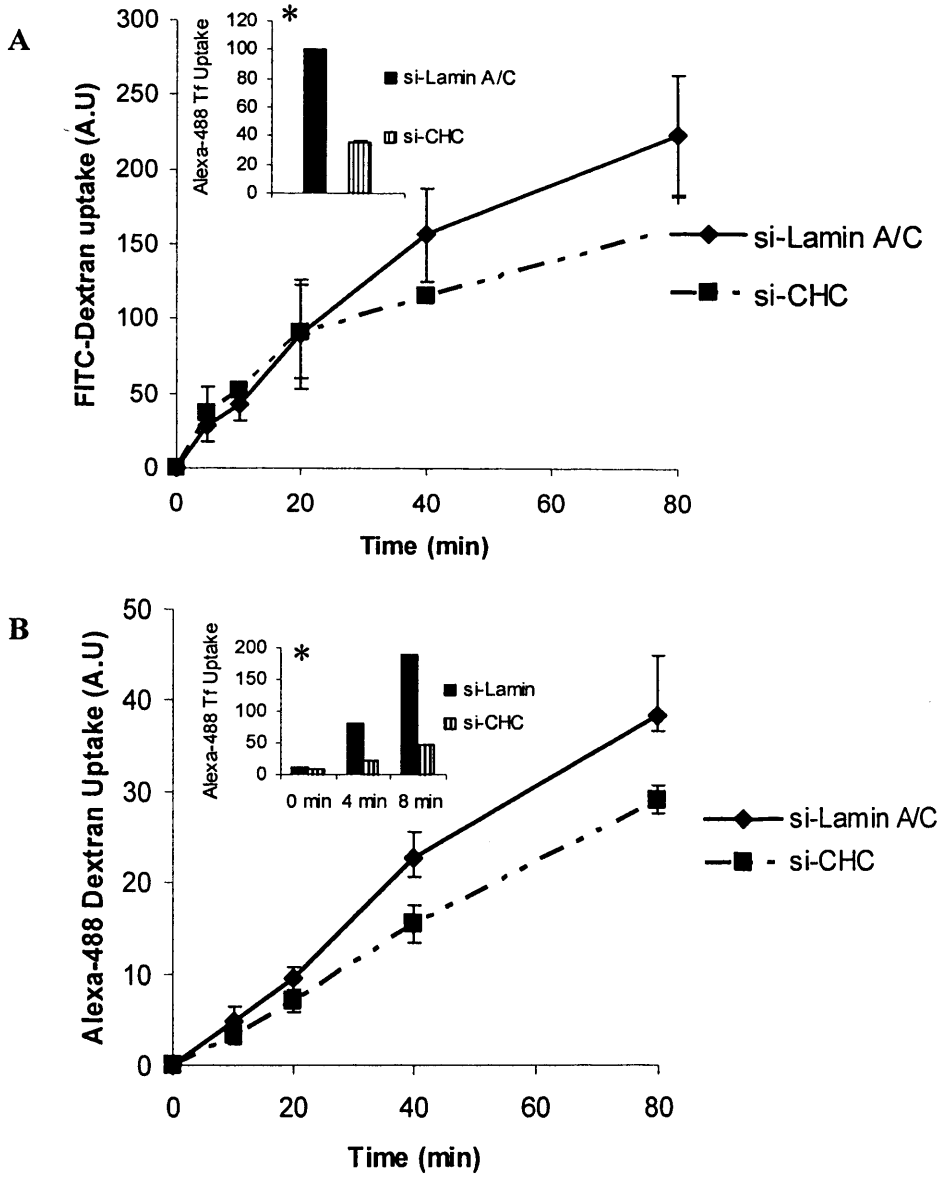

Figure 3.5. Evaluation of Dextran Internalisation via CME.

HeLa cells were transfected with si-Lamin A/C or si-CHC for 48hr, then incubated for the indicated time points with either 5mg/ml FITC-dextra **(A)** or 0.2mg/ml Alexa488-Dextran **(B)** at 37^0 C before washing and analysis by Flow cytometry. The data represents cell associated fluorescence for three independent experiments (n=3). * Parallel uptake experiments with transferrin (siRNA Internal Control) was performed to ensure protein depletion and an effect on CME.

3.4. Discussion

The uptake of CPPs such as R8 and HIV Tat has been intensely studied and in the most the peptides are covalently coupled to one of the many fluorophores that are now available and analysis is performed using flow cytometry and/or fluorescence microscopy. However new methods such as mass spectrometry of radiolabelled peptides are now emerging to support the fluorescence approach or raise questions about the suitability of fluorescence-peptides (Jiao et al. 2009). Despite these studies there is still controversy in the field and it is important to note that it is likely that different CPPs will have their own entry mechanism thus one model is unlikely to emerge that fits all peptides. It is generally accepted that some variants can enter in an energy dependant and independent mechanism but for this thesis the main focus was on studying the endocytic uptake rather than direct translocation and here it is seen that at 2μM that 85% of uptake can be inhibited by performing the internalisation experiments on ice. In collaboration with the Futaki laboratory has focused on D and L forms of octaarginine and Tat peptides but the main focus of this thesis was the L forms of these two peptides.

Most of the reports on these two peptides and other fluorescent CPPs have described experiments using endocytosis inhibitors that as discussed in Chapter 1 have their own problems of lack of specificity (Ivanov 2008). Mutant proteins such as dynamin have also been used to

characterise uptake (Wadia et al. 2004) but it is now known that dynamin II regulates more than one endocytic pathway (Doherty and McMahon 2009).

For this thesis attempts were made to inhibit several endocytic pathways through the use of siRNA depletion of endocytic proteins. This was a new technique in the laboratory and the earlier part of the work concentrated on developing this method. CME is by far the best characterised uptake route and therefore the initial work focused on this pathway. CME is regulated by several proteins including CHC, clathrin light chain and adaptor proteins and there is data available of the use of siRNA to deplete these proteins (Motley et al. 2003; Poupon et al. 2008; Thiery et al. 2010). From screening siRNAs from a number of proteins regulating CME, CHC and adaptor proteins were identified the most effective targets (Johannessen et al. 2000). For the project, CHC was chosen as the target protein and HeLa cells were used as they have been a model used in the laboratory to study CPPs, they are known to be relatively easy to transfect and studies have been published on using siRNA to affect endocytosis in these cells (Motley et al. 2003).

Fluorescently labelled endocytic probes transferrin and dextrans were employed as markers on CME and fluid phase uptake. The use of fluorescein isothiocyanite (FITC) as a fluorescence label is attractive due to the fact that FITC labels are relatively cheap compared with Alexa variants however it is known that the emission of this probe is sensitive to pH thus careful analysis needs to be made when interpreting data using this probe to study endocytosis. Therefore, two different fluorescence labelled dextrans were chosen to validate the results noting that Alexa dyes are not known to be pH sensitive.

The uptake of transferrin was initially studied and it was decided at the start of the project that time course experiments would be used as choosing a single time point could mean the loss of important information. This however is much more labour intensive especially as three independent experiments were required to allow statistical analysis of the data. The siRNA concentration was also briefly investigated and 50nM was finally selected due it giving slightly better inhibition of transferrin uptake. Over 85% of CHC expression could be depleted with CHC siRNA sequence shown in Table 3.1. This sequence was then used to look at timed uptake of the probe and viability of the cells. The relative inhibition in transferrin uptake was found to be time dependent being very high at early time points 0-15 min and then reducing at longer incubations. This is probably due to the fact that clathrin coated pits are also known to be required for recycling of this probe (van Dam and Stoorvogel 2002). Therefore, in CHC deficient cells there would also be a fault in recycling and that the material entering at a reduced levels compared to control cells would also be retained at a higher level.

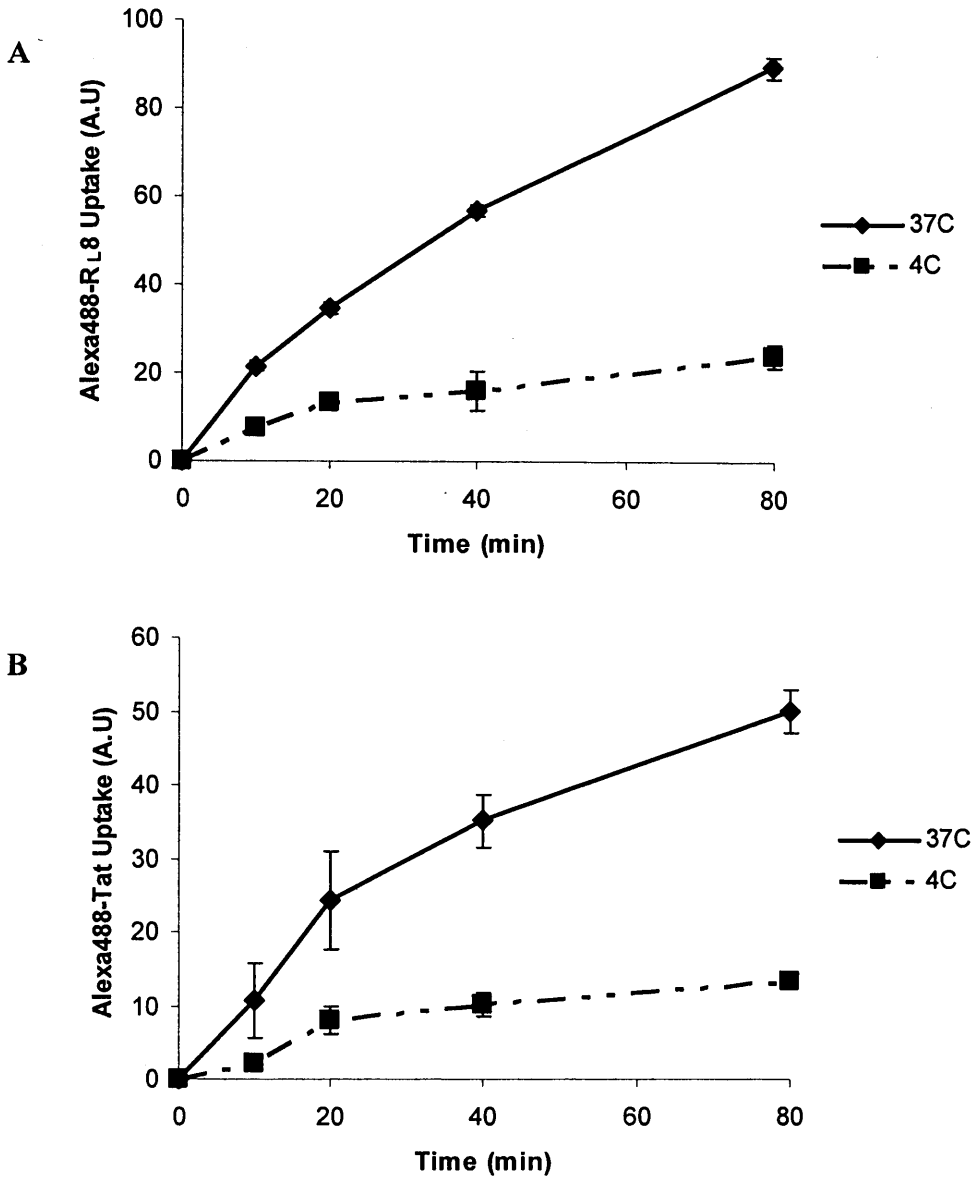

Figure 3.6. Effect of temperature on Alexa488-R8 and -Tat uptake.

HeLa cells were incubated with 2 μM Alexa488-R8 (A) and –Tat (B) at 37^0 C and at 4^0 C for 0-80 min, followed by washing, trypsinisation and analysis by flow cytometry (n=3).

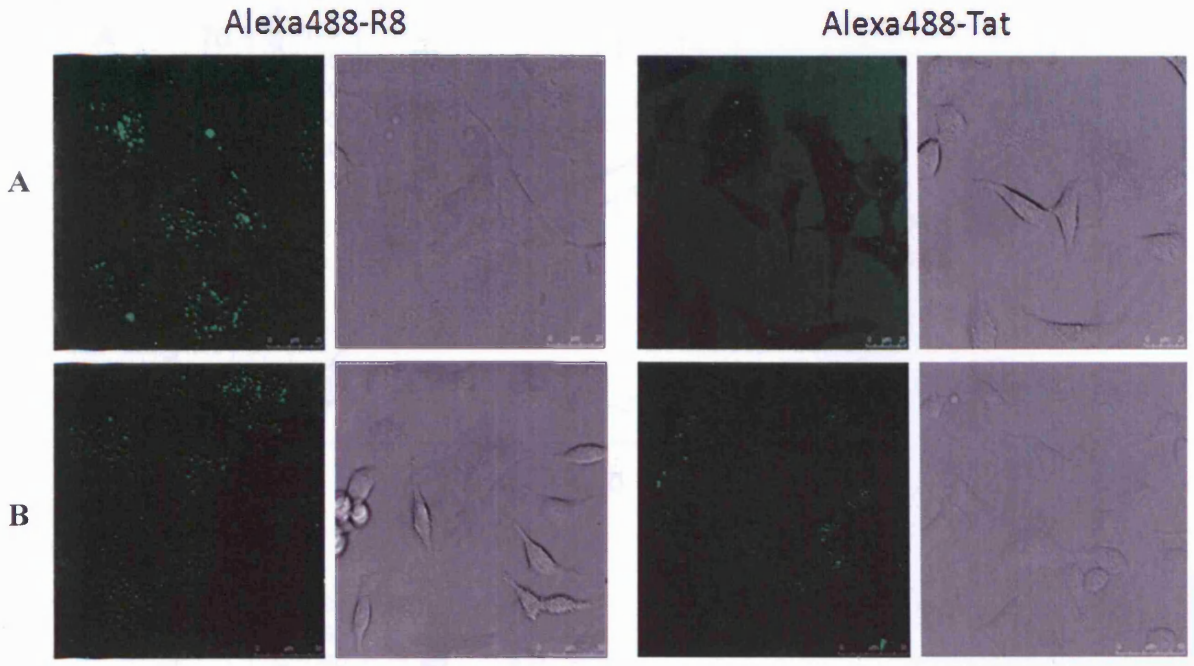

Figure 3.7 Subcellular distribution of Alexa488-R8 and -Tat in HeLa cells

HeLa cells were washed and incubated with 2μM of Alexa488-R8 or -Tat in DMEM media for 1 hr, then the cells were either unwashed **(A)** or washed **(B)** and analysed immedietly by confocal microscopy on the 37^0 C temperature stage. Shown are fluorescence and bright field images.

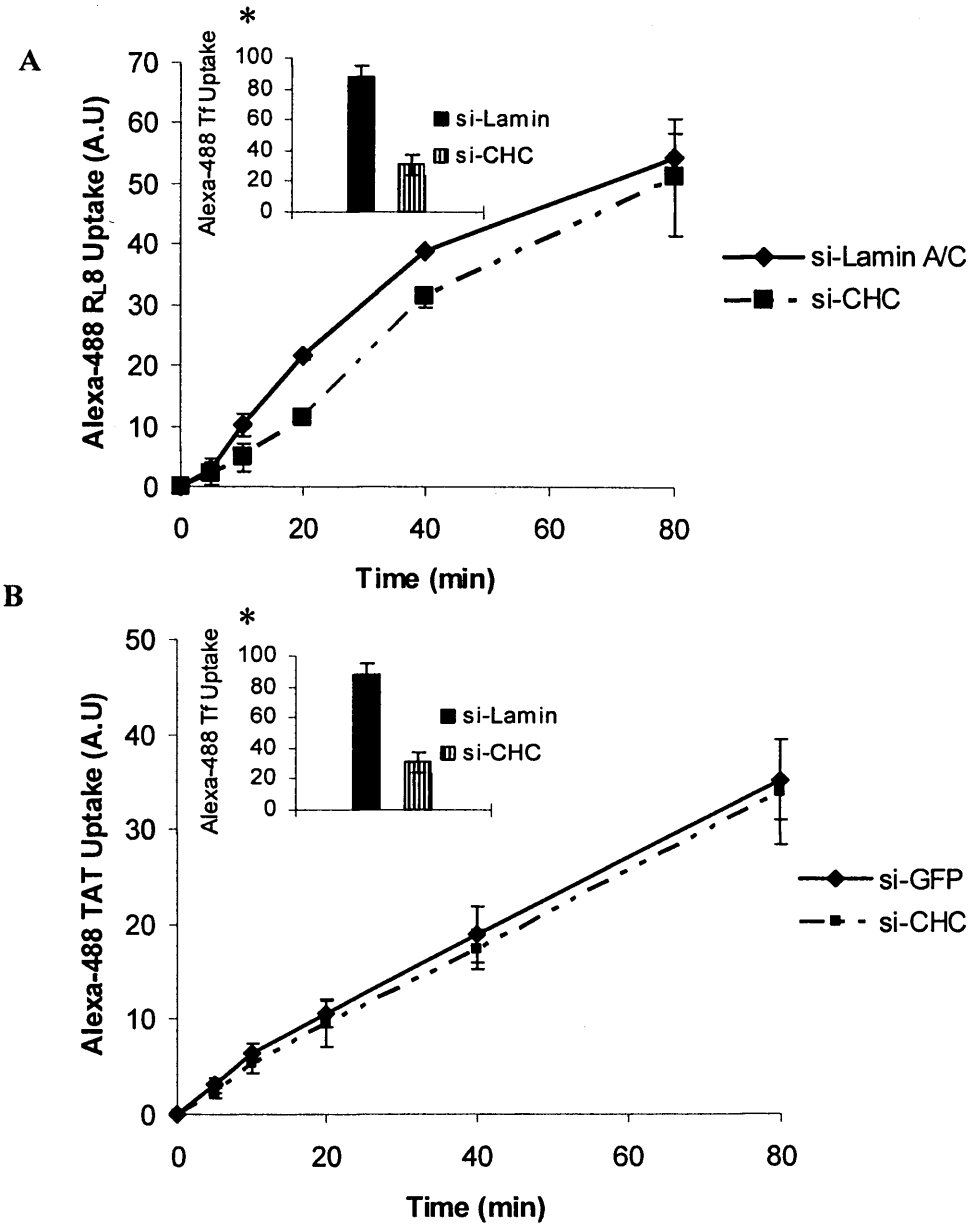

Figure 3.8. Uptake of Alexa488-R_L8 and -Tat uptake in CHC depleted cells.

HeLa cells were transfected with si-CHC, si-Lamin A/C or si-GFP for 48hr, then incubated for the indicated time points with 2 μM Alexa488-R8 (A) or –Tat (B) at 370 C for the indicated time points. Cells were washed, trypsinised and immediately analysed by flow cytometry. Values above obtained from three independent experiments (n=3) *Parallel uptake experiments with transferrin (siRNA Internal Control) is performed to ensure protein depletion and an effect on CME.

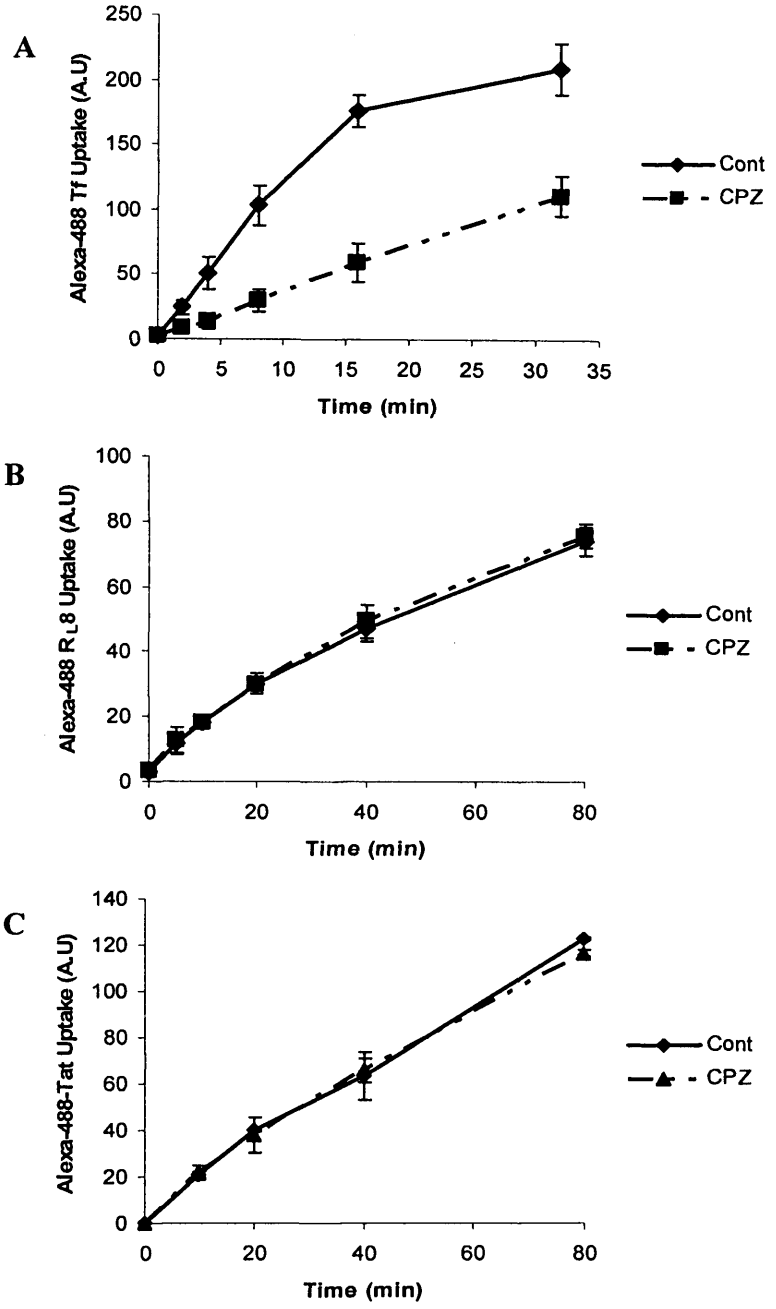

Figure 3.9 Effect of using pharmacological CME inhibitor (CPZ) on CPPs uptake

Cells were pre-incubated for 30 min in the absence (Control) or presence (CPZ) of 10μM CPZ at 37∘C, prior to washing and incubation with 100 nM Alexa488-Tf **(A)** or with 2 μM Alexa488-R_L8 **(B)** or –Tat **(C)** at 37^0 C for the indicated time points. Cells were washed, trypsinised and analysed by flow cytometry. Results represent data from three independent experiments.

The viability of the cells at following these siRNA treatments was tested using MTT assays and the results in Figure 3.2 show that cell viability remained >85% 48 hrs following transfection. siRNA targeting LaminA/C has often been used as a control for these kinds of experiments (Schmid et al. 2007), but microscopy revealed that the nucleus of Lamin A/C depleted cells had unusual shapes (Figure 3.10). Although, they had control uptake of Tf it was decided to use siRNA against a protein not expressed in these cells thus GFP was chosen for all subsequent experiments.

There is a possibility that inhibiting one pathway may affect the efficiency of another pathway and the uptake of Dextran was investigated in siRNA CHC cells. The studies show that uptake of both FITC and Alexa488 dextran was reduced at later time points but this was not statistically significant. This may have been a consequence of the slight effect on cell viability of the transfection procedure. The data are essentially in agreement with another study that investigated dextran uptake in CHC depleted cells (Zhang et al. 2009).

The development of these methods then allowed us to reach the main objective here, namely to study the uptake of the two CPPs Alexa488-R8 and –Tat. Again, the effect of temperature was initially investigated at different time points. Unlike Tf there was some temperature independent uptake of both R8 and Tat amounting to approximately 15% of the uptake. This is in agreement with other studies (Jiao et al. 2009; Nakase et al. 2004). It is however very difficult to distinguish between peptide that is actually inside the cells and peptide that may still be present on the surface of the plasma membrane or

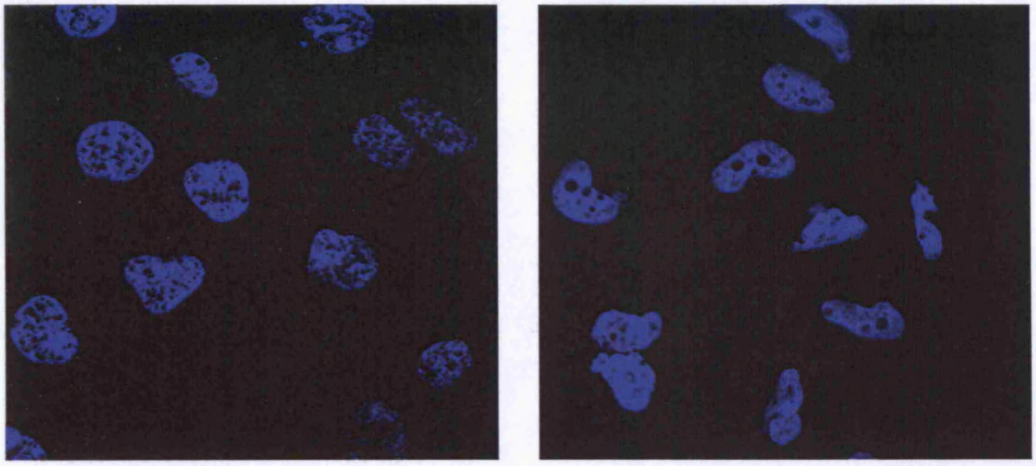

Figure 3.10. Effects of lamin depletion on nuclear shape.

HeLa cells were transfected with si-CHC (left) or si-Lamin A/C for 48hr, washed with PBS and the fixed in 3% PFA before incubation with PBS/0.2 Triton-X 100 for 5min. 10 μM of Hoechst was then added to the cells for 10 min before washing and mounting on coverslips and analysis by confocal microscopy.

even in the plasma membrane and this is despite washing with heparin and trypsinisation. There was no effect on uptake on uptake of either CPPs in CHC depleted cells leading to the conclusion that CME endocytosis plays no role in endocytosis of these peptides an this is contrary to results obtained using inhibitors (Richard et al. 2003).

Other studies also suggest that arginine rich CPPs utilise CME pathway to gain entry to the cytoplasm (Potocky et al. 2003) and Tat has been shown to be partially colocalized with transferrin (Richard et al. 2003). The uptake of retro-inverso form of a Tat peptide, R.I.-CKTat9, was also studied highlighting a concentration- and energy-dependent uptake mechanism. In addition, the labelled R.I.-CKTat9 colocalized with labeled transferrin in the punctate structure, suggesting that the peptide enters HeLa cells by CME. And in support of this they also show a significant inhibition in R.I.-CKTat9 in siRNA CHC depleted cells and in CME inhibitors (monodansylcadaverine & sucrose) pretreated cells (Zhang et al. 2009). However, these results were gained from very few cells using microscopy methods and from appearance the viability of the cells needs to be questioned. It may be that in the results presented in this thesis, 100% depletion CHC was not observed that the remaining fraction was sufficient for CPP uptake; but this is very unlikely. To make sure that transfection was successful in each experiment, control experimental points were employed for each assay, and this proved to be a highly efficient way of validating the data. It is very rare that these kinds of control experiments are performed.

The data is supported by another study using the BHK21-tTA/anti-clathrin heavy chain (CHC) cell line that can be induced to become defective in CME

(Ter-Avetisyan et al. 2009). They confirmed that the uptake of Tat is not mediated by CME.

To validate the data obtained using siRNA method, the CME inhibitor chlorpromazine (CPZ) was used in experiments using Tf and CPPs. The data shows a significant inhibition in transferrin uptake, whereas it failed to inhibit the uptake of both Alexa488-R_L8 and -Tat. Information on Dynasore, another CME inhibitor, is given in Chapter 4 and the data is supportive of the results obtained here. It has been reported that at peptide concentrations <5 μM, CPZ has no effect on cellular uptake of R9 and Tat, however, by increasing peptide concentration, the inhibitory effect of CPZ increased (Duchardt et al. 2007). Additionally studies from independent laboratories show that the higher the extracellular concentrations of cationic CPPs, the greater the fraction that is diffusely localized in the cytoplasm (Duchardt et al. 2007; Fretz et al. 2007; Tunnemann et al. 2008). Thus, the concentration of CPPs is a critical factor that may affect the uptake mechanism and possibly the type of endocytic pathway utilised. The concentration, used here was 2 μM and as shown 85% of the uptake occurs via an energy dependent manner. However, different cell-lines may have different threshold concentrations, due to the differences in the composition of the plasma membrane -lipids, proteins and their associated carbohydrates.

In conclusion, methods were developed for depleting CHC from HeLa cells, showing a strong inhibitory effect on Tf uptake. Using these methods paralleled with inhibitor studies allowed for us to conclude that there was no requirement for CME on uptake of CPPs R8 and Tat. Parallel studies using siRNA depletion were running in the University of Ghent as they attempted to

study the uptake of disulfide-based poly(amido-amine)/DNA polyplexes as part of their drug delivery programme. For the project, all the immunolabelling of lysates was developed and conducted by myself as part of this thesis. This was recently published in *Biomaterials* (Vercauteren et al. 2011) and they were able to successfully deplete CHC and show that internalisation of p(CBA-ABOL) polyplexes in ARPE-19 cells is independent of CME.

Efforts for this thesis were then concentrated on investigating other pathways that are less well characterised and more of a challenge to study.

Chapter 4: Evaluation of the role of Dynamin-2, Caveolin-1 and Flotillin-1 in cellular uptake of CPPs Tat and R8

4.1. Introduction

It has been shown that several molecules and receptors are internalised into cells via vesicular carriers, which are not clathrin or caveolin 1 dependent. The caveolin-1 dependent pathway will be discussed later in this chapter. The products of invagination called clathrin-independent carriers (CLIC), or GPI-enriched endocytic compartments (GEEC) are still poorly described. Actin and small GTPases like dynamin, RhoA, ARF1, ARF6 and Cdc42 have been shown to mediate the formation of CLICs. The most well known examples of molecules that enter cells via clathrin- and caveolin independent endocytosis are interleukin receptor 2, major histocompatibility complex class I (MHC I) and GPI-anchored proteins. The first plasma membrane receptor to be shown to utilize CLIC is Interleukin-2 and it also has been shown to be dependent on RhoA (Cheng et al. 2006; Lamaze et al. 2001; Sabharanjak et al. 2002). Rho A is also required in fluid phase uptake of dextran (Sabharanjak et al. 2002). However, the internalisation of the folate receptor, which is a GPI-anchored protein occurring through a Cdc42-dependent pathway (Sabharanjak et al. 2002). Arf6 has been shown to regulate the dynamin independent endocytosis of proteins such as class β1 integrin, E-cadherin, GPI-APs, I major histocompatibility complex molecule (MHC I) (Mayor and Pagano 2007). Recently, the McMahon group have reported that a Rho-GAP-domain-containing protein GRAF1 to be the first non cargo marker for the CLIC/GEEC endocytic membranes (Lundmark et al. 2008). This protein was shown to be associated with dynamic tubular and vesicular lipid structures together with phosphoinositides PtdIns(4,5)P2, and Cdc42.

Flotillin-1 (Flot-1) and flotillin-2 (Flot-2), also termed Reggie-2 and 1, respectively, are ubiquitously expressed proteins (Solis et al. 2007) and been reported to be associated with cholesterol rich membrane microdomains and in invaginations that do not contain caveolins (Frick et al. 2007; Stuermer et al. 2001). Lately, flotillin mediated endocytosis is considered as a new clathrin- and caveolin-independent endocytic pathway (Glebov et al. 2006) and more recently the same group have suggested it is involved in uropod dynamics of neutrophils (Szakacs et al. 2006). Flotillin-1 and 2 have however been studied for a number of years and their association with lipid rafts have long been established though the flotillin domains on the plasma membrane seem to be separate from those enriched in caveolin-1. But in common with caveolin-1 it seems that uptake of flotillin-1 structures is a slow and/or infrequent process; flotillin has also been implicated in phagocytosis (Dermine et al. 2001). The original work in flotillin-1 and endocytosis demonstrated that an antibody against CD59 was internalised into HeLa cells in a flotillin-1 dependant manner (Glebov et al. 2006). This was shown using siRNA targeting of flotillin-1 and investigating the uptake of a fluorescent anti-CD59 antibody. CD59 is also known as protectin, and it is a complement regulatory protein, or MIRL (membrane inhibitor of reactive lysis) (Venneker et al. 1994). Three activities for CD59 have been recognized including downregulation of the activation of the C cascade at membrane attack complex formation stage, participation in T-cell rosette formation with erythrocytes and it is necessary for T-cell activation (Venneker and Asghar 1992; Venneker et al. 1994). CD59 is present on most tissues and this is compatible with its function of protecting cells and tissues from incidentally activated autologous C. Mature CD59 is

made up of 103 amino acids and 20% of its molar mass is carbohydrate. The protein part of the molecule is covalently linked to an oligosaccharide, which is glycosydically linked to phosphatidylinositol (PI). Decreased expression of CD59 has been shown in two diseases; paroxysmal nocturnal hemoglobinuria, and in psoriasis (Venneker and Asghar 1992; Venneker et al. 1994). Like many proteins, advances in CD59 biology have been made through the use of antibodies recognising this protein and several have been described including A35, YTH53.1, BRIC229, MEM34, and HC2 (Bodian et al. 1997). For this thesis A35 and YTH53.1 clones were investigated. As CD59 is a GPI linked protein most studies on the uptake of this protein have concentrated on this fact and the protein was found to be localised to ARF6 compartments before merging with cargo internalised via CME (Naslavsky et al. 2004). Interestingly CD59 was found in tubular structures after 30 min of uptake and mutant AP180 protein involved in CME did not affect uptake of the molecule but filipin significantly reduced uptake (Naslavsky et al. 2004).

Caveolae are 50–80 nm flask-shaped membrane regions also rich in GPI-anchored proteins, sphingolipids, cholesterol. The caveolae shape was discovered 50 years ago by electron microscopy (Parton and Richards 2003; Yamada 1955), whereas its structural components were identified later. The main protein in caveolae is caveolin, which is a 21 kDa integral membrane protein and is inserted as a hairpin loop into the membrane, and its amino- and carboxy-terminal regions are directed toward the cytosol (Dupree et al. 1993). Caveolin has three known isoforms, caveolin-1 (Cav-1), caveolin-2 (Cav-2) and caveolin-3 (Cav-3). Both Cav-1 and Cav-2 have similar distribution and

they are highly expressed in adipocytes, endothelial cells, fibroblasts and smooth muscle cells. While Cav-3 is highly expressed in cardiac and skeletal muscle (Parton and Richards 2003). It has been reported that cellular internalisation of caveolae is dependent on active dynamin and the actin cytoskeleton (Nichols 2002; Thomsen et al. 2002). Caveolae have been implicated in delivering a number of different cargoes and integral plasma membrane proteins and lipids (Parton and Richards 2003). It was initially thought that cholera toxin B was internalised solely through this pathway and this was usually termed 'the caveolae marker' but subsequently it was discovered that this toxin can enter through other clathrin dependent and independent pathways (Pang et al. 2004; Torgersen et al. 2001). The endocytosis of fluorescent glycosphingolipid (GSL) analogs in various cell types was studied by Pagano's group, using pharmacological inhibitors and colocalization studies with fluorescent lactosylceramide as a GSL probe and DsRed caveolin-1 as a marker protein. They found that, all GSLs tested were internalised mainly by a clathrin-independent, caveolar-related mechanism, regardless of cell type. Their results show that the internalisation of fluorescent LacCer was reduced 80-90% in cell types with low Cav-1, but was dramatically stimulated by Cav-1 overexpression. However, even in cells with low levels of Cav-1, residual LacCer internalisation was clathrin independent. In contrast, cholera toxin B subunit was internalised via clathrin-independent endocytosis in cells with high Cav-1 expression. There results suggest that GSL analogs are selectively internalised via a caveolar-related mechanism in most cell types, whereas CtxB may undergo "pathway switching" when Cav-1 levels are low (Singh et al. 2003).

In this chapter the role of DNM2, Flot-1, and Cav-1 was investigated using chemical inhibitors and siRNA depletion of these three proteins. The goal here was to find a specific probe for distinct pathways regulated by these proteins and then test the siRNA developed models for uptake of Tat and R8. Alexa488-Tf was used as a marker probe for DNM2 dependent endocytic pathway as this protein is known to be involved in CME and caveolin dependent uptake. But most important here is the recent evidence suggesting that DNM2 is involved in fluid phase uptake (Cao et al. 2007). There is every possibility that the peptides are entering via fluid phase uptake but this pathway does not have a true siRNA target and thus DNM2 was studied. If CPPs are entering cells in the fluid phase then it should be possible to inhibit their entry in DNM2 depleted cells. Based on literature it was decided to study the uptake of anti-CD59 and BODIPY LacCer for Flot-1-dependent and Cav-1 dependent endocytic pathways respectively.

4.2. Methods

HeLa cells and A431 cells were used to study DNM2 dependent pathways, while Flot-1 dependent and Cav-1 dependent pathways were studied using HeLa cells only.

Initially, Alexa488-Tf, Alexa488-R8, and -Tat uptake was investigated in HeLa and A431 cells treated with the DNM2 inhibitor dynasore and cell associated fluorescence was measured by flow cytometry as shown in section 2.3.5.4. Alexa488-Tf uptake was also investigated in dynasore treated cells using confocal microscopy as described in section 2.3.4.2. HeLa cells and A431 cells were also transfected with different siRNA sequences as described

in chapter 2 and as shown in Table 4.1. Alexa488-Tf, Alexa488-R8 and -Tat uptake was investigated in control (siRNA GFP) and DNM2 depleted cells and cell associated fluorescence was measured by flow cytometry as described in section 2.3.5.3

To study the role of Flot-1 in CPP uptake, methods were developed for analysing the uptake of anti-CD59 antibody in Flot-1 depleted HeLa cells using different siRNA sequences as described in chapter 2 and as shown in Table 4.1. Thereafter Alexa488-R8 and -Tat uptake was investigated in Flot-1 depleted cells and cell associated fluorescence was measured by flow cytometry as described in section 2.3.5.2 and 2.3.5.3.

In order to characterize the requirement of Cav-1 in CPP uptake methods were developed for investigating the uptake of BODIPY-LacCer in Cav-1 depleted cells. Due to the excessive plasma membrane binding of this marker, even following extensive washing, trypan blue quenching and back extraction methods was investigated as described in section 2.3.5.2. The uptake of Alexa488-R8 and -Tat was finally investigated in Cav-1 depleted HeLa cells using a single siRNA sequence as described in chapter 2 and as shown in Table 4.1.

Finally, SDS-PAGE electrophoresis and Western blotting techniques were used to measure DNM2, Flot-1, and Cav-1 depletion from cell lysates as described in section 2.3.7 and 2.3.8.

This chapter also shows Western blotting data on lysates sent from the University of Ghent and preliminary analysis of the effects of transfecting cells with siRNAs targeting ARF6 and GRAF-1

siRNA-Target	Sequences	Ref.
GFP	GGC UAC GUC CAG GAG CGC AdTdT	Designed by MWG
DNM2-A	5'-GACAUGAUCGUGCAGUUUATT-3'	(Cao et al. 2007)
DNM2-B	Set of 4 oligo's: 5'-GGCCCUACGUAGCAAACUA-3' 5'-GAGAUCAGGUGGACACUCU-3' 5'-CCGAAUCAAUCGCAUCUUC-3' 5'-GAGCGAAUCGUCACCACUU-3'	Designed by Dharmacon
DNM2-C	GGA CAU GAU CCU GCA GUU dTdT	(Romer et al. 2007)
Flot-1-A	AGA UGC ACG GAU UGG AGA AdTdT	Designed by MWG
Flot-1-B	CACACUGACCCUCAAUGUCdTdT	(Glebov et al. 2006)
Cav-1	AGA CGA GCU GAG CGA GAA GdTdT	Designed by MWG
Arf6	Set of 4 oligo's: CGG CAU UAC UAC ACU GGG AdTdT UCA CAU GGU UAA CCU CUA AdTdT GAG CUG CAC CGC AUU AUC AdTdT GAU GAG GGA CGC CAU AAU CdTdT	Designed by Dharmacon
GRAF1	CCA CUC AUG AUG UAC CAG UUU CAA A	Designed by Invitrogen

Table 4.1. siRNA sequences used in this Chapter

4.3. Results

4.3.1. Characterisation of the requirement of dynamin-2 protein in cellular uptake of Alexa488-R_L8 and –Tat

The uptake of both Alexa488-R8 and -TAT were investigated in this chapter using the two methods, which have been described in previous chapters detailing methods for siRNA depletion and chemical inhibitors (section 2.3.5.3 and 2.3.5.4). As described in Chapter 2, one of the most important regulators of CME is dynamin and it acts as a scissor to separate the CCV from the plasma membrane. However it is now known to be involved in uptake through caveolae (Yao et al. 2005) and in fluid phase endocytosis (Cao et al. 2007). Alexa488-Tf was used as a marker for dynamin dependent endocytosis as methods were already in place for quantifying the uptake of this probe (section 2.3.5.3). Dynasore is a recently discovered dynamin 1 and dynamin 2 inhibitor that was shown to be a powerful inhibitor of CME (Macia et al. 2006). It inhibits the action of dynamin by interfereing with the GTPase activity of dynamin1 and dynamin2 and rapidly blocking coated vesicle formation (Macia et al. 2006). HeLa cells were pre-incubated with 80μM dynasore for 30 min, then incubated with 100 nM Alexa488-Tf for the indicated time points. Transferrin uptake was significantly inhibited in dynasore treated cells (Figure 4.1.A). Uptake was inhibited by 60-70% from 5-15 min then the inhibition was reduced to 40-50% from 20-30 min (Figure 4.1.B), Again this may be due to the requirement for this protein, as for CHC, in transferrin recycling. These flow cytometry results were also confirmed by confocal microscopy, that was performed after incubating untreated cells (Figure 4.2.A) or dynasore treated cells for 30 min (Figure 4.2.B). This then allowed analysis of the uptake of

both CPPs in dynasore treated cells and the data in Figure 4.1C and D highlights the fact that the drug had no effect on CPP uptake. Experiments were then performed to determine whether there was any requirement for DNM2 by depleting this protein from cells.

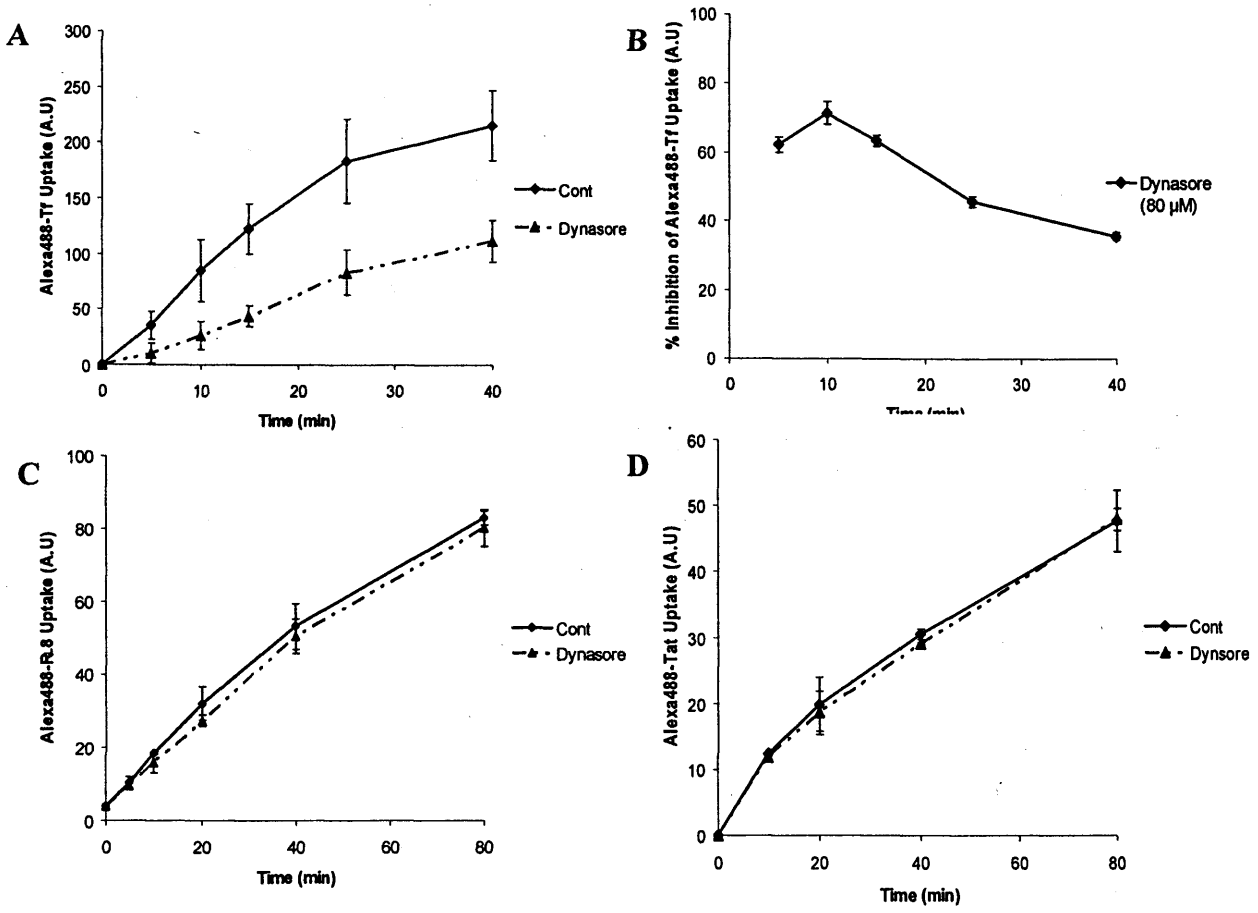

Figure 4.1. The effect of Dynasore on CPPs uptake in HeLa cells

Cells were pre-incubated for 30 min in the absence (Control) or presence (Dynasore) of 80µM dynasore at 37°C, prior to washing and incubation with 100 nM Alexa488-Tf **(A-B)** , 2 μM Alexa488-R_L8 **(C)** or Alexa488-Tat **(D)** at 37° C for the indicated time points. Cells were washed and immediately analysed by flow cytometry under standard conditions for CPP uptake. Values above obtained from three independent experiments (n=3). **(B)** Results from A expressed as percentage inhibition compared with control siRNA cells.

A B

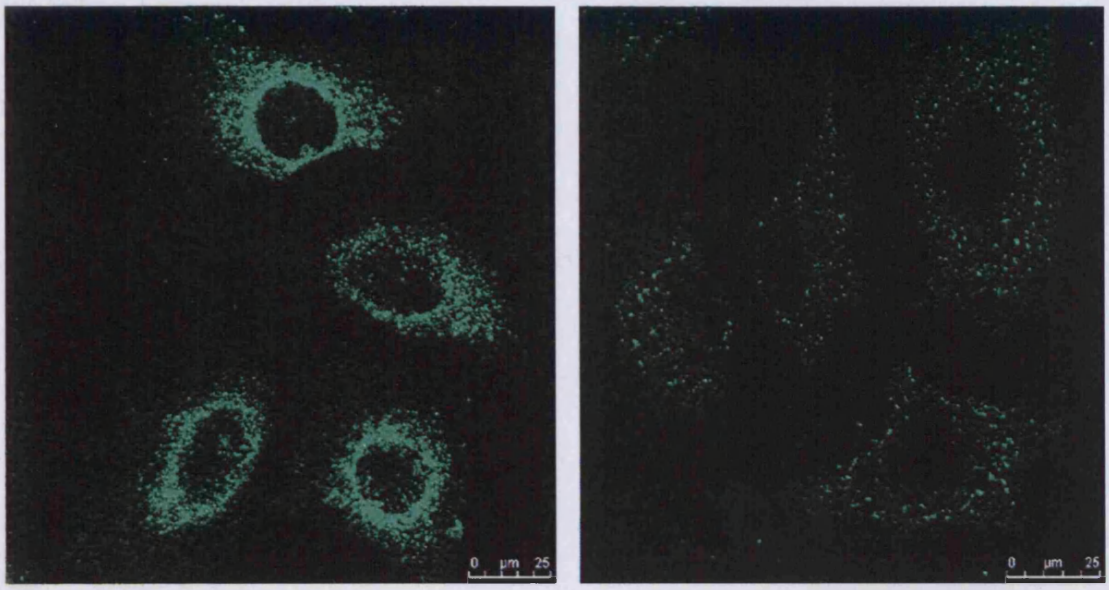

Figure 4.2. Uptake of Alexa488-Tf in control and dynasore treated HeLa cells.

Cells were pre-incubated for 30 min in the absence (Control) **(A)** or presence (Dynasore) **(B)** of 80µM dynasore at 37^0 C, prior to washing and incubation with 100 nM Alexa488-Tf before washing, fixation and analysis by confocal microscopy. Confocal images represent maximum projection images. Scale bars = 25µm.

HeLa cells were transfected with a number of different siRNA sequences against this protein (si-DNM2-A, si-DNM2-B, and si-DNM2-C in Table 4.1). However, all of these siRNAs failed to deplete DNM2 efficiently using the standard methods used successfully for depleting CHC; this involves incubating the cells for 48 hrs after transfection before performing endocytosis assays and immunodetection from SDS gels (Figure 4.3). It was clear that some depletion was observed but this was not of a level that would have allowed for subsequent functional endocytosis assays in these cells (Figure 4.3.A, B, and D). At this time lystates were also sent from Ghent University to study the depletion of this protein from Retinal pigment epithelial cells and similar to data shown in Figure 4.3.C, complete depletion was not observed.

It was then decided to attempt to deplete this protein from A431 cells, using the standard 48 hr period and extended 72 hr periods, i.e. from start of transfection to analysis. A431 were chosen here because studies had already been investigated with these cells for studying macropinocytosis (Chapter 5). Both si-DNM2-B and si-DNM2-C were investigated here. The results in Figure 4.3.E show that successful depletion of DNM2 was obtained with sequence si-DNM2-C after 72 hrs. Following this successful depletion the uptake of Alexa488-R8 and -Tat, were investigated in A431 cells depleted of DNM2 or treated with dynasore. The data in Figure 4.4.A supports the data in HeLa cells showing that dynasore inhibits transferrin uptake but has no effect on uptake of CPPs (Figure 4.4.B & C). The same effects were seen in DNM2 depleted cells that were deficient in endocytosis of transferrrin (Figure 4.5. A) but had normal uptake of both CPPs (Figure 4.5.B & C).

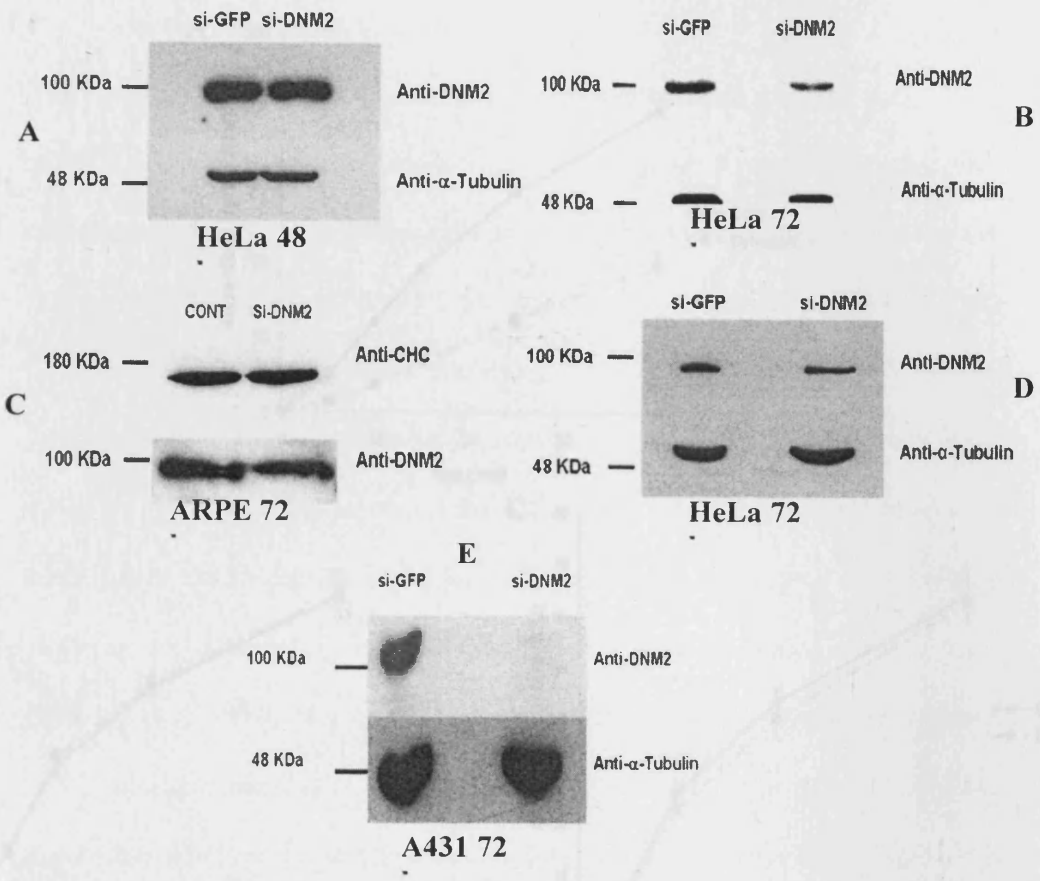

Figure 4.3. Analysis of DNM2 expression following transfections with siRNA targeting DNM2

Cells were transfected with siRNA targeting DYN2 and incubated for 72 hrs before preparing cell lysates. The lysates were then separated by electrophoresis and transferred to nitrocellulose papers, probed with antibodies against DNM2 or α-tubulin that were then detected with HRP conjugated secondary antibodies and Enhanced Chemiluminescence (ECL). **(A), (B),** and **(D)** represent data obtained from HeLa cells using si-DNM2-A, si-DNM2-C, and si-DNM-B respectively, while **(C)** represent ARPE cells (Ghent lysates samples) using DNM-C and (E) represent data obtained from A431 cells using si-DNM2-C.

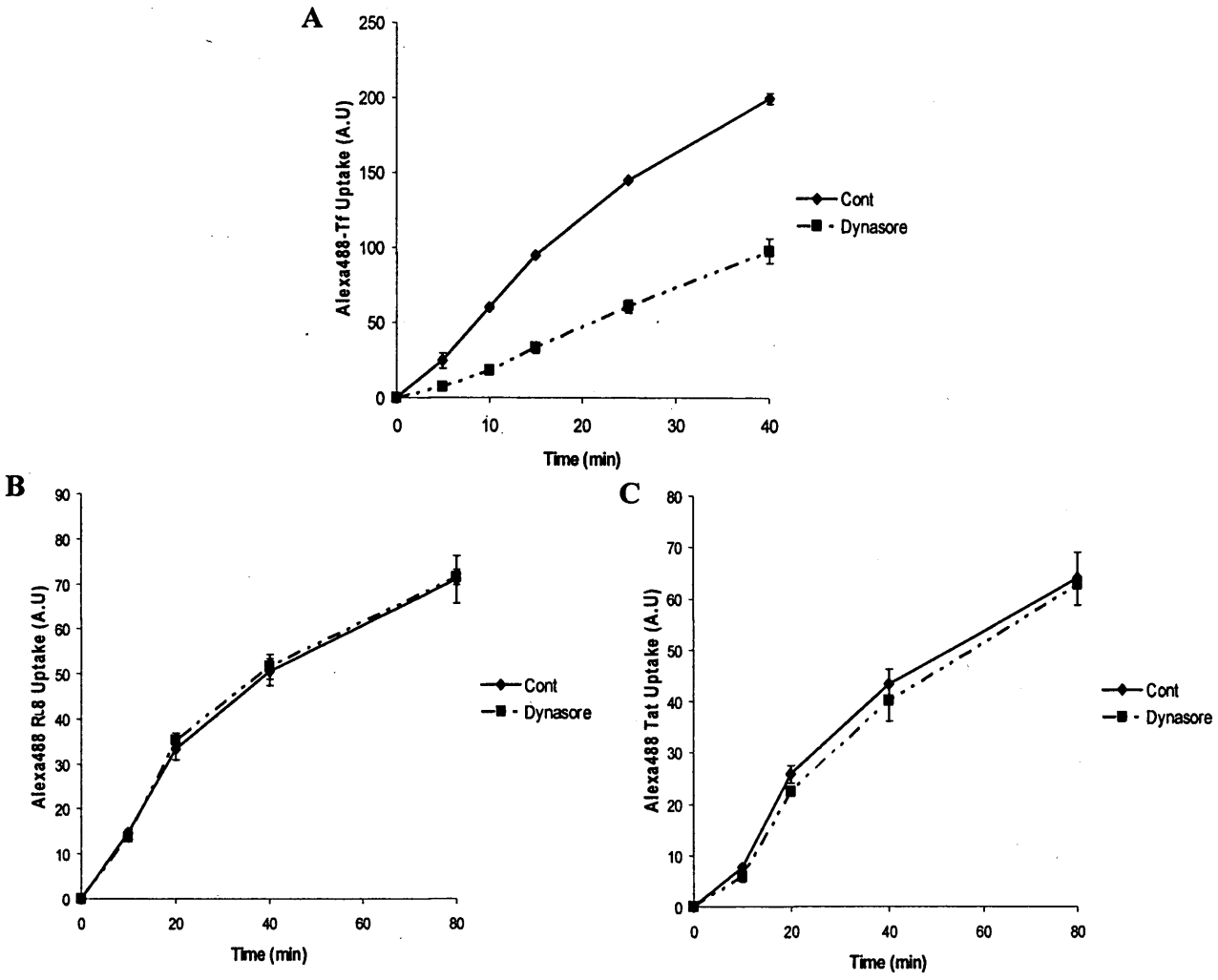

Figure 4.4 The effect of the DNM2 inhibitor Dynasore on CPP uptake in A431 Cells

Cells were pre-incubated for 30 min in the absence (Control) or presence (Dynasore) of 80μM dynasore at 37°C, prior to washing and incubation with 100 nM Alexa488-Tf **(A)** or with 2 μM Alexa488-R_L8 **(B)** or -Tat **(C)** at 37^0 C for the indicated time points. Cells were then processed for analysis by flow cytometry under standard conditions for CPP uptake. Values above obtained from three independent experiments (n=3).

4.3.2. Characterisation of the requirement for flotillin-1 in cellular uptake of Alexa488-R_L8 and –Tat

The main obstacle in investigating the flotillin dependent pathway is to find a specific and easily available marker for this pathway. As mentioned, flotillin-mediated endocytosis is a relatively new discovery and characterised by the finding that the uptake of anti-CD59 was reduced in flotillin-1 depleted cells (Glebov et al. 2006). However, the exact antibody used in this study was no longer available and of note is the fact that no specific chemical inhibitor is yet available or indeed characterised for inhibiting this pathway. The School of Medicine at the University of Wales Hospital have for a number of years been studying the biology of CD59 as part of its role in the complement system (Rooney et al. 1991). We were fortunate in having available some pre prepared FITC labelled anti-CD59 antibodies that we could investigate initially to determine whether we could measure and quantify its uptake in cells. For experiments analysing transferrin uptake in cells it is common to include an acid wash step to remove the fraction that is still bound to the plasma membrane and not inside the cells. Experiments were performed to see if acid washing reduced the cell associated fluorescence of cells incubated with this antibody. Initially, 2 different anti CD59 epitopes were tested, FITC-CD59-A35 and FITC-CD59-YTH-53.1. HeLa cells were incubated with 2.5mg/ml FITC-CD59 antibody for 30 min then cells were washed with PBS +/- acid washing prior to trypsinisation and flow cytometry analysis. The acid wash method was successful in removing the plasma membrane binding of FITC-CD59-YTH-53.1by 55% compared to the non acid washed cells (Figure 4.6.A). FITC-CD59-YTH-53.1 gave extremely high fluorescence values that

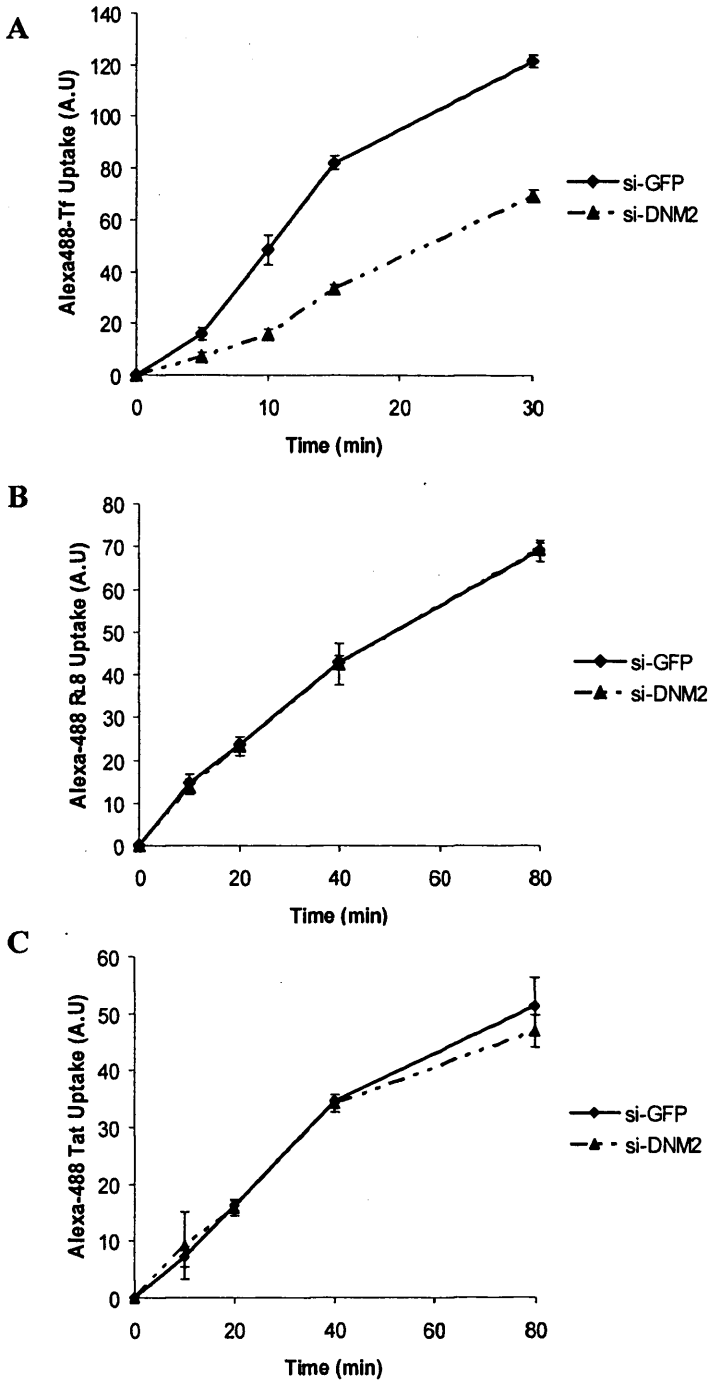

Figure 4.5. Uptake of Alexa488-R_L8 and -Tat in DNM2 depleted cells

A431 cells were transfected with si-DNM2, or si-GFP for 72hr, then incubated for the indicated time points with 100 nM Alexa488-Tf (**A**) or with 2 μM Alexa488-R_L8 (**B**) or -Tat (**C**) at 37^0 C. Cells were then processed for analysis by flow cytometry under standard conditions for CPP uptake. Values above obtained from three independent experiments (n=3).

were on the whole non resistant to acid washing (Figure 4.6.A) and it was determined at this stage to continue experiments with FITC-CD59-A35.

Once methods were in place for quantifying the uptake of this fluorescent antibody siRNA sequences were investigated to determine whether they depleted Flot-1 expression and whether this resulted in a reduction in the endocytosis of anti-CD59. Initially, two different siRNA sequences against Flot-1 were tested, si-Flot-1-A was designed by MWG, while, si-Flot-1-B was obtained form the Gelbov et al study (Glebov et al. 2006). Both of them were able to reduce Flot-1 expression, however si-Flot-1-A showed higher depletion compared with si-Flot-1-B (Figure 4.7). Note that CHC was used as an internal control here as the usual tubulin control has a molecular weight similar to that of Flot-1. Consequently, only si-Flot-1-A was used for subsequent experiments. HeLa cells were then transfected for 48 hrs using si-Flot-1-A, prior to adding 2.5 mg/ml of FITC-CD59 antibody for 0-40 min, acid washing, trypsinisation and flow cytometry analysis. The results in Figure 4.6.B show a significant inhibition of approximately 30% between 20 min- 40 min in the uptake of anti-CD59 in siRNA-Flot-1 cells; there was no inhibition at earlier time points.

The role of Flot-1 was also investigated in the uptake of both FITC-dextran and Alexa488-Tf. Flot-1 was depleted for 48 hrs in HeLa cells that were then incubated with 5mg/ml of FITC-dextran (Figure 4.6.C) or 100nM of Alexa488-Tf (Figure 4.6.D) for the indicated times. The cells were then processed for flow cytometry analysis as previously described. The results show no inhibition of FITC-dextran uptake and though there was a consistent inhibition

(15-19%) in the uptake of Alexa488-Tf this was statistically insignificant at P>0.05. The development of these methods then allowed for analysis of the uptake of R8 and Tat and the results in Figure 4.8.A and 4.8.B show that there is no requirement for Flotillin dependent endocytosis in the internalisation of these two CPPs.

4.3.3. Characterize the requirement of caveolin-1 protein in Alexa488-R_L8 and -Tat cellular uptake

Similar to problems encountered with Flotillin dependent endocytosis one of the main issues regarding uptake through caveolin is to find a suitable endocytic probe whose uptake is dependent on this pathway. It has been shown in literature that lactosylceramide (LacCer) is internalised specifically via a caveolae-mediated pathway (Puri et al. 2001; Rejman et al. 2004). Therefore, BODIPY®(4,4-difluoro-4-bora-3a,4adiaza-s-indacene)–LacCer (lactosylceramide), here termed Bodipy-LacCer was used in this chapter as a Cav-1 dependent probe. As described in Chapter 1 Bodipy- LacCer with its ceramide backbone will partition into lipid rafts where most of the caveolae are located. Lipids such as sphingomyelin that have a ceramine backbone are predominantly found in lipid rafts (Silva et al. 2007) and BODIPY-LacCer will therefore partition into these structures. Caveolin and cavaeolae are known to be enriched in lipid rafts and thus are likely to be internalised with these structures. Thus one of the main problems with using this probe is the very high fraction that localises to the plasma membrane and is not internalised (Singh et al. 2003; Vercauteren et al. 2010). Thus the cell associated fluorescence is very high but the fraction of the probe that is inside the cells

may be a very small part of that. The Pagano's group have used the so called back exchange washing method to remove the plasma membrane fraction. This involves extensive washing of cells in several changes of buffer containing 5% fatty acid-free BSA. Throughout this procedure lipids on the cell surface are extracted from the cell surface and transferred to the BSA acceptor in the medium. This back-exchange procedure is usually carried out at low temperature to stop any consequent endocytic transport of the lipid analoges during the required incubations (Singh et al. 2003).

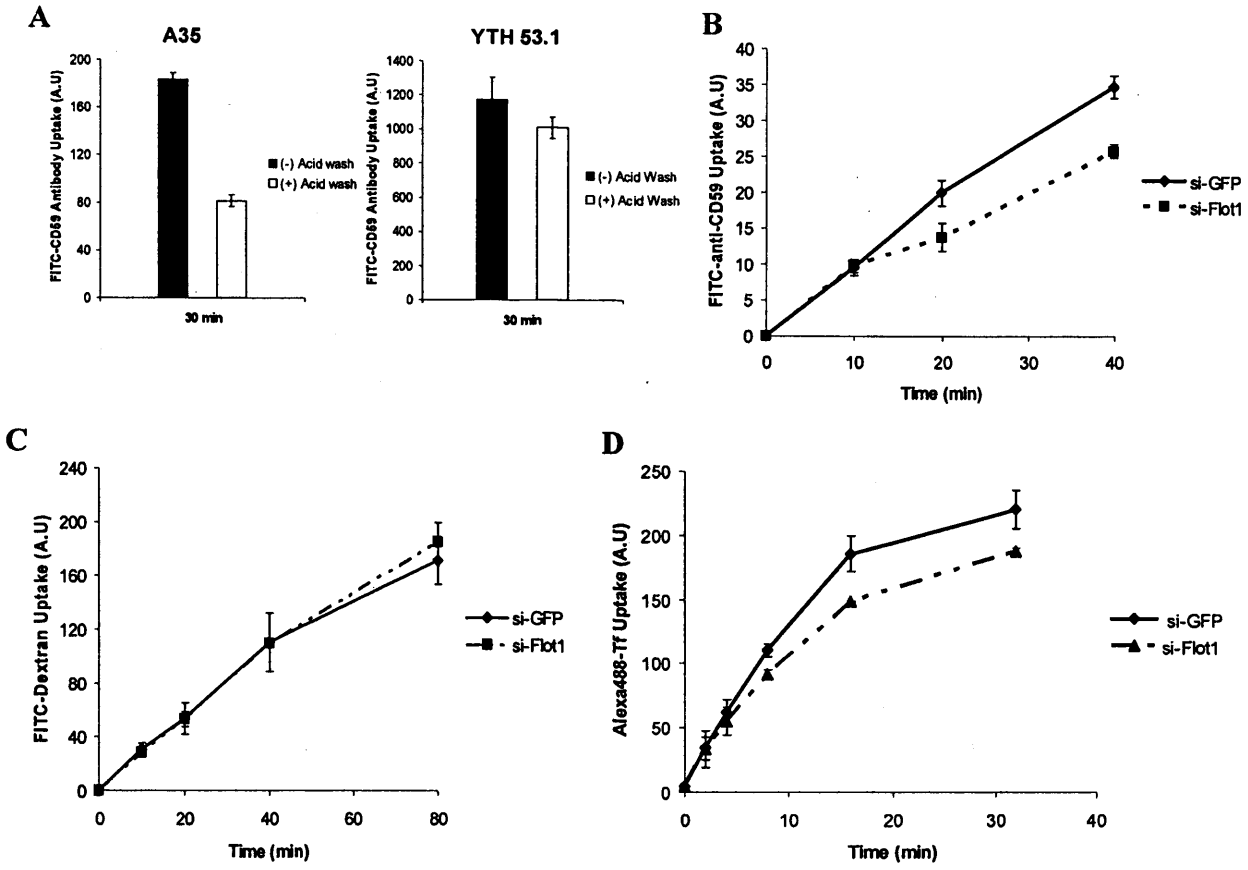

Figure 4.6. The effect of depleting Flot-1 on the uptake of FITC-CD59 antibody, FITC-Dextran, and Alexa488-Tf.

HeLa cells were either transfected **(B,C, D)** or non-transfected **(A)** with si-Flot-1-A, or si-GFP for 48hr, then incubated for the indicated time points with 2.5 mg/ml FITC-CD59 antibody **(A)** & **(B)**, 5mg/ml FITC-Dextran **(C)**, or 100nM Alexa488-Tf **(D)** at 37^0 C for the indicated time points. Cells were acid washed and followed by PBS wash and then trypsinized before analysed by flow cytometry. Values above obtained from three independent experiments (n=3).

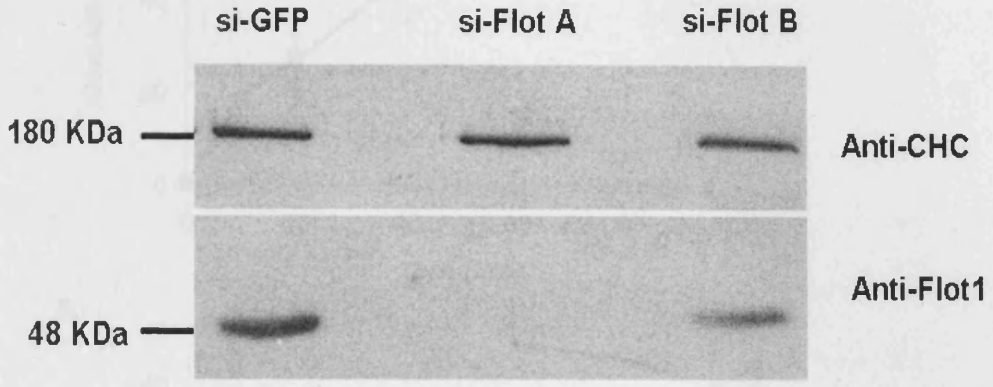

Figure 4.7. Analysis of Flot-1 expression following transfections with siRNAs targeting Flot-1

Cells were transfected with siRNA targeting Flot-1-A or Flot-B and incubated for 48 hrs before preparing cell lysates. The lysates were separated by electrophoresis transferred to nitrocellulose papers, probed with antibodies against Flot-1, or α-CHC that were then detected with HRP conjugated secondary antibodies and Enhanced Chemiluminescence (ECL).

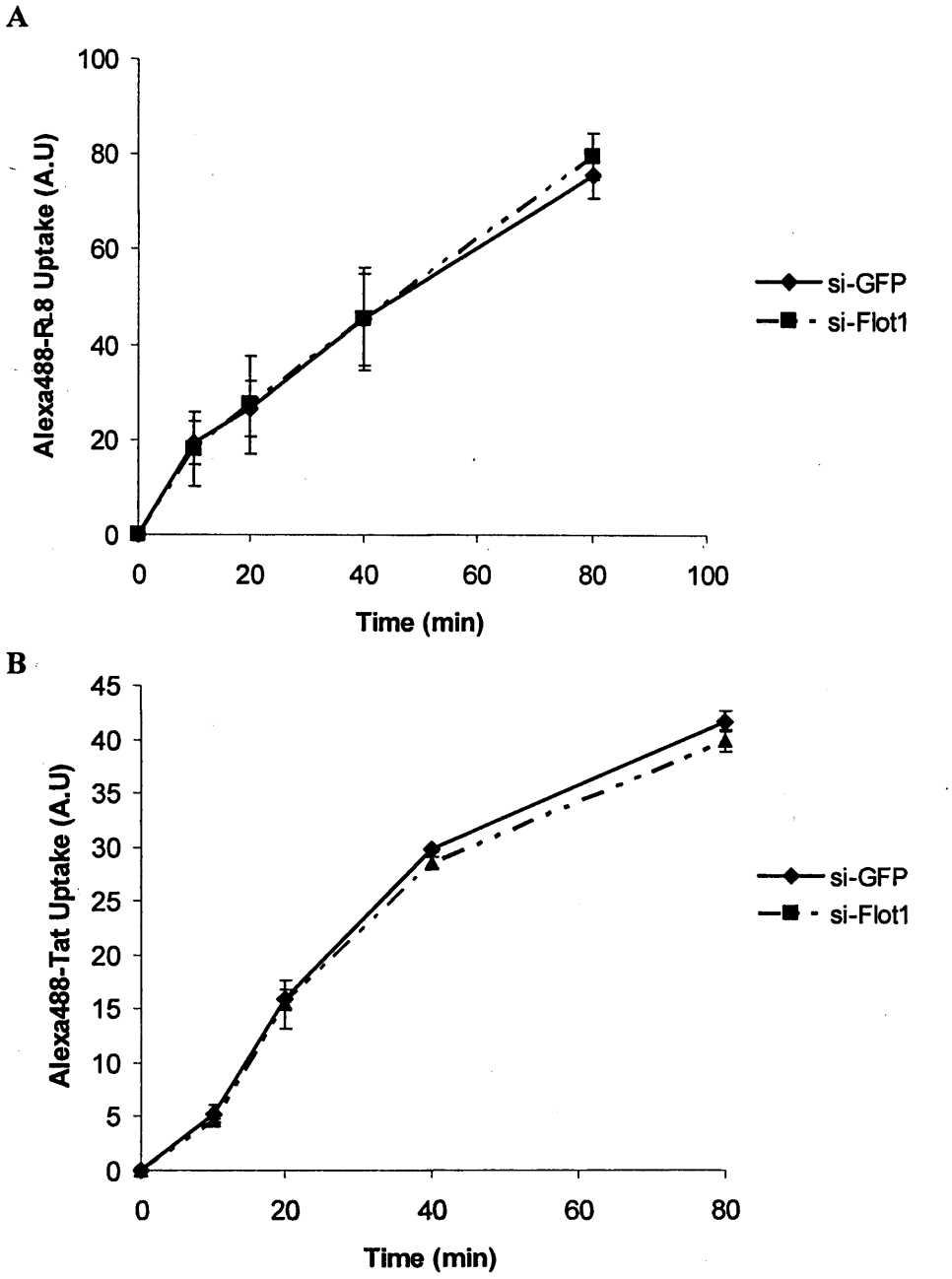

Figure 4.8. The effect of depleting Flot-1 on the uptake of Alexa488-R8 and -Tat.

HeLa cells were transfected with si-Flot-1-A, or si-GFP for 48hr, then incubated for the indicated time points with 2μM Alexa488-R8 **(A)** or -Tat **(B)** at 37^0 C for the indicated time points. Cells were washed, trypsinized and processed for flow cytometry under standard conditions for CPP uptake. Values above obtained from three independent experiments (n=3).

(Aoki et al. 2010; Chen et al. 1998; Marks et al. 2005). Although it has been shown that the back exchange method is an effective in removing plasma membrane binding of BODIPY-LacCer, it was unable to remove extremely high BODIPY-LacCer fluorescence from three separate attempts (Figure 4.9.A). An alternative method was therefore investigated and it was based on a live cell study for measuring fatty acid import (Li et al. 2005a). The assay use the chromophore, trypan blue, to quench the extracellular fluorescence of the fatty acid analoge C1-BODIPY-C12 instead of the back exchange method. This method was therefore investigated. HeLa cells were incubated with 1 μM BODIPY-LacCer at 10°C for 30 min to load the plasma membrane with the lipid analog. The cells were then washed 3 times with SFM at 10°C, followed by incubation at 37° C for 15 min to allow a short pulse of endocytosis. To remove the plasma membrane binding, the cells were rinsed twice with ice-cold PBS and trypsinised at room temperature. This was followed by adding 0.33 mM trypan blue in PBS for 30 min at room temperature. After, the suspension was washed with ice cold PBS, before measuring cell associated fluorescence by flow cytometry. The results in Figure 4.9.B show that the fluorescence of cells incubated with trypan blue was reduced to 69% of the control cells. This developed method was then suitable for further analysis once siRNA methods were developed for depleting Cav-1. A number of reports have been published whereby Cav-1 has been silenced with siRNA (Glebov et al. 2006; Vassilieva et al. 2009). A predesigned sequence from MWG was selected for these analysis, based on the fact that the previous purchase from this company has shown a successful depletion with pedesigned sequences.

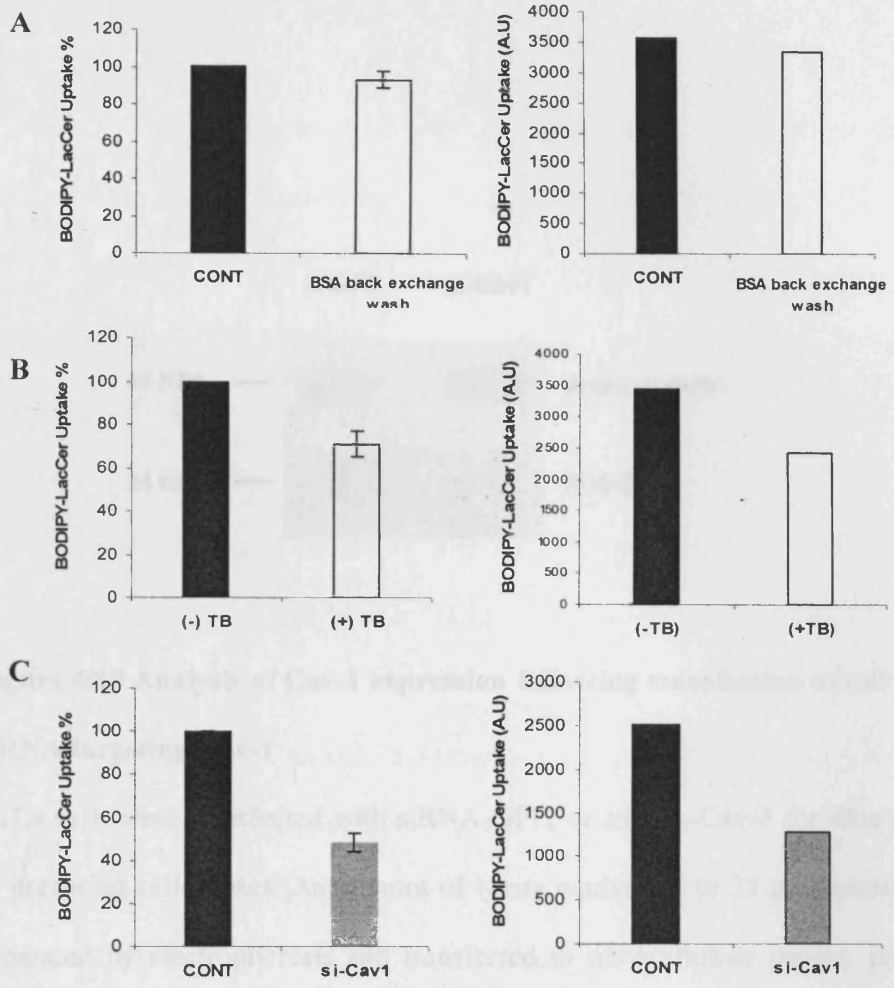

Figure 4.9. The effect of trypan blue Quenching vs. BSA back exchanged method on cell associated fluorescence and the effect of depleting Cav-1 on the uptake of of BODIPY-LacCer

HeLa cells were incubated with 1 μM BODIPY-LacCer at 10°C for 30 min then washed 3X times with SFM at 10°C, followed by incubation at 37° C for 15 min to promote endocytosis. Cells were then washed, either by BSA back exchange method **(A)** or trypan blue method **(B).** Then the cells suspension was washed with ice cold PBS, before measuring cell associated fluorescence by flow cytometry. n=3 from three independent experiments **(C)**. Cells were transfected with si-Cav-1-A, or si-GFP for 48hr, and analysed for the uptake of BODIPY-LacCer as described for A. Values above obtained from three independent experiments (n=3) and are represented in (A.U) values (right).

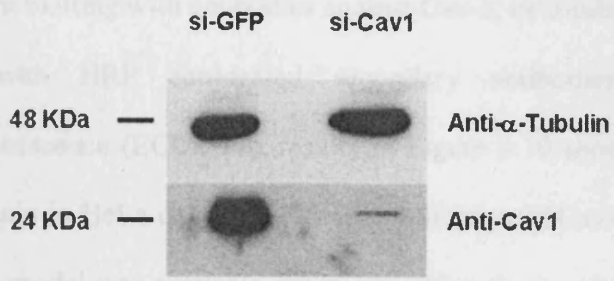

Figure 4.10 Analysis of Cav-1 expression following transfection of cell with siRNA targeting Cav-1

HeLa cells were transfected with siRNA-GFP, or siRNA-Cav-1 for 48hr prior to preparing cell lysates. An amount of lysate equivalent to 25 μg protein was separated by electrophoresis and transferred to nitrocellulose papers, probed with antibodies against Cav-1, or α-tubulin that were then detected with HRP conjugated secondary antibodies and Enhanced Chemiluminescence (ECL).

(Table 4.1). HeLa cells were transfected using siRNA against Cav-1 for 48 hrs, and then 25μg of protein from cell lysates were analyzed by SDS-PAGE and Western blotting with antibodies against Cav-1, or α-tubulin that were then detected with HRP conjugated secondary antibodies and Enhanced Chemiluminescence (ECL). The results in Figure 4.10 show clear expression of this protein in HeLa cells and efficient inhibition of Cav-1 protein. Thus a siRNA cell model was available for investigating the involvement of Cav-1 in endocytosis of the lipid raft marker Bodipy-LacCer using the earlier described method but also the two CPPs.

Previous to this all the uptake experiments are presented as time dependent uptake but the methodological issues surrounding analysis of BODIPY-LacCer uptake made this very difficult. Therefore a single time point of 15 min as previously described (Li et al. 2005a) and developed for this thesis (Figure 4.9) was utilised. HeLa cells were transfected with si-Cav-1 for 48 hrs before incubation with BODIPY-LacCer. The results in Figure 4.9.C shows that BODIPY-LacCer is inhibited by 60% in Cav-1 depleted cells, and thus providing us with a very good siRNA model to study the involvement of this protein and pathway in internalisation of CPPs.

Cells were then transfected as above with siRNA targeting Cav-1 and incubated for normal time course experiments in the presence of either Alexa488-R8 or -Tat. The data in Figure 4.11 show identical uptake of both peptides in control siRNA cells and those depleted of Cav-1. This confirms that there is no involvement of cavaeolae in uptake of these two CPPs.

It was previously shown that depleting Flot-1 from intestinal epithelial cells lead to a decrease in the expression of Cav-1 (Vassilieva et al. 2009). To test the effect of depleting Cav-1 on Flot-1 expression and vice versa, HeLa cells were transfected with siRNAs targeting GFP, Cav-1, or Flot-1 and incubated fro 48 hrs. Lysates (25μg)

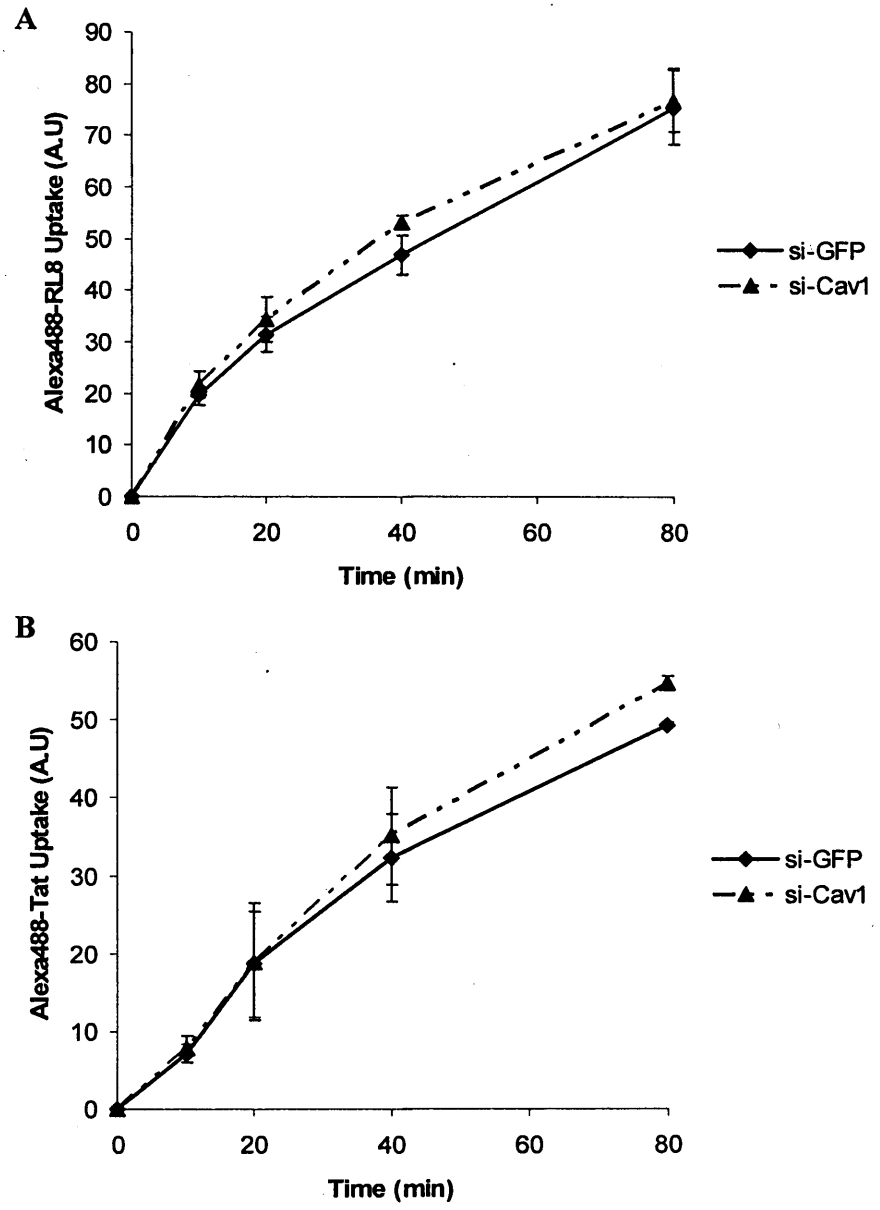

Figure 4.11. The effect of depleting Cav-1 on the uptake of of Alexa488-R8 and -Tat

HeLa cells were transfected with si-Cav-1-A, or si-GFP for 48hr, then incubated for the indicated time points with 2 μM Alexa488-R8 **(A)** or -Tat **(B)** at 37^0 C. Cells were then washed and processed for flow cytometry under standard conditions for CPP uptake. Values above obtained from three independent experiments (n=3).

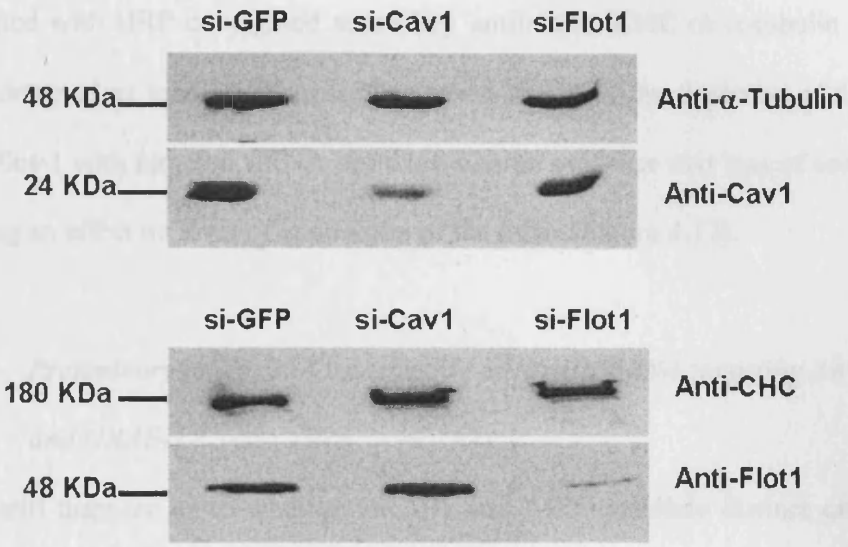

Figure 4.12. Analysis of Cav-1 and Flot-1 expression following siRNA targeting.

HeLa cells were transfected with siRNA-GFP, siRNA-Flot-1 or siRNA-Cav-1 for 48hr prior to preparing cell lysates. An amount of lysate equivalent to 25g protein was separated by electrophoresis and transferred to nitrocellulose papers, probed with antibodies against Cav-1, Flot-1, CHC or α-tubulin that were then detected with HRP conjugated secondary antibodies and Enhanced Chemiluminescence (ECL). CHC and α-tubulin were used as loading controls.

were separated by electrophoresis, transferred to nitrocellulose papers and probed with antibodies against Cav-1, Flot-1, CHC or α-tubulin that were then detected with HRP conjugated secondary antibodies. CHC or α-tubulin were also detected as loading controls. The results confirm the depletion of Cav-1 and Flot-1 with targeted siRNA but there was no evidence that loss of one was having an effect on level of expression of the other (Figure 4.12).

4.3.4. Preliminary analysis of transfecting cells with siRNA targeting ARF6 and GRAF-1

It is still disputed as to whether GRAF1 and ARF6 mediate distinct clathrin independent endocytic pathways. For example ARF6 has also been implicated in clathrin mediated endocytosis and recycling and also in phagocytosis (D'Souza-Schorey et al. 1995; Someya et al. 2010). For distinguishing these as distinct endocytic pathways researchers have studies MHC class one proteins and carboxypeptidease E (ARF6) or bacterial exotoxins and also fluid phase markers (Doherty and McMahon 2009). Though these are interesting findings it was not clear as to what endocytic probe to use and time did not allow for extensive analysis that was performed for other endocytic pathways.

siRNA sequences against these two proteins were however acquired (Table 4.1) and tested to see if they could deplete these proteins. Methods were initially developed for detecting the proteins in HeLa cells using Western blotting and this then allowed for siRNA targeting experiments and the combined results are shown in Figure 4.13. A single band was detected for ARF6 at the correct molecular weight of approx. 23KDa and this could not be detected in siRNA ARF6 treated cells. Two bands were detected for GRAF1

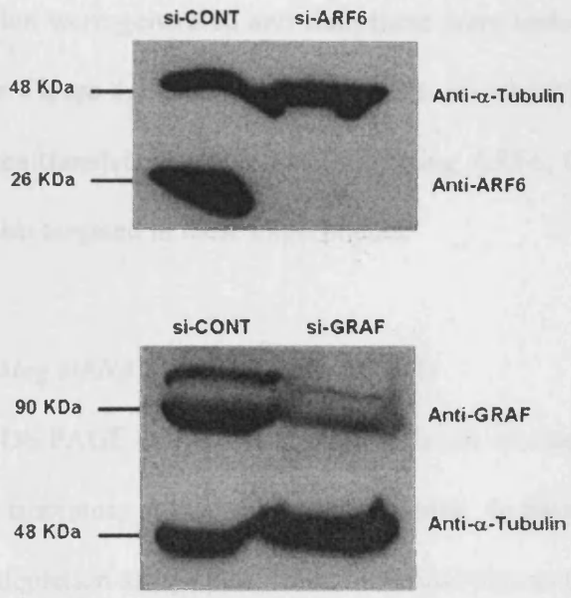

Figure 4.13. Analysis of ARF6 and GRAF1 expression in ARPE following transfection with siRNA.

ARPE cells were transfected with siRNA-GFP, siRNA-ARF6, or siRNA-GRAF1 for 72hr prior to preparing cell lysates (Ghent samples). An amount of lysate equivalent to 20 μg protein were separated by electrophoresis, transferred to nitrocellulose papers, probed with antibodies against ARF6, GRAF1, or α-tubulin that were then detected with HRP conjugated secondary antibodies and Enhanced Chemiluminescence (ECL).

and both were reduced significantly in siRNA GRAF1 treated cells but there was still residual expression. Thus cell models for either full depletion or partial depletion were generated and then these were tested for internalisation of R8. Data in Figure 4.14 shows that there was no inhibition on the uptake of R8 in cell lines transfected with siRNA targeting ARF6, GRAF-1, Cav-1 and DNM2 was also targeted in these experiments.

4.3.5. Analysing siRNA targeting in ARPE cells

Performing SDS PAGE and Western Blotitng is not routinely performed at our collaborating laboratory at the University of Ghent. In parallel with our studies were siRNA depletion assays performed on retinal pigment epithelial cells. For this thesis methods were developed for detection of CHC, Flot-1, Cav-1, DNM2 and Pak-1 in HeLa and A431 cells (chapter 3, 4, and 5). These methods were then used to detect protein expression from siRNA experiments performed in Ghent. Typically this would involve the sending over of cell lysates for electrophoresis and immunodetection. Figure 4.15 is taken from Dries et al (Vercauteren et al. 2011) showing data from analysis performed as part of this thesis. The data specifically highlights the problems in a separate cell line in depleting DNM2. Interestingly rather than observing that Flot-1 depletion indirectly reduces Cav-1 expression as previously described (Vassilieva et al. 2009), the opposite was determined in that Cav-1 depletion led to a significant decrease in Flot-1 expression.

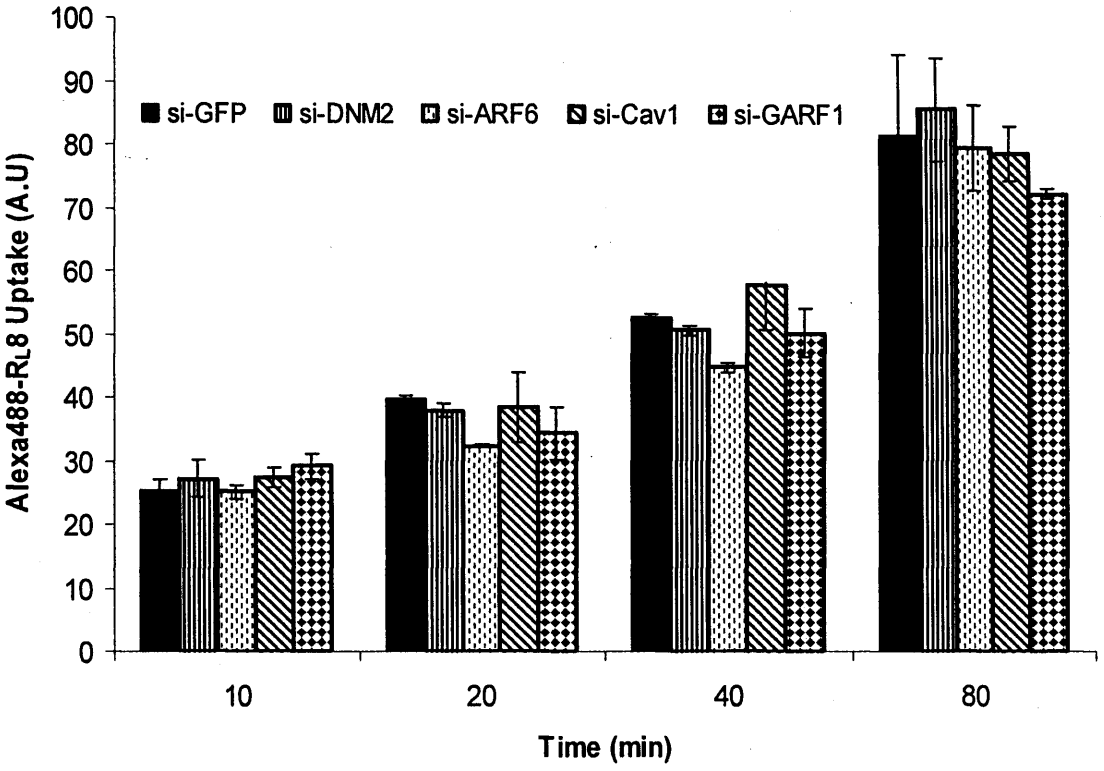

Figure 4.14. The effect of depleting DNM2, ARF6, Cav-1, and GRAF1 on the uptake of of Alexa488-R8.

HeLa cells were transfected with si-GFP, si-DNM2-C, si-ARF6, si-Cav-1-A, or si-GRAF1 for 48hr, then incubated for the indicated time points with 2μM Alexa488-R8 at 37^0 C for the indicated time points. Cells were washed, trypsinized and processed for flow cytometry under standard CPP conditions. Values above obtained from two independent experiments (n=2).

4.4. Discussion

In this chapter endocytic pathways regulated by DNM2, Flot-1 and Cav-1 were investigated with a view to silencing the proteins using siRNA and investigating the effects of this depletion on uptake of endocytic probes and finally CPPs. Dynamin II, was originally identified as a protein regulating CME, but it has also been associated in regulating uptake through other endocytic pathways including those regulated by Cav-1 and more recently was associated in regulating constitutive fluid phase uptake using 70 KDa dextran as a marker (Cao et al. 2007). It was the later data that was of most interest to us as it gave a possibility of measuring the fraction of CPPs that enter via fluid phase endocytosis. Different published single and pooled siRNA sequences (Table 4.1) failed to give effective depletion in HeLa cells (>50%) such that its role in mediating CPP uptake could not be investigated. Problems of depleting this protein using siRNA was also noted in collaborative studies with the University of Ghent (Vercauteren et al. 2011). This proved to be a major problem and a great deal of time was lost in before the decision was taken to move to a different cell line, namely A431 cells. Here for the first time DNM2 was effectively and consistently depleted to <20%. In these DNM2 depleted A431 cells a strong inhibition of transferrin uptake was shown, however fluid phase endocytosis of dextran was unaffected, and this completely contradicts an earlier study that directed our studies towards this protein (Cao et al. 2007). The reason for this is unknown but it should be noted that we observed very strong depletion of transferrin uptake in siRNA DNM2 cells thus proving that there was an effect on endocytosis. Similarly there was no effect on the uptake of either Alexa488-R8 or -Tat in DNM2 depleted cells thus confirming the

earlier results with CHC depletion, which similarly showed no effect on CPP uptake. A431 and HeLa cells were also incubated with Dynasore, a DNM1 and DNM2 inhibitor and this drug as expected was a strong inhibitor of CME but had no effect on uptake of Dextran or Alexa488-R8 and -Tat in HeLa cells. In spite of the strong functional effects of DNM2 depletion on CME, its involvement in fluid phase uptake or internalisation of these cationic peptides was not confirmed.

An assay was developed for analysing anti- CD59 antibody and in line with a previous study (Glebov et al. 2006) it was found that uptake of this probe was reduced in cells depleted of Flot-1. It was, however, far from complete inhibition but highly consistent and significant ($P<0.05$) after 10 min uptake. The data highlight that a major fraction of this protein also enters cells independent of the requirement of Flot-1. It must be noted here that the level of inhibition observed in this thesis is entirely consistent with that observed in the first study to highlight a role for Flot-1 in mediating a distinct endocytic pathway (Glebov et al. 2006). It has been more recently shown that Flot-1 depleted cells have reduced endocytosis of polyethylenimine/DNA complexes and disulfide-based poly(amido amine)/DNA polyplexes (Payne et al. 2007; Vercauteren et al. 2011). For the later study it was also shown that Flot-1 depleted cells were also more difficult to transfect with plasmid DNA. It will be interesting to test this further as these polymers may be more suitable probes compared with anti-CD59 antibody to analyse the involvement of this pathway. From our initial studies it was clear that analysing the uptake of this antibody was not a trivial issue but by employing additional acid washing it was possible

to more accurately measure internalised antibody. There are alternative sources of commercial anti-CD59 antibodies and it would be interesting to test these. As methods were developed for analysing protein depletion using immunodetection and functionally in endocytosis assays it was then possible to investigate the effects of Flot-1 depletion on uptake of CPPs Tat and R8. The data clearly shows that this pathway is not involved in their uptake.

Caveolin-1 labels flask shaped invaginations on the plasma membrane of cells called caveolae that upon splitting from the plasma membrane form caveosomes (Nabi and Le 2003). The sphingolipid lactosylceramide has been shown to be internalised from the plasma membrane in a clathrin independent mechanism involving cavaeolae (Singh et al. 2003; Vassilieva et al. 2009). GFP-Tat peptide was shown to be localized to caveaolae suggesting this may be an uptake route preferred by this peptide (Ferrari et al. 2003; Fittipaldi et al. 2003). In addition siRNA depletion of Cav-1 from HeLa cells or the use of caveolin-1 knockout (Cav-$1^{-/-}$) mouse embryonic fibroblasts cells suggested a role for cavaeolae in uptake of transportan-avidin complexes (Saalik et al. 2009). Blood cells such as the K562 cells that our laboratory have used for CPP studies are also Cav-$1^{-/-}$ and these internalise CPPs such as R8 and Tat very efficiently (Al-Taei et al. 2006). This suggests that caveolae are not absolutely required for CPP uptake but it may be the case that in Cav-1 positive cells this pathway is utilized. As cavaeolae are enriched in lipid rafts, cholesterol sequestering drugs such as MßCD and nystatin are used to disrupt these domains prior to performing endocytosis assays. However loss of

integrity of these domains has multiple effects on cells and can affect a number of endocytic pathways (Rodal et al. 1999). In addition is has been shown that results with CPPs and, for example, MßCD are very difficult to interpret as the effects depend on the CPP concentration (Duchardt et al. 2007). Previous studies from our lab also highlight the problems of using this drug for CPP uptake studies (Watkins et al. 2009b).

In order to study this pathway it was important to confirm the presence of Cav-1 expression and this was clearly confirmed in HeLa cells; this is in agreement with other publications (Simon et al. 2009a; Spoden et al. 2008). siRNA depletion was very successful here and this then allowed us to develop a functional assay for Cav-1 depletion. We made use of the BODIPY LacCer but as for CD59 antibodies problems were encountered due to extensive partitioning of this lipid into the plasma membrane that was then very difficult to remove. This has previously been documented and rigorous washing methods including lipid extraction a been employed to reduce this fraction (Aoki et al. 2010; Chen et al. 1998; Li et al. 2005a; Marks et al. 2005; Vercauteren et al. 2010). Here trypan blue quenching proved to be the most effective method for reducing the plasma membrane bound fraction and once this method had been optimised, it has moved on to look at the effects of depleting Cav-1 on the uptake of this probe. Investigating LacCer uptake assay at multiple time points in control siRNA and Cav-1 depleted cells proved to be technically difficult and therefore a single time point (15 min) was selected. LacCer uptake was however significantly depleted in Cav-1 depleted cells and this is the first time that this has been determined experimentally. However

these cells had control levels of internalised Alexa488-R8 and –Tat and together with data from Cav-1 negative leukameic cell lines this suggested strongly that cavaeole were not required for uptake, even if expressed.

Recent data has shown that down-regulation of Flot-1 expression, which disrupted lipid raft-mediated endocytosis of BODIPY FL C(5)-lactosylceramide, also significantly decreased Cav-1 levels in SK-CO15 human intestinal epithelial cells. They revealed that the decrease in caveolin-1 expression is specifically related to Flot-1 depletion as they did not observe the same results after down-regulating Flot-2. They also show that the decrease in Cav-1 levels in Flot-1-depleted cells was not due to suppression of its mRNA synthesis and was not mimicked by cholesterol depletion. In addition, they show that Flot-1 dependent down-regulation of Cav-1 was reversible after exposing cells to a lysosomal/acidification inhibitor such as chloroquine. They suggest that Flot-1 regulates Cav-1 level by preventing its lysosomal degradation in intestinal epithelial cells. In contrast, the data in this chapter revealed that Flot-1-depleted HeLa cells have control level of Cav-1 expression and vice versa. In contrast to these two sets of data, the studies in Ghent, suggested an alternative relationship between the two proteins as depleting Cav-1 also led to a reduction in Flot-1 levels. This may suggest some relationship between these proteins and the pathways that they regulate but how one regulates the other remains to be fully determined.

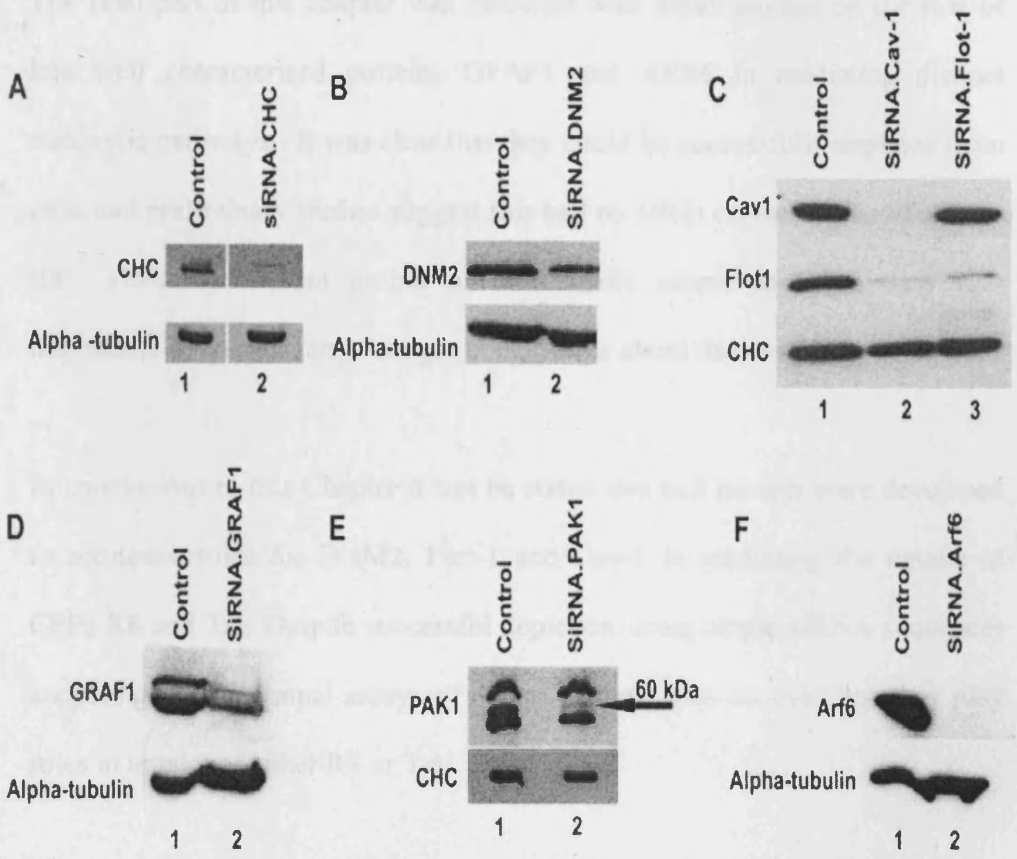

Figure 4.15. siRNA depletion of endocytic proteins in ARPE cells

All siRNA experiments were performed at the University of Ghent (Vercauteren et al. 2011) and lysates sent to Cardiff for analysis. For (A), (B), (D) and (F) the expression of α-Tubulin served as an internal control for equal protein loading, while CHC expression levels were used as a reference in (C) and (E). In (E), the (depleted) PAK-1 band at approx. 60 kDa is marked with a black arrow.

The final part of this chapter was involved with initial studies on the role of less well characterised proteins GFAF1 and ARF6 in mediating distinct endocytic pathways. It was clear that they could be successfully depleted from cells and preliminary studies suggest this had no effect on the uptake of at least R8. However without probes to functionally assess depletion then it is impossible to come to any stronger conclusions about this work.

In conclusions to this Chapter it can be stated that cell models were developed to scrutinise roles for DNM2, Flot-1 and Cav-1 in mediating the uptake of CPPs R8 and Tat. Despite successful depletion using single siRNA sequences and design of functional assays of depletion there was no evidence they play roles in uptake of either R8 or Tat.

Chapter 5: Evaluation of the role of Macropinocytosis in the cellular uptake of CPPs Tat and R8

5.1. Introduction

Macropinocytosis is an actin-dependent and growth factor induced process that associated with plasma membrane ruffling lead to intrnalization of fluid and macromolecules. It has however also been termed a constitutive process and there is much confusion regarding this definition of the process and the most characterised response to growth factor activation (Jones 2007b). These, such as epidermal growth factor (EGF) and platelet derived growth factor (PDGF) (Brunk *et al.*, 1976; Hewlett *et al.*, 1994) are known to activate signalling pathways when they bind to their receptors leading to activation of Rac GTPase, which has been shown to regulate actin dynamics and therefore macropinocytosis that in its own right is dependant on actin rearrangement (Ridley *et al.*, 1992). P21-Activated Kinase (PAK-1) is reported to have a role in regulating macropinocytosis and has been shown to induce the formation of circular dorsal ruffles similar to those associated with the macropinocytic uptake process (Liberali et al. 2008; Mercer and Helenius 2010). It has been shown that endogenous PAK-1, identified with PAK-1 antibody, localized to pinocytic vesicles containing BSA-rhodamine, a marker for bulk fluid-phase uptake, while the distribution of PAK-1 in PDGF stimulated cells was detected in membrane ruffles and at the edges of lamellipodia. Moreover, treatment of the PDGF-stimulated cells with either cytochalasin D or wortmannin caused the complete loss of membrane ruffles, and the absence of the membrane-associated PAK-1 observation (Dharmawardhane et al. 1997). Another study showed that inhibition of endogenous PAK-1 activity using a PAK-specific autoinhibitory domain blocks growth factor-induced macropinocytosis, indicating that PAK activity is required for this process. Furthermore, the study

revealed that PDGF-stimulated macropinocytosis is enhanced by activated PAK-1 mutants (Dharmawardhane et al. 2000). These data strongly indicate a regulatory role for PAK-1 in the macropinocytic process, involving PAK-1 kinase activity and downstream cytoskeletal remodelling.

In recent studies investigating internalisation of mainly cationic CPPs, macropinocytosis has emerged as a strong candidate for the mechanism of uptake (Kaplan et al. 2005; Nakase et al. 2004; Suzuki et al. 2002; Wadia et al. 2004). Additionally different studies show that the activation of Rac1 and organization of the actin is induced by arginine-rich CPPs and that this is the trigger for macropinocytosis or a macropinocytosis-like pathway (Gerbal-Chaloin et al. 2007; Nakase et al. 2007). In line with this cationic CPPs have been demonstrated to enhance the uptake of fluorescent dextran suggesting some of their effects may be similar to the actin rearranging properties of growth factors (Gump et al. 2010; Wadia et al. 2004).

It should however be noted that all studies here have used pharmacological inhibitors of endocytic pathways as study tools and the most common such as CytD, amiloride and amiloride analogues have other effects on cells. There is therefore a strong requirement for a protein target regulating macropinocytosis to be targeted with the hope that this can reveal the true requirement of this process in uptake of CPPs and also other drug delivery vectors (Sahay et al. 2010).

Due to the fact that CPPs are thought to enter cells by macropinocytosis and that PAK-1 regulates this process the studies in this Chapter concentrated on

initial characterisation of PAK-1 expression and macropinocytosis in different cell types. Once this was achieved the role of this pathway and in uptake of R8 and TAT was investigated in cells depleted of PAK-1.

5.2. Methods

Both HeLa and A431 cells were used to study different aspects of macropinocytosis. Cells were transfected with two different PAK-1 siRNA sequences as shown in Table 5.1; siRNA targeting GFP was used as control.

To study the role of macropinocytosis in dextran internalisation, different dextran conjugates were used: Alexa488-Dextran (10 kDa), FITC-Dextran (40 kDa), and TMR-Dextran (70 KDa). These were incubated with cells either alone or in the presence of CPPs or following stimulation by EGF. The full methods are given in section 2.3.5.6

In order to, characterize the involvement of macropinocytosis in Alexa488-R8 and -Tat uptake, 2 μM of extracellular CPP was added to PAK-1 depleted HeLa and A431 cells following pre-incubation with macropinocytosis inhibitors such as cytochalasin D (CytD), blebbistatin (Blebb) and 5-(*N*-ethyl-*N*-isopropyl) amirolide (EIPA). The full methods are given in section 2.3.5.5 and 2.3.5.4

SDS-PAGE electrophoresis and Western blotting techniques were used to detect PAK-1 and EGFR, expression levels. The full methods are given in section 2.3.7 and 2.3.8

siRNA	Sequences	Ref.
PAK-1-A	AACUUCUCUUGACGUUGACdTdT	(Mercer and Helenius 2008)
PAK-1-B	AUAACGGCCUAGACAUUCAdTdT	Designed by MWG
GFP	GGCUACGUCCAGGAGCGCAdTdT	Designed by MWG
CHC	UAAUCCAAUUCGAAGACCAAUdTdT	(Motley et al. 2003)

Table 5.1. siRNA sequences used in this Chapter

5.3. Results

5.3.1. EGFR and PAK-1 expression in HeLa and A431 Cells

It was initially important to establish a macropinocytosis model and traditionally this has been performed in cells with high levels of EGFR or PDGFR so that they can then be stimulated with growth factors. However our initial CPP model was HeLa cells and comparisons were made of the expression of EGFR in these cells and a well described EGFR high-expressor, A431 cells. At the same time the levels of PAK-1 was determined. SDS-PAGE electrophoresis and immunolabeling methods were therefore developed (sections 1.3.7 & 1.3.8) to detect the expression level of EGFR and PAK-1 from cell lysates. The data shows that EGFR could not be detected in HeLa cells using this method and exposure, but a strong single band at approximately 180KDa was observed in A431 cells (Figure 5.1.A). PAK-1 was detected in both cell lines at the predicted mass of 60 KDa, however three bands were detected with the antibody at both lower and higher molecular weight than predicted. Similar to expression of EGFR the A431 cells had much higher expression of PAK-1 compared with HeLa cells. The two faint bands higher than the predicted mass were not always observed as can be seen later.

Two different siRNA sequences were selected for depleting PAK-1 in these cells. Cells were transfected with 50nM of these sequences and then PAK-1 was detected following SDS-PAGE and immunoblotting. Figure 5.1.C shows highly effective PAK-1 depletion in A431 cells, while partial depletion was observed in HeLa cells (Figure 5.1.B). Note in Figure 5.1.C that only the lower band is depleted and the higher band can then act as a positive loading control and α-Tubulin staining was used to confirm these results. In HeLa cells CHC

was used as a loading control but there was evidence that both detected bands were reduced in PAK-1 depleted cells.

Repeat experiments showed a consistent reduction of over 90% expression in A431 cells (Figure 5.2). Two PAK-1 siRNA sequences were tested here, si-PAK-1-A and –B. si-PAK-1-A was obtained from a previous publication (Mercer and Helenius 2008) but there was concern that depletion by this sequence was not sufficient to then perform functional assays. si-PAK-1-B, which was predesigned by MWG was then investigated and found to consistently reduce PAK-1 levels to <10% (Figure 5.2)

In order to investigate these findings further repeat transfections were performed on cells plated on coverslips. Following 48 hr transfections the cells we fixed and then labelled with anti-PAK-1 antibody and Alexa-488 labelled secondary antibodies (Section 2.3.4.3). This was the first time that the laboratory had used immunofluorescence to investigate the distribution of this protein in any cell line and of note was the localisation of the protein to large amorphous structures in control cells and there was little evidence of plasma membrane labelling but there was significant labelling of the nucleus (Fig. 5.3). In PAK-1 depleted cells there was a clear reduction cell associated fluorescence, indeed it was very difficult to observe any staining.

5.3.2. Stimulation of uptake of the fluid phase marker dextran in response to growth factor stimulation

In order to study the macropinocytosis process, it is essential to find a specific endocytic probe for this pathway. Unfortunately, none as yet exists however it

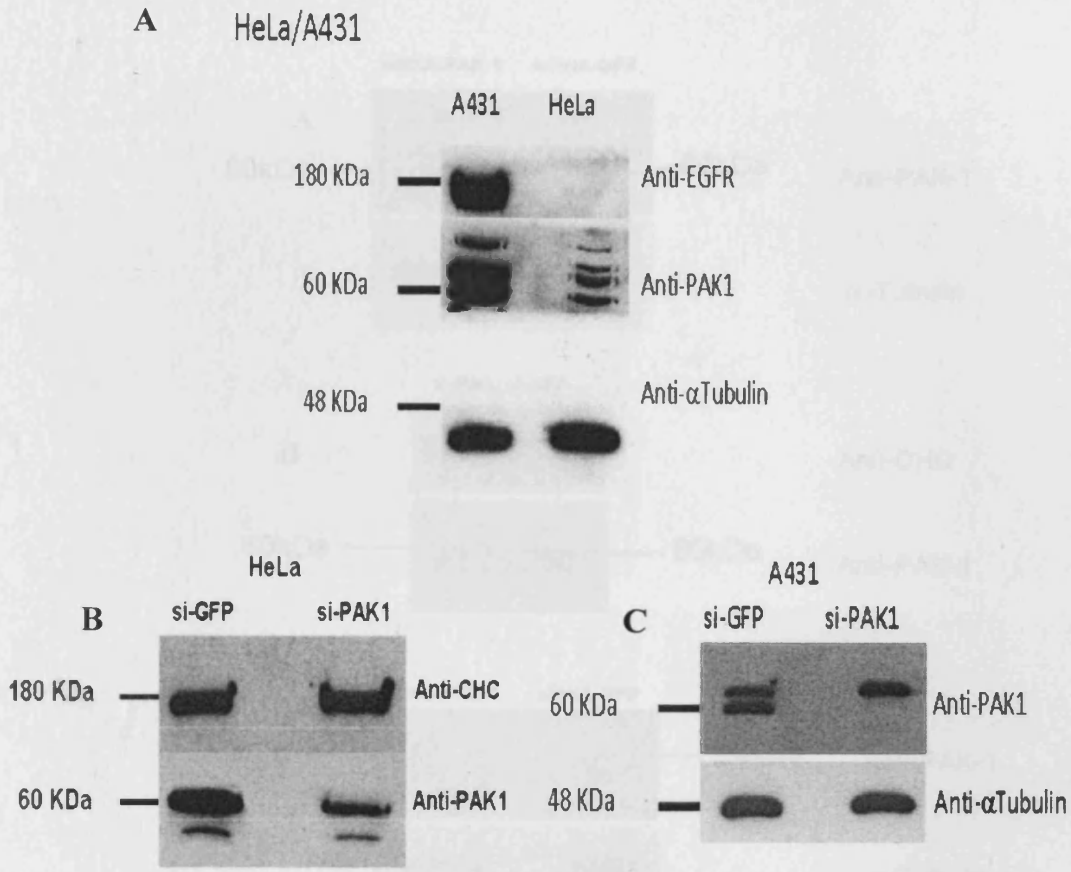

Figure 5.1. EGFR expression in A431 cells and PAK-1 depletion via siRNA targeting.

(A) Lysates from HeLa or A431 cells were separated by electrophoresis and proteins transferred to nitrocellulose papers that were probed with antibodies recognizing PAK-1, EGFR or tubulin that were then detected with HRP conjugated secondary antibodies and Enhanced Chemiluminescence (ECL). HeLa (B) or A431 (C) cells were transfected for 48 hrs with siRNA targeting PAK-1 using si-PAK-1-A (B) and si-PAK-1-B (C) and lysates were separated by electrophoresis and proteins transferred to nitrocellulose papers that were probed with antibodies recognizing PAK-1, EGFR CHC, or α-tubulin that were then detected with HRP conjugated secondary antibodies and Enhanced Chemiluminescence (ECL). CHC and α-tubulin antibodies were used as loading controls.

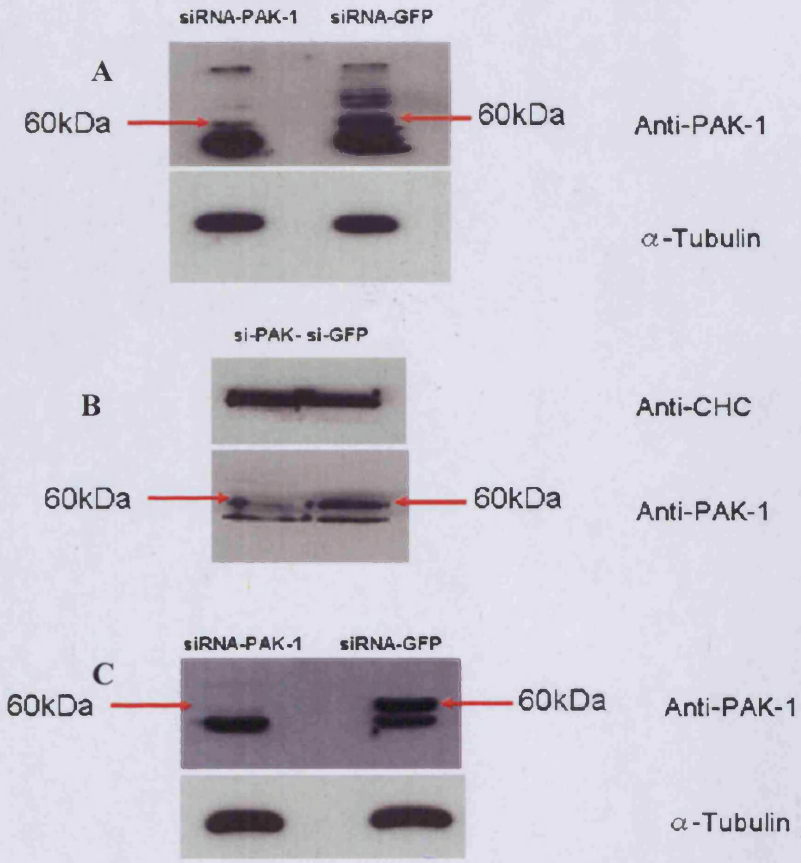

Figure 5.2. Analysis of PAK-1 following siRNA targeting in A431 cells.

A431 cells were transfected for 48 hrs with siRNA targeting PAK-1 and lysates were separated by electrophoresis and proteins transferred to nitrocellulose papers that were probed with antibodies recognizing PAK-1, CHC, or α-tubulin that were then detected with HRP conjugated secondary antibodies and Enhanced Chemiluminescence (ECL). CHC and α-tubulin antibodies were used as loading controls. (A), (B), and (C) are all obtained from si-PAK-1-B and they represent 3 independent experiments.

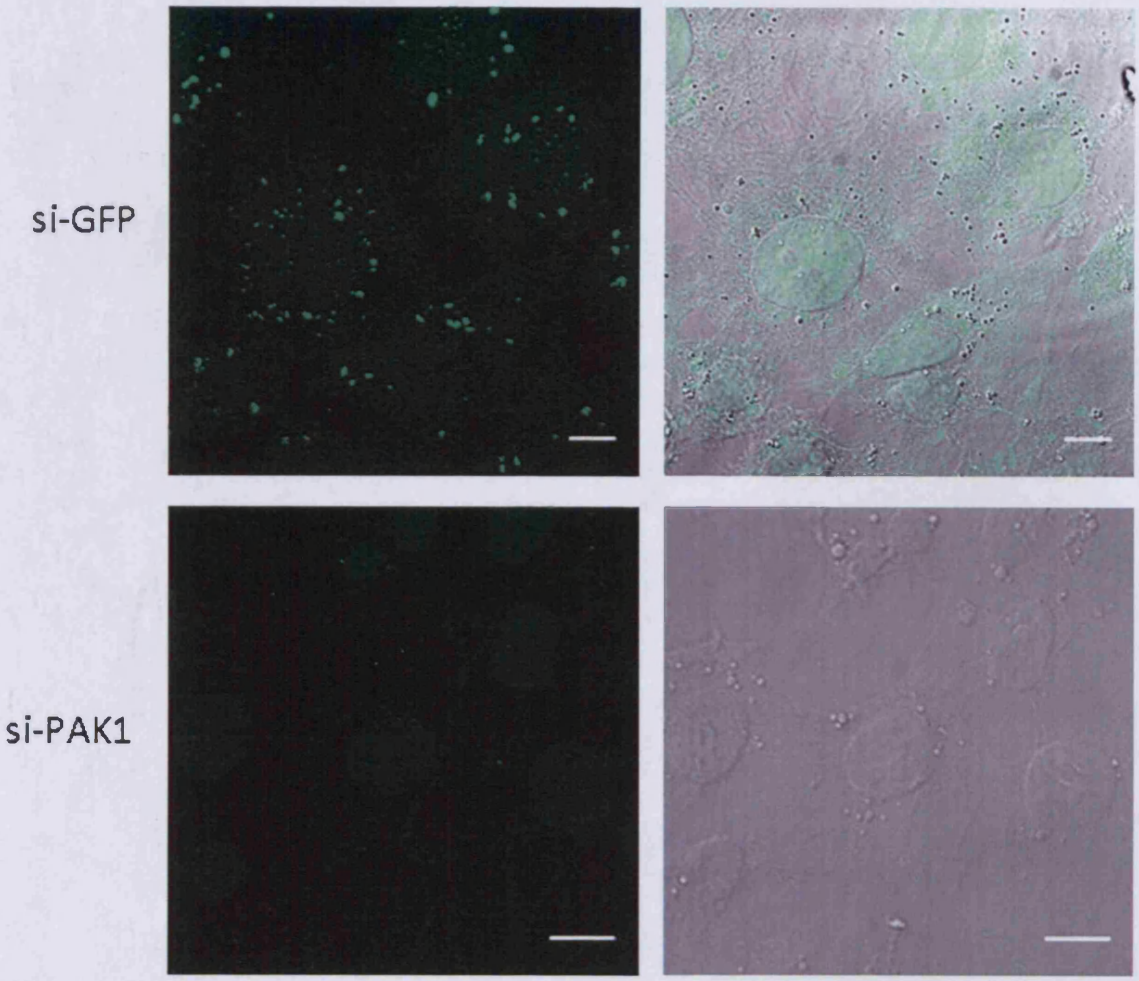

Figure 5.3. PAK-1 immunolabelling in si-GFP vs. si-PAK-1 transfected A431 cells.

A431 cells were transfected with si-GFP or with is-PAK-1 for 48hr, then washed and fixed with 3% PFA, followed by washing and immunolabelling with PAK-1 antibody. Confocal images shown, represent maximum projection images (left) and direct interference contrast (DIC) images (right) of the same cells. Scale bars = 20μm.

is known that growth factor binding activates the pathway and leads to a concomitant increase in the uptake of fluid phase markers such as dextran (Dharmawardhane et al. 2000). Therefore, experiments were performed to investigate whether an increase in dextran uptake could be observed in both HeLa and A431 cells and specifically whether this could be inhibited in PAK-1 depleted cells. Initially, dextran uptake in EGF treated cells was tested under two conditions, serum starvation and non-starvation. Non-starved HeLa cells and A431 cells were incubated with either 5 mg/ml FITC-Dextran or 0.2 mg/ml Alexa488-Dextran with and without 50 nM EGF in Ringer's buffer for 0-80 min. Then cells were washed (including acid washing) prior to trypsinisation and analysis of internalised dextran by flow cytometry. Figure 5.4 shows that EGF did not cause an increase in dextran uptake when cells were incubated with EGF. The same experiments were then performed in serum starved cells (1hr) and here there was a significant increase in dextran uptake in serum starved A431 cells incubated with EGF (Fig. 5.5.A). In HeLa cells growth factor addition had no effect on the uptake of this probe even when they were serum starved (Fig. 5.5B). The results confirms that cellular starvation is an essential step to initiate and stimulate EGF induced macropinocytosis process, however HeLa cells are not responsive to this growth factor in terms of macropinocytosis and as discussed later this may be due to the low levels of EGFR in this cell line.

5.3.3. Effect of depleting PAK-1 expression on macropinocytosis

Initially, A431 cells were transfected with 50 nM of siRNA against GFP and PAK-1 for 48 hrs. Cells were then starved for 1 hr prior to incubation with 5

mg/ml of FITC-dextran with or without EGF as previously described. The cells were subsequently washed and trypsinised prior to analysis of dextran uptake by flow cytometry. The results in Figure 5.6 show that by depleting PAK-1, the EGF stimulated uptake of dextran is inhibited by 25% approximately after 40 min and by ~30 % at 80 min but not at earlier time points and there was also a very minor inhibition in the basal uptake of dextran but this was not statistically significant (Figure 5.6.A). The uptake of FITC-dextran was also examined in PAK-1 depleted HeLa cells, without EGF stimulation (Figure 5.6.B). The data again shows some inhibition in the basal uptake of dextran but this was not significant as $P > 0.05$. From these experiment it was decided to use the A431 cells as a macropinocytosis model allowing for comparison of the effects of EGF vs CPPs.

Macropinocytosis is actin-dependent and therefore the distribution of actin in PAK-1 depleted cells was investigated by confocal microscopy. A431 cells were transfected for 48 hrs with si-PAK-1-B and - GFP as previously described and then fixed with and incubation with with rhodamine-phalloidin, to stain actin. As shown in Figure 5.7 actin in control cells is localized to long filaments and also on the periphery of the cells. However in PAK-1 depleted cells there is a lack of filamentous actin and the staining is concentrated on the periphery of the cells and also in a perinuclear region. The cells are also significantly smaller than control

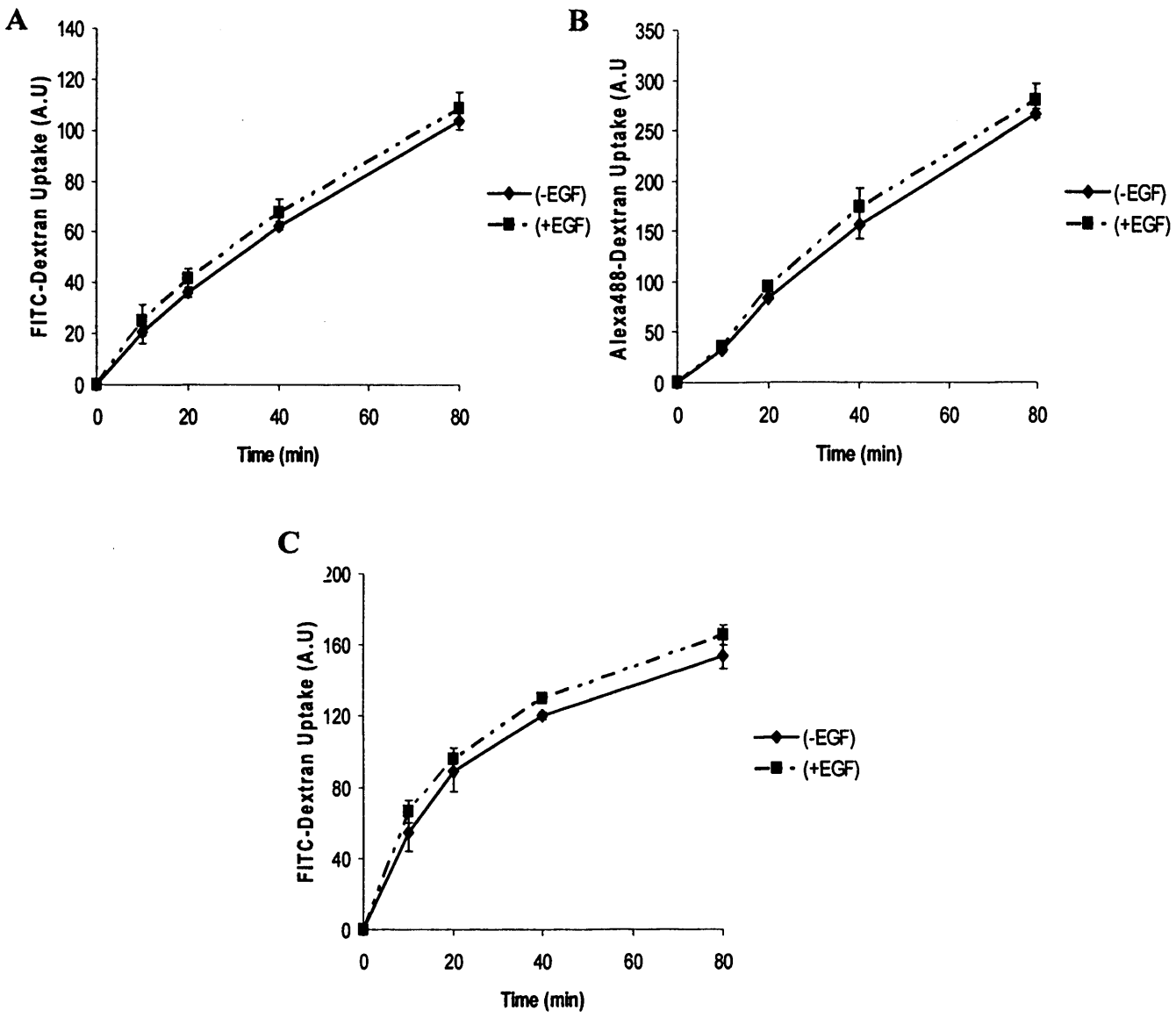

Figure 5.4. Effect of EGF stimulation on dextran uptake in serum non-starved cells.

HeLa cells **(A & B)** and A431 cells **(C)** were incubated with either 5mg/ml FITC-dextran or 0.2mg/ml Alexa488-Dextran +/- 50nM EGF at 37^0 C, prior washing and analysis by flow cytometry. Results represent data from three independent experiments (n=3).

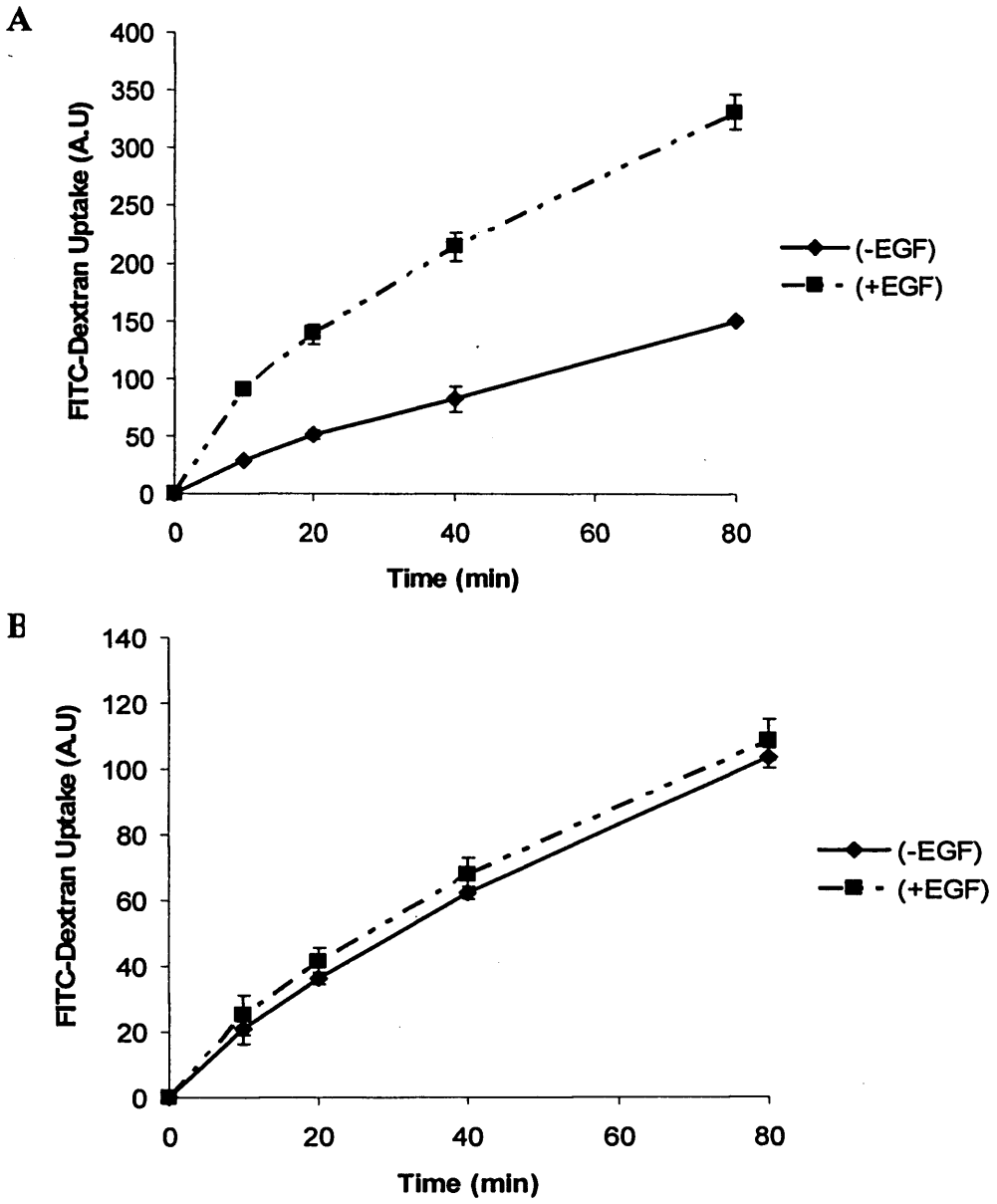

Figure 5.5. Effect of EGF stimulation on dextran uptake in serum starved cells.

A431 cells **(A)** and HeLa cells **(B)** were serum starved in Ringer's buffer for 1 hr then incubated with 5mg/ml FITC-dextran +/- 50nM EGF at 37^0 C, prior washing and analysis by flow cytometry. Results represent data from three independent experiments.

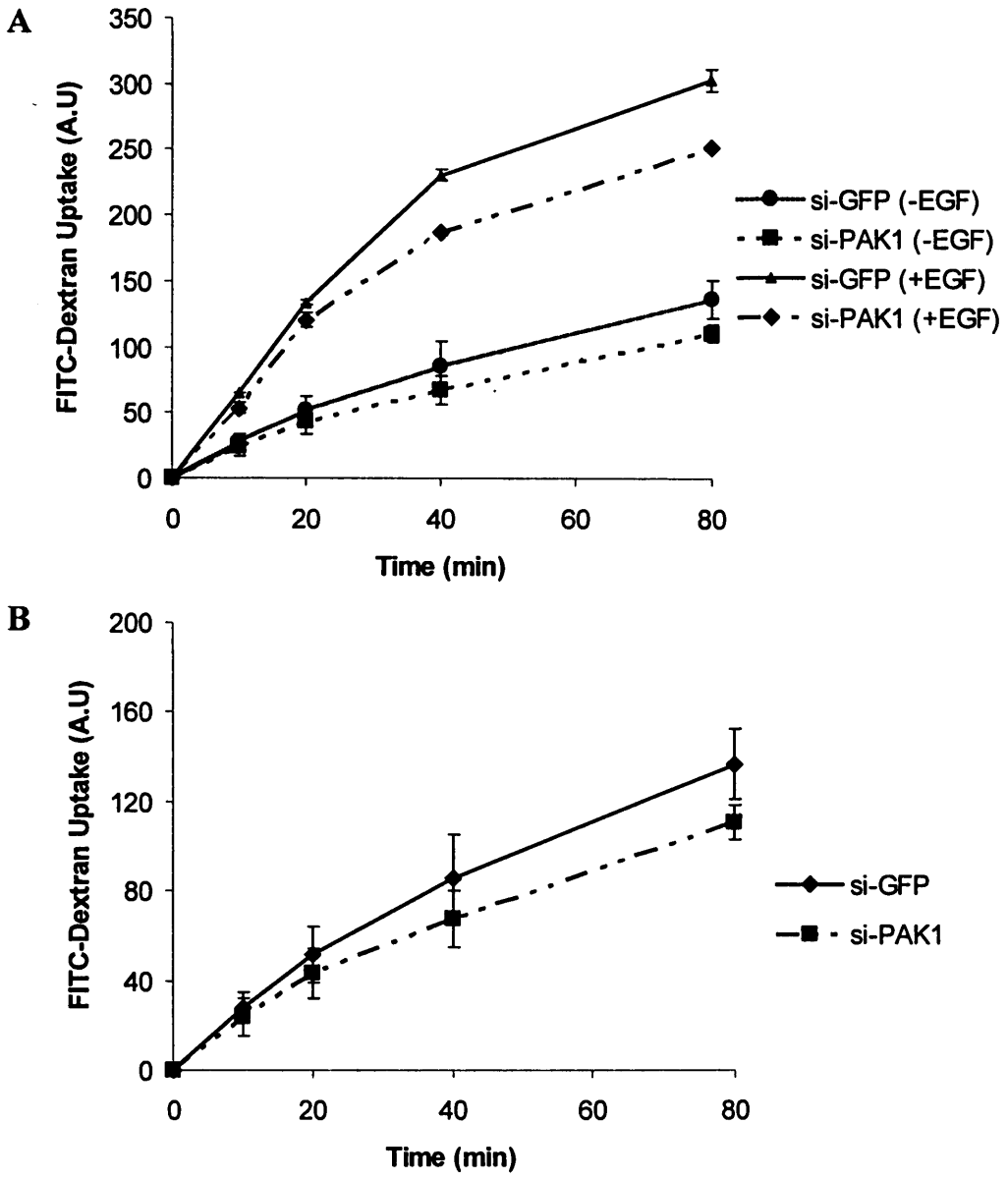

Figure 5.6. Evaluation of dextran internalisation in PAK-1 depleted cells. A431 cells **(A)** and HeLa cells **(B)** were transfected with si-GFP or si-PAK-1 for 48hr, then incubated for the indicated time points with 5mg/ml FITC-dextran +/- 50 nM EGF at 37^0 C before washing and analysis by flow cytometry. The data represents cell associated fluorescence for three independent experiments (n=3).

5.3.4. Characterisation of the requirement for PAK-1 in cellular uptake of Alexa488-R8 and –Tat

Previous studies have reported that macropinocytosis is involved in the endocytic uptake of CPPs and this is mainly based on the use of pharmacological inhibitors such as EIPA (Nakase et al. 2004; Wadia et al. 2004). Thus, the uptake of both Alexa488-R8 and -TAT were investigated further using siRNA depletion of PAK-1 compared with pharmacological inhibition.

The two cell-lines were transfected with si-PAK-1-B or with control -GFP for 48 hrs, then incubated with 2μM Alexa488-R8 or –TAT for different periods prior to trypsinisation, heparin washing and flow cytometry (Figure 5.8). The data in HeLa cells (Figure 5.8 A-B) show a slight reduction in uptake of both peptides but this was not significant but in A431 cells the there was a much stronger inhibition and this was statistically significant at $P<0.05$ (Figure 5.8 C-D). Traditionally results from these types of experiments are presented as percentage of controls and Figure 5.8.C shows how this same data set would appear as a comparison for each time point of the equivalent siRNA control. The uptake of Alexa488-R8 was inhibited approximately 50 % at early time points < 20 min and by 30-40 % after 20 min (Figure 5.8.E). Alexa488-Tat uptake was inhibited by 30 % for early rime point <20 and at later time point the percentage inhibition increased to 55% and then decreased; again the inhibition was significant at $P <0.05$ (Figure 5.8.F).

5.3.5. Analysing the capacity of CPPs to induce uptake of dextran.

The previous experiments had shown that the uptake of R8 and Tat could be inhibited in PAK-1 depleted cells but the capacity of these two peptides to stimulate macropinocytosis was yet to be determined. To investigate this effect, two different types of neutral dextran conjugates were used: 40 KDa FITC-, and 70 KDa TMR-dextran at 5mg/ml and 0.75 mg/ml respectively. Initially, cells were incubated for 1 h at 37°C in serum-free Ringer's buffer (serum starved), then incubated in Ringer's buffer containing the dextran conjugate and either 2μM unlabeled R8 or Tat for different incubation periods. Figure 5.9.A (HeLa cells) and Figure 5.9.B (A431 cells) shows no-significant increase in FITC-dextran uptake as a result of CPP incubation. When A431 cells were incubated with CPPs and 70 KDa TMR dextran both were able to promote significant uptake of the probe (Figure 5.9.C). The results from this experiment are also represented as percentage of controls (Figure 5.9.D).

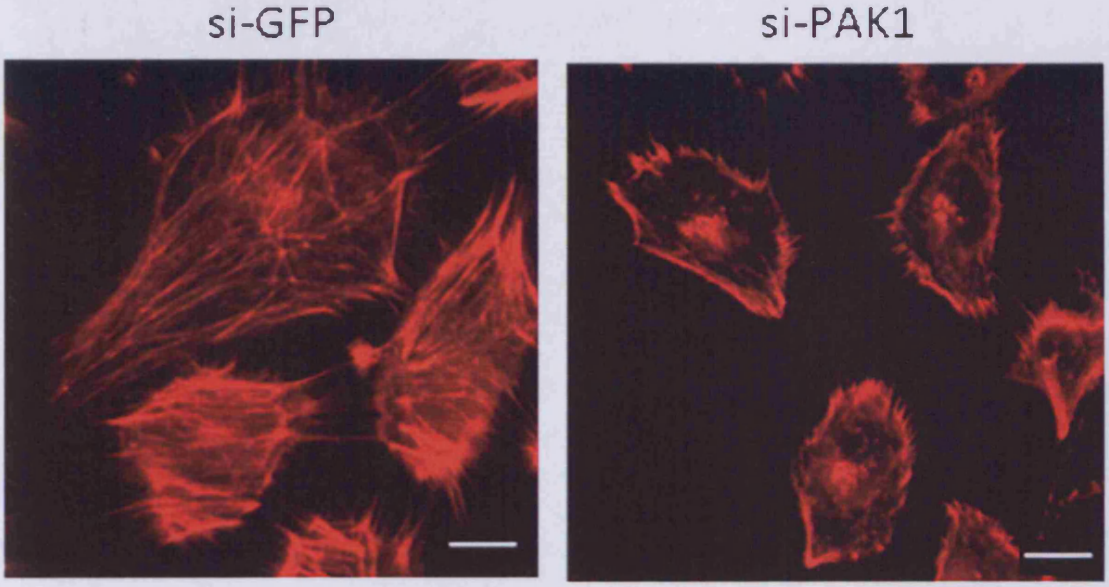

Figure 5.7 Effect of depleting PAK-1 on cellular actin distribution.

A431 cells were transfected with si-GFP or si-PAK-1 for 48hr, then washed fixed and labelled with rhodamine-phalloidin prior to confocal microscopy. Scale bars = 20μm.

In order to investigate this further, similar experiments were performed with cells plated on 35mm imaging dishes and analysis by confocal microscopy. A431 cells were seeded 24 hrs before the experiment in 35 mm dish for live cell imaging. Cells were serum starved for 1 hr before incubation for a further 1 hr with 0.75 mg/ml TMR-dextran +/- 50 nM EGF, or 2μM unlabeled R8 or Tat. Then cells were washed and immediately analyzed by confocal microscopy (Figure 5.10). For control cells it was rather difficult to observe clear staining suggesting that only low amounts of this probe was entering the cells. However some staining was observed in punctate structures and in the main these were observed close to the plasma membrane. EGF increased uptake dramatically and now clear TMR labeled vesicles could be observed throughout the cell. There was also an obvious increase in cell associated TMR-Dextran labeling in R8 treated cells but a significant portion of this was localized on or very close to the plasma membrane. The increase in dextran uptake was less apparent in Tat treated cells. EGF also causes a clear effect on the morphology of the cells that are more rounded at the end of the incubation period and a similar but less pronounced effect was seen in cells incubated with R8 or TAT.

5.3.6. The effect of pharmacological inhibitors on macropinocytosis and on the uptake of CPPs

Pharmacological inhibitors cytochalasin D (CytD), blebbistatin (Blebb) and 5-(N-Ethyl-N-isopropyl) amiloride (EIPA) have been used to study macropinocytosis and CPP uptake section 2.3.5.4. These drugs were used here to investigate their effects on uptake of both dextran and CPPs.

5.3.6.1.Cytochalasin D (CytD)

Cytochalasin D (CytD) is an effective inhibitor of actin polymerization as it binds with high affinity to growing ends of actin nuclei and filaments (F-actin), and prevents addition of monomers (G-actin) to these sites. A431 cells were pre-incubated with 10 μM CytD for 15 min then incubated with 2 μM Alexa488-R8 or -Tat in the presence of the drug for the indicated time points. Then the cells were washed with PBS, trypsinized and heparin washed prior to analysis with flow cytometry (Figure 5.11). The uptake of Alexa488-R8 and -Tat was significantly inhibited by up to 50% and 35% in CytD treated cells respectively.

The same experiment was then performed with three different dextran conjugates: 40KDa FITC-Dextran, 10KDa Alexa488-Dextran or 70 KDa TMR-dextran. Surprisingly, the uptake of all these conjugates was increased to different extents in CytD incubated cells (Figure 5.12) and this was most apparent at longer incubation periods. For FITC Dextran this was investigated further using confocal microscopy and here A431 cells were pre-incubated for 15 min in the absence (Control) or presence (CytD) of 10μM CytD at 37^0 C, prior to washing and incubation with 5mg/ml FITC-Dextran at 37^0 C for the indicated time points. Cells were then washed and processed for live-cell imaging (Figure 5.12.F & G) or fixed and actin stained with rhodamine-phalloidin (Figure 5.12.D & E). Figure 5.12.F shows that FITC-dextran in control cells is enriched in a perinuclear region, while cells treated with CytD there was the expected breakdown of actin (Figure 5.12.E) but the dextran was scattered throughout the cell and there was little evidence of enrichment in the perinuclear region (Figure 5.12.D).

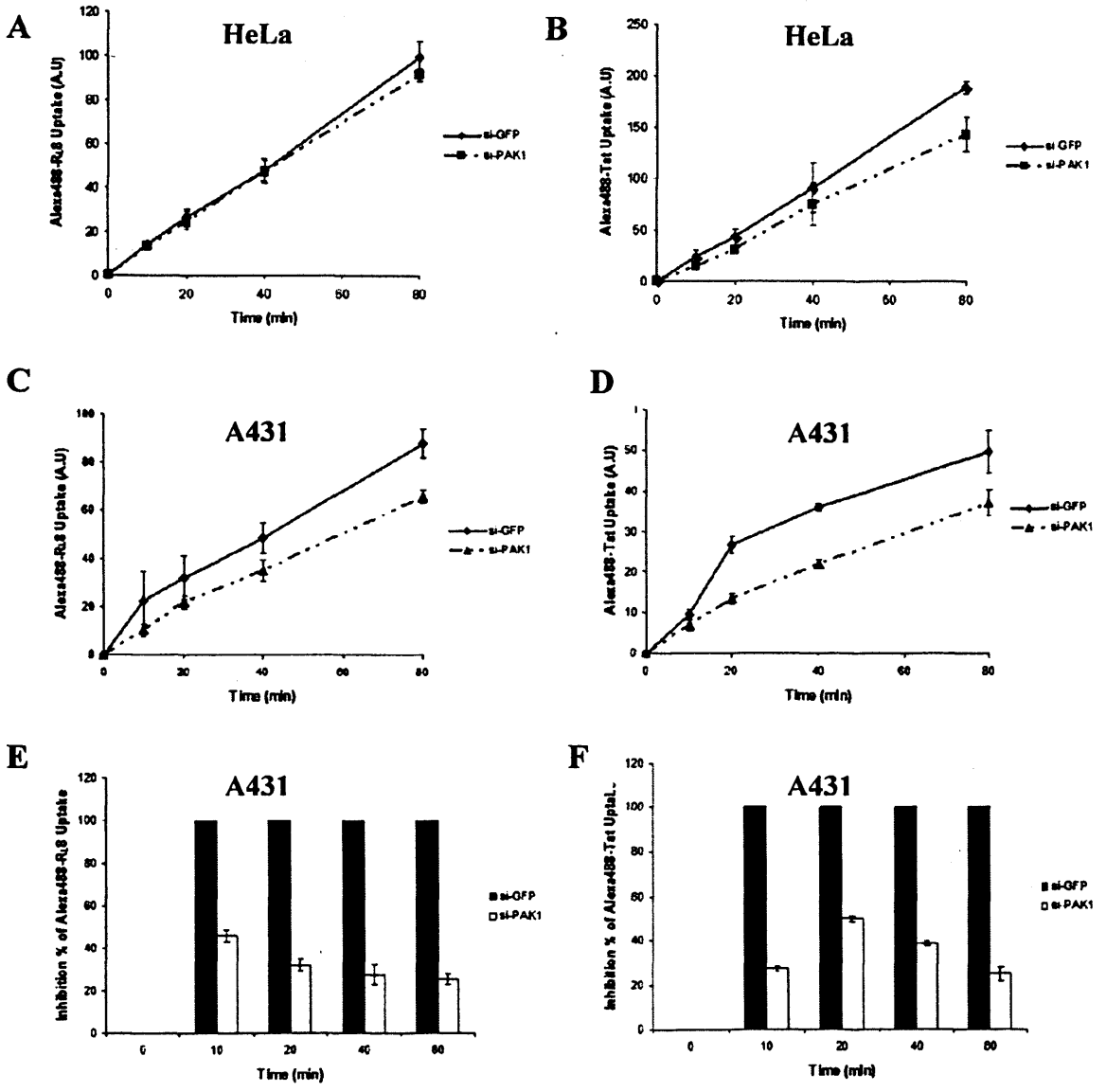

Figure 5.8. Uptake of Alexa488-RL8 and -Tat uptake in PAK-1 depleted cells.

HeLa cells (A & B) and A431 cells (C & D) were transfected with si-GFP and si-PAK-1 for 48hr, then incubated for the indicated time points with 2 μM Alexa488-R8 or –Tat at 370 C for the indicated time points. Cells were washed and analysed by flow cytometry. Data obtained from A431 cells are also represented as a percentage of control for each time point (E & F). Values above obtained from three independent experiments (n=3)

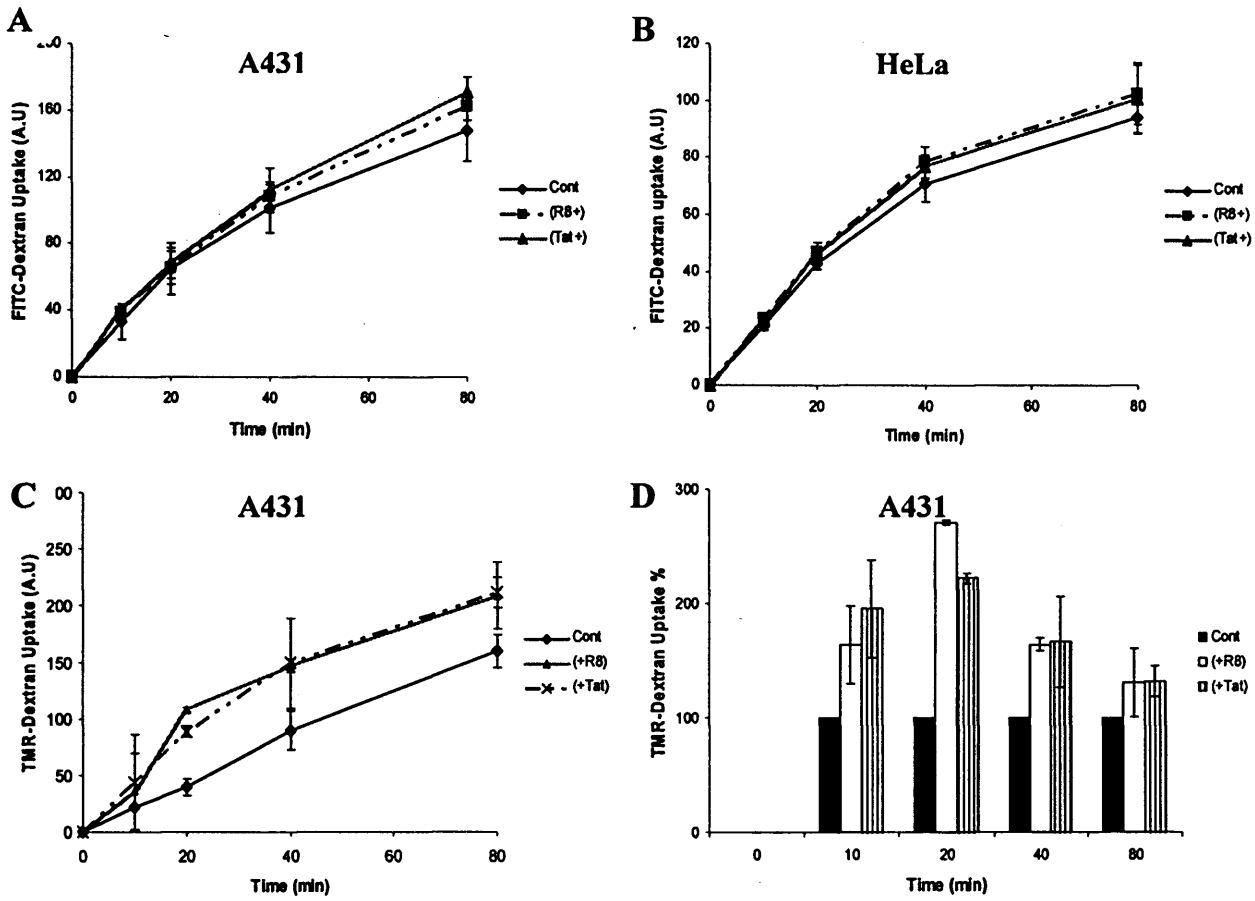

Figure 5.9. Effect of co-incubating CPPs with different molecular weight dextrans.

A431 cells **(A, C, D)** and HeLa cells **(B)** were serum starved in Ringer's buffer for 1 hr then incubated with 5 mg/ml FITC-dextran or 0.75 mg/ml TMR-dextran +/- 2μM R8 or Tat at 37^0 C, prior washing and analysis by flow cytometry. TMR-dextran data are also represented as a percentage of control for each time point **(D)**. Results represent data from three independent experiments.

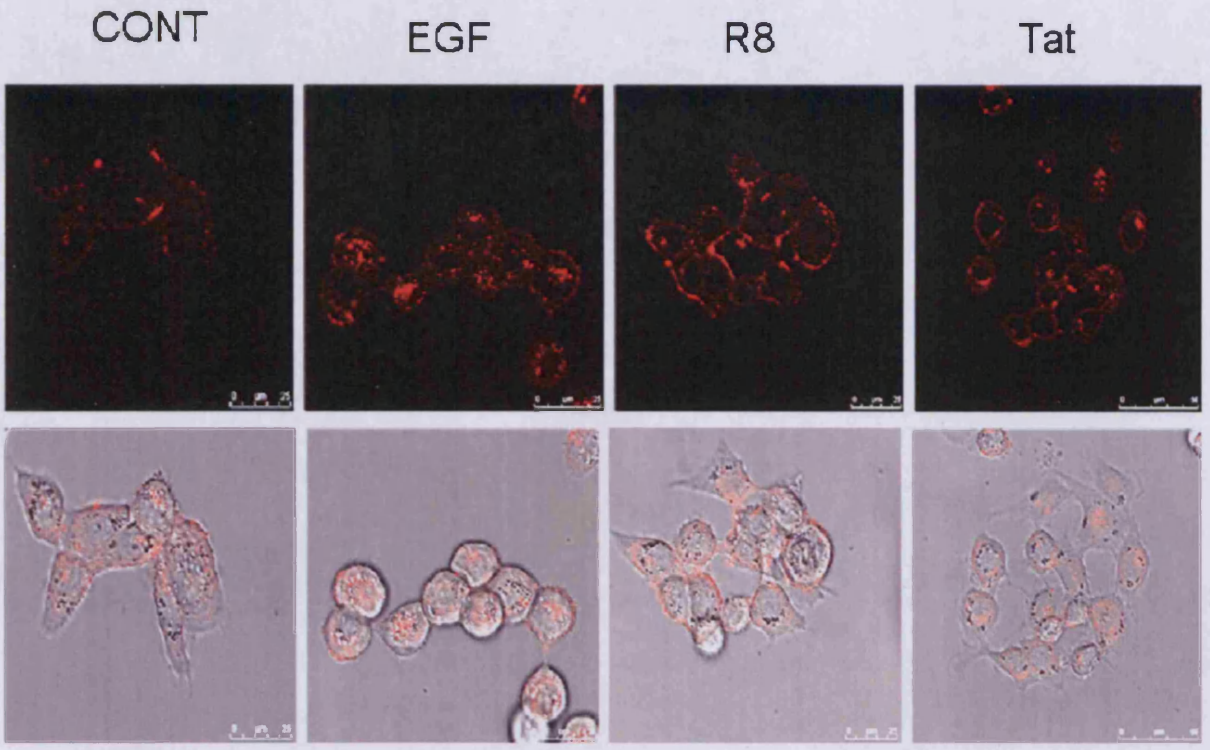

Figure 5.10. TMR-dextran uptake in the presence of EGF and CPPs.

A431 cells were serum starved for 1 hr, and then incubated with 0.75 mg/ml TMR-dextran +/- 50 nM EGF, 2μM unlabeled R8 or Tat for 1hr before washing and analysis by confocal microscopy. Images are of single sections through the middle of cells. Scale bars = 25μm.

5.3.6.2.Blebbistatin (Blebb)

Blebbistatin is a small molecule inhibitor showing high affinity and selectivity toward myosin II, binds to the myosin-ADP-P_i complex with high affinity and interferes with the phosphate release process. Thus, the inhibitor blocks myosin in an actin-detached state (Kovacs et al. 2004). Blebb is now gaining ground as a specific inhibitor for macropinocytosis (Section 2.3.5.5) and was recently used to identify this pathway as an uptake mechanism for vaccinia virus (Mercer and Helenius 2008). It was, therefore, used in this chapter to investigate its effect on CPP and dextran uptake.

Initially the effect of Blebb on the fluid phase uptake of dextran was investigated. A431 cells were pre-incubated with or without 100 μM Blebb for 30 min followed by incubation of 5 mg/ml FITC-dextran for 0-80 min in the presence of the drug. Cells then were washed and trypsinized and cellular FITC was quantified using flow cytometry. Figure 5.13.A demonstrates that Blebb had no effect on uptake of FITC-dextran, thus the drug has no effect on fluid phase endocytosis. For the next experiment macropinocytosis was stimulated as described in section 2.3.5.5 by treating 1 hr serum starved cells with EGF. Cells were serum-starved and stimulated with FITC-dextran +/- EGF +/- Blebb, followed by washing and analysis by flow cytometry. As shown in Figure 5.13.B Blebb treated cells incubated with EGF were only able to induce dextran uptake to levels slightly higher than basal levels. Thus the drug proved to be a powerful inhibitor of enhanced fluid phase uptake in response to EGF.

The effect of Blebb on actin distribution after EGF stimulation was studied further by confocal microscopy. A431 cells were serum starved for 1 hr then incubated with or without 100 μM Blebb for 30 min followed by incubation

with 50 nM EGF for 10 min. Then cells were washed and fixed prior to actin staining with rhodamine-phalloidin and analysis by confocal microscopy (Figure 5.14). There was a clear difference in the distribution of actin in the two cell populations. The clear membrane ruffling that was apparent in EGF treated cells was not observed in cells pretreated with the drug. The effect of this drug on the uptake of the CPPs was then investigated in A431 and in HeLa cells. The results show significant inhibition in the uptake of Alexa488-R8 (Figure 5.15.A) in A431 cells, whereas the uptake of Alexa488-Tat is not affected (Figure 5.15.B). The drug has no significant effect on uptake of either CPPs uptake in HeLa cells (Figure 5.15.C & D).

5.3.6.3.5-(N-Ethyl-N-isopropyl) Amiloride (EIPA)

The amiloride analogue EIPA has been widely used as a macropinocytosis inhibitor to study this pathway and its role in the uptake of viruses and CPPs. It was used in this chapter to assess its effect on CPPs uptake in A431 and HeLa cells, and support the earlier data with other pharmacological inhibitors and PAK-1 depletion. Cells were pretreated with 100μM EIPA, and then incubated with 2 μM Alexa488-R8 or -Tat in the continued presence of the drug. The cells were then processed for analysis of cell associated fluorescence. Figure 5.16.A-D reveals that there was no effect of this drug on the uptake of either R8 or Tat in either cell line.

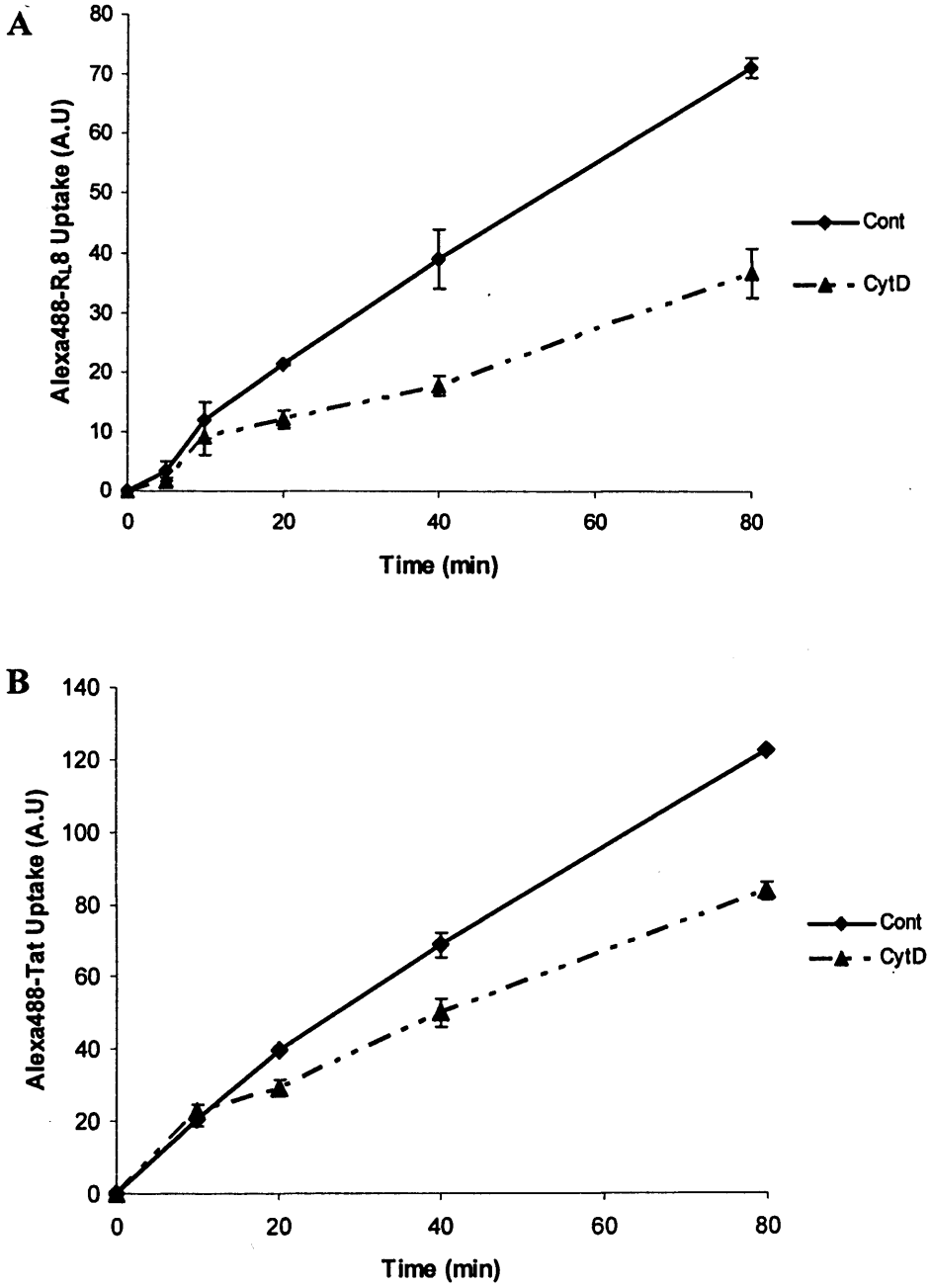

Figure 5.11 Effect of Cytochalasin D on CPPs uptake

Cells were pre-incubated for 15 min in the absence (Control) or presence (CytD) of 10μM CytD at 37^0 C, prior to washing and incubation with 2 μM Alexa488-R_L8 **(A)** or –Tat **(B)** at 37^0 C for the indicated time points. Cells were washed and analysed by flow cytometry. Results represent data from three independent experiments (n=3).

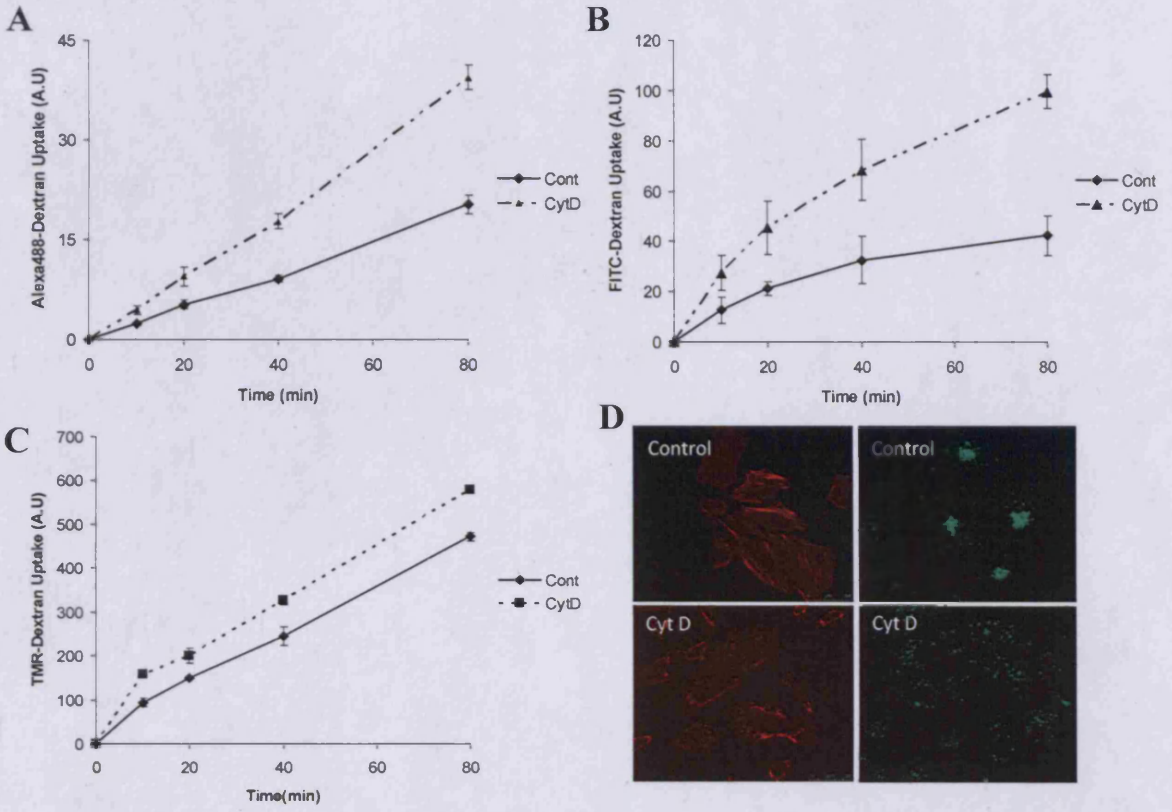

Figure 5.12 Effects of cytochalasin D on Dextran uptake and actin distribution.

A431 cells were pre-incubated for 15 min in the absence (Control) or presence (CytD) of 10μM CytD at 37^0 C, prior to washing and incubation with 5mg/ml FITC-Dextran **(A)**, 0.2 mg/ml Alexa488-Dextran **(B)** or 0.75 mg/ml TMR-dextran **(C)** at 37^0 C for the indicated time points. Cells were then washed and analysed by flow cytometry. Results represent data from three independent experiments. Live-cell images of 5 mg/ml FITC-Dextran distribution in A431 cells after internalising dextran for 60 mins in the presence **(G)** or absence **(F)** of CytD, and then cells were washed and processed for live cell imaging immediately. Actin staining of fixed control A431 cells **(D)** and CytD pre-treated cells **(E).**

5.3.7. *The effect EGF, CPPs and cationic transfection reagents on PAK-1 distribution in A431 Cells*

EGF treatment was shown to redistribute PAK-1 localisation to the plasma membrane in A431 cells (Liberali et al. 2008). As PAK-1 depletion inhibited CPP uptake experiments were performed to investigate whether CPPs cause a similar redistribution of this protein. As a positive control, cells were initially incubated with EGF for 10 min and then fixed, immunolabelled with antibodies recognizing PAK-1 and Alexa488 labelled secondary antibodies and the actin distribution was also determined by incubating the cells with rhodamine-phalloidin. As previously shown in Figure 5.17 PAK-1 antibodies in control cells highlighted cytoplasmic structures and the nucleus, however in EGF treated cells there was a dramatic redistribution of this protein to the cell periphery. Close inspection revealed that the PAK-1 labelling did not colocalize with the actin in this region that had also been redistributed in response to EGF stimulation (Fig 5.17).

The same labeling was then performed in cells incubated for 10 min with either 2μM R8 or Tat. In these cells there was also sign of that PAK-1 was being redistributed to the plasma membrane but the effects were not as obvious or consistent as those observed following growth factor stimulation. To investigate whether this was a product of positive charge, A431 cells were incubated with the cationic polymers PEI, Oligofectamine™, Lipofectamine™ and Fugene6™, all complexed with either plasmid DNA (Fugene6, PEI) or siRNA (Oligfectamine, lipofectamine) (Section 2.3.4.6). The cells were then labeled as above for PAK-1 and actin. None of these commonly used transfection systems had any effect on PAK-1 distribution (Figure 5.17) and in

the interest of time no further experiments were performed to investigate whether these reagents in the absence of siRNA or DNA had effects on cellular PAK-1 distribution.

5.4. Discussion

Macropinocytosis is emerging as a difficult pathway to study as no clearly identifiable protein has been shown to specifically regulate it, and and an endocytic probe that only enters by this pathway has not been identified (Jones 2007b; Kerr and Teasdale 2009). Some cells are known to use this pathway constitutively but it has been most studied following growth factor activation by agents such as EGF and PDGF. Here an obvious effect is a stimulation in fluid pahse uptake measured using probes that normally enter cells by fluid phase endocytosis such as dextran and horseradish peroxidase. It has also been shown that pathogens and viruses utilize this pathway to gain access to cells (Kalin et al. 2010; Mercer and Helenius 2010)

A role for macropinocytosis in mediating CPP uptake was originally suggested based on inhibitor studies with the amiloride analogue EIPA and an ability of CPPs to modify the actin cytoskeleton and enhance the uptake of the fluid phase marker, 70 KDa dextran. From these studies 70 KDa Dextran has emerged as a marker for macropinocytosis suggesting it does not enter cells by any other route.

P21-activated kinase (PAK-1) is a member of the PAK family of serine/threonine kinases that are activated by Cdc42/Rac and play roles in cell motility migration and in the main this is through interactions with the cell

cytoskeleton (Arias-Romero and Chernoff 2008). PAK-1 was recently shown to be involved in growth factor induced macropinocytosis (Dharmawardhane et al. 2000) and in uptake of vaccinia virus (Mercer and Helenius 2008). In addition it has been shown that inhibiting endogenous PAK-1 activity using a PAK-1 specific autoinhibitory domain blocks growth factor-induced macropinocytosis, which indicates PAK-1 requirement in activating macropinocytosis (Dharmawardhane et al. 2000). CPPs including R8 and TAT were also shown to activate Rac-1 to levels comparable if not exceeding Rac-1 activation by EGF (Gerbal-Chaloin et al. 2007). It is therefore clear that there is a link between the actin cytoskeleton and cationic CPPs but depleting Rac-1 from cells is likely to have many effects and based on recent data with PAK-1 and macropinocytosis it was decided to investigate this protein further. In order to do this it was very important that a macropinocytosis model could be established in the laboratory and that PAK-1 could be effectively depleted. A431 cells have been widely used as models for macropinocytosis as they have high levels of EGFR (Hamasaki et al. 2004; Liberali et al. 2008). It has been reported that the number of EGFR in A431 cells was about 100-fold higher than HeLa cells (Masui et al. 1984). This was confirmed in this thesis but in addition it was found that PAK-1 levels were also much higher in this cell line. Attempts were made to deplete PAK-1 expression in HeLa cells and A431 cells, but only in the later was effective depletion consistently obtained. This was less problematic than predicted as these cells turned out to be the most effective models for measuring the effects of macropinocytosis.

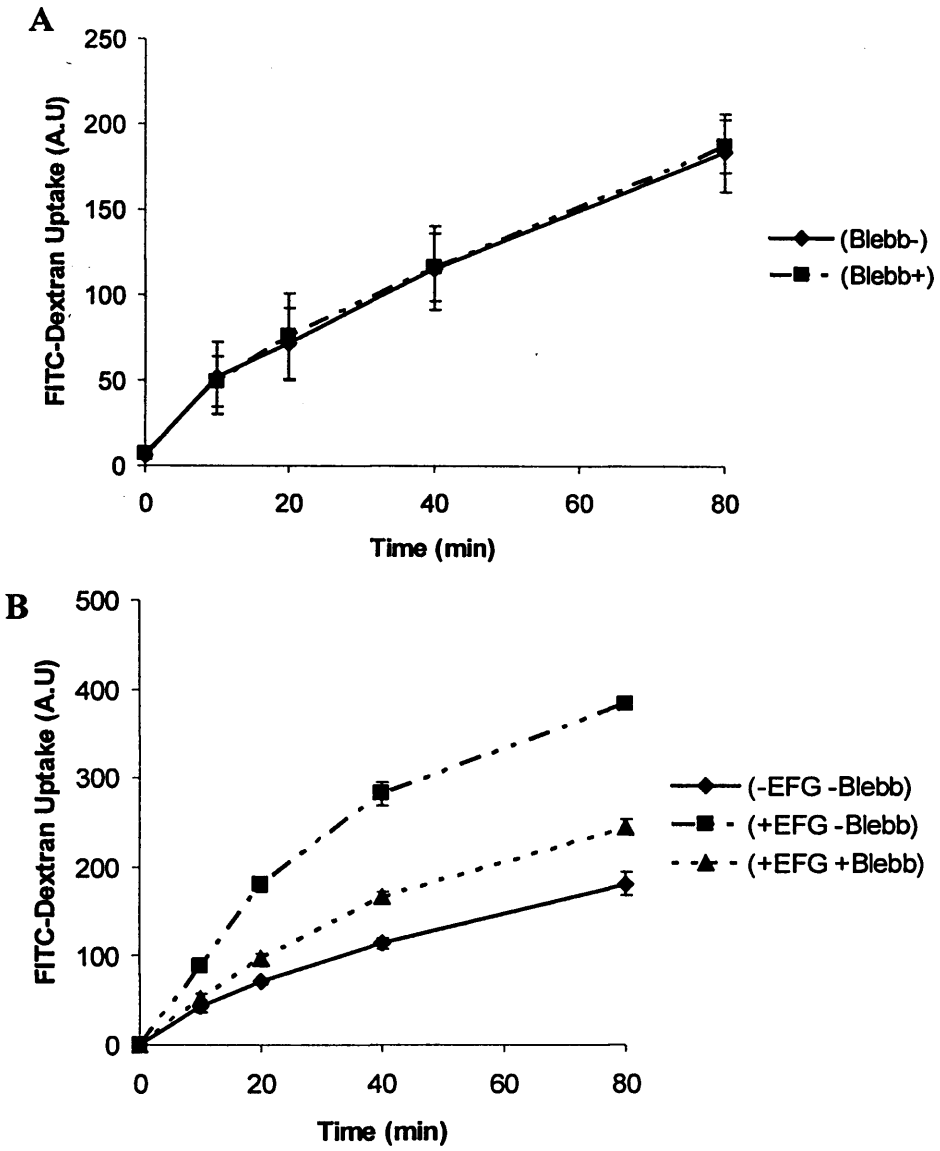

Figure 5.13 Effect of using myosin II inhibitor Blebbistatin on dextran uptake in the presence or absence of EGF.

(A) Serum starved cells were pre-incubated for 30 min in the absence (Blebb-) or presence (Blebb+) of 100μM Blebb, prior to washing and incubation with 5mg/ml FITC-Dextran at 37^0 C for the indicated time points prior to washing and analysis by flow cytometry. (B) Serum starved cells were pre-incubated for 30 min in the absence (Blebb-) or presence (Blebb+) of 100μM Blebb, prior to washing and incubation with 5mg/ml FITC-Dextran in the absence (-EGF) or presence of EGF (+) for the indicated time points. The cells were then analysed by flow cytometry Results represent data from three independent experiments.

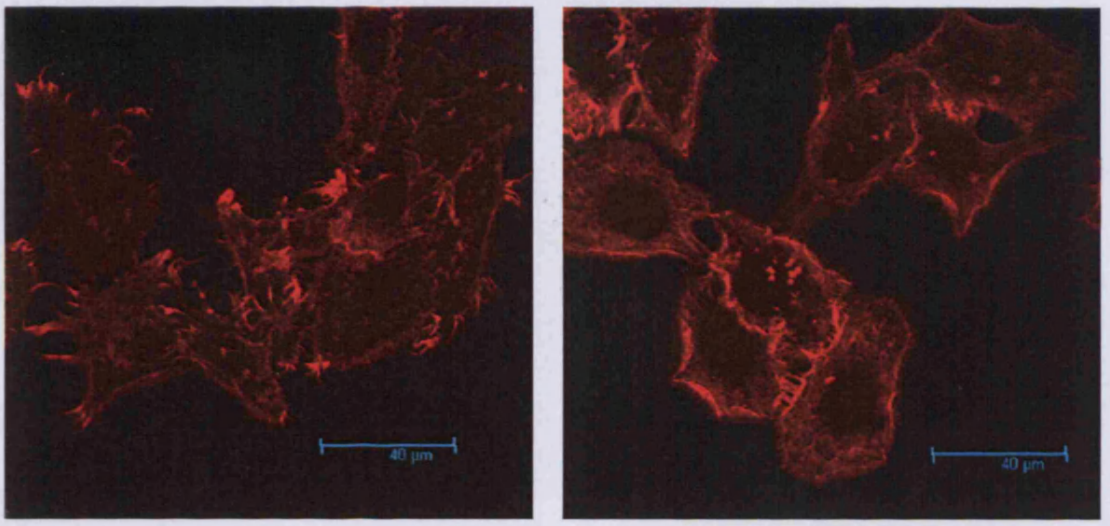

+EGF -Blebb +EGF +Blebb

Figure 5.14 Effect of Blebbistatin on cellular actin distribution in EGF stimulated A431 cells.

A431 cells were serum starved for 1 hr, then pre-incubated with +/- Blebb for 30 min then incubated with 50 nM EGF for 10 min. The cells were washed, fixed and incubated with rhodamine-phalloidin for 10 min and analysed by confocal microscopy. Scale bars = 40µm.

The same antibody used for Western blotting also proved to be effective for immunofluorescence microscopy revealing the location of the protein in vesicles and also tubular structures. It was also obvious that there was a large fraction of the protein in the nucleus. This nuclear fraction was shown to be increased with EGF stimulation (Singh et al. 2005), but this was not particularly noticeable from my experiments. Also documented is the fact that this protein is recruited to the plasma membrane by growth factor activation and this was also observed here. It was also found that both CPPs to some degree caused a reorganisation of this protein to the plasma membrane. It is known that EGF causes actin reorganisation and this is in part caused by activating the cytoplasmic domain of EGFR to recruit proteins such as PI 3-kinase that affect actin reorganisation through Rac and Rho but also through activating PAK-1 (Papakonstanti and Stournaras 2002). PAK-1 is known to interact with many proteins that affect the cell cytoskeleton including PI 3-kinase, Rac-1 and cdc42 and it is therefore heavily involved with actin dynamics (Sells et al. 1997).

As the CPPs studies here are highly cationic some experiments were performed whereby transfection agents complexed with DNA or siRNA were incubated with cells prior to labelling for PAK-1 and actin redistribution. Neither of them showed any evidence of being able to do this even to the extent demonstrated by the CPPs. Important to note however is that complexation with negative DNA or RNA will reduce the overall charge on these molecules and possibly minimising their capacity to redistribute actin and PAK-1. This remains to be determined but would make for interesting studies. When A431 cells were depleted of PAK-1 it was clear that there was a clear effect on the

cell cytoskeleton but this has not been previously documented. Overall from these studies a PAK-1 depletion model was generated that could then be used to study macropinocytosis induced by EGF and then a role for this pathway in the uptake of CPPs.

To characterise growth factor induced macropinocytosis, cells were incubated with EGF and then the uptake of FITC-dextran was measured. This uptake is known to be dependent on expression of EGF receptor (EGFR), and this explains the small increase in the uptake of dextran observed in HeLa cells compared to A431 cells. These experiments however showed that the two cell lines have a similar relative basal upatke of dextran, however EGF stimulated fluid phase endocytosis in A431 is higher than that seen in HeLa cells. Identical experiment was performed with TMR-dextran and similar effect has been obtained. Though there is a clear difference in the response of these two cell lines to growth factor stimulation it has yet to be determined whether constitutive macropinocytosis, if it exists, is the same in the two cell variants.

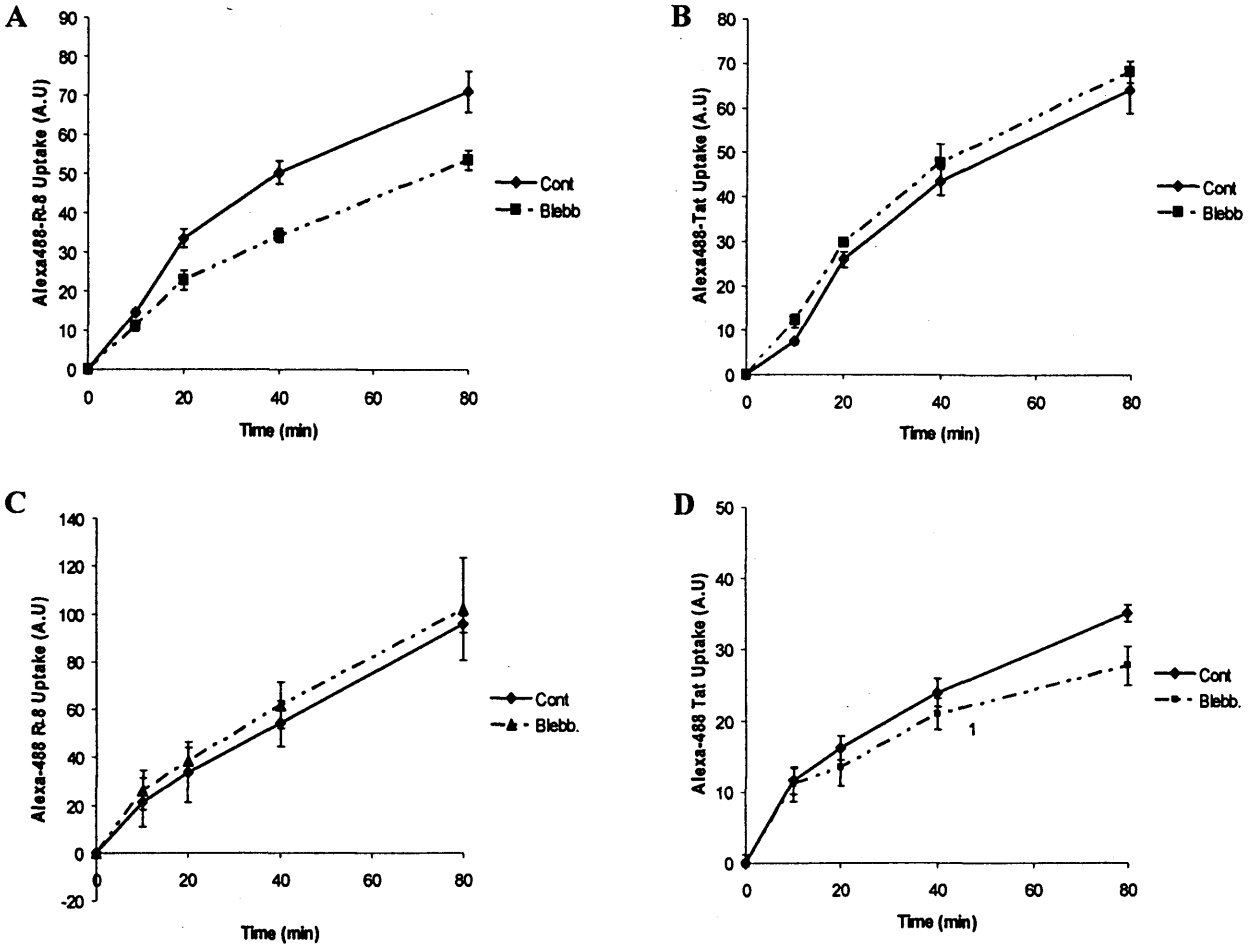

Figure 5.15 Effect of Blebbistatin on CPPs uptake.

A431 cells **(A & B)** and HeLa cells **(C & D)**, were pre-incubated for 30 min in washing and incubation with 2 μM Alexa488-R_L8 or –Tat at 37^0 C for the indicated time points. Cells were washed and analysed by flow cytometry. Results represent data from three independent experiments (n=3).

Expression of auto inhibitory domain (AID) of PAK-1 have been shown to dramatically reduce the uptake of FITC-dextran in presence of PDGF but had no effect on basal levels of FITC-Dextran uptake (Dharmawardhane et al. 2000). In comparison, siRNA depletion of PAK-1 (Figure 5.6), failed to completely inhibit the increase in dextran uptake to baseline values and it did not affect the overall basal dextran uptake (without EGF stimulation) (Figure 5.5). Labelling PAK-1 depleted A431 cells with rhodamine phalloidin revealed that all the cells had a reorganised cytoskeleton but as described these cells had normal levels of dextran uptake but reduced stimulation of dextran caused by EGF and interestingly also had lower levels of CPP uptake compared with control cells. However it must also be noted that CPP uptake was not totally inhibited in PAK-1 depleted A431 cells suggesting a large fraction enters via a process that is independent of the requirement for this protein. The data was more difficult to interpret in HeLa cells as very high efficiency of PAK-1 depletion was not achieved.

Dowdy and co-workers show that TAT induces macropinocytic fluid-phase uptake in CHO and glycan mutant cells. They co-incubated unlabeled (0.5 and 2 μM) TAT peptide in the presence of 70 kDa neutral TMR- for 1 h at 37^0 C, and their results suggest that Tat and possibly other cationic CPPs may induce macropinocytic uptake and transduction via binding to a protein on the cell surface rather than through interactions with glycans or direct interaction with the membrane. In addition, the increase in dextran uptake increased with increasing the concentration of Tat (Gump et al. 2010). In this thesis two dextrans were investigated of molecular weights 40 and 70 KDa under conditions and concentrations that have previously been shown to be effective

at demonstrating macropinocytosis (Ellinger and Fuchs 2010; Gump et al. 2010). Neither R8 or Tat had any effect on uptake of FITC-dextran but both peptides were able to stimulate uptake of TMR- 70 KDa dextran. The reason for this is unlear and it should be noted that the concentration of the two dextrans were quite different. The high costs of TMR-Dextran was prohibitive to repeating all the experiments at 5mg/ml as was used for FITC-dextran.

Based on the effects of PAK-1 depletion on the actin cytoskeleton (Figure 5.7) it was predicted that cytochalasin D would have some effect on CPP uptake in A431 cells. In previous studies this agent has been shown to inhibit CPPs by up 45% (Gomez and Matsuyama 2010; Tunnemann et al. 2006). Here CytD also proved to be a powerful though not complete inhibitor of the uptake of R8 and Tat. Interestingly the effects of this drug were only noticeable after approximately 15 min and were more apparent for R8 compared with Tat. The reason for this delayed response is unclear but may be due to the fact that it is only affecting the later macropinocytic engulfment of the peptides into the cells. As 70 KDa dextran is regarded as a macropinocytosis marker it was predicted that its uptake would also be inhibited in CytD treated cells but this was not the case for this probe or 40 KDa dextran. For the later there was a dramatic increase in cell associated dextran and the relative effect increased

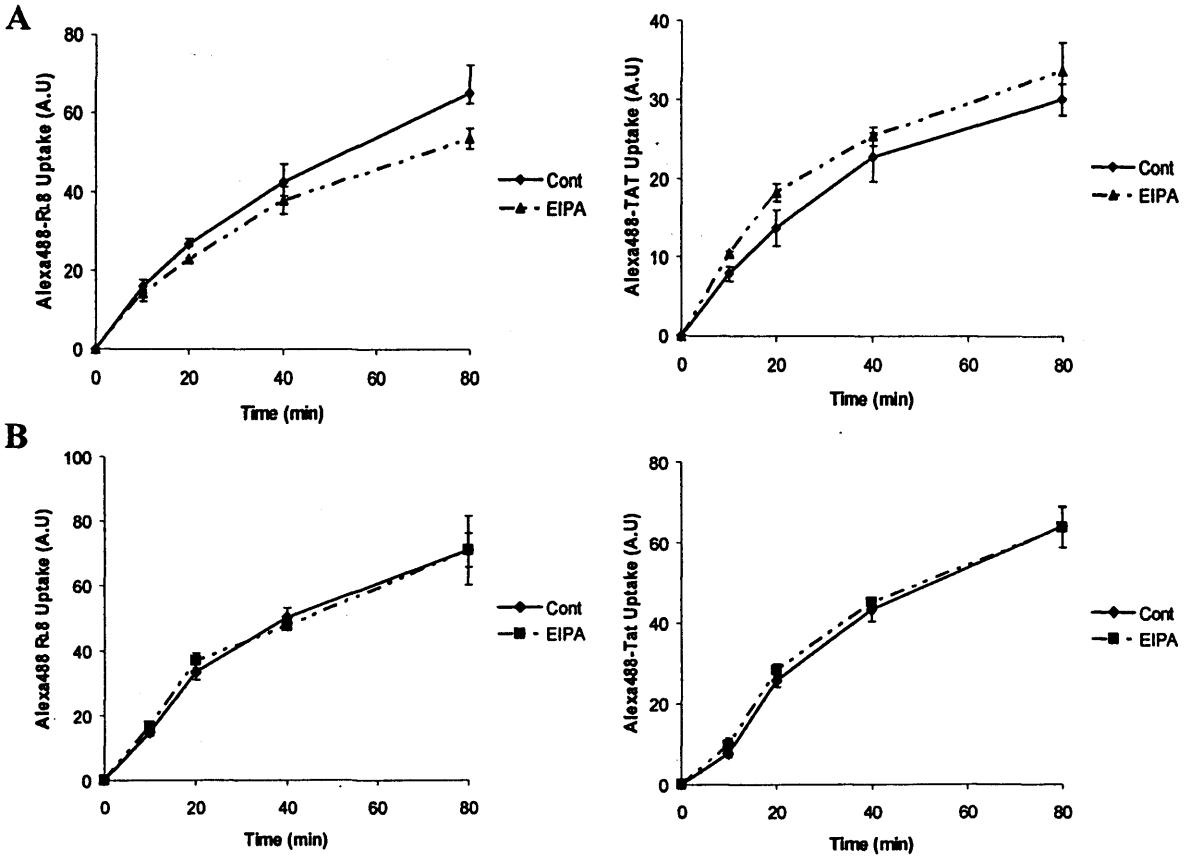

Figure 5.16 The effect of EIPA on cellular uptake of R8 and Tat.

HeLa (**A**) and A431 cells (**B**) were pre-incubated for 30 min in the absence (Cont) or presence (EIPA) of 100μM EIPA at 37^0 C, prior to washing and incubation with 2 μM Alexa488-R_L8 or –Tat at 37^0 C for the indicated time points. Cells were washed trypsinized and analysed by flow cytometry. Results represent data from three independent experiments (n=3).

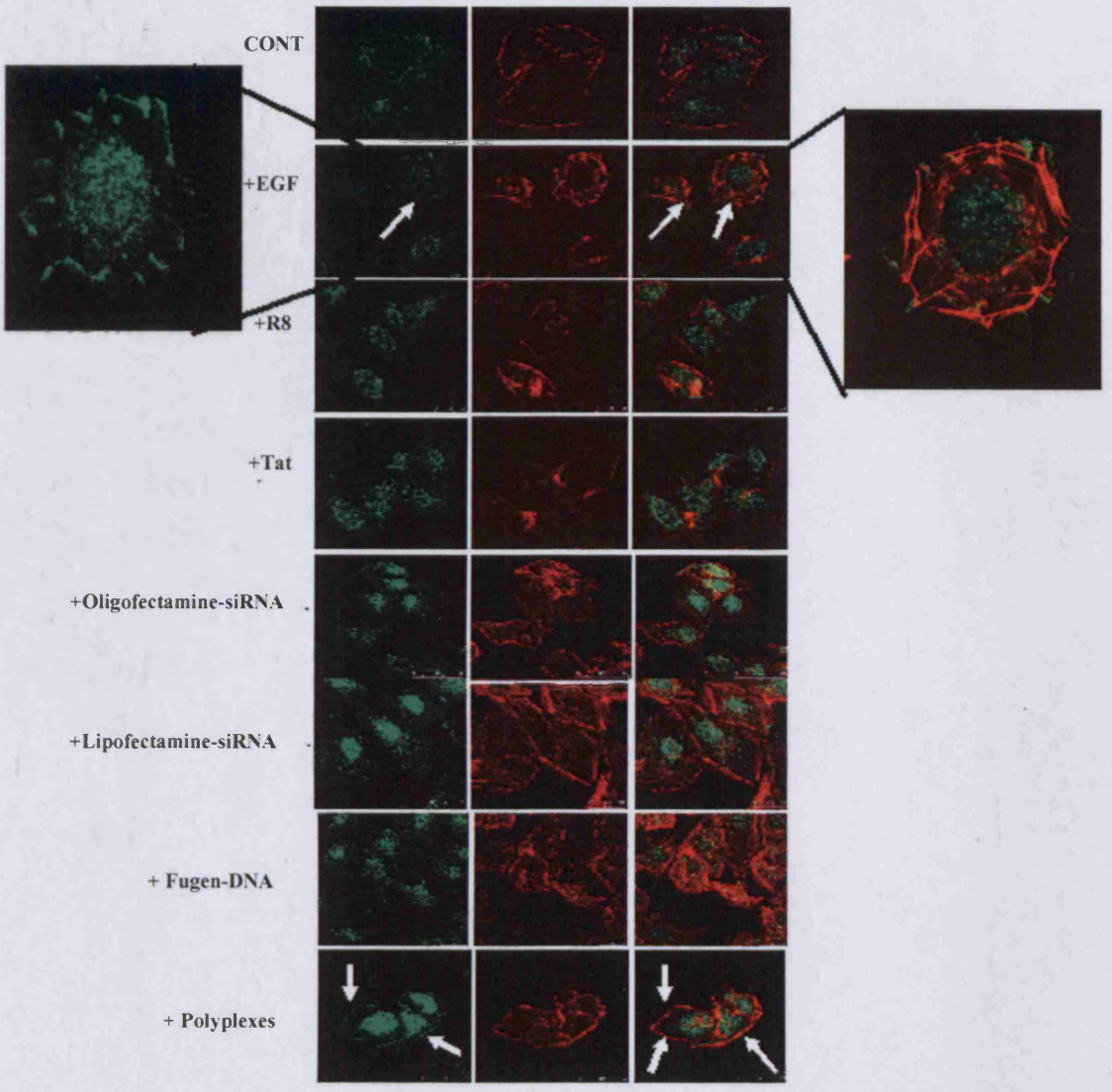

Figure 5.17. The effect of cationic lipids, cationic polymers, EGF, and CPPs on PAK-1 distribution in A431 Cells.

A431 cells were treated with 50 nM EGF, 2μM unlabelled R8 or Tat or transfected with oligofectamine-siRNA, lipofectamine-siRNA, Fugene-6-DNA or PEI-DNA (polyplexes) for 10 min, followed by washing and fixation prior to immunulabelling with PAK-1 antibody and actin labeling with rhodamine-phalloidin. Analysis was then performed by confocal microscopy. Scale bars = 20μm.

over time. This was highly unexpected but a search in the literature identified other studies showing an increase of dextran in T84 cells (Song et al. 1999) and no effect in uptake of dextran in other cell types (Gold et al. 2010). Studies investigating CytD on receptor mediated endocytosis have revealed that its effects are highly dependant on the choice of cell line and interestingly only A431 cells were resistant to CytD with respect to its capacity to inhibit CME (Fujimoto et al. 2000). Indeed in parallel studies performed at the Unversity of Ghent it was found that CytD inhibited dextran (Oregon Green labeled 70 kDa dextran, 0.5 mg/ml) uptake by 40% (Vercauteren et al. 2011). Recycling may be an important aspect here and no studies have looked in detail at the possibility that CPPs are recycled. However Dextran is known to be recycled (Seib et al. 2007) and if an actin cytoskeleton is involved in this it may be the case that in CytD treated cells that the fraction of dextran that is internalised is not able to recycle and so accumulates. This is similar to the observations obtained with ransferrin in CHC depleted cells in Chapter 3.

Blebb inhibits the interaction of actin with myosin II and has been used to reduce membrane ruffling and macropinocytosis (Mercer and Helenius 2010). The data obtained with this inhibitor were interesting in that it was able to reduce EGF stimulated uptake of Dextran to almost basal levels thus proving to be more effective than PAK-1 depletion. The morphological effects of this drug on actin in EGF treated cells were also clear to see. With regards to CPPs it inhibited R8 uptake but had no effects on Tat. Time did not allow for further analysis of the effects of this drug on CPP mediated stimulation of fluid phase uptake to see if it was affective as it was in inhibiting this when caused by EGF (Figure 5.13).

Amiloride and the amiloride analogue EIPA are now widely used as macropinocytosis inhibitors and have also been shown to inhibit uptake of R8 and Tat (Nakase et al. 2004; Wadia et al. 2004). However, other studies have shown very little effects of this drug on CPP uptake (Al-Taei et al. 2006; Fretz et al. 2006). The later study shows that treatment of cells with EIPA affects the morphology and subcellular location of early, late endosomes and lysosomes. Enlarged early and late endocytic structures were observed in EIPA-treated cells, and these organelles accumulated in a perinuclear region. EIPA-treated cells were additionally characterized by increased localization of the HIV-TAT peptide and octaarginine peptides in the cytosol and that EIPA was without major effect on uptake of both peptides in leukaemic KG1a cells (Al-Taei et al. 2006). The results in this thesis clearly show that there were no effects of this drug on CPP uptake.

In conclusion it was identified that stimulation of fluid phase uptake by cationic CPPs Tat and R8 was highly dependent on the nature of the dextran and also the cell line. By generating a model for macropinocytosis it was found that the effects on fluid phase uptake could be partially decreased in cells depleted of PAK-1 however the majority of the peptide was able to enter cells in a PAK-1 independent manner. Studies with the actin disrupting agent CytD revealed extensive differences between the requirements for actin between CPPs and dextran(s) and it still remains to be determined whether this is at the level of endocytosis or downstream processing including recycling. Overall the data show a strong requirement for functional actin for cell entry but it is difficult to refute the possibility that actin disruption may also inhibit the direct

translocation of these peptides across the plasma membrane as well as their uptake via endocytic mechanisms.

Chapter 6: Designing new methods to study the uptake of CPP-protein conjugates

6.1. Introduction

An ability to deliver intact proteins into cells would have wide ranging implications for both academic research and the pharmaceutical industry (Futaki et al. 2004; Wadia and Dowdy 2003). Here CPPs have been extensively studied through purifying CPP sequences linked at the C- or N-terminus of proteins and these conjugates are often simply added to the culture media. The researcher can then either analyse the uptake of the protein and CPP by microscopy or if the protein has biological activity (e.g. enzymic) then this can be measured. Various CPPs have now been shown to be successful for delivering protein cargo of molecular weight as large as ~ 150 kDa (immunoglobulins and ß-galactosidase at 120 KDa (Schwarze et al. 1999). Most important here is that there is plenty of evidence to show that the delivered proteins retain their functions either as enzymes (ß-galactosidase) or as regulators of processes such as cell division and signal transduction (Wadia and Dowdy 2003). Of the CPPs studied HIV-Tat protein has again been prominent and it is known that in this sequence and also in other arginine rich peptides that the guanidino moiety plays an important role (Futaki et al. 2001; Wender et al. 2000). The group of Pooga has been active in studying the ability of biotinylated CPPs such as penetratin, Tat, pVEC and transportan to deliver avidin thus representing another mechanism for linking the CPP to the cargo (Saalik et al. 2004).

Unless the proteins can complex to the CPP through linkages such as biotin-avidin there is most often a requirement to purify the protein and CPP and this is most often done in *E. Coli* and an additional histidine tag is incorporated into the expressed protein. Histidine-tagging is based on preparing proteins of

interest that have usually six residues of histidine at the N- or the C-terminus and passing an *E. Coli* lysate through an immobilized Ni(II), column will trap the histidine tagged proteins whereas other molecules that lack histidine tags will be eluted (Hochuli et al. 1987). Elution of the tagged protein is then achieved using an imidazole-containing buffer. A number of plasmids and kits are now available for efficient production and purification of these histidine-tagged proteins (Terpe 2003). In addition, this method is not only used for protein purification but also for detecting cross-linking between proteins. The Futaki group developed this further by making a nitriliotraiacetic acid derivatised octaarginine peptide NTA. This forms non-covalent complexes with histidine residues and consequently this was shown to enable the peptide to bind to His6-EGFP and deliver it into mammalian cells (Futaki et al. 2004)

GFP or EGFP has been widely used as a tool for assessing the capacities of CPPs to deliver proteins into cells and this was the protein that first highlighted the fixing artefacts associated with CPPs (Lundberg et al. 2003). More recently use was made of variants of GFP (green red) and Fluorescence resonance energy transfer (FRET) to monitor both uptake and endosomal escape and this study highlighted the large fraction of HIV-Tat-GFP that is held up in endosomes and lysosomes. Most of the mechanistic studies using GFP have been focused on HIV TAT providing evidence for uptake through macropinocytosis and also caveolae (Ferrari et al. 2003; Wadia et al. 2004). In the main, these studies have focused on using pharmacological inhibitors and colocalisation experiments using confocal microscopy however a role for macropinocytosis was also demonstrated using the HIV-TAT-Cre system

developed by the Dowdy group (Gump et al. 2010). More recently the use of siRNA depletion was described to suggest that protein delivery by transportans is mediated by caveolae. For analysing CPP-protein uptake new techniques are also required to gain a better understanding of how they enter cells and then escape form the endosomal pathway.

The work described in this Chapter represent the final stages of the thesis whereby hsitidine tagged (His_6) EGFP-R8 protein was purified from *E. coli* BL21(DE3)pLysS competent cells transformed using a pEV3b plasmid encoding for His_6-EGFP-R8 and Ampicillin resistance (Figure 6.1) and then purified using histidine-tag method. The quantitative uptake of this protein was analysed using two different tools flow cytometry and a newly developed tool by which the protein uptake quantified directly from SDS Gels following electrophoresis under non-denaturing conditions.

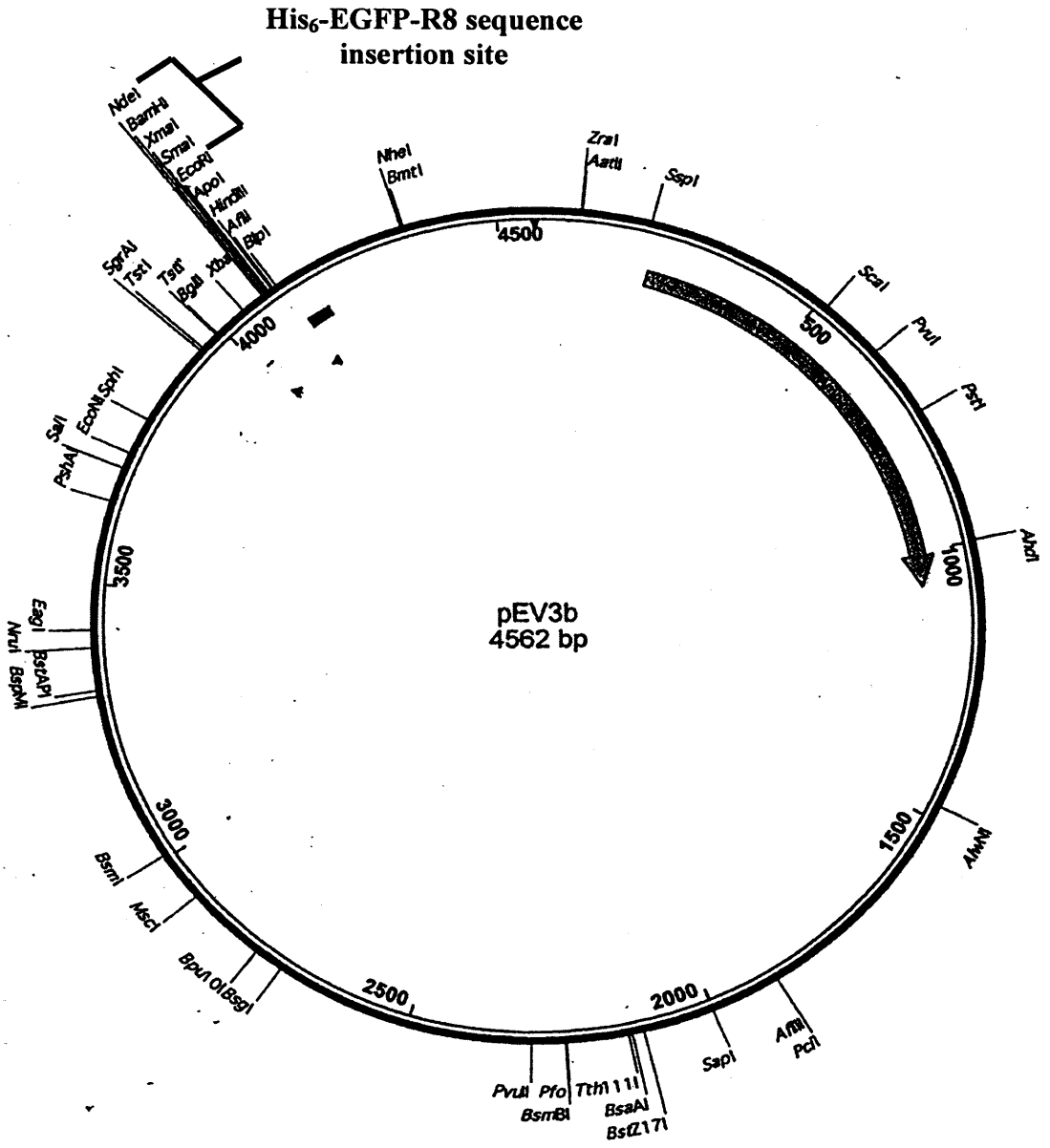

Figure 6.1. His_6-EGFP-R8 Plasmid map.

The sequence for His_6-EGFP-R8 was inserted between Ndel-Ecorl restrict

6.2. Methods

As a major aspect here is protein purification the entire methods are provided in this chapter rather than under the main Materials and Methods chapter. Under all experimental procedures here of protein purification only sterilised consumables such as pipette tips and tubes were used. The plasmid DNA used was a kind gift of Professor Shiroh Futaki, Kyoto University and was prepared as a 1mg/ml stock solution via a separate project performed in the laboratory. Thus no detail of plasmid preparation is provided here.

6.2.1. Preparation of LB^{Amp} agar plates

35g of LB agar was placed in 1L of dH_2O and autoclaved for 50 min. The agar was allowed to cool down to ~ 50°C before adding 100 µl of 100 mg/ml stock of ampicillin in dH_2O. The plates were allowed to set in the biological safety cabinet and were stored upside down at 4°C (in the fridge or cold room) until required.

6.2.2. Transformation

First the water bath was preheated to 42°C and 200 µl aliquots of competent cells (***E. coli* BL21(DE3)pLysS)** were removed from the -80°C freezer and transfered to an ice bath to let the cells thaw. Plasmid DNA (no more than 50 ng in ≤ 10 µl) was then added to the cells and the contents were mixed by pipetting up and down very gently. Negative control were also prepared containing competent cells only. All tubes were then placed on ice for 30 minutes and then placed in a preheated 42°C water bath for exactly 90 seconds. The tubes were then transferred rapidly to an ice bath to allow the cells to chill

for 1-2 min. SOC medium (Invitrogen®; containing 2% tryptone, 0.5% yeast extract, 10 mM NaCl, 2.5 mM KCl, 10 mM $MgCl_2$, 10 mM $MgSO_4$, 20 mM glucose) was added to each tube (800µl) and the contents were mixed gently before sealing the lids with parafilm. The cultures were incubated for 45 minutes in the orbital shaker at 37^0 C and 100 rpm. 200 µl of transformed competent cells and non-transformed competent cells respectively (negative control) was pipetted onto a LB^{Amp} agar plate. The cells were gently spread over the surface of the agar plate by using a sterile bent polypropylene rod then they were incubated at room temperature for 10-15 min to allow the cells to settle in the agar. The plates were then inverted and incubated at 37^0 C over night (16-20 hours). Transformed colonies appear only in the cells incubated with plasmid (Figure 6.1). The agar plates were sealed with parafilm and stored upside down at 4^0 C and were used as a supply of colonies for protein purification.

6.2.3. Expression of His_6-EGFP-R8 protein

LB broth medium were prepared in 4 sterile McCartney bottles (5ml/bottle), 4 autoclaved 250 ml conical flasks (20 ml/flask,) and 4 autoclaved 1 L conical flasks (490ml/flask) and all were autoclaved and finally stored in room temperature. A single colony was picked and added to a 5ml LB bottle containing ampicillin at 100µg/ml and this was incubated for 6 hrs at 37^0 C at 100 rpm in the orbital shaker. 0.5 ml of the incubated culture was added to each of the 20 ml LB^{Amp} broth and these were incubated overnight on the orbital shaker. The following day, 4 x 490 ml culture flasks that containg Ampicillin, were inoculated with 10 ml of the overnight noninduced culture

and the flasks were incubated in Orbital shaker at 37^0 C, 200 rpm until an OD_{600} of ~0.6 was reached. The absorbance was measured after 2 hrs and then every 1 hr using the photometer and blank LB broth as a reference. Before induction a 1 ml sample from each conical flask was taken and stored at -20^0 C as a marker for non-incuction. Protein expression was induced by adding 250 µl of 1M IPTG stock (C_{final}=500µM) to each conical flask and the cultures were incubated for an additional 3 hrs. 1 ml sample from the induced flasks was taken after every 1 hr and stored at -20^0 C. At the end of the reaction, the flasks were placed in the cold room overnight. The following day the cell culture volume was split into four autoclaved 250-ml centrifuge bottles, and centrifuged at 4000 x g and 4^0 C for 20 min on Aventi centrifuge (rotor JS 7.5). This step was repeated and each time the supernatant was removed a new volume was added to each bottle. Following removal of the last supernatant, the pellets were snap-frozen in liquid nitrogen and then thawed for 5 min on ice before resuspending them in one centrifuge tube using ice-cold filtered solution A (500 mM Tris-HCl, 600 mM NaCl, 1 M Imidazole, 1 protease mix inhibitor tablet, complete with ddH_2O). The green and thick laysates were transferred to 2 sterile 50 ml falcons and sonicated on ice until good cell lysis was achieved. The cell debris then was then centrifuged on the JA 14 rotor at 10,000 x g at 4^0 C for 30 min. The supernatants were the transferred to a sterile falcon tube and kept on ice.

6.2.4. Purification of His6-EGFP-R8 protein

An experimental set-up as shown in Figure 6.2 was arranged for the final purification steps after washing the peristaltic pump with 50 ml of sterile water

and then with 70% ethanol. The Ni-Nitrilotriactetic acid (NTA) superflow material was equilibrated with solution A then the cold *E. Coli* preparation (lysate) was pumped slowly to the column at a rate of approximately xml/min. It is important that the flow is not so strong as to rise the level above the column to > 0.5 cm above the first filter with flow rate 2-4 x 10. Once all the sample was passed down the column the His6-EGFP-R8 protein was eluted with 8 ml ice cold filtered solution B (500 mM Tris-HCl, 500 mM NaCl, of 1M Imidazole, complete with dd H_2O). The eluted sample was then collected in eppendorf tubes. The column was washed with 0.5 M NaOH and stored with 30% ethanol at 4^0 C to inhibit microbial growth. The eluted fraction was then dialysed in the cold room for 24 hrs against 3x 2L of PBS using dialysis tubing with a 10 KDa molecular weight cut off. The concentration of the dialysed protein was then determined with the BCA assay (section 2.3.6) and was typically around 10 mg/ml. This was then immediately aliquoted and stored at -80°C. To assess purity it was then loaded on to 12% SDS PAGE gels.

This CPP protein conjugate was then available for analysis with cells to investigate it uptake and also to design methods for analysing the fraction that was intracellular.

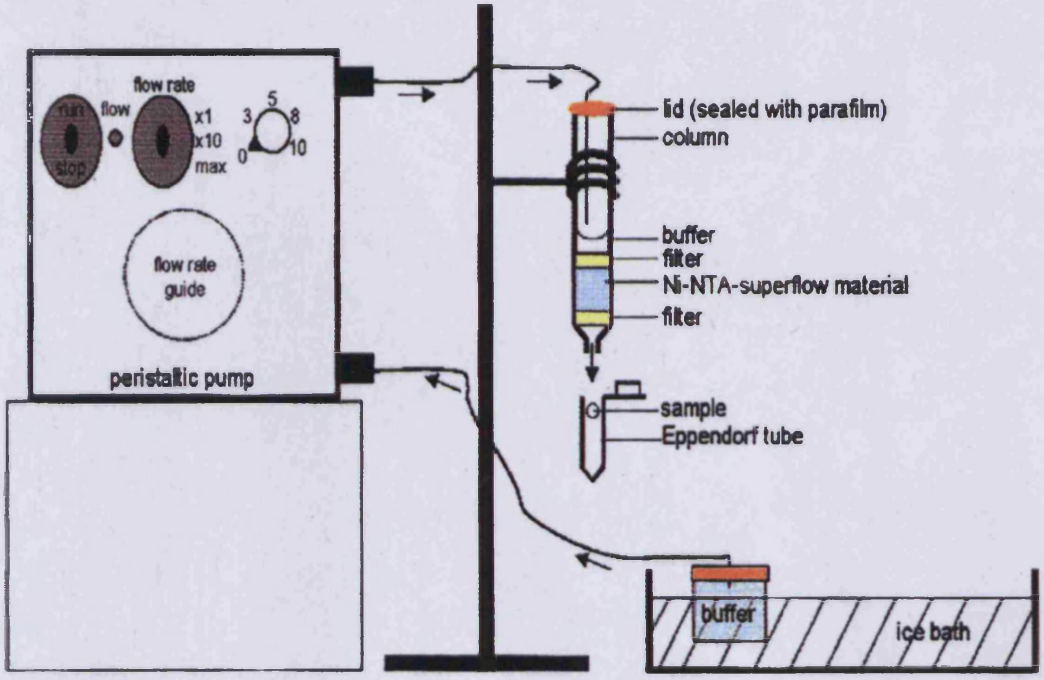

Figure 6.2. An experimental set-up of the peristaltic pump and column used to purify the protein.

6.2.5. Uptake of His_6-EGFP-R8 in HeLa cells (Live cell imaging)

HeLa cells were seeded into glass-bottomed, 35 mm culture dishes and allowed to adhere for 24 h. The cells were washed 2x with PBS before incubating with either 2μM **(A)** or 5μM **(B)** of His_6-EGFP-R8 in DMEM media for 1 hr. The cells were washed 3x with PBS and 2x imaging media, before being processed to live cell imaging analysed via confocal microscopy on the 37^0 C temperature stage.

6.2.6. Uptake of His_6-EGFP-R8 in +/- CytD pretreated HeLa cells

HeLa cells were seeded in DMEM media, 24 hrs before the experiment at a seeding density 220,000 cells/well in 6-well plates, then the cells were PBS washed and pre treated +/- 10 μM CytD for 15 min. Then 2 μM of His_6-EGFP-R8 in DMEM media was added to the cells in presence or absence of 10 μM CytD for 0, 30, 60 and 90 min at 37^0 C or for 60 min at 4^0 C. The 0 time point here refer to cells incubated for a few seconds with the protein that was then immediately removed from the cells. The cells were then washed with ice cold PBS, followed by addition of lysis buffer (50mM Tris-HCl, 150mM NaCl, dd H_2O and pH to 8.0 using 5M HCl, 1%) on ice for 5 min. Then cell lysates were removed and centrifuged at 13,000 x g for 10 min at 4^0 C. The supernatant was removed protein concentration detected using BCA method. A volume equivalent to 20 μg of protein was then mixed with sample buffer +/- DTT and loaded in 12 % gel SDS-PAGE as shown in section 2.3.7. DTT was omitted so that a non-denaturing gel could be run that retained the integrity of the GFP and also its fluorescence. The non-denatured gel was scanned on the Typhoon Variable Mode Imager while the denatured gel was processed

further by electrophoresis and immunoblotting method as shown in section 2.3.8.

6.3. Results

A typical preparation from 4 L of *E.coli* yielded 10 mg of protein that was highly fluorescent (Figure 6.3). During purification, samples were retained and Figure 6.4 highlight the appearance of a very prominent band at 30 KDa in the induced cells. Passing the supernatant through the column identified this to be the retained protein from loading up to 20 μg of this protein on gels no other band appeared suggesting this was a very pure preparation.

To analyse the protein sample 20 μg of protein either denatured or nondenatured was loaded on to gels and following electrophoresis these were immediately scanned on the Typhoon analyser. Only the non denatured protein was observed (Figure 6.4A) as a clear band of 30 KDa. However when the same gel was stained with Coomassie Brilliant Blue both bands were observed (Figure 6.5.B).

Figure 6.3. Purified and highly fluorescent His_6-EGFP-R8 Protein.

6.3.1 His_6-EGFP-R8 protein concentration and analysis

For microscopy experiment, HeLa cells were washed with PBS before incubation under tissue culture conditions with 2 or 5 μM of His_6-EGFP-R8 protein for 1 hr. Then the cells were then processed for live cell imaging confocal microscopy (section 6.2.5). The results in (Figure 6.7.A), show that at 2 μM EGFP labelled vesicles were observed but were very faint against the background labelling, whereas at 5 μM (Figure 6.7.B), the vesicles are much easier to observe and were prominent throughout the cytoplasm.

In order to attempt to quantify His_6-EGFP-R8 the protein was similarly incubated, for 60 min in 6 well plates with HeLa cells at external concentrations of 4 and 8μM. The cells were then washed with PBS and trypsinized followed by heparin washing and flow cytometry analysis.

The cell associated fluorescence (Figure 6.6) was very low compared to an equal molarity of Alexa-R8 shown in other chapters and it was impossible to then compare this control uptake with those whereby different endocytic pathways have been inhibited. Alternative methods was therefore investigated based on loading cell lysates from His_6-EGFP-R8 treated cells on SDS gels and then either scanning the gels on the Typhoon imager or alternatively by transferring the proteins from gels on to nitrocellulose membranes that were then probes with anti-EGFP antibody and HRP conjugated secondary antibodies.

HeLa cells were incubated with 2 μM of His6-EGFP-R8 for 0, 30, 60, and 90 min at 37^0 C or for 60 min at 4^0 C. The cells were then washed and trypsinized then washed 3X with PBS before being lysed using lysis buffer containing protease inhibitors and trypsin inhibitor. Following quantification of the lysate

20μg was loaded on to 12% gel followed by transfer and immunolabelling with anti EGFP antibody. The results in Figure 6.8.A show that at 0 min (Cont) and with incubations performed at 4^0 C, no band was detected. However, clear EGFP bands were detected for 30 and 60 min time points but surprisingly the signal at 90 min was significantly lower. The same experiment was repeated ,excluding 4^0 C point, and identical data was obtained including a reduced signal from 60 to 90 min. Samples from these uptake experiments were also analysed via direct scanning of the gels on the Typhoon analyser and similar to results shown in Figure 6.8A and B an increased uptake was observed between 30 and 60 minutes and then a reduction at 90 min (Figure 6.8.C). Here another band was also observed at 50 KDa in all lanes except the control but this did not appear to decrease between 60 and 90 min.

6.3.2. His_6-EGFP-R8 Uptake in HeLa cells

For microscopy experiment, HeLa cells were washed with PBS before incubation under tissue culture conditions with 2 or 5 μM of His_6-EGFP-R8 protein for 1 hr. Then the cells were then processed for live cell imaging confocal microscopy (section 6.2.5). The results in (Figure 6.7.A), show that at 2 μM EGFP labelled vesicles were observed but were very faint against the background labelling, whereas at 5 μM (Figure 6.7.B), the vesicles are much easier to observe and were prominent throughout the cytoplasm.

In order to attempt to quantify His_6-EGFP-R8 the protein was similarly incubated, for 60 min in 6 well plates with HeLa cells at external concentrations of 4 and 8 μM. The cells were then washed with PBS and trypsinized followed by heparin washing and flow cytometry analysis.

The cell associated fluorescence (Figure 6.6) was very low compared to an equal molarity of Alexa-R8 shown in other chapters and it was impossible to then compare this control uptake with those whereby different endocytic pathways have been inhibited. Alternative methods was therefore investigated based on loading cell lysates from His_6-EGFP-R8 treated cells on SDS gels and then either scanning the gels on the Typhoon imager or alternatively by transferring the proteins from gels on to nitrocellulose membranes that were then probes with anti-EGFP antibody and HRP conjugated secondary antibodies.

HeLa cells were incubated with 2 μM of His6-EGFP-R8 for 0, 30, 60, and 90 min at 37^0 C or for 60 min at 4^0 C. The cells were then washed and trypsinized then washed 3X with PBS before being lysed using lysis buffer containing protease inhibitors and trypsin inhibitor. Following quantification of the lysate 20μg was loaded on to 12% gel followed by transfer and immunolabelling with anti EGFP antibody. The results in Figure 6.8.A show that at 0 min (Cont) and with incubations performed at 4^0 C, no band was detected. However, clear EGFP bands were detected for 30 and 60 min time points but surprisingly the signal at 90 min was significantly lower. The same experiment was repeated excluding the 4^0 C point and identical data was obtained including a reduced signal from 60 to 90 min. Samples from these uptake experiments were also analysed via direct scanning of the gels on the Typhoon analyser and similar to results shown in Figure 6.8A and B an increased uptake was observed between 30 and 60 minutes and then a reduction at 90 min (Figure 6.8.C). Here another band was also observed at 50 KDa in all lanes except the control but this did not appear to decrease between 60 and 90 min.

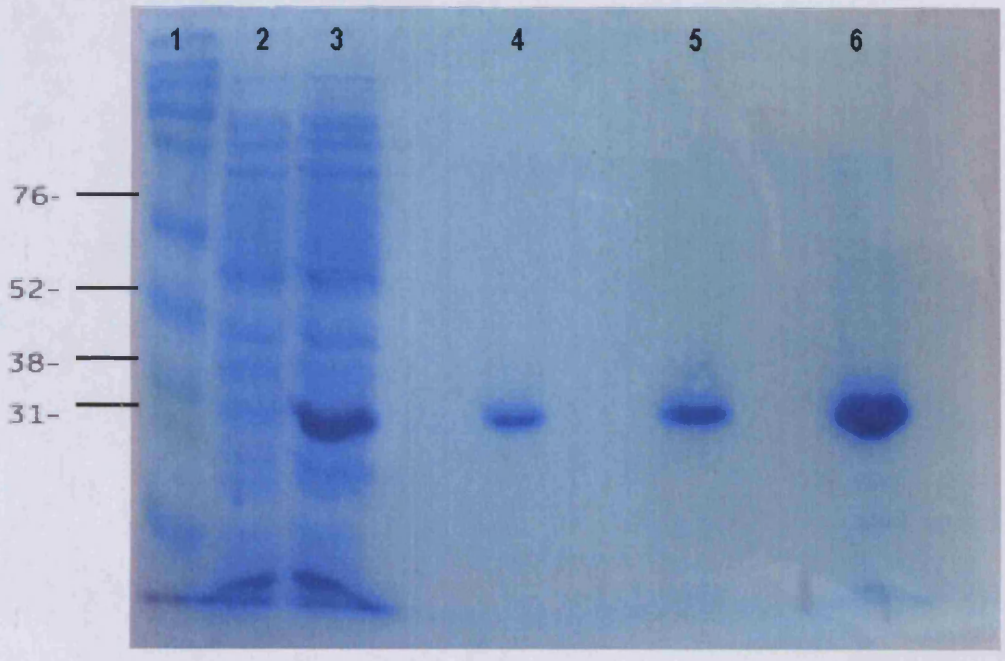

Figure 6.4. Steps towards purification of His6-EGFP-R8

Samples were loaded on to SDS PAGE gels, stained with Coomassie Brilliant Blue and then destained. (1) Molecular weight markers (2) Noninduced *E. Coli* lysates, (3) induced lysates (4-6) 5, 10, 20 μg of the purified protein.

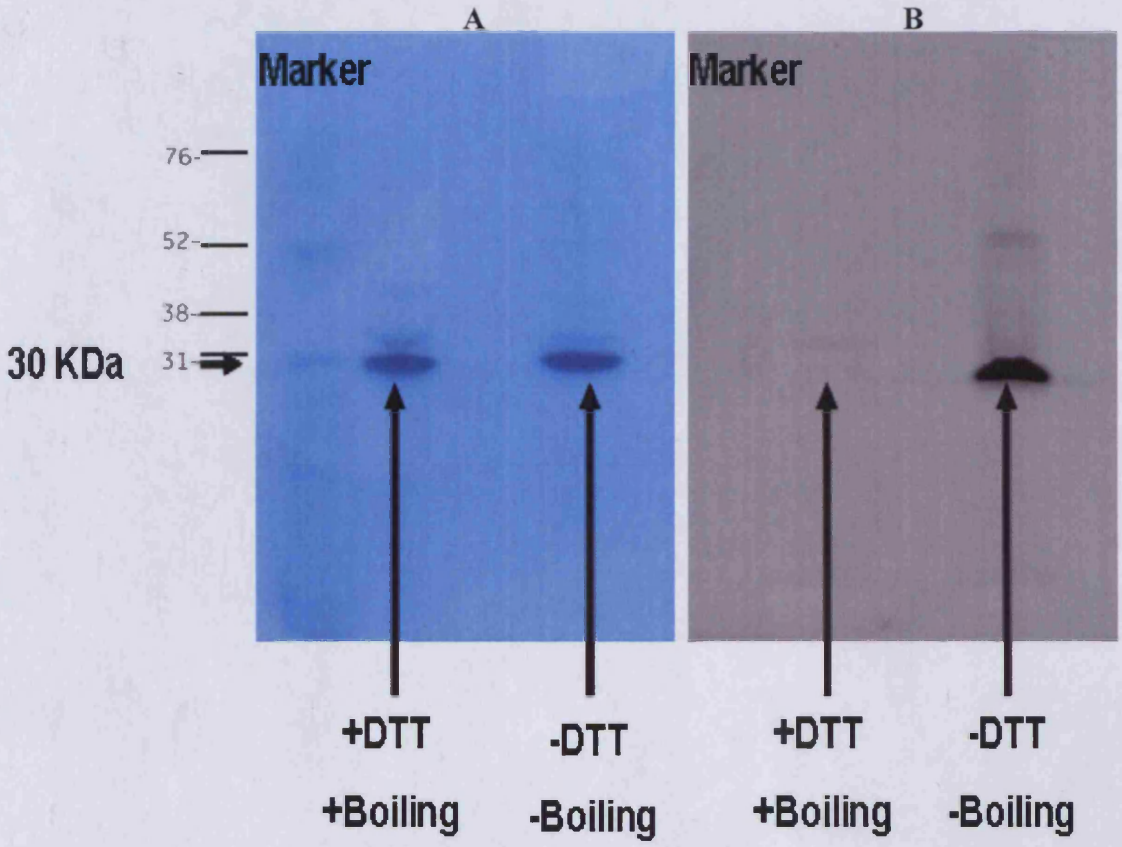

Figure 6.5 Analysis of denatured and non denatured His_6-EGFP-R8 using electrophoresis and Typhoon laser scanning.

20 µg of His6-EGFP-R8 was mixed with SDS sample buffer +/-DTT and +/-boiling and then loaded on to a 12% SDS PAGE gel. Following electrophoresis the fluorescence of the samples was measured directly from the gel on the scanner **(A)** and the same gel was then stained with Coomassie brilliant blue stain for and destained (**B**)

6.3.3. Internalisation of His_6-EGFP-R8 uptake and analysing the effect of CytD on its uptake

To study the effect of CytD on uptake of His_6-EGFP-R8, HeLa cells were washed with PBS and pre treated +/- 10 μM CytD for 15 min. Then 2 μM of His_6-EGFP-R8 was added to the cells in presence or absence of 10 μM CytD for 1 hr at 37^0 C. The cells were then washed with ice cold PBS, followed by adding lysis buffer on ice for 5 min. Following protein quantification 20 μg of lysate was analysed by non denaturing electrophoresis and the gel was then immediately scanned by the Typhoon imager. The results show an inhibition in uptake in CytD treated cells but the quality of the data was poor and time did not allow for follow up experiments to assess whether this method could be used to analyse the uptake of this protein under conditions which affect endocytic pathways (Figure 6.9).

6.4. Discussion

CPPs have been shown to be able to promote the delivery of several different types of proteins that have also been shown to retain their activities inside cell. The ability of HIV TAT to deliver β-galactosidase protein into several mouse tissues following IV injection triggered the initial interest in this field and increased the importance of CPPs as potential delivery vectors (Fawell et al. 1994; Schwarze et al. 1999). Generally, researchers couple CPPs to proteins via either covalent bonds, avidin-biotin affinity or via fusion constructs (Deshayes et al. 2008; Gros et al. 2006; Jones 2010; Patel et al. 2007). R8 as shown here in this work has previously been shown to deliver GFP to the cells (Lundberg et al. 2003; Takeuchi et al. 2006). In the later study the distribution

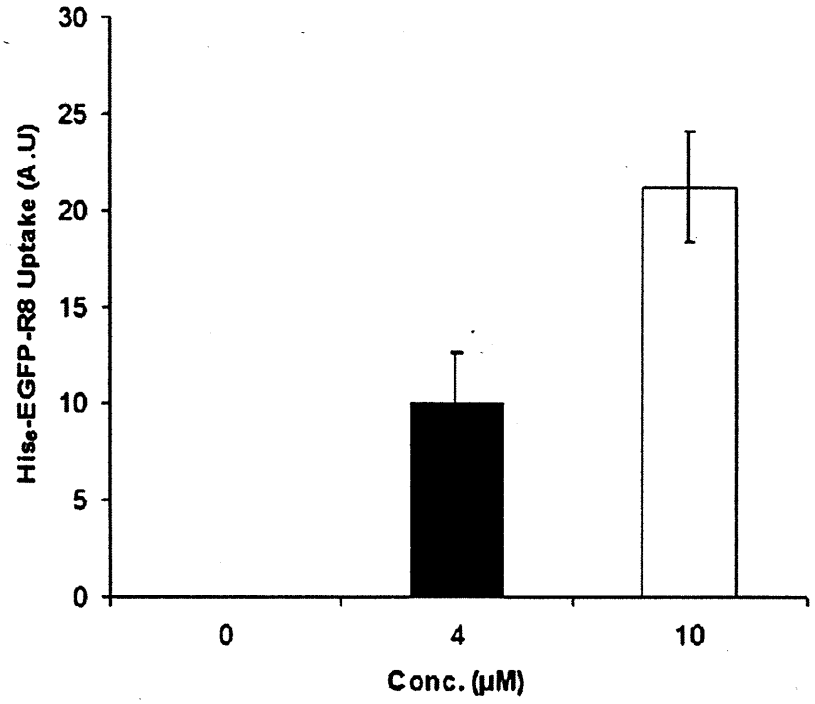

Figure 6.6. His6-EGFP-R8 uptake in HeLa cells

HeLa cells were incubated with 0, 4, 10 μM of His6-EGFP-R8 in SFM for 1 hr at 37^0 C. Then the, cells were washed with PBS and trypsinized followed by heparin washing and flow cytometry analysis (n=3).

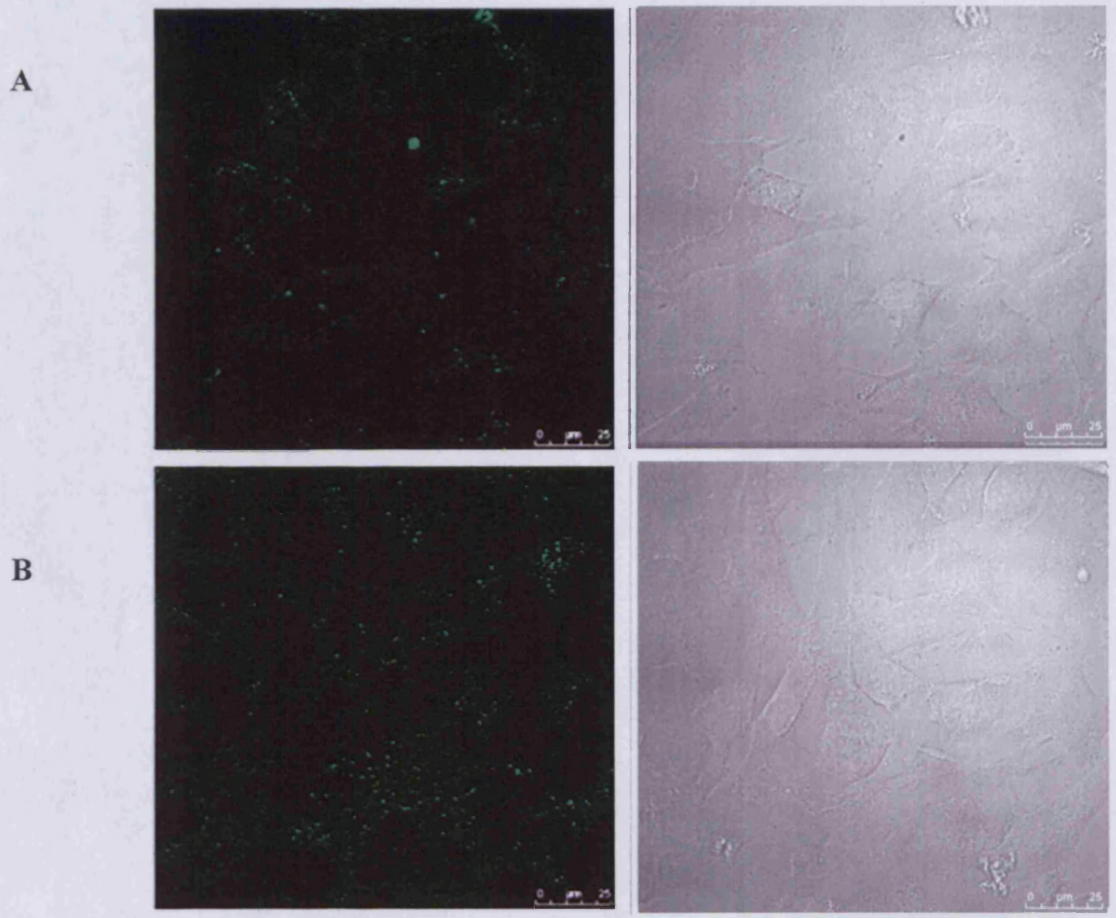

Figure 6.7 Subcellular distribution of His_6-EGFP-R8 in HeLa cells

HeLa cells were washed and incubated with either 2μM **(A)** or 5μM **(B)** of His_6-EGFP-R8 in DMEM media for 1 hr, washed and analysed by confocal microscopy on the 37^0 C temperature stage. Shown are fluorescence and bright field images.

of R8-EGFP was not shown by microscopy but in the earlier study and in this thesis it was shown to bind strongly to the plasma membrane. (Lundberg et al. 2003).

In Figure 6.7 it is seen that plasma membrane labelling is also accompanied by vesicular labelling and overall this suggests, for this CPP and others, a basic mechanism of endocytosis followed by endosomal escape for at least a fraction of the internalised protein. The exact mechanism by which these CPP conjugates enter cells in the first place and then escape from the endosomal is largely unknown. Studying protein delivery, as found in this thesis, is much more difficult than studying the uptake of fluorescent peptides. But in this chapter some preliminary experiments were performed to assess alternative methods for quantifying the uptake of EGFP-R8 protein in cells.

It was clear that by using the flow cytometry equipment available that quantifying uptake through this method would be difficult. The signal following a1 hr incubation was barely above baseline and this makes further experiments with inhibitors or siRNA treated cells very difficult. It should also be noted that trypsinisation was used here to detach the cells and to remove plasma membrane bound protein and thus may explain the further the signal weakness. One alternative would be to label the cells with a fluorescent antibody recognising EGFP and add this to cells treated with this conjugate.

Alternative methods were then investigated and successful attempt were made at measuring the uptake of the protein using electrophoresis of cell lysates from cells incubated with His6-EGFP-R8. The intact and internalised protein was

then identified either by directly scanning the fluorescence of the gel on the Typhoon analyser with 488nm excitation or alternatively through immunolabelling the protein with an anti-EGFP antibody. The data shows that initially a time dependent and temperature dependent uptake but surprising was the fact that at 90 mins the signal was reduced compared with 60 min suggesting a high degree of degradation that was occurring at a higher rate than the rate of internalisation. It may also be due to the fact that degradation was accompanied by recycling thus further reducing the signal.

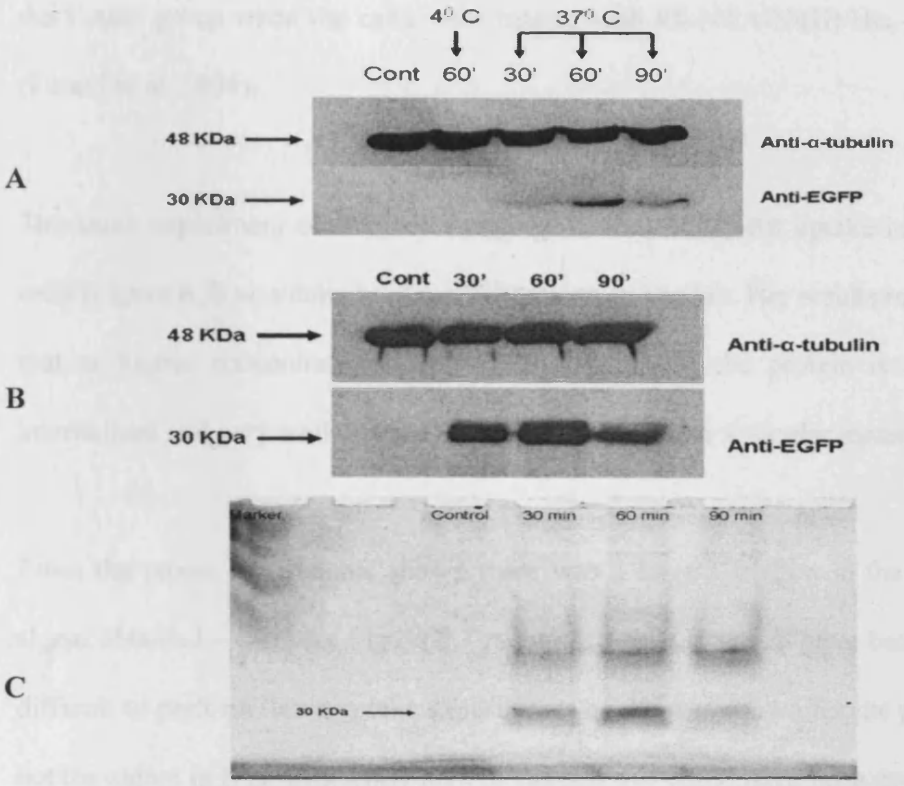

Figure 6.8 Measuring the uptake of His6-EGFP-R8 Uptake into HeLa cells

Cells were incubated with 2 μM of His6-EGFP-R8 for 60 min at 4^0 C or for 0, 30, 60, and 90 min at 37^0C (A) and the same experiment was repeated but without the 4^0 C point **(B)**. The cells were then washed and lysed and 20 μg of the cell lysates was then loaded on to 12% SDS PAGE transferred on to nitrocellulose papers that were then probed with a anti EGFP antibody and a HRP conjugated secondary antibody. Tubulin was detected as an internal control for protein loading; samples obtained from

experiment B were also loaded as non denatured proteins on to gels that following electrophoresis were scanned on the Typhoon analyser at 488nm excitation **(C).**

The requirement for energy for uptake of this conjugate was also observed by the Futaki group when the cells were treated with R8-NTA-Ni(II)/His_6-EGFP (Futaki et al. 2004).

The same experiment of live cell imaging of His_6-EGFP-R8 uptake in HeLa cells (Figure 6.7) was done by Anja Schermann in our lab. Her results revealed that at higher concentrations such as 10 or 20 μM the protein is clearly internalised and very well distributed inside the cells in a vesicular manner.

From the repeat experiments shown there was a large variation in the EGFP signal obtained – compare Figure 6.7 A and B. For A it would have been very difficult to perform timed uptake experiments of the sort shown for the peptide but the signal in B is sufficiently high to suggest this could have been done. There may be a possibility that the six histidine residues lying at the N-terminus to the protein were affecting uptake and could also influence endosomal escape. The vector was obtained from the Futaki group and was designed that the His_6 portion should be cleaved via thrombin cleavage site engineered between the His_6 and the EGFP. The intention was to perform thrombin cleavage and then re-purify the EGFP-R8 through dialysis; the His_6 portion would have been very small and would easily flow through a 10KDa dialysis membrane. However is a separate project performed in the laboratory it was discovered that there was a mutation at this site and that the thrombin would not have cleaved this purification tag from the EGFP-R8.

Time did not allow for full optimisation of the methods for quantification but an experiment was conducted to investigate whether the uptake of this probe is as sensitive to actin disruption as shown in chapter 5 for the fluorescent peptide and also for Tat-EGFP or Tat-Cre. Under microscopy the TAT-EGFP/Cre conjugates in cytochalasin D treated cells are shown lining the plasma membrane but there is very little evidence of intracellular vesicular structures (Tunneman, Ferrari). As observed with CPPs in chapter 5 treatment with this agent causes massive disruption of cell morphology and it is no surprising that this effects uptake of both CPPs as fluorescent probes and also CPP-protein conjugates.

The data in Figure 6.9 is of rather low quality but does suggest that the uptake is reduced in the Cytochalasin D treated cells thus suggesting that this method with further optimisation could be used to analyse the uptake of this protein and others provided they are fluorescent or that there are suitable antibodies available to detect them following transfer from gels. It would be interesting to now test the siRNA models developed in other chapters to see if there is parity between results for peptide uptake compared with protein uptake.

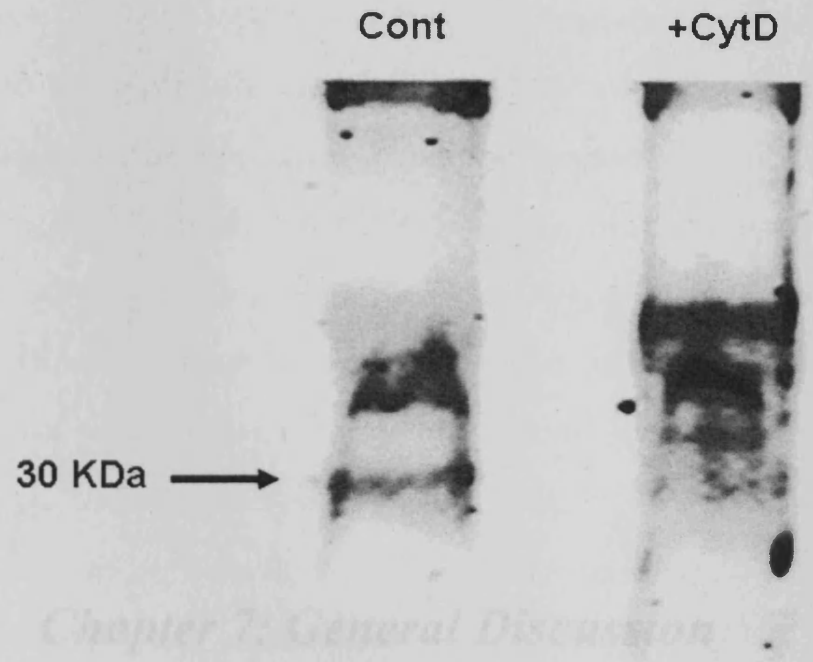

Figure 6.9 Studying the effect of CytD on His_6-EGFP-R8 Uptake

HeLa cells were treated +/- 10 μM CytD for 15 min prior to incubation with 2 μM of His_6-EGFP-R8 in presence or absence of 10 μM CytD for 1 hr at 37^0 C. The cells were then washed lysed and 20 μg undenatured protein was then separated by electrophoresis and the gel was scanned on the Typhoon analyser.

Chapter 7: General Discussion

7.1. General Discussion

A major obstacle to successful delivery of macromolecular therapeutics is getting membrane impermeable drugs such as peptides, proteins, and nucleotides to the inside of cells and defined intracellular locations. Therefore, over last 20 years, considerable effort has been invested in the design of new technologies to improve cellular uptake of therapeutic compounds (Jarver and Langel 2004; Torchilin 2005b). Although, many non-viral strategies have been introduced, including lipid-, polymeric-, nanoparticle- and peptide-based methods (Morris et al. 2000; Ogris and Wagner 2002; Torchilin 2005b), only a few of these methods have shown promise in vivo and progressed into clinical trials. The major limitations of these technologies are the poor stability of the complexes and the rapid degradation of the cargo, as well as an insufficient ability to reach the intracellular target.

Researchers are constantly looking for new vectors to deliver therapeutics into cells and prominent candidates during the last 20 years have been CPPs (Moschos et al. 2007). They are attractive as they have been shown to efficiently improve intracellular delivery of several types of macromolecules, including plasmid DNA, oligonucleotides, siRNA, PNA, proteins and peptides, liposomes and nanoparticles. Further, the they have been developed to overcome both extracellular and intracellular limitations, and to improve the movement of a cargo across the cell membrane into the cytoplasm and intracellular trafficking to reach its target (Foerg and Merkle 2008; Johnson et al. 2011; Morris et al. 2000; Snyder et al. 2005). This is important as so many vectors are able to gain access into cells but then are poor at endosomal escape and this is necessary especially if the therapeutic is sensitive to enzymes that

are found in lysosomes. It is clear that some CPPs (HIV-Tat and R8) are also delivered to lysosomes (Al-Taei et al. 2006) but numerous studies have shown that a large enough fraction of the cargo is delivered to mediate a biological response. There is still controversy regarding the uptake mechanism itself and even less is understood regarding the mechanism by which they traverse the endosomal membranes. It should not be forgotten that data is strong for a mechanism by which endosytosis is not required and this is especially the case where the cargo is small such as a fluorophore and the extracellular peptide concentration is relatively high at > 5 μM. Here only R8 and Tat were studied for the reason that most of the work from the laboratory has focused on these two CPPs and that it would have been difficult to study more CPPs in this kind of detail. In this study a concentration of 2 μM was chosen for all studies as it was found here, and others have published, that uptake at this concentration, for these peptides, can be inhibited by at least 85 % by performing the uptake experiments on ice. This allowed for studies performed here to investigate in detail the endocytic pathways that CPPs use to gain access with minimal influence from direct plasma membrane penetration.

The organization of mammalian cells is however highly complex and this system is maintained through the organization of the cytoplasm into multiple intracellular structures and each of these structures has their own specific identity and function (Bonifacino and Glick 2004). Endocytic pathway controls the transport of molecules, such as receptor ligands and solutes entering the cells (Maxfield and McGraw 2004). But these systems are also highly complex involving hundereds of different proteins and lipids (Doherty and McMahon 2009). For drug delivery research that is interested in using endocytosis for

cellular delivery it is important that this complexity is appreciated and that tools are in place to study the different entry routes. This was one of the main objectives of this thesis as a failure to understand this may lead to insufficient cell entry or intracellular traffic to an inappropriate cell location or alternatively into the recycling pathway leading to exit from the cell. Cell biologists are mainly focused on studying specific pathways or even a single protein mediating endocytosis but for drug delivery it is often required to be able to study several endocytic pathways at once or at least be able to study the involvement of one pathway in the uptake of a candidate drug delivery system. Thus especially important for the drug delivery researcher is tools that can be used to pinpoint the type of endocytic pathway(s) that a cell uses to internalise a vector. These need to be simple, reproducible, affordable methods and most importantly they need to be specific for a particular pathway. By far the most commonly used tools are pharmacological or chemical inhibitors. As mentioned previously, there are several advantages to using these inhibitors over the more sophisticated molecular biological tools, however, they suffer enormously from toxicity and lack of specificity (Ivanov 2008; Vercauteren et al. 2010). Introducing a mutant protein into a cell system can also be used and this was not studied in this thesis but the problem here is controlling expression levels and maintaining that the protein does not then sequester other proteins in the cell that may be needed. Alternatively, the possibility now exists whereby single proteins can be depleted from cells using siRNA targeting and this was the main focus of this thesis. Previously in the lab this method was not used but now cells models are in place that allow for depletion and phenotypic

characterisation of cells depleted in several endocytic pathways and this was the main achievement of the thesis.

Targeted pathways were those regulated by CHC, Flot-1, DNM2, Cav-1 and PAK-1 and I successfully depleted each protein and then identified probes that could be used to show the effects on one or more aspect of endocytosis. Unlike most studies using pharmacological inhibition or siRNA depletion, experiments using single time points were not employed and rather I have developed assays whereby uptake was studies for various periods of time. This was more of an experimental challenge but very useful information was gained from this approach including showing the effects of CHC depletion on transferrin recycling and also that the effects of CytD on CPP was not immediate but occurred after an initial phase where uptake was identical. This approach was however difficult for analyzing the role of cavaeolae in endocytosis of BODIPY-LacCer as the probe penetrated into the plasma membrane and required extensive washing to remove this fraction so that the internalised fraction could be measured. This suggests an alternative probe is required for this pathway and the same is true for the pathway regulated by Flot-1. Here anti-CD59 was used but only one type of antibody proved suitable for these studies. During the course of these studies the effect of Flot-1 depletion on uptake of the cationic polymer polyethylenimine was shown (Payne et al. 2007) and the group in Ghent also identified that Flot-1 depletion also affected uptake of disulphide-based polyamidoamine polyplexes (Vercauteren et al. 2011) suggesting these may also be used as novel probes for the flotillin pathway. It is however important to note that Cav-1 and Flot-1 are known to organize domains on the plasma membrane thus depleting these

proteins form cells may change the landscape of the membrane completely and affect other endocytic pathways. This needs further experimentation.

DNM2 proved to be the most difficult protein to deplete and it is most famous for regulating uptake through the clathrin pathway. However, one study led us to believe that depleting this protein could also help answer the roles that fluid phase endocytosis had in CPP uptake (Cao et al. 2007). Eventually, and only in A431 cells the protein was depleted but I could not see any effect on fluid phase uptake in cells depleted of this protein, yet uptake through clathrin was significantly reduced. This, together with the data using Dynasore questions the role of this protein in fluid phase endocytosis and there is still a need for a suitable protein marker fro this pathway that could be depleted with a siRNA sequence.

To cell lines HeLa and A431 were used throughout this thesis and ideally all the work would have been performed in a single cell line. But this was not possible because of the work required to study macropinocytosis and to deplete DNM2. Macropinocytosis proved difficult to study and it was important that a protein was available to deplete with a siRNA sequence and also that a good assay was available to study this process. Adding EGF to cells proved to be very effective for measuring growth factor induced macropinocytosos but the HeLa cell line proved to deficient for this. This was due to the known fact that they express low levels of EGFR but I also discovered that expression of PAK-1 is also very low in this line and thus it became very difficult to study the effects of depleting this protein on macropinocytosis. Thus the skin epithelia

A431 cell-line was chosen to extensively study this pathway, as there is a lot of literature on its capacity to perform this process; especially in response to addition of EGF. The choice of probe for this pathway was also a problem as there is no macropinocytosis specific probe. I eventually used the concept of EGF stimulation, in which the cells increase the fluid phase uptake of a fluid phase marker, such as dextran, which then reflects on their capacity to perform macropinocytosis. Consequently, inhibiting PAK-1, that was shown to regulate macropinocytosis, inhibited the increase in dextran uptake thus a model for this pathway was in place to study the role of this pathway in uptake of R8 and Tat. No single siRNA sequence or pharmacological inhibitor completely inhibits the uptake of the two peptides studied here thus further questioning whether even at these low concentrations, the role endocytosis has to play. It may be that a fraction, and in a temperature dependent manner, moves directly across the plasma membrane or it may be that the roles of simple fluid phase uptake, independent of DNM2, is mediating uptake. This requires further characterization.

Of all the siRNAs tested only the one targeting PAK-1 had any effect on uptake of CPPs and this was significant but not complete. During the studies it also became clear that PAK-1 depleted cells also had strange distribution of the actin cytoskeleton thus it may be that the effects of PAK-1 depletion may be on the cell cytoskeleton that then indirectly effects uptake of the CPPs. The work clearly showed that actin disruption with CytD also inhibited uptake but this drug causes huge effects on cell morphology and again this may be the reason as to why it is such a strong inhibitor of CPP entry rather than being a specific

inhibitor of macropinocytosis. During these studies, I also identified some rather unexpected findings regarding the role of action or the effects of CytD on uptake of dextran. Rather than finding an inhibition in uptake I found that the drug increased uptake of several variants of this probe but a search of the literature identified other examples of this (Gold et al. 2010; Song and Schmid 2003). This may be due to its effects on recycling but more work on other cell lines is required to better understand the mechanism by which it is doing this and these are underway.

The project finally moved to look at the capacity of R8 to internalise a much larger cargo into cell namely EGFP. Time did not allow for extensive studies here and progress was much slower due to the fact that the protein had to be purified from *E. Coli* before it could be loaded on to cells. In order to compare R8-fluorophore uptake with R8-protein uptake it was decided to keep the extracellular concentration at 2μM. However in my hands uptake of the protein at this concentration was difficult to detect using both microscopical methods and more quantifiable methods. However the use of the Typhoon analyser showed that the intact protein could be detected in cells thus allowing for the future developments of an assay that not only measures uptake but also degradation. This could be performed by combining detection systems measuring fluorescence of EGFP and also EGFP (whole and degraded) using an antibody and ECL. Overall however though there was evidence that the method could be used to show again that CytD affected uptake time did not allow for a screen of the siRNAs and pathways that were developed for investigating peptide uptake.

The methods developed in this thesis have already revealed some very important issues relating to the uptake of CPPs but the hope is that they can now be used to prepare a manuscript and then study a host of other drug delivery systems. This would be to gain a better understanding of their mode of internalisation, intracellular traffic and endosomal escape thus allowing them easier progression from the laboratory to the clinic.

References:

Al-Taei, S. et al. 2006. Intracellular traffic and fate of protein transduction domains HIV-1 TAT peptide and octaarginine. Implications for their utilization as drug delivery vectors. *Bioconjug Chem* 17(1), pp. 90-100.

Alberts, B. 2002. *Molecular biology of the cell.* 4th ed. New York: Garland Science, p. 1463p. +.

Amand, H. L. et al. 2008. Stimulated endocytosis in penetratin uptake: effect of arginine and lysine. *Biochem Biophys Res Commun* 371(4), pp. 621-625.

Anderson, R. G. 1998. The caveolae membrane system. *Annu Rev Biochem* 67, pp. 199-225.

Aniento, F. et al. 1996. An endosomal beta COP is involved in the pH-dependent formation of transport vesicles destined for late endosomes. *J Cell Biol* 133(1), pp. 29-41.

Aoki, S. et al. 2010. The role of proline in the membrane re-entrant helix of caveolin-1. *J Biol Chem* 285(43), pp. 33371-33380.

Araki, N. et al. 2007. Phosphoinositide metabolism during membrane ruffling and macropinosome formation in EGF-stimulated A431 cells. *Exp Cell Res* 313(7), pp. 1496-1507.

Arias-Romero, L. E. and Chernoff, J. 2008. A tale of two Paks. *Biol Cell* 100(2), pp. 97-108.

Aubry, S. et al. 2010. MALDI-TOF mass spectrometry: a powerful tool to study the internalization of cell-penetrating peptides. *Biochim Biophys Acta* 1798(12), pp. 2182-2189.

Beattie, E. C. et al. 2000. Regulation of AMPA receptor endocytosis by a signaling mechanism shared with LTD. *Nat Neurosci* 3(12), pp. 1291-1300.

Beauvais, D. M. and Rapraeger, A. C. 2004. Syndecans in tumor cell adhesion and signaling. *Reprod Biol Endocrinol* 2, p. 3.

Belting, M. 2003. Heparan sulfate proteoglycan as a plasma membrane carrier. *Trends Biochem Sci* 28(3), pp. 145-151.

Bernheimer, A. W. and Rudy, B. 1986. Interactions between membranes and cytolytic peptides. *Biochim Biophys Acta* 864(1), pp. 123-141.

Billy, E. et al. 2001. Specific interference with gene expression induced by long, double-stranded RNA in mouse embryonal teratocarcinoma cell lines. *Proc Natl Acad Sci U S A* 98(25), pp. 14428-14433.

Bodian, D. L. et al. 1997. Mutational analysis of the active site and antibody epitopes of the complement-inhibitory glycoprotein, CD59. *J Exp Med* 185(3), pp. 507-516.

Bolton, S. J. et al. 2000. Cellular uptake and spread of the cell-permeable peptide penetratin in adult rat brain. *Eur J Neurosci* 12(8), pp. 2847-2855.

Bonifacino, J. S. and Glick, B. S. 2004. The mechanisms of vesicle budding and fusion. *Cell* 116(2), pp. 153-166.

Brodsky, F. M. et al. 2001. Biological basket weaving: formation and function of clathrin-coated vesicles. *Annu Rev Cell Dev Biol* 17, pp. 517-568.

Cao, G. et al. 2002. In Vivo Delivery of a Bcl-xL Fusion Protein Containing the TAT Protein Transduction Domain Protects against Ischemic Brain Injury and Neuronal Apoptosis. *J Neurosci* 22(13), pp. 5423-5431.

Cao, H. et al. 2007. Dynamin 2 mediates fluid-phase micropinocytosis in epithelial cells. *J Cell Sci* 120(Pt 23), pp. 4167-4177.

Caron, N. J. et al. 2001. Intracellular delivery of a Tat-eGFP fusion protein into muscle cells. *Mol Ther* 3(3), pp. 310-318.

Chen, C. S. et al. 1998. Abnormal transport along the lysosomal pathway in mucolipidosis, type IV disease. *Proc Natl Acad Sci U S A* 95(11), pp. 6373-6378.

Cheng, Z. J. et al. 2006. Distinct mechanisms of clathrin-independent endocytosis have unique sphingolipid requirements. *Mol Biol Cell* 17(7), pp. 3197-3210.

Chico, D. E. et al. 2003. Binding of cationic cell-permeable peptides to plastic and glass. *Peptides* 24(1), pp. 3-9.

Coniglio, S. J. et al. 2008. Pak1 and Pak2 mediate tumor cell invasion through distinct signaling mechanisms. *Mol Cell Biol* 28(12), pp. 4162-4172.

Conner, S. D. and Schmid, S. L. 2003. Regulated portals of entry into the cell. *Nature* 422(6927), pp. 37-44.

Console, S. et al. 2003. Antennapedia and HIV transactivator of transcription (TAT) "protein transduction domains" promote endocytosis of high molecular weight cargo upon binding to cell surface glycosaminoglycans. *J Biol Chem* 278(37), pp. 35109-35114.

Couet, J. et al. 2001. Cell biology of caveolae and caveolin. *Adv Drug Deliv Rev* 49(3), pp. 223-235.

D'Souza-Schorey, C. and Chavrier, P. 2006. ARF proteins: roles in membrane traffic and beyond. *Nat Rev Mol Cell Biol* 7(5), pp. 347-358.

D'Souza-Schorey, C. et al. 1995. A regulatory role for ARF6 in receptor-mediated endocytosis. *Science* 267(5201), pp. 1175-1178.

Damke, H. et al. 1994. Induction of mutant dynamin specifically blocks endocytic coated vesicle formation. *J Cell Biol* 127(4), pp. 915-934.

Damke, H. et al. 2001. Dynamin GTPase domain mutants block endocytic vesicle formation at morphologically distinct stages. *Mol Biol Cell* 12(9), pp. 2578-2589.

De Camilli, P. and Takei, K. 1996. Molecular mechanisms in synaptic vesicle endocytosis and recycling. *Neuron* 16(3), pp. 481-486.

de Fougerolles, A. et al. 2007. Interfering with disease: a progress report on siRNA-based therapeutics. *Nat Rev Drug Discov* 6(6), pp. 443-453.

Dermine, J. F. et al. 2001. Flotillin-1-enriched lipid raft domains accumulate on maturing phagosomes. *J Biol Chem* 276(21), pp. 18507-18512.

Derossi, D. et al. 1996. Cell internalization of the third helix of the Antennapedia homeodomain is receptor-independent. *J Biol Chem* 271(30), pp. 18188-18193.

Derossi, D. et al. 1994. The third helix of the Antennapedia homeodomain translocates through biological membranes. *J Biol Chem* 269(14), pp. 10444-10450.

Deshayes, S. et al. 2008. Delivery of proteins and nucleic acids using a non-covalent peptide-based strategy. *Adv Drug Deliv Rev* 60(4-5), pp. 537-547.

Dharmawardhane, S. et al. 1997. Localization of p21-activated kinase 1 (PAK1) to pinocytic vesicles and cortical actin structures in stimulated cells. *J Cell Biol* 138(6), pp. 1265-1278.

Dharmawardhane, S. et al. 2000. Regulation of macropinocytosis by p21-activated kinase-1. *Mol Biol Cell* 11(10), pp. 3341-3352.

Di Fiore, P. P. and De Camilli, P. 2001. Endocytosis and signaling. an inseparable partnership. *Cell* 106(1), pp. 1-4.

Dietz, G. P. and Bahr, M. 2004. Delivery of bioactive molecules into the cell: the Trojan horse approach. *Mol Cell Neurosci* 27(2), pp. 85-131.

Ding, H. et al. 2003. Selective silencing by RNAi of a dominant allele that causes amyotrophic lateral sclerosis. *Aging Cell* 2(4), pp. 209-217.

Doherty, G. J. and Lundmark, R. 2009. GRAF1-dependent endocytosis. *Biochem Soc Trans* 37(Pt 5), pp. 1061-1065.

Doherty, G. J. and McMahon, H. T. 2009. Mechanisms of endocytosis. *Annu Rev Biochem* 78, pp. 857-902.

Drab, M. et al. 2001. Loss of caveolae, vascular dysfunction, and pulmonary defects in caveolin-1 gene-disrupted mice. *Science* 293(5539), pp. 2449-2452.

Drin, G. et al. 2003. Studies on the internalization mechanism of cationic cell-penetrating peptides. *J Biol Chem* 278(33), pp. 31192-31201.

Duchardt, F. et al. 2007. A comprehensive model for the cellular uptake of cationic cell-penetrating peptides. *Traffic* 8(7), pp. 848-866.

Dupree, P. et al. 1993. Caveolae and sorting in the trans-Golgi network of epithelial cells. *Embo J* 12(4), pp. 1597-1605.

Eguchi, A. and Dowdy, S. F. 2010. Efficient siRNA delivery by novel PTD-DRBD fusion proteins. *Cell Cycle* 9(3), pp. 424-425.

El-Andaloussi, S. et al. 2007. Cargo-dependent cytotoxicity and delivery efficacy of cell-penetrating peptides: a comparative study. *Biochem J* 407(2), pp. 285-292.

El-Sayed, A. et al. 2009. Delivery of macromolecules using arginine-rich cell-penetrating peptides: ways to overcome endosomal entrapment. *Aaps J* 11(1), pp. 13-22.

Ellinger, I. and Fuchs, R. 2010. Receptor-mediated and fluid-phase transcytosis of horseradish peroxidase across rat hepatocytes. *J Biomed Biotechnol* 2010, p. 850320.

Elmquist, A. et al. 2006. Structure-activity relationship study of the cell-penetrating peptide pVEC. *Biochim Biophys Acta* 1758(6), pp. 721-729.

Elmquist, A. et al. 2001. VE-cadherin-derived cell-penetrating peptide, pVEC, with carrier functions. *Exp Cell Res* 269(2), pp. 237-244.

Embury, J. et al. 2001. Proteins linked to a protein transduction domain efficiently transduce pancreatic islets. *Diabetes* 50(8), pp. 1706-1713.

Fawell, S. et al. 1994. Tat-mediated delivery of heterologous proteins into cells. *Proc Natl Acad Sci U S A* 91(2), pp. 664-668.

Ferrari, A. et al. 2003. Caveolae-mediated internalization of extracellular HIV-1 tat fusion proteins visualized in real time. *Mol Ther* 8(2), pp. 284-294.

Ferrari, M. E. et al. 1998. Analytical methods for the characterization of cationic lipid-nucleic acid complexes. *Hum Gene Ther* 9(3), pp. 341-351.

Fischer, R. et al. 2005. Break on through to the other side-biophysics and cell biology shed light on cell-penetrating peptides. *Chembiochem* 6(12), pp. 2126-2142.

Fischer, R. et al. 2004. A stepwise dissection of the intracellular fate of cationic cell-penetrating peptides. *J Biol Chem* 279(13), pp. 12625-12635.

Fittipaldi, A. et al. 2003. Cell membrane lipid rafts mediate caveolar endocytosis of HIV-1 Tat fusion proteins. *J Biol Chem* 278(36), pp. 34141-34149.

Foerg, C. and Merkle, H. P. 2008. On the biomedical promise of cell penetrating peptides: limits versus prospects. *J Pharm Sci* 97(1), pp. 144-162.

Fra, A. M. et al. 1994. Detergent-insoluble glycolipid microdomains in lymphocytes in the absence of caveolae. *J Biol Chem* 269(49), pp. 30745-30748.

Fra, A. M. et al. 1995. De novo formation of caveolae in lymphocytes by expression of VIP21-caveolin. *Proc Natl Acad Sci U S A* 92(19), pp. 8655-8659.

Frank, P. G. et al. 2003. Caveolin, caveolae, and endothelial cell function. *Arterioscler Thromb Vasc Biol* 23(7), pp. 1161-1168.

Frankel, A. D. and Pabo, C. O. 1988. Cellular uptake of the tat protein from human immunodeficiency virus. *Cell* 55(6), pp. 1189-1193.

Fretz, M. et al. 2006. Effects of Na+/H+ exchanger inhibitors on subcellular localisation of endocytic organelles and intracellular dynamics of protein transduction domains HIV-TAT peptide and octaarginine. *J Control Release* 116(2), pp. 247-254.

Fretz, M. M. et al. 2004. OVCAR-3 cells internalize TAT-peptide modified liposomes by endocytosis. *Biochim Biophys Acta* 1665(1-2), pp. 48-56.

Fretz, M. M. et al. 2007. Temperature-, concentration- and cholesterol-dependent translocation of L- and D-octa-arginine across the plasma and nuclear membrane of CD34+ leukaemia cells. *Biochem J* 403(2), pp. 335-342.

Frick, M. et al. 2007. Coassembly of flotillins induces formation of membrane microdomains, membrane curvature, and vesicle budding. *Curr Biol* 17(13), pp. 1151-1156.

Fujimoto, L. M. et al. 2000. Actin assembly plays a variable, but not obligatory role in receptor-mediated endocytosis in mammalian cells. *Traffic* 1(2), pp. 161-171.

Furuchi, T. and Anderson, R. G. 1998. Cholesterol depletion of caveolae causes hyperactivation of extracellular signal-related kinase (ERK). *J Biol Chem* 273(33), pp. 21099-21104.

Futaki, S. et al. 2004. Arginine carrier peptide bearing Ni(II) chelator to promote cellular uptake of histidine-tagged proteins. *Bioconjug Chem* 15(3), pp. 475-481.

Futaki, S. et al. 2001. Arginine-rich peptides. An abundant source of membrane-permeable peptides having potential as carriers for intracellular protein delivery. *J Biol Chem* 276(8), pp. 5836-5840.

Gammon, S. T. et al. 2003. Quantitative analysis of permeation peptide complexes labeled with Technetium-99m: chiral and sequence-specific effects on net cell uptake. *Bioconjug Chem* 14(2), pp. 368-376.

Gerbal-Chaloin, S. et al. 2007. First step of the cell-penetrating peptide mechanism involves Rac1 GTPase-dependent actin-network remodelling. *Biol Cell* 99(4), pp. 223-238.

Glebov, O. O. et al. 2006. Flotillin-1 defines a clathrin-independent endocytic pathway in mammalian cells. *Nat Cell Biol* 8(1), pp. 46-54.

Gold, S. et al. 2010. A clathrin independent macropinocytosis-like entry mechanism used by bluetongue virus-1 during infection of BHK cells. *PLoS One* 5(6), p. e11360.

Gomez, J. and Matsuyama, S. 2010. Cell-penetrating penta-peptides and Bax-inhibiting peptides: protocol for their application. *Methods Mol Biol* 683, pp. 465-471.

Grassme, H. U. et al. 1996. Gonococcal opacity protein promotes bacterial entry-associated rearrangements of the epithelial cell actin cytoskeleton. *Infect Immun* 64(5), pp. 1621-1630.

Gros, E. et al. 2006. A non-covalent peptide-based strategy for protein and peptide nucleic acid transduction. *Biochim Biophys Acta* 1758(3), pp. 384-393.

Gump, J. M. et al. 2010. Revised role of glycosaminoglycans in TAT protein transduction domain-mediated cellular transduction. *J Biol Chem* 285(2), pp. 1500-1507.

Gupta, B. et al. 2005. Intracellular delivery of large molecules and small particles by cell-penetrating proteins and peptides. *Adv Drug Deliv Rev* 57(4), pp. 637-651.

Haigler, H. T. et al. 1979. Rapid stimulation of pinocytosis in human carcinoma cells A-431 by epidermal growth factor. *J Cell Biol* 83(1), pp. 82-90.

Hamasaki, M. et al. 2004. Association of early endosomal autoantigen 1 with macropinocytosis in EGF-stimulated A431 cells. *Anat Rec A Discov Mol Cell Evol Biol* 277(2), pp. 298-306.

Hansen, G. H. et al. 2005. Cholera toxin entry into pig enterocytes occurs via a lipid raft- and clathrin-dependent mechanism. *Biochemistry* 44(3), pp. 873-882.

Harasaki, K. et al. 2005. Sorting of major cargo glycoproteins into clathrin-coated vesicles. *Traffic* 6(11), pp. 1014-1026.

Harper, S. Q. et al. 2005. RNA interference improves motor and neuropathological abnormalities in a Huntington's disease mouse model. *Proc Natl Acad Sci U S A* 102(16), pp. 5820-5825.

Hill, M. M. et al. 2008. PTRF-Cavin, a conserved cytoplasmic protein required for caveola formation and function. *Cell* 132(1), pp. 113-124.

Hochuli, E. et al. 1987. New metal chelate adsorbent selective for proteins and peptides containing neighbouring histidine residues. *J Chromatogr* 411, pp. 177-184.

Hofmann, C. et al. 2004. The genetics of Pak. *J Cell Sci* 117(Pt 19), pp. 4343-4354.

Holm, T. et al. 2005. Uptake of cell-penetrating peptides in yeasts. *FEBS Lett* 579(23), pp. 5217-5222.

Huang, F. et al. 2004. Analysis of clathrin-mediated endocytosis of epidermal growth factor receptor by RNA interference. *J Biol Chem* 279(16), pp. 16657-16661.

Ivanov, A. I. 2008. Pharmacological inhibition of endocytic pathways: is it specific enough to be useful? *Methods Mol Biol* 440, pp. 15-33.

Jacque, J. M. et al. 2002. Modulation of HIV-1 replication by RNA interference. *Nature* 418(6896), pp. 435-438.

Jarver, P. and Langel, U. 2004. The use of cell-penetrating peptides as a tool for gene regulation. *Drug Discov Today* 9(9), pp. 395-402.

Jarver, P. and Langel, U. 2006. Cell-penetrating peptides--a brief introduction. *Biochim Biophys Acta* 1758(3), pp. 260-263.

Jiao, C. Y. et al. 2009. Translocation and endocytosis for cell-penetrating peptide internalization. *J Biol Chem* 284(49), pp. 33957-33965.

Jin, L. H. et al. 2001. Transduction of human catalase mediated by an HIV-1 TAT protein basic domain and arginine-rich peptides into mammalian cells. *Free Radic Biol Med* 31(11), pp. 1509-1519.

Johannes, L. and b Lamaze, C. 2002. Clathrin-dependent or not: is it still the question? *Traffic* 3(7), pp. 443-451.

Johannessen, L. E. et al. 2000. Epidermal growth factor receptor efficiently activates mitogen-activated protein kinase in HeLa cells and Hep2 cells conditionally defective in clathrin-dependent endocytosis. *Exp Cell Res* 260(1), pp. 136-145.

Johnson, R. M. et al. 2011. Therapeutic applications of cell-penetrating peptides. *Methods Mol Biol* 683, pp. 535-551.

Jones, A. T. 2007. Macropinocytosis: searching for an endocytic identity and role in the uptake of cell penetrating peptides. *J Cell Mol Med* 11(4), pp. 670-684.

Jones, A. T. 2008. Gateways and tools for drug delivery: endocytic pathways and the cellular dynamics of cell penetrating peptides. *Int J Pharm* 354(1-2), pp. 34-38.

Jones, A. T. 2010. *Uptake and Intracellular Dynamics of Proteins Internalized by Cell-Penetrating Peptides*. John Wiley & Sons, Inc., pp. 263-288.

Jones, S. W. et al. 2005. Characterisation of cell-penetrating peptide-mediated peptide delivery. *Br J Pharmacol* 145(8), pp. 1093-1102.

Kalin, S. et al. 2010. Macropinocytotic uptake and infection of human epithelial cells with species B2 adenovirus type 35. *J Virol* 84(10), pp. 5336-5350.

Kaplan, I. M. et al. 2005. Cationic TAT peptide transduction domain enters cells by macropinocytosis. *Journal of controlled release* 102(1), pp. 247-253.

Kerr, M. C. and Teasdale, R. D. 2009. Defining macropinocytosis. *Traffic* 10(4), pp. 364-371.

Khalil, I. A. et al. 2006. Uptake pathways and subsequent intracellular trafficking in nonviral gene delivery. *Pharmacol Rev* 58(1), pp. 32-45.

Kimberley, F. C. et al. 2007. Alternative roles for CD59. *Mol Immunol* 44(1-3), pp. 73-81.

Kirchhausen, T. et al. 2008. Use of dynasore, the small molecule inhibitor of dynamin, in the regulation of endocytosis. *Methods Enzymol* 438, pp. 77-93.

Koivusalo, M. et al. 2010. Amiloride inhibits macropinocytosis by lowering submembranous pH and preventing Rac1 and Cdc42 signaling. *J Cell Biol* 188(4), pp. 547-563.

Kong, H. J. and Mooney, D. J. 2007. Microenvironmental regulation of biomacromolecular therapies. *Nat Rev Drug Discov* 6(6), pp. 455-463.

Kosuge, M. et al. 2008. Cellular internalization and distribution of arginine-rich peptides as a function of extracellular peptide concentration, serum, and plasma membrane associated proteoglycans. *Bioconjug Chem* 19(3), pp. 656-664.

Kovacs, M. et al. 2004. Mechanism of blebbistatin inhibition of myosin II. *J Biol Chem* 279(34), pp. 35557-35563.

Laakkonen, P. and Vuorinen, K. 2010. Homing peptides as targeted delivery vehicles. *Integr Biol (Camb)* 2(7-8), pp. 326-337.

Lamaze, C. et al. 2001. Interleukin 2 receptors and detergent-resistant membrane domains define a clathrin-independent endocytic pathway. *Mol Cell* 7(3), pp. 661-671.

Lee, Y. J. et al. 2008. Real-time fluorescence detection of protein transduction into live cells. *J Am Chem Soc* 130(8), pp. 2398-2399.

Letoha, T. et al. 2003. Membrane translocation of penetratin and its derivatives in different cell lines. *J Mol Recognit* 16(5), pp. 272-279.

Li, H. et al. 2005a. A live-cell high-throughput screening assay for identification of fatty acid uptake inhibitors. *Anal Biochem* 336(1), pp. 11-19.

Li, Y. et al. 2005b. Selective induction of apoptosis in mutant p53 premalignant and malignant cancer cells by PRIMA-1 through the c-Jun-NH2-kinase pathway. *Mol Cancer Ther* 4(6), pp. 901-909.

Liberali, P. et al. 2008. The closure of Pak1-dependent macropinosomes requires the phosphorylation of CtBP1/BARS. *Embo J* 27(7), pp. 970-981.

Limouze, J. et al. 2004. Specificity of blebbistatin, an inhibitor of myosin II. *J Muscle Res Cell Motil* 25(4-5), pp. 337-341.

Lundberg, M. et al. 2003. Cell surface adherence and endocytosis of protein transduction domains. *Mol Ther* 8(1), pp. 143-150.

Lundmark, R. et al. 2008. The GTPase-activating protein GRAF1 regulates the CLIC/GEEC endocytic pathway. *Curr Biol* 18(22), pp. 1802-1808.

Macia, E. et al. 2006. Dynasore, a cell-permeable inhibitor of dynamin. *Dev Cell* 10(6), pp. 839-850.

Maiolo, J. R. et al. 2005. Effects of cargo molecules on the cellular uptake of arginine-rich cell-penetrating peptides. *Biochim Biophys Acta* 1712(2), pp. 161-172.

Manceur, A. et al. 2007. Flow cytometric screening of cell-penetrating peptides for their uptake into embryonic and adult stem cells. *Anal Biochem* 364(1), pp. 51-59.

Marechal, V. et al. 2001. Human immunodeficiency virus type 1 entry into macrophages mediated by macropinocytosis. *J Virol* 75(22), pp. 11166-11177.

Marina-Garcia, N. et al. 2009. Clathrin- and dynamin-dependent endocytic pathway regulates muramyl dipeptide internalization and NOD2 activation. *J Immunol* 182(7), pp. 4321-4327.

Marks, D. L. et al. 2005. Use of fluorescent sphingolipid analogs to study lipid transport along the endocytic pathway. *Methods* 36(2), pp. 186-195.

Marsh, M. and McMahon, H. T. 1999. The structural era of endocytosis. *Science* 285(5425), pp. 215-220.

Masters, J. R. 2002. HeLa cells 50 years on: the good, the bad and the ugly. *Nat Rev Cancer* 2(4), pp. 315-319.

Masui, H. et al. 1984. Growth inhibition of human tumor cells in athymic mice by anti-epidermal growth factor receptor monoclonal antibodies. *Cancer Res* 44(3), pp. 1002-1007.

Maxfield, F. R. and McGraw, T. E. 2004. Endocytic recycling. *Nat Rev Mol Cell Biol* 5(2), pp. 121-132.

Mayor, S. and Pagano, R. E. 2007. Pathways of clathrin-independent endocytosis. *Nat Rev Mol Cell Biol* 8(8), pp. 603-612.

Mayor, S. et al. 1998. Cholesterol-dependent retention of GPI-anchored proteins in endosomes. *Embo J* 17(16), pp. 4626-4638.

Meade, B. R. and Dowdy, S. F. 2007. Exogenous siRNA delivery using peptide transduction domains/cell penetrating peptides. *Adv Drug Deliv Rev* 59(2-3), pp. 134-140.

Meier, O. et al. 2002. Adenovirus triggers macropinocytosis and endosomal leakage together with its clathrin-mediated uptake. *J Cell Biol* 158(6), pp. 1119-1131.

Meier, O. and Greber, U. F. 2004. Adenovirus endocytosis. *J Gene Med* 6 Suppl 1, pp. S152-163.

Mercer, J. and Helenius, A. 2008. Vaccinia virus uses macropinocytosis and apoptotic mimicry to enter host cells. *Science* 320(5875), pp. 531-535.

Mercer, J. and Helenius, A. 2010. Apoptotic mimicry: phosphatidylserine-mediated macropinocytosis of vaccinia virus. *Ann N Y Acad Sci* 1209, pp. 49-55.

Morris, M. C. et al. 2000. Translocating peptides and proteins and their use for gene delivery. *Curr Opin Biotechnol* 11(5), pp. 461-466.

Morris, M. C. et al. 2001. A peptide carrier for the delivery of biologically active proteins into mammalian cells. *Nat Biotechnol* 19(12), pp. 1173-1176.

Morris, M. C. et al. 2008. Cell-penetrating peptides: from molecular mechanisms to therapeutics. *Biol Cell* 100(4), pp. 201-217.

Morris, M. C. et al. 1997. A new peptide vector for efficient delivery of oligonucleotides into mammalian cells. *Nucleic Acids Res* 25(14), pp. 2730-2736.

Moschos, S. A. et al. 2007. Cell-penetrating-peptide-mediated siRNA lung delivery. *Biochem Soc Trans* 35(Pt 4), pp. 807-810.

Motley, A. et al. 2003. Clathrin-mediated endocytosis in AP-2-depleted cells. *J Cell Biol* 162(5), pp. 909-918.

Mueller, J. et al. 2008. Comparison of cellular uptake using 22 CPPs in 4 different cell lines. *Bioconjug Chem* 19(12), pp. 2363-2374.

Murriel, C. L. and Dowdy, S. F. 2006. Influence of protein transduction domains on intracellular delivery of macromolecules. *Expert Opin Drug Deliv* 3(6), pp. 739-746.

Nabi, I. R. and Le, P. U. 2003. Caveolae/raft-dependent endocytosis. *J Cell Biol* 161(4), pp. 673-677.

Nakase, I. et al. 2009. Cell-surface accumulation of flock house virus-derived peptide leads to efficient internalization via macropinocytosis. *Mol Ther* 17(11), pp. 1868-1876.

Nakase, I. et al. 2004. Cellular uptake of arginine-rich peptides: roles for macropinocytosis and actin rearrangement. *Mol Ther* 10(6), pp. 1011-1022.

Nakase, I. et al. 2007. Interaction of arginine-rich peptides with membrane-associated proteoglycans is crucial for induction of actin organization and macropinocytosis. *Biochemistry* 46(2), pp. 492-501.

Naslavsky, N. et al. 2004. Characterization of a nonclathrin endocytic pathway: membrane cargo and lipid requirements. *Mol Biol Cell* 15(8), pp. 3542-3552.

Nekhotiaeva, N. et al. 2004. Cell entry and antimicrobial properties of eukaryotic cell-penetrating peptides. *Faseb J* 18(2), pp. 394-396.

Neumann-Giesen, C. et al. 2007. Role of EGF-induced tyrosine phosphorylation of reggie-1/flotillin-2 in cell spreading and signaling to the actin cytoskeleton. *J Cell Sci* 120(Pt 3), pp. 395-406.

Nichols, B. J. 2002. A distinct class of endosome mediates clathrin-independent endocytosis to the Golgi complex. *Nat Cell Biol* 4(5), pp. 374-378.

Oehlke, J. et al. 1997. Evidence for extensive and non-specific translocation of oligopeptides across plasma membranes of mammalian cells. *Biochim Biophys Acta* 1330(1), pp. 50-60.

Oehlke, J. et al. 1998. Cellular uptake of an alpha-helical amphipathic model peptide with the potential to deliver polar compounds into the cell interior non-endocytically. *Biochim Biophys Acta* 1414(1-2), pp. 127-139.

Ogris, M. and Wagner, E. 2002. Targeting tumors with non-viral gene delivery systems. *Drug Discov Today* 7(8), pp. 479-485.

Palm-Apergi, C. et al. 2011. PTD-DRBD siRNA delivery. *Methods Mol Biol* 683, pp. 339-347.

Pang, H. et al. 2004. Ganglioside GM1 levels are a determinant of the extent of caveolae/raft-dependent endocytosis of cholera toxin to the Golgi apparatus. *J Cell Sci* 117(Pt 8), pp. 1421-1430.

Papakonstanti, E. A. and Stournaras, C. 2002. Association of PI-3 kinase with PAK1 leads to actin phosphorylation and cytoskeletal reorganization. *Mol Biol Cell* 13(8), pp. 2946-2962.

Parente, R. A. et al. 1990. Association of a pH-sensitive peptide with membrane vesicles: role of amino acid sequence. *Biochemistry* 29(37), pp. 8713-8719.

Parrini, M. C. et al. 2005. Spatiotemporal regulation of the Pak1 kinase. *Biochem Soc Trans* 33(Pt 4), pp. 646-648.

Parton, R. G. and Richards, A. A. 2003. Lipid rafts and caveolae as portals for endocytosis: new insights and common mechanisms. *Traffic* 4(11), pp. 724-738.

Patel, L. N. et al. 2007. Cell penetrating peptides: intracellular pathways and pharmaceutical perspectives. *Pharm Res* 24(11), pp. 1977-1992.

Payne, C. K. et al. 2007. Internalization and trafficking of cell surface proteoglycans and proteoglycan-binding ligands. *Traffic* 8(4), pp. 389-401.

Pooga, M. et al. 1998. Cell penetration by transportan. *FASEB J* 12(1), pp. 67-77.

Potocky, T. B. et al. 2003. Cytoplasmic and nuclear delivery of a TAT-derived peptide and a beta-peptide after endocytic uptake into HeLa cells. *J Biol Chem* 278(50), pp. 50188-50194.

Poupon, V. et al. 2008. Clathrin light chains function in mannose phosphate receptor trafficking via regulation of actin assembly. *Proc Natl Acad Sci U S A* 105(1), pp. 168-173.

Razani, B. et al. 2002. Caveolae: from cell biology to animal physiology. *Pharmacol Rev* 54(3), pp. 431-467.

Richard, J. P. et al. 2005. Cellular uptake of unconjugated TAT peptide involves clathrin-dependent endocytosis and heparan sulfate receptors. *J Biol Chem* 280(15), pp. 15300-15306.

Richard, J. P. et al. 2003. Cell-penetrating peptides. A reevaluation of the mechanism of cellular uptake. *J Biol Chem* 278(1), pp. 585-590.

Rodal, S. K. et al. 1999. Extraction of cholesterol with methyl-beta-cyclodextrin perturbs formation of clathrin-coated endocytic vesicles. *Mol Biol Cell* 10(4), pp. 961-974.

Romer, W. et al. 2007. Shiga toxin induces tubular membrane invaginations for its uptake into cells. *Nature* 450(7170), pp. 670-675.

Rooney, I. A. et al. 1991. The complement-inhibiting protein, protectin (CD59 antigen), is present and functionally active on glomerular epithelial cells. *Clin Exp Immunol* 83(2), pp. 251-256.

Rothbard, J. B. et al. 2000. Conjugation of arginine oligomers to cyclosporin A facilitates topical delivery and inhibition of inflammation. *Nat Med* 6(11), pp. 1253-1257.

Rothbard, J. B. et al. 2004. Role of membrane potential and hydrogen bonding in the mechanism of translocation of guanidinium-rich peptides into cells. *J Am Chem Soc* 126(31), pp. 9506-9507.

Rothe, R. et al. 2010. Characterization of the cell-penetrating properties of the Epstein-Barr virus ZEBRA trans-activator. *J Biol Chem* 285(26), pp. 20224-20233.

Rousselle, C. et al. 2000. New advances in the transport of doxorubicin through the blood-brain barrier by a peptide vector-mediated strategy. *Mol Pharmacol* 57(4), pp. 679-686.

Rousselle, C. et al. 2002. Improved brain delivery of benzylpenicillin with a peptide-vector-mediated strategy. *J Drug Target* 10(4), pp. 309-315.

Rousselle, C. et al. 2001. Enhanced delivery of doxorubicin into the brain via a peptide-vector-mediated strategy: saturation kinetics and specificity. *J Pharmacol Exp Ther* 296(1), pp. 124-131.

Royle, S. J. and Lagnado, L. 2010. Clathrin-mediated endocytosis at the synaptic terminal: bridging the gap between physiology and molecules. *Traffic* 11(12), pp. 1489-1497.

Ruter, C. et al. 2010. A newly identified bacterial cell-penetrating peptide that reduces the transcription of pro-inflammatory cytokines. *J Cell Sci* 123(Pt 13), pp. 2190-2198.

Saalik, P. et al. 2004. Protein cargo delivery properties of cell-penetrating peptides. A comparative study. *Bioconjug Chem* 15(6), pp. 1246-1253.

Saalik, P. et al. 2009. Protein delivery with transportans is mediated by caveolae rather than flotillin-dependent pathways. *Bioconjug Chem* 20(5), pp. 877-887.

Sabharanjak, S. et al. 2002. GPI-anchored proteins are delivered to recycling endosomes via a distinct cdc42-regulated, clathrin-independent pinocytic pathway. *Dev Cell* 2(4), pp. 411-423.

Saeed, M. F. et al. 2010. Cellular entry of ebola virus involves uptake by a macropinocytosis-like mechanism and subsequent trafficking through early and late endosomes. *PLoS Pathog* 6(9).

Sahay, G. et al. 2010. Endocytosis of nanomedicines. *J Control Release* 145(3), pp. 182-195.

Saleh, A. F. et al. 2010. Synthesis and splice-redirecting activity of branched, arginine-rich peptide dendrimer conjugates of peptide nucleic acid oligonucleotides. *Bioconjug Chem* 21(10), pp. 1902-1911.

Sandgren, S. et al. 2004. The human antimicrobial peptide LL-37 transfers extracellular DNA plasmid to the nuclear compartment of mammalian cells via lipid rafts and proteoglycan-dependent endocytosis. *J Biol Chem* 279(17), pp. 17951-17956.

Schmid, D. et al. 2007. Antigen-loading compartments for major histocompatibility complex class II molecules continuously receive input from autophagosomes. *Immunity* 26(1), pp. 79-92.

Schmid, S. L. 1997. Clathrin-coated vesicle formation and protein sorting: an integrated process. *Annu Rev Biochem* 66, pp. 511-548.

Schnatwinkel, C. et al. 2004. The Rab5 effector Rabankyrin-5 regulates and coordinates different endocytic mechanisms. *PLoS Biol* 2(9), p. E261.

Schwarze, S. R. et al. 1999. In vivo protein transduction: delivery of a biologically active protein into the mouse. *Science* 285(5433), pp. 1569-1572.

Schweitzer, J. K. et al. 2010. ARF6-mediated endocytic recycling impacts cell movement, cell division and lipid homeostasis. *Semin Cell Dev Biol* 22(1), pp. 39-47.

Seib, F. P. et al. 2007. Comparison of the endocytic properties of linear and branched PEIs, and cationic PAMAM dendrimers in B16f10 melanoma cells. *J Control Release* 117(3), pp. 291-300.

Sells, M. A. et al. 1997. Human p21-activated kinase (Pak1) regulates actin organization in mammalian cells. *Curr Biol* 7(3), pp. 202-210.

Senatus, P. B. et al. 2006. Restoration of p53 function for selective Fas-mediated apoptosis in human and rat glioma cells in vitro and in vivo by a p53 COOH-terminal peptide. *Mol Cancer Ther* 5(1), pp. 20-28.

Simon, M. et al. 2009a. Crimean-Congo hemorrhagic fever virus entry and replication is clathrin-, pH- and cholesterol-dependent. *J Gen Virol* 90(Pt 1), pp. 210-215.

Simon, M. J. et al. 2009b. TAT-mediated intracellular protein delivery to primary brain cells is dependent on glycosaminoglycan expression. *Biotechnol Bioeng* 104(1), pp. 10-19.

Simpson, J. C. et al. 2004. A role for the small GTPase Rab21 in the early endocytic pathway. *J Cell Sci* 117(Pt 26), pp. 6297-6311.

Singh, R. D. et al. 2003. Selective caveolin-1-dependent endocytosis of glycosphingolipids. *Mol Biol Cell* 14(8), pp. 3254-3265.

Singh, R. R. et al. 2005. Nuclear localization and chromatin targets of p21-activated kinase 1. *J Biol Chem* 280(18), pp. 18130-18137.

Sinha, B. et al. 2011. Cells respond to mechanical stress by rapid disassembly of caveolae. *Cell* 144(3), pp. 402-413.

Skarnes, R. C. and Watson, D. W. 1957. Antimicrobial factors of normal tissues and fluids. *Bacteriol Rev* 21(4), pp. 273-294.

Snyder, E. L. et al. 2005. Enhanced targeting and killing of tumor cells expressing the CXC chemokine receptor 4 by transducible anticancer peptides. *Cancer Res* 65(23), pp. 10646-10650.

Solis, G. P. et al. 2007. Reggie/flotillin proteins are organized into stable tetramers in membrane microdomains. *Biochem J* 403(2), pp. 313-322.

Someya, A. et al. 2010. The guanine nucleotide exchange protein for ADP-ribosylation factor 6, ARF-GEP100/BRAG2, regulates phagocytosis of monocytic phagocytes in an ARF6-dependent process. *J Biol Chem* 285(40), pp. 30698-30707.

Song, B. D. and Schmid, S. L. 2003. A molecular motor or a regulator? Dynamin's in a class of its own. *Biochemistry* 42(6), pp. 1369-1376.

Song, J. C. et al. 1999. PKC-epsilon regulates basolateral endocytosis in human T84 intestinal epithelia: role of F-actin and MARCKS. *Am J Physiol* 277(6 Pt 1), pp. C1239-1249.

Spoden, G. et al. 2008. Clathrin- and caveolin-independent entry of human papillomavirus type 16--involvement of tetraspanin-enriched microdomains (TEMs). *PLoS One* 3(10), p. e3313.

Stuermer, C. A. et al. 2001. Glycosylphosphatidyl inositol-anchored proteins and fyn kinase assemble in noncaveolar plasma membrane microdomains defined by reggie-1 and -2. *Mol Biol Cell* 12(10), pp. 3031-3045.

Suzuki, T. et al. 2002. Possible existence of common internalization mechanisms among arginine-rich peptides. *J Biol Chem* 277(4), pp. 2437-2443.

Swanson, J. A. and Watts, C. 1995. Macropinocytosis. *Trends Cell Biol* 5(11), pp. 424-428.

Szakacs, G. et al. 2006. Targeting multidrug resistance in cancer. *Nat Rev Drug Discov* 5(3), pp. 219-234.

Takeshima, K. et al. 2003. Translocation of analogues of the antimicrobial peptides magainin and buforin across human cell membranes. *J Biol Chem* 278(2), pp. 1310-1315.

Takeuchi, T. et al. 2006. Direct and rapid cytosolic delivery using cell-penetrating peptides mediated by pyrenebutyrate. *ACS Chem Biol* 1(5), pp. 299-303.

Tan, M. L. et al. 2009. Recent developments in liposomes, microparticles and nanoparticles for protein and peptide drug delivery. *Peptides* 31(1), pp. 184-193.

Temsamani, J. and Vidal, P. 2004. The use of cell-penetrating peptides for drug delivery. *Drug Discov Today* 9(23), pp. 1012-1019.

Ter-Avetisyan, G. et al. 2009. Cell entry of arginine-rich peptides is independent of endocytosis. *J Biol Chem* 284(6), pp. 3370-3378.

Terpe, K. 2003. Overview of tag protein fusions: from molecular and biochemical fundamentals to commercial systems. *Appl Microbiol Biotechnol* 60(5), pp. 523-533.

Thiery, J. et al. 2010. Perforin activates clathrin- and dynamin-dependent endocytosis, which is required for plasma membrane repair and delivery of granzyme B for granzyme-mediated apoptosis. *Blood* 115(8), pp. 1582-1593.

Thomsen, P. et al. 2002. Caveolae are highly immobile plasma membrane microdomains, which are not involved in constitutive endocytic trafficking. *Mol Biol Cell* 13(1), pp. 238-250.

Thoren, P. E. et al. 2003. Uptake of analogs of penetratin, Tat(48-60) and oligoarginine in live cells. *Biochem Biophys Res Commun* 307(1), pp. 100-107.

Todaro, G. J. et al. 1980. Transforming growth factors produced by certain human tumor cells: polypeptides that interact with epidermal growth factor receptors. *Proc Natl Acad Sci U S A* 77(9), pp. 5258-5262.

Torchilin, V. P. 2005a. Fluorescence microscopy to follow the targeting of liposomes and micelles to cells and their intracellular fate. *Adv Drug Deliv Rev* 57(1), pp. 95-109.

Torchilin, V. P. 2005b. Recent advances with liposomes as pharmaceutical carriers. *Nat Rev Drug Discov* 4(2), pp. 145-160.

Torchilin, V. P. et al. 2001. TAT peptide on the surface of liposomes affords their efficient intracellular delivery even at low temperature and in the presence of metabolic inhibitors. *Proc Natl Acad Sci U S A* 98(15), pp. 8786-8791.

Torgersen, M. L. et al. 2001. Internalization of cholera toxin by different endocytic mechanisms. *J Cell Sci* 114(Pt 20), pp. 3737-3747.

Trushina, E. et al. 2006. Mutant huntingtin inhibits clathrin-independent endocytosis and causes accumulation of cholesterol in vitro and in vivo. *Hum Mol Genet* 15(24), pp. 3578-3591.

Tseng, Y. L. et al. 2002. Translocation of liposomes into cancer cells by cell-penetrating peptides penetratin and tat: a kinetic and efficacy study. *Mol Pharmacol* 62(4), pp. 864-872.

Tung, C. H. et al. 2002. Novel branching membrane translocational peptide as gene delivery vector. *Bioorg Med Chem* 10(11), pp. 3609-3614.

Tunnemann, G. et al. 2006. Cargo-dependent mode of uptake and bioavailability of TAT-containing proteins and peptides in living cells. *Faseb J* 20(11), pp. 1775-1784.

Tunnemann, G. et al. 2008. Live-cell analysis of cell penetration ability and toxicity of oligo-arginines. *J Pept Sci* 14(4), pp. 469-476.

van Dam, E. M. and Stoorvogel, W. 2002. Dynamin-dependent transferrin receptor recycling by endosome-derived clathrin-coated vesicles. *Mol Biol Cell* 13(1), pp. 169-182.

Vassilieva, E. V. et al. 2009. Flotillin-1 stabilizes caveolin-1 in intestinal epithelial cells. *Biochem Biophys Res Commun* 379(2), pp. 460-465.

Veithen, A. et al. 1996. v-Src induces constitutive macropinocytosis in rat fibroblasts. *J Cell Sci* 109 (Pt 8), pp. 2005-2012.

Venneker, G. T. and Asghar, S. S. 1992. CD59: a molecule involved in antigen presentation as well as downregulation of membrane attack complex. *Exp Clin Immunogenet* 9(1), pp. 33-47.

Venneker, G. T. et al. 1994. Glycosylphosphatidylinositol (GPI)-anchored membrane proteins are constitutively down-regulated in psoriatic skin. *J Pathol* 172(2), pp. 189-197.

Vercauteren, D. et al. 2011. Flotillin-dependent endocytosis and a phagocytosis-like mechanism for cellular internalization of disulfide-based poly(amido amine)/DNA polyplexes. *Biomaterials* 32(11), pp. 3072-3084.

Vercauteren, D. et al. 2010. The use of inhibitors to study endocytic pathways of gene carriers: optimization and pitfalls. *Mol Ther* 18(3), pp. 561-569.

Vives, E. et al. 1997. A truncated HIV-1 Tat protein basic domain rapidly translocates through the plasma membrane and accumulates in the cell nucleus. *J Biol Chem* 272(25), pp. 16010-16017.

Vives, E. et al. 2003. TAT peptide internalization: seeking the mechanism of entry. *Curr Protein Pept Sci* 4(2), pp. 125-132.

Wadia, J. S. and Dowdy, S. F. 2003. Modulation of cellular function by TAT mediated transduction of full length proteins. *Curr Protein Pept Sci* 4(2), pp. 97-104.

Wadia, J. S. and Dowdy, S. F. 2005. Transmembrane delivery of protein and peptide drugs by TAT-mediated transduction in the treatment of cancer. *Adv Drug Deliv Rev* 57(4), pp. 579-596.

Wadia, J. S. et al. 2004. Transducible TAT-HA fusogenic peptide enhances escape of TAT-fusion proteins after lipid raft macropinocytosis. *Nat Med* 10(3), pp. 310-315.

Walton, S. P. et al. 2010. Designing highly active siRNAs for therapeutic applications. *Febs J* 277(23), pp. 4806-4813.

Watkins, C. L. et al. 2009a. Cellular uptake, distribution and cytotoxicity of the hydrophobic cell penetrating peptide sequence PFVYLI linked to the proapoptotic domain peptide PAD. *J Control Release* 140(3), pp. 237-244.

Watkins, C. L. et al. 2009b. Low concentration thresholds of plasma membranes for rapid energy-independent translocation of a cell-penetrating peptide. *Biochem J* 420(2), pp. 179-189.

Wender, P. A. et al. 2008. The design of guanidinium-rich transporters and their internalization mechanisms. *Adv Drug Deliv Rev* 60(4-5), pp. 452-472.

Wender, P. A. et al. 2000. The design, synthesis, and evaluation of molecules that enable or enhance cellular uptake: peptoid molecular transporters. *Proc Natl Acad Sci U S A* 97(24), pp. 13003-13008.

West, M. A. et al. 1989. Distinct endocytotic pathways in epidermal growth factor-stimulated human carcinoma A431 cells. *J Cell Biol* 109(6 Pt 1), pp. 2731-2739.

Wilda, M. et al. 2002. Killing of leukemic cells with a BCR/ABL fusion gene by RNA interference (RNAi). *Oncogene* 21(37), pp. 5716-5724.

Yamada, E. 1955. The fine structure of the gall bladder epithelium of the mouse. *J Biophys Biochem Cytol* 1(5), pp. 445-458.

Yao, Q. et al. 2005. Caveolin-1 interacts directly with dynamin-2. *J Mol Biol* 348(2), pp. 491-501.

Yoon, H. Y. et al. 2002. TAT-mediated delivery of human glutamate dehydrogenase into PC12 cells. *Neurochem Int* 41(1), pp. 37-42.

Zaro, J. L. and Shen, W. C. 2005. Evidence that membrane transduction of oligoarginine does not require vesicle formation. *Exp Cell Res* 307(1), pp. 164-173.

Zhang, X. et al. 2009. Endocytosis and membrane potential are required for HeLa cell uptake of R.I.-CKTat9, a retro-inverso Tat cell penetrating peptide. *Mol Pharm* 6(3), pp. 836-848.

Ziegler, A. 2008. Thermodynamic studies and binding mechanisms of cell-penetrating peptides with lipids and glycosaminoglycans. *Adv Drug Deliv Rev* 60(4-5), pp. 580-597.

Ziegler, A. et al. 2005. The cationic cell-penetrating peptide CPP(TAT) derived from the HIV-1 protein TAT is rapidly transported into living fibroblasts: optical, biophysical, and metabolic evidence. *Biochemistry* 44(1), pp. 138-148.

Appendix I

Appendix I:

1- **Poster Abstract contribution for the MicroRNAs and the regulation of biological function Biomedical Society Meeting Imperial College London, UK, 8th of July 2008**

siRNA Inhibition of Endocytic Pathways for Studying Cellular Uptake of Cell Penetrating Peptides:

Al-Soraj M; Watkins C; Jones A T

Welsh School of pharmacy, Redwood Building, King Edward VII Avenue, Cardiff, Wales, UK, CF10 3NB

Plasma membrane represents an impermeable barrier for most macromolecules, however, some peptides such as cell-penetrating peptides (CPPs) translocate cells efficiently, but the mechanism of entry is still unresolved. Of particular interest, they are able to deliver cargoes up to 100 times their own size. It has been shown that different endocytic pathways contribute to the import of these molecules, for example clathrin-mediated endocytosis (CME), macropinocytosis and cavoelae-mediated endocytosis. In this study, we have used RNA interfering tool to silence endocytic pathways by knocking down proteins, such as clathrin heavy chain (CHC), to investigate the mechanism of the uptake of arginin peptide (R8) and Tat peptide. Different incubation periods were tested for both R8 and TAT. Alexa-488 Transferrin was used as a marker for CME, since its uptake is predominately via CME a reduction in cell associated fluorescence would indicate successful transfection.

2- **Poster Abstract for the 3th Intracellular Delivery of Therapeutics Molecules: From Bench to Bedside Montpellier, France, August 31st - September 2nd 2009 (PRIZE WINNER)**

siRNA Inhibition of Endocytic Pathways for Studying Cellular Uptake of Cell Penetrating Peptides

Monerah H. Al-Soraj[1], Catherine L. Watkins[1], Dries Vercauteren[2], Stefaan De Smedt[2], and Arwyn T. Jones[1]

[1]*Welsh School of Pharmacy, Cardiff University, Cardiff, Wales,CF10 3NB*
[2]*Laboratory of General Biochemistry & Physical Pharmacy, Ghent University, Harelbekestraat 72 (2nd floor), B-9000 Ghent, Belgium*

Cell-penetrating peptides (CPPs) have the potential to deliver several different types of therapeutic macromolecules into cells including peptides, proteins, and nucleic acids. Endocytosis is thought to be of significant importance for allowing access of CPP-cargo molecules but there is currently little consensus regarding the exact uptake mechanism used by different CPPs. A single cell can endocytose via multiple pathways and uptake of CPPs has been documented to occur through clathrin coated vesicles, cavaeolae and via macropinocytosis. This work aims enhance the use of cell penetrating peptides as intracellular delivery vectors by further characterizing their uptake mechanisms and the contribution of endocytosis to this. Traditionally the uptake of CPPs and other drug delivery vectors has been performed using chemical inhibitors of endocytosis but these lack specificity and can be toxic. In this study, we have used siRNA technology to silence critical endocytic proteins such as clathrin heavy chain, flotillin-1 and dynamin isoforms to inhibit distinct endocytic pathways. The success of this approach is dependent on depleting cells of specific proteins but also on identifying marker proteins whose uptake is limited to one specific pathway and a series of experiments have been performed to better define markers for alternative pathways to that regulated by clathrin. Our data shows that siRNA could effectively deplete expression of clathrin heavy chain, flotillin-1 and dynamin II but whereas uptake of markers such as transferrin was reduced in some of these cells the uptake of CPPs octaarginine and HIV-TAT was relatively unaffected. Comparative analysis of these experiments with those performed using traditional endocytosis inhibitors were also performed and highlight the difficulty in interpretation of data from these studies compared to siRNA depletion. In conclusion, the study demonstrated the usefulness and pitfalls of using siRNA technology, compared with endocytosis

inhibitors, to study the internalization of drug delivery vectors and their associated cargoes.

3- Paper contribution for the 11th European Symposium on Controlled Drug Delivery Egmond aan Zee, The Netherlands, 6th-9th April 2010.

siRNA Inhibition of Endocytic Pathways for Studying Cellular Uptake of Cell Penetrating Peptides.

Monerah H. Al-Soraj[1], Catherine L. Watkins[1], Dries Vercauteren[2], Stefaan De Smedt[2], Kevin Braeckmans[2] and Arwyn T. Jones[1]

[1]Welsh School of Pharmacy, Cardiff University, Cardiff, Wales, UK, CF10 3NB

[2]Laboratory of General Biochemistry & Physical Pharmacy, Ghent University, Harelbekestraat 72 (2nd floor), B-9000 Ghent, Belgium

Abstract Summary: The debate, regarding the main mechanism of uptake of cell penetrating peptides (CPPs), is still unresolved. Different endocytic pathways has been shown to be contributed, for example clathrin-mediated endocytosis (CME), macropinocytosis and clathrin and cavoelin independent endocytosis. In this study, we have used RNA interfering tool to silence different proteins, such as clathrin heavy chain (CHC), flotillin-1 and PAK-1 to investigate the mechanism of the uptake of arginin-rich peptides such as R8 and HIV-Tat.

Introduction: Cell-penetrating peptides (CPPs) have the potential to deliver a host of therapeutic macromolecules into cells including peptides, proteins, and nucleic acids. Endocytosis is thought to be of significant importance for allowing access of CPP-cargo molecules but identifying the uptake mechanisme of different CPPs is still debatable[1]. Multiple pathways has been reported to contribute in CPPs uptake, such as clathrin dependent, cavaeolin and clathrin-independent and via macropinocytosis[2]. This work aims enhance the use of cell penetrating peptides as drug delivery vectors by investigating and studying their

mechanisms of uptake. Traditionally the uptake of these molecules and other drug delivery vectors has been performed using chemical inhibitors of endocytosis but there are often toxic and lack specificity[3,4]. In this study, we have used siRNA technology to silence critical endocytic proteins such as clathrin heavy chain[5], flotillin-1[6] and PAK-1[7] to inhibit distinct endocytic pathways.

Experimental Methods: For cell culture HeLa cells and A431 cells were grown in DMEM-GlutaMAX-I media containing 10% FBS and 100 U/ml penicillin and 100μg/ml streptomycin. 24 hrs prior to transfection cells were seeded onto 6- or 12-well plates, and were 50%-60% confluent on the day of transfection. Clathrin heavy chain (CHC), Flotillin-1(Flot-1) Caveolin-1 (Cav-1) and P21-activated kinase 1 (PAK-1) were depleted using siRNA and siRNA against GFP is used as a control. Uptake of endocytic pathways markers and CPPs was measured by a FACS Calibur Flow Cytometer. Protein depletion was assessed by western blot and 25 μg of protein lysate was loaded in a 10% or 11% SDS-PAGE gel. CHC, flot-1, Cav-1, PAK-1 and ∝-tubulin was detected by enhanced chemiluminescence using anti-CHC and anti-flot-1 (BD Biosciences) , anti-Cav-1 (Cell signalling), anti-PAK-1 (Santacruz) and anti-∝-tubulin (Sigma) antibodies respectively followed by HRP conjugated secondary antibody (Pierce).

Results and Discussion: The success of this approach is dependent of identifying marker proteins whose uptake is limited to one specific pathway and a series of experiments have been performed to better define markers for alternative pathways to that regulated by clathrin. Our data shows that siRNA could effectively deplete expression of clathrin heavy chain, flotillin-1 and PAK-1 but whereas uptake of markers such as transferrin was reduced in some of these cells the uptake of CPPs octaarginine and HIV-TAT was relatively unaffected. Moreover, depleting flotillin-1 shows 30-35% inhibition in the uptake of anti-CD59 antibody, which was used as a marker for flotillin-1

dependent uptake[6] and no inhibition has been found in R8 uptake. Comparatively, the uptake of R8 and HIV-Tat shows a dependency on PAK-1, whereas depleting PAK-1 has no effect on fluid phase endocytosis of FITC-Dextran. The results also show depleting PAK-1 inhibits the increase in the uptake of FITC-Dextran following EGF ruffling stimulation in A431 cells. Comparative analysis of these experiments with those performed using traditional endocytosis inhibitors were also performed and the results show that the uptake of R8 is inhibited following actin depolymerization with cytochalasin D. Whereas, no effect has been shown following chlorpromazine, and EIPA treatment.

Conclusion: The study aimed to determine the requirement for CHC, flot-1 and PAK1-dependent endocytosis in the uptake of CPPs that are of interest as vectors for intracellular delivery of therapeutic macromolecules. The data shows that clathrin mediated and flotillin-1 dependent endocytosis are not the main route of internalization for Alexa-488-R8 peptide and contradicts previous studies using endocytic inhibitors[3]. On the other hand, the cellular uptake of R8 and Tat peptide is reduced by 25% by depleting PAK-1. Similar methods of targeting other endocytic proteins that regulate alternative uptake routes can now be utilized to further study CPP uptake. These will also provide us with tools to study the uptake of other candidate drug delivery vectors. In conclusion, the study illustrates the usefulness of using siRNA technology, compared with endocytosis inhibitors, to study the internalization of CPPs and their associated cargoes.

4- Paper contribution for the 3rd International Cellular Delivery of Therapeutic Macromolecules Symposium (CDTM) 26th- June – 29th June 2010, Welsh School of Pharmacy, Cardiff University, UK.

Monerah H. Al-Soraj[1], Catherine L. Watkins[1], Dries Vercauteren[2], Stefaan De Smedt[2], Kevin Braeckmans[2] and Arwyn T. Jones[1]

[1]*Welsh School of Pharmacy, Cardiff University, Cardiff, Wales, UK, CF10 3NB*
[2]*Laboratory of General Biochemistry & Physical Pharmacy, Ghent University, Harelbekestraat 72 (2nd floor), B-9000 Ghent, Belgium*

Cell-penetrating peptides (CPPs) have the potential to deliver numerous therapeutic macromolecules into cells including peptides, proteins, and nucleic acids. Under defined conditions endocytosis is thought to be of significant importance for CPP entry but identifying the exact uptake mechanism and pathway(s) involved has been difficult. Multiple pathways have been reported to contribute to uptake, including macropinocytosis and those regulated by clathrin and cavaeolin-1. This project aims enhance the use of cell penetrating peptides as drug delivery vectors by developing new technologies to study their mechanisms of uptake. Traditionally studies investigating the uptake of these molecules, and other drug delivery vectors, have been performed using chemical inhibitors but these are often toxic and lack specificity (1). We have developed siRNA-based assays to silence endocytic proteins that have previously been shown to regulate distinct endocytic pathways. The effect of depleting these proteins was then assessed to investigate their roles in mediating the uptake of well characterised endocytic probes and CPPs.

Two cell lines were predominantly used, HeLa (cervical cancer epithelial) and A431 (human epithelial carcinoma). Endocytic proteins clathrin heavy chain, flotillin-1, dynamin II, caveolin-1 and P21-activated kinase (PAK-1) were depleted using single siRNA sequences; siRNA against GFP was used as a control. In siRNA treated cells the uptake of fluorescent endocytic markers including; Alexa488-transferrin (Clathrin mediated endocytosis), 40KDa FITC Dextran (fluid phase uptake and macropinocytosis), FITC conjugated anti-CD59 antibody (Flotillin-1 dependent uptake) and the uptake of Alexa488 CPPs (RRRRRRRRGC-Alexa488-R8, and GRKKRRQRRRPPQ-Alexa488-HIV-TAT) were measured by flow cytometry. Protein depletion was assessed from protein lysates using SDS PAGE and Western blotting.

The overall data shows that siRNA transfection method could effectively reduce expression of clathrin heavy chain, caveolin-1 and flotillin-1 from HeLa cells and this then allowed for us to study effects on endocytosis of various probes. PAK-1 has been shown to regulate macropinocytosis and we show that the induction of macropinocytosis and PAK-1 expression are highly cell line dependent. Paralleled with this was our findings that cationic CPPs induce an increase in fluid phase uptake of dextran and the extent of this was cell line dependent. Comparative analysis of these experiments with those performed using pharmacological inhibitors, allowed us to determine the usefulness of this approach for drug delivery research.

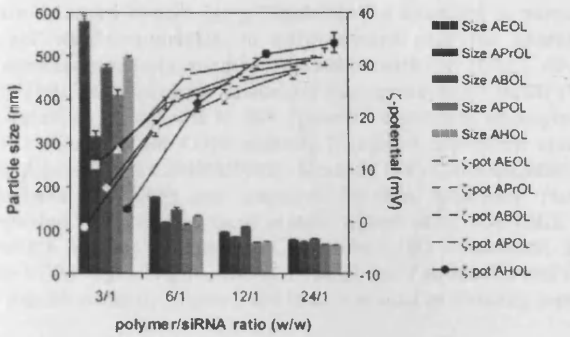

Fig. 2. Particle size and zeta potential of complexes of siRNA with SS-PAA copolymers having various ω-hydroxyalkyl chains, as determined by DLS.

None of the polymers are toxic during the transfection. This was derived from the remaining luciferase expression after treatment with non coding siRNA complexes (Fig. 3b). To zoom in on the cytotoxicity of the materials, H1299 Fluct cells were treated for 2 h (similar to transfection protocol) with polymer solutions of concentrations ranging from 1.5 to 800 μg/ml and two days later their proliferation was measured using XTT (Fig. 4a). All polymers show a similar toxicity profile, except for the ABOL polymer, which is tolerated by the cells up to much higher concentrations. The toxicity may be related to the ability to lyse the membrane of the cells; therefore the hemolytic activity of the polymers was investigated against human erythrocytes (Fig. 4b). Although the total lysis is relatively low, increasing hydrophobicity leads to more disruption of the lipid membrane. This is best represented at the highest polymer concentration. Interestingly, the AHOL polymer differs significantly from the others in giving much higher lysis.

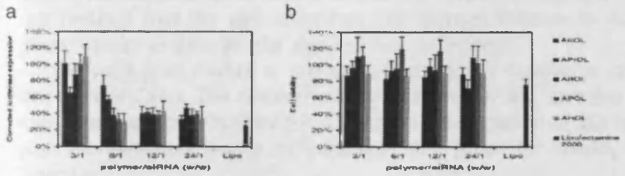

Fig. 3. Knockdown of firefly luciferase in H1299 Fluct cells in the absence of serum by (a) anti-Luc siRNA and (b) non coding siRNA. Luciferase knockdown is corrected for the cell viability and Lipofectamine 2000 was used as a positive control.

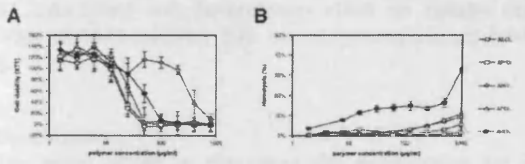

Fig. 4. (a) Cell viability of H1299 Fluct cells two days after treatment with polymer solutions; (b) hemoglobin leakage from human erythrocytes after 30 min incubation in a polymer solution.

Cellular uptake is generally favored by (hydrophobic) membrane interactions, although too heavy interactions may lead to cell lysis. It may be possible that AHOL gives an early cytotoxicity by damaging the cell membrane, which is in accordance with the hemolysis experiment. The cytotoxicity of the other polymers may be attributed to post-endocytotic effects, but more detailed studies are necessary to elucidate these effects.

Conclusion

Five analogous SS-PAAs were synthesized with ethylene diamine in the main chain and ω-hydroxyalkyl chain side chains of different chain lengths. All polymers showed excellent gene silencing properties in H1299 Fluct cells. The polymer with the ω-hydroxybutyl side chain appeared to be the least toxic gene carrier and is a very promising material for siRNA delivery in the near future.

References

[1] C. Lin, Z. Zhong, M.C. Lok, X. Jiang, W.E. Hennink, J. Feijen, J.F.J. Engbersen, Novel Bioreducible Poly(amido amine)s for Highly Efficient Gene Delivery, Bioconjugate Chem. 18 (1) (2007) 138–145.

[2] D.G. Anderson, A. Akinc, N. Hossain, R. Langer, Structure/property studies of polymeric gene delivery using a library of poly(β-amino esters), Mol. Ther. 11 (3) (2005) 426–434.

doi:10.1016/j.jconrel.2010.07.061

siRNA versus pharmacological inhibition of endocytic pathways for studying cellular uptake of cell penetrating peptides

Monerah H. Al-Soraj[1], Catherine L. Watkins[1], Dries Vercauteren[2], Stefaan C. De Smedt[2], Kevin Braeckmans[2], Arwyn T. Jones[1]

[1]*Welsh School of Pharmacy, Cardiff University, Cardiff, Wales, CF10 3NB, United Kingdom*

[2] *Laboratory of General Biochemistry & Physical Pharmacy, Ghent University, Harelbekestraat 72, B-9000 Ghent, Belgium*

Abstract summary

The exact mechanism by which cell penetrating peptides (CPPs) enter cells is still debated. Direct translocation and different endocytic pathways have been shown to contribute, including clathrin-mediated endocytosis (CME), macropinocytosis, uptake through caveolae and clathrin and cavoelin independent pathways. In this study, we show comparative data from the use of siRNA depletion of endocytic proteins versus the use of endocytic inhibitors to investigate the mechanism of the uptake of arginine-rich CPPs R8 and HIV-Tat.

Introduction

Cell-penetrating peptides (CPPs) have the potential to deliver a host of therapeutic macromolecules into cells including peptides, proteins, and nucleic acids. Under defined conditions endocytosis is thought to be of significant importance for allowing CPP entry but identifying the exact uptake mechanism and pathway(s) involved has been difficult [1]. Multiple pathways have been reported to contribute to uptake, including macropinocytosis and those regulated by clathrin and cavaeolin [2]. This work aims to enhance the use of cell penetrating peptides as drug delivery vectors by investigating and studying their mechanisms of uptake. Traditionally studies investigating the uptake of these molecules and other drug delivery vectors have been performed using chemical inhibitors but there are often toxicity and lack of specificity [3,4]. In this study, we have used siRNA technology to silence endocytic proteins such as clathrin heavy chain [5], flotillin-1 [6] caveolin-1 and PAK-1 [7] that have previously been shown to regulate distinct endocytic pathways. The effects of depleting these proteins were then assessed to investigate their roles in mediating the uptake of CPPs and well characterised endocytic probes.

Experimental methods

Cell lines HeLa (cervical cancer epithelial) and A431 (human epithelial carcinoma) were grown in DMEM-GlutaMAX-I media containing 10% FBS and 100 U/ml penicillin and 100 μg/ml streptomycin. 24 h prior to transfection cells were seeded onto 6- or 12-well plates, and were 50%–60% confluent on the day of transfection. Clathrin heavy chain (CHC), Flotillin-1 (Flot-1) Caveolin-1 (Cav-1) and P21-activated kinase 1 (PAK-1) were depleted using single siRNA sequences; siRNA against GFP was used as a control. siRNA (50 nM)

were delivered to cells using Oligofectamine according to manufacturers' recommendations. In siRNA treated cells the uptake of fluorescent endocytic markers Alexa488-transferrin (CME), 40 KDa FITC Dextran (fluid phase uptake and macropinocytosis), BODIPY® FL C_5-ceramide complexed to BSA (caveolin dependent endocytosis), FITC conjugated anti-CD59 antibody (Flotillin-1 dependent uptake) and Alexa488 CPPs RRRRRRRRGC-Alexa488 (R8), GRKKRRQRRRPPQ-Alexa488 (HIV-TAT) was measured by flow cytometry. Protein depletion was assessed from protein lysates using SDS PAGE and Western blotting using anti-CHC, anti-Flot-1 (BD Biosciences), anti-Cav-1 (Cell signalling), anti-PAK-1 (Santa Cruz) antibodies and anti-∝-tubulin antibody (Sigma); the latter was used as a loading control.

Result and discussion

The success of this siRNA approach to study endocytosis is dependent of identifying marker proteins that regulate specific pathways and that probes are available to effectively assess uptake through a defined pathway. We were successful in depleting clathrin heavy chain, caveolin-1 and flotillin1 from HeLa cells and this then allowed us to study the effects on endocytosis of various probes. We find that critical to these studies is performing multiple time point experiments as opposed to using a single time point and this is especially true if the endocytic probe or vector to be measured is recycled – transferrin. The uptake of transferrin was effectively inhibited in cells incubated with siRNA targeting CHC and we were also able to inhibit uptake of FITC-CD59 antibody in Flot-1 depleted cells. But cells depleted of CHC and Flot-1 had normal uptake rates of CPPs R8 or HIV-TAT.

PAK-1 has been shown to regulate macropinocytosis and our preliminary studies show that the induction of macropinocytosis is cell line dependent. We find that PAK-1 expression or macropinocytosis is not essential for uptake of these CPPs. Paralleled with this was our findings that the well described CPP induced increase in fluid phase uptake of dextran was also cell line dependent.

We were also unable to see any effect on CPP uptake in cells depleted of Cav-1. The involvement of this protein and caveolae in mediating uptake of BODIPY® FL C5-ceramide complexed to BSA was also analysed thus testing its suitability as a probe for uptake via caveolae.

Comparative analysis of these experiments with those performed using traditional endocytosis inhibitors was also performed and the results show that CPP uptake is inhibited by approximately 50% following actin depolymerization with cytochalasin D. In line with the siRNA data there was however no effect on uptake using the macropinocytosis inhibitor EIPA or chlorpromazine, an inhibitor of CME.

Conclusions

The study aimed to determine the requirement for distinct endocytic pathways in the uptake of CPPs that are of intense interest as vectors for intracellular delivery of therapeutic macromolecules. The data shows that macropinocytosis, clathrin mediated and flotillin-1, caveolin-1 dependent endocytosis are not the main routes of internalization for two cationic variants R8 and HIV-TAT. However specifying a requirement for a particular endocytic protein for mediating the uptake of a defined probe is not a trivial undertaking for a number of less well characterised pathways. Our studies continue to assess the roles for endocytic proteins regulating alternative uptake routes such that these methods can be utilized to further study CPP uptake. These technologies will also provide us with a mechanism to study in more detail the uptake of other candidate drug delivery vectors. In conclusion, the study illustrates the usefulness of using siRNA technology, compared with endocytosis inhibitors, to study the internalization of CPPs and their associated cargoes.

Acknowledgements

This work was supported by the Kuwait University and the BBSRC.

References

[1] A.T. Jones, Gateways and tools for drug delivery: endocytic pathways and the cellular dynamics of cell penetrating peptides, Int. J. Pharm. 354 (1–2) (2008) 34–38.
[2] J.P. Richard, et al., Cell-penetrating peptides. A reevaluation of the mechanism of cellular uptake, J. Biol. Chem. 278 (1) (2003) 585–590.
[3] A.I. Ivanov, Pharmacological inhibition of endocytic pathways: is it specific enough to be useful? Methods Mol. Biol. 440 (2008) 15–33.
[4] D. Vercauteren, et al., The use of inhibitors to study endocytic pathways of gene carriers: Optimisation and pitfalls, Mol. Ther. 18 (3) (2010) 561–569.
[5] A. Motley, et al., Clathrin-mediated endocytosis in AP-2-depleted cells, J. Cell Biol. 162 (5) (2003) 909–918.
[6] O.O. Glebov, N.A. Bright, B.J. Nichols, Flotillin-1 defines a clathrin-independent endocytic pathway in mammalian cells, Nat. Cell Biol. 8 (1) (2006) 46–54.
[7] J. Mercer, A. Helenius, Virus entry by macropinocytosis, Nat. Cell Biol. 11 (5) (2009) 510–520.

doi:10.1016/j.jconrel.2010.07.062

Programmed packaging of multicomponent envelope-type nanoparticle system (MENS)

Daniela Pozzi[1], Carlotta Marianecci[2], Maria Carafa[2], Cristina Marchini[3], Maura Montani[3], Augusto Amici[3], Giulio Caracciolo[1]
[1] *Department of Chemistry, Faculty of Medicine, 'Sapienza' University of Rome, P.le A. Moro 5, 00185 Rome, Italy*
[2] *Dipartimento di Chimica e Tecnologie del Farmaco, Faculty of Pharmacy 'Sapienza' University of Rome, P.le A. Moro 5, 00185 Rome, Italy*
[3] *Department of Molecular Cellular and Animal Biology, University of Camerino, Via Gentile III da Varano, 62032 Camerino (MC), Italy*

Abstract summary

Here we apply a recently proposed programmed packaging strategy to develop a novel multicomponent envelope-type nanoparticle system (MENS). To this end, we took specific advantage of using multicomponent liposomes that have recently exhibited intrinsic endosomal rupture properties that allow plasmid DNA to escape from endosomes and to enter the nucleus with extremely high efficiency. Transfection efficiency experiments on NIH 3T3 mouse fibroblasts indicate that MENS is a promising transfection candidate.

Introduction

Non-viral DNA delivery systems have been developed to facilitate gene entry into mammalian cells. The cell presents multiple barriers to DNA/vector complexes en route to the nucleus. Very early steps in the transfection process involve binding of the vector to the cell surface and its internalization via multiple mechanisms. Once in the cell, plasmid DNA must be able to escape endosomal trafficking. If DNA is not released from endosomes, it is shuttled to the lysosomes, where it is degraded by the abundant nucleases and transfection may fail. An efficient nanocarrier should therefore incorporate different functional devices, but it is difficult to integrate them into a single system and to have each function exerted at the appropriate time and correct place. Recently, a new programmed packaging concept in which various tools that control intracellular trafficking are packed into single nanoparticles has been proposed [1]. Here we apply such a novel strategy to develop a multicomponent envelope-type nanoparticle system (MENS) for overcoming intracellular membrane

50% silencing efficiency whereas incubation with pHPMA-MPPM and TMC polyplexe made at N/P ratios of 8 and 16 showed 30–40% gene silencing. Incubation of cells with branched PEI polyplexes led to 25–30% silencing of luciferase. The XTT cell viability assays show low cytotoxicity of the polymer complexes (except PE 1) made at an N/P ratio of 8 (less than 15%) and by increasing the N/P ratio to 16, cytotoxicity level is increased. In the case of pDMAEMA, pHPMA-MPPM and TMC the cytotoxicity of the polyplexes at the N/P ratio of 16 is about two folds higher than the N/P ratio of 8 which is correlated to the increased concentration of the polymers in the formulations and subsequently in the culture medium (Fig. 5).To facilitate the endosomal release of the siRNA complexes, photochemical internalization (PCI) was applied. PCI is a technique based on the use of a photosensitizer that photochemically destabilizes endosomal membranes after illumination [6]. By application of PCI, the silencing efficiency of the pDMAEMA polyplexes made at N/P ratios of 8 and 16 increased up to 70% and 60% respectively whereas for both N/P ratios of 8 and 16, the silencing efficiency of the pHPMA-MPPM and TMC—33% polyplexes increased up to 70% and 80% respectively.

The gene silencing efficiency of PEI polyplexes, after application of PCI showed a slight increase (5%) which is not significant and is probably due to the intrinsic endosomolytic properties of PEI which makes it independent of PCI [7]. In the case of lipofectamine, the silencing efficiency of the complexes increased up to 60% after application of PCI (Fig. 4). These results show that biodegradable polymethacrylates and TMC polymers are much more in favor of PCI as an endosome disruptive technique. For all formulations, the observed increase in gene silencing efficiency was not due to PCI-associated cytotoxicity (Fig. 5).

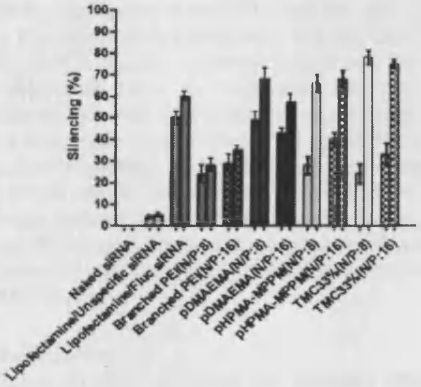

Fig. 4. Luciferase gene silencing after incubation of H1299 cells with polyplexes in medium without serum, with and without application of PCI (mean ± standard deviation (n = 3)).

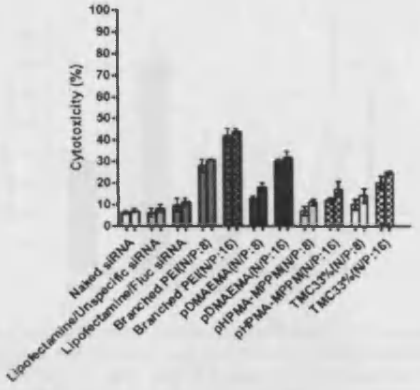

Fig. 5. Cell viability as measured by XTT assay after incubation of siRNA complexes in medium without serum with and without application of PCI (mean ± standard deviation (n = 3)). In all formulations, the left and the right bars show the silencing efficiency without and with PCI respectively.

Conclusion

Biodegradable pHPMA-MPPM and TMC (33%) polymers are efficient and safe vectors for siRNA delivery and gene silencing, which by facilitating their endosomal escape, show a promising gene silencing efficiency.

References

[1] J. Park, M. Ye, M.K. Park, Biodegradable Polymers for Microencapsulation of Drugs, Molecules 10 (1) (2005) 146–161. doi:10.3390/10010146.
[2] J. Luten, N. Akeroyd, A. Funhoff, M.C. Lok, H. Talsma, W.E. Hennink, Methacrylamide polymers with hydrolysis-sensitive cationic side groups as degradable gene carriers, Bioconjugate Chem. 17 (2006) 1077–1084.
[3] R.J. Verheul, M. Amidi, S. van de. Wal, E. van Riet, W. Jiskoot, W.E. Hennink, Synthesis, characterization and in vitro biological properties of O-methyl free N,N,N-trimethylated chitosan, Biomaterials 29 (27) (2008) 3642–3649.
[4] K. Berg, P.K. Selbo, L. Prasmickaite, T.E. Tjelle, K. Sandvig, J. Moan, G. Gaudernack, O. Fodstad, S. Kjølsrud, H. Anholt, G.H. Rodal, S.K. Rodal, A. Høgset, Photochemical internalization: a novel technology for delivery of macromolecules into cytosol, Cancer Res. 59 (1999) 1180–1183.
[5] R.B. Arote, S.K. Hwang, M.K. Yoo, D. Jere, H.L. Jiang, Y.K. Kim, Y.J. Choi, J.W. Nah, M. H. Cho, C.S. Cho, Biodegradable poly(ester amine) based on glycerol dimethacrylate and polyethylenimine as a gene carrier, J. Gene Med. 10 (11) (2008) 1223–1235.
[6] A. Bonsted, B.O. Engesæter, A. Høgset, G.M. Mælandsmo, L. Prasmickaite, C. D'Oliveira, W.E. Hennink, J.H. van Steenis, K. Berg, Photochemically enhanced transduction of polymer-complexed adenovirus targeted to the epidermal growth factor receptor, J. Gene Med. 8 (2006) 286–297.
[7] T. Xia, M. Kovochich, M. Liong, H. Meng, S. Kabehie, S. George, J.I. Zink, A.E. Nel, Polyethyleneimine coating enhances the cellular uptake of mesoporous silica nanoparticles and allows safe delivery of siRNA and DNA constructs, ACS Nano. 3 (10) (2009) 3273–3286.

doi:10.1016/j.jconrel.2010.07.072

Unraveling the cellular uptake of bioreducible poly(amido amine) — Gene complexes in cells of the retinal pigment epithelium

D. Vercauteren[1,*], M. Piest[2], M. Al Soraj[3], A.T. Jones[3], J.F.J. Engbersen[2], S.C. De Smedt[1], K. Braeckmans[1]
[1] *Lab of General Biochemistry and Physical Pharmacy, Ghent University, Ghent, East Flanders, B9000, Belgium*
[2] *MIRA Institute for Biomedical Technology and Technical Medicine, Dept. of Biomedical Chemistry and Dept. of Polymer Chemistry and Biomaterials, University of Twente, P.O. Box 217, 7500 AE Enschede, The Netherlands*
[3] *Welsh School of Pharmacy, Cardiff University, Cardiff, CF10 3XF, Wales, United Kingdom*
**Corresponding author.*
E-mail: dries.vercauteren@UGent.be.

Abstract summary

In vitro endocytosis of gene complexes composed of a bioreducible polyamidoamine CBA ABOL and plasmid DNA, in cells of the retinal pigment epithelium (RPE) was studied, the latter being an interesting target for ocular gene therapy. We found that cationic CBA ABOL DNA polyplexes attach to cell surface proteoglycans of these RPE cells and get subsequently internalized via a phagocytosis-like mechanism, as well as Flotillin dependent endocytosis.

Introduction

Proper delivery of therapeutic genes to designated cells and their availability at the intracellular site of action are crucial requirements for successful gene therapy. To this end, typically sub-micron sized particles are made by combining the therapeutic genes with a carrier material, such as cationic polymers, that aid in delivering the genes to the target site. In this work, for the first time, we have evaluated the ability of the highly promising bioreducible polymer carrier cystamin bisacrylamid aminobutanol (CBA ABOL) [1] (Fig. 1) to deliver plasmid DNA in cultured cells of the retinal pigment epithelium (ARPE-19) and characterized *in vitro* the cellular interactions with these target

cells. These studies are of crucial importance since the further design and functionalization of polymeric gene carriers depend strongly on our understanding of the mechanisms involved in cellular adhesion, intracellular uptake and intracellular processing of the polyplexes.

Experimental methods

ARPE-19 cells (retinal pigment epithelial cell line; ATCC number CRL-2302) were cultured in DMEM:F12 supplemented with 10% fetal bovine serum, 2 mM l-glutamine, and 2% penicillin-streptomycin. All cells were grown at 37 °C in a humidified atmosphere containing 5% CO_2. CBA ABOL gene complexes with an average hydrodynamic diameter of 130 nm and an average zeta potential of +45 mV in 20 mM HEPES buffer were obtained by adding the polymer in a mass ratio of 48/1 in 20 mM HEPES to the plasmid and vortexing the mixture for 10 min. For every transfection, fresh polyplexes were prepared and applied to the cells within 30 min after complexation. For all uptake studies, YOYO-1™ (λ_{ex} = 491 nm, λ_{em} = 509 nm, Molecular Probes, Merelbeke, Belgium) labeled pGL4.13 plasmid (Promega, Leiden, The Netherlands) was used. For all transfection studies, gWiz™GFP plasmid (Aldevron, Freiburg, Germany) was used. siRNAs were all purchased from Dharmacon and transfected in cells with the help of LipofectaminRNAiMAX (Invitrogen, Merelbeke, Belgium). Protein knockdown was assessed on Western Blot. Uptake of polyplexes or endocytic markers or GFP expression was measured on a FACS Calibur Flow Cytometer (Beckton Dickinson, Erembodegem, Belgium). For genetic labeling of endosomes, cells were transfected with GFP-fusion proteins.

For fluorescence colocalization studies with GFP labeled cellular structures, cells were transfected with GFP-fusion proteins using Lipofectamin2000 (Invitrogen, Merelbeke, Belgium) and 24 h later exposed to red fluorescent labeled polyplexes. For this, CBA ABOL was complexed with pGL4.13 plasmid, covalently labeled with Cy5 (Label IT Nucleic Acid Labeling Kit, Mirus Bio Corporation, WI, USA). Live cell fluorescence colocalization was then performed on a custom built laser epi-fluorescence microscope set-up. A Nikon Plan Apo VC 100× 1.4 NA oil immersion objective lens (Nikon Belux, Brussels, Belgium) was used for imaging. GFP and Cy5 were excited with 491 nm and 636 nm laser light and emission was detected on an EMCCD camera (Roper Scientific, Nieuwegein, The Netherlands). For live cell imaging the cells were placed in a stage top incubation chamber (Tokai Hit, Shizuoka, Japan), set at 37 °C, 5% CO_2 and 100% humidity.

Result and discussion

First, we found evidence that these net positively charged CBA ABOL polyplexes adhere to the negatively charged heparan sulfate proteoglycans (HSPGs) at the cell surface and that polyplex internalization is blocked by antibodies against Toll-like receptor 9.

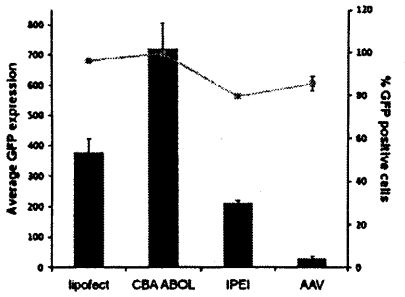

Fig. 1. Comparison of transfection efficacy of different gene delivery vehicles carrying the GFP reporter gene in ARPE-19 cells. Cells were incubated for 2 h in OptiMEM with different gene carriers: Lipofectamin2000, CBA ABOL, Exgen500 (linear PEI) and Adeno Associated Virus (AAV). Transfection analysis was performed 24 h later with flow cytometry. The square data points represent the percentage of transfected (GFP expressing) cells, the grey bars represent the amount of expression (average GFP fluorescence intensity) per cell. It appears that the performances for CBA ABOL in RPE cells are in these conditions competitive to Exgen500 and AAV mediated transfection and even with Lipofectamin2000 lipofection.

Second, in an extensive study on the characterization of the endocytic pathways that are involved in the cellular internalization of these polyplexes, we learned by the use of endocytic inhibitors [2] that polyplex uptake is for a large part very similar to the uptake of *Escherichia coli*, which indicates a substantial contribution by phagocytosis. We also learned from these studies that clathrin dependent endocytosis is not involved and that the internalization of polyplexes is highly dependent on actin, dynamin, cholesterol and tyrosine kinase activities. In a complementary study, where we used RNAi to knock down specific key endocytic proteins, not only we could confirm that polyplex uptake is independent of clathrin, but also of Caveolin-1, Arf6, PAK1 and GRAF-1. On the other hand we did find a dependency on Dynamin-2 and Flotillin-1. This indicates that, next to phagocytosis, probably a second endocytic pathway dependent on Flotillin-1 [3] is involved, which is in agreement with what has been reported for gene complexes based on the polymer polyethylenimine [4]. Finally, using live-cell dual colour fluorescence colocalization microscopy, we could confirm the involvement of Flotillin during polyplex internalization at early time-points while no colocalization was found with Caveolin-1 containing vesicles.

Conclusion

In conclusion, we learned by combining three different methodological approaches that these polyplexes stimulate their own cellular uptake and are rapidly internalized in RPE cells via two endocytic pathways, being Flotillin mediated endocytosis and phagocytosis. We would like to note that this conclusion was only possible by combining the use of chemical inhibitors, siRNA downregulation of essential endocytic proteins and live cell colocalization microscopy. By getting a detailed insight into the uptake and subsequent intracellular processing of these polyplexes, we want to provide the knowledge necessary for a further rational optimization of the design and composition of this polymer carrier.

Acknowledgements

D. Vercauteren is a doctoral fellow of the Institute for the Promotion of Innovation through Science and Technology in Flanders (IWT), Belgium. We gratefully acknowledge the European Commission for the funding through the Integrated 6th Framework Programme MediTrans. The contribution provided by A.T. Jones was supported by the BBSRC.

References

[1] C. Lin, Z.Y. Zhong, M.C. Lok, X.L. Jiang, W.E. Hennink, J. Feijen, J.F.J. Engbersen, Novel bioreducible poly(amido amine)s for highly efficient gene delivery, Bioconjugate Chem. 18 (2007) 138–145.
[2] D. Vercauteren, R.E. Vandenbroucke, A.T. Jones, J. Rejman, J. Demeester, S.C. De Smedt, N.N. Sanders, K. Braeckmans, The Use of Inhibitors to Study Endocytic Pathways of Gene Carriers: Optimization and Pitfalls, Mol. Ther. 18 (3) (2009) 561–569.
[3] O.O. Glebov, N.A. Bright, B.J. Nichols, Flotillin-1 defines a clathrin-independent endocytic pathway in mammalian cells, Nat. Cell Biol. 8 (2006) 46-U16.
[4] C.K. Payne, S.A. Jones, C. Chen, X.W. Zhuang, Internalization and trafficking of cell surface proteoglycans and proteoglycan-binding ligands, Traffic 8 (2007) 389–401.

doi:10.1016/j.jconrel.2010.07.073

Sustained delivery of oncolytic adenovirus in alginate gel for local tumor virotheraphy

Pyung-Hwan Kim[1], Eunah Kang[2], Jung Woo Choi[2], Tae Jin Yun[2], Hong-Kwan Park[3], Jung Hyun Kim[c], Chae-Ok Yun[1,2,*]
[1] *Graduate Program for Nanomedical Science, Yonsei University 1661 College of Medicine, Seoul, South Korea*
[2] *Brain Korea 21 Project for Medical Sciences and Institute for Cancer Research, Yonsei University College of Medicine, Seoul, South Korea*
[3] *Department of Chemical and Biomolecular Engineering, Yonsei University, 134 Shinchon-Dong, Seodaemun-Gu, Seoul, South Korea*
**Corresponding author.*
E-mail: chaeok@yuhs.ac.

3. Sánchez-Martín RM, et al. *Angew Chem Int Ed* 2006;**45**:5472–4.
4. Alexander LM, et al. *Bioconjug Chem* 2009;**20**:422–6.
5. Sánchez-Martín RM, et al. *ChemBioChem* 2009;**10**:1453–6.

doi:10.1016/j.drudis.2010.09.410

A63

siRNA versus pharmacological inhibition of endocytic pathways for studying cellular uptake of cell penetrating peptides and other drug delivery vectors

Monerah H. Al-Soraj[1,*], Catherine L. Watkins[1], Dries Vercauteren[2], Stefaan De Smedt[2], Kevin Braeckmans[2], Arwyn T. Jones[1]

[1] *Welsh School of Pharmacy, Cardiff University, Cardiff, Wales CF10 3NB, UK*

[2] *Laboratory of General Biochemistry & Physical Pharmacy, Ghent University, Harelbekestraat 72, Ghent, Belgium*

*Corresponding author.
E-mail: alsorajm@cf.ac.uk (M.H. Al-Soraj).

Cell-penetrating peptides (CPPs) have the potential to deliver numerous therapeutic macromolecules into cells including peptides, proteins, and nucleic acids. Under defined conditions endocytosis is thought to be of significant importance for CPP entry but identifying the exact uptake mechanism and pathway(s) involved has been difficult. Multiple pathways have been reported to contribute to uptake, including macropinocytosis and those regulated by clathrin and cavaeolin-1. This project aims enhance the use of cell penetrating peptides as drug delivery vectors by developing new technologies to study their mechanisms of uptake. Traditionally studies investigating the uptake of these molecules, and other drug delivery vectors, have been performed using chemical inhibitors but these are often toxic and lack specificity [1]. We have developed siRNA-based assays to silence endocytic proteins that have previously been shown to regulate distinct endocytic pathways. The effect of depleting these proteins was then assessed to investigate their roles in mediating the uptake of well characterised endocytic probes and CPPs. Two cell lines were predominantly used, HeLa (cervical cancer epithelial) and A431 (human epithelial carcinoma). Endocytic proteins clathrin heavy chain, flotillin-1, dynamin II, caveolin-1 and P21-activated kinase (PAK-1) were depleted using single siRNA sequences; siRNA against GFP was used as a control. In siRNA treated cells the uptake of fluorescent endocytic markers including; Alexa488-transferrin (clathrin mediated endocytosis), 40 kDa FITC Dextran (fluid phase uptake and macropinocytosis), FITC conjugated anti-CD59 antibody (flotillin-1 dependent uptake) and the uptake of Alexa488 CPPs (RRRRRRRRGC-Alexa488-R8, and GRKKRRQRRRPPQ-Alexa488-HIV-TAT) were measured by flow cytometry. Protein depletion was assessed from protein lysates using SDS PAGE and Western blotting. Overall, the data shows that siRNA transfection method could effectively reduce expression of clathrin heavy chain, caveolin-1 and flotillin-1 from HeLa cells and this then allowed for us to study effects on endocytosis of various probes. PAK-1 has been shown to regulate macropinocytosis and we show that the induction of macropinocytosis and PAK-1 expression are highly cell line dependent. Paralleled with this was our findings that cationic CPPs induce an increase in fluid phase uptake of dextran and the extent of this was cell line dependent. Comparative analysis of these experiments with those performed using pharmacological inhibitors, allowed us to determine the usefulness of this approach for drug delivery research.

Reference

1. Vercauteren D, et al. The use of inhibitors to study endocytic pathways of gene carriers: optimisation and pitfalls. *Mol Ther* 2010;**18**:561–9.

doi:10.1016/j.drudis.2010.09.411

A64

SAINTargs, a novel lipid-based targeting device for siRNA delivery

Niek G.J. Leus[1,*], Piotr S. Kowalski[1], Sigridur A. Ásgeirsdóttir[1], Eduard G. Talman[2], Marcel H.J. Ruiters[2], Grietje Molema[1], Jan A.A.M. Kamps[1]

[1] *University Medical Center Groningen, Department of Pathology & Medical Biology, Laboratory of Endothelial Medicine & Vascular Drug Targeting, Hanzeplein 1, 9713 GZ Groningen, The Netherlands*

[2] *Synvolux Therapeutics, L.J. Zielstraweg 1, 9713 GX Groningen, The Netherlands*

*Corresponding author.
E-mail: n.g.j.leus@med.umcg.nl (N.G.J. Leus).

The endothelium represents an important therapeutic target because its pivotal role in many diseases such as chronic inflammation and cancer and its accessibility for systemic administration. RNA interference by small interfering RNA (siRNA) has become in the last decade a very powerful tool in basic research, and has huge potential to become an important new class of therapeutics for humans. However, due to their size and charge, siRNAs have no bioavailability to enter unperturbed cells. To overcome this problem, our laboratory developed a non-viral lipid-based targeting device which efficiently and specifically delivers siRNA into endothelial cells. Molecular determinants expressed on the surface of inflammation-activated endothelial cells, like certain adhesion molecules and receptors involved in endocytosis, are excellent candidates to increase carrier-mediated siRNA uptake. Therefore we conjugated monoclonal anti-E-selectin antibodies to the cationic amphiphilic lipid, 1-methyl-4-(cis-9-dioleyl)methyl-pyridinium-chloride (SAINT-18) which was complexed in a 1:2000 molar ratio with the transfection agent SAINT-MIX (SAINT:DOPE, 1:1), and siRNA, resulting in a siRNA containing lipoplex called anti-E-selectin-SAINTarg [1]. Our findings demonstrate that anti-E-selectin-SAINTargs maintained the antigen recognition capacity of the parental antibody and showed increased siRNA uptake in otherwise difficult-to-transfect primary human umbilical vein endothelial cells (HUVEC) as compared to non-targeted SAINT-MIX. Moreover, anti-E-selectin-SAINTargs superior binding and uptake efficiency was corroborated by improved silencing of both gene- and protein expression of VE-cadherin in activated HUVEC. The VE-cadherin gene expression could be silenced up to 95% by VE-cadherin specific siRNA, at low siRNA concentrations (30 pmol/ml). Furthermore, no non-specific silencing by scrambled or VE-cadherin specific siRNA was observed. To optimize siRNA delivery into activated endothelial cells we also synthesized anti-VCAM-1-SAINTargs which were as efficient in VE-cadherin silencing as anti-E-selectin-SAINTargs. Because of the heterogeneous expression of adhesion molecules on inflammation-activated endothelial cells *in vivo*, a combination of these two SAINTargs may result in enhanced siRNA effects. Taken together, SAINTargs demonstrate specific and efficient targeting to inflammation-activated difficult-to-transfect primary endothelial cells and results in strong siRNA specific gene silencing at low siRNA concentrations.

Reference

1. Asgeirsdottir SA, Talman EG, de GI, Kamps JA, Satchell SC, Mathieson PW, Ruiters MH, Molema G. Targeted transfection increases siRNA uptake and gene silencing of primary endothelial cells in vitro - A quantitative study. *J Control Release* 2010 Jan 25;**141**(2):241–51.

doi:10.1016/j.drudis.2010.09.412

Biomaterials 32 (2011) 3072–3084

Contents lists available at ScienceDirect

Biomaterials

journal homepage: www.elsevier.com/locate/biomaterials

Flotillin-dependent endocytosis and a phagocytosis-like mechanism for cellular internalization of disulfide-based poly(amido amine)/DNA polyplexes☆

Dries Vercauteren[a], Martin Piest[b], Leonardus J. van der Aa[b], Monerah Al Soraj[c], Arwyn T. Jones[c], Johan F.J. Engbersen[b], Stefaan C. De Smedt[a], Kevin Braeckmans[a,*]

[a] Laboratory of General Biochemistry and Physical Pharmacy, Ghent University, Harelbekestraat 72, B-9000 Ghent, Belgium
[b] Department of Biomedical Chemistry, MIRA Institute for Biomedical Technology and Technical Medicine, Faculty of Science and Technology, University of Twente, P.O. Box 217, 7500 AE Enschede, The Netherlands
[c] Welsh School of Pharmacy, Redwood Building, Cardiff University, CF10 3NB, Cardiff, Wales, UK

ARTICLE INFO

Article history:
Received 28 October 2010
Accepted 27 December 2010
Available online 22 January 2011

Keywords:
Non-viral gene delivery
Endocytosis
Retinal pigment epithelium
Polyplexes

ABSTRACT

Extensive research is currently performed on designing safe and efficient non-viral carriers for gene delivery. To increase their efficiency, it is essential to have a thorough understanding of the mechanisms involved in cellular attachment, internalization and intracellular processing in target cells. In this work, we studied *in vitro* the cellular dynamics of polyplexes, composed of a newly developed bioreducible poly(amido amine) carrier, formed by polyaddition of *N,N*-cystamine bisacrylamide and 1-amino-4-butanol (p(CBA-ABOL)) on retinal pigment epithelium (RPE) cells, which are attractive targets for ocular gene therapy. We show that these net cationic p(CBA-ABOL)/DNA polyplexes require a charge-mediated attachment to the sulfate groups of cell surface heparan sulfate proteoglycans in order to be efficiently internalized. Secondly, we assessed the involvement of defined endocytic pathways in the internalization of the polyplexes in ARPE-19 cells by using a combination of endocytic inhibitors, RNAi depletion of endocytic proteins and live cell fluorescence colocalization microscopy. We found that the p(CBA-ABOL) polyplexes enter RPE cells both via flotillin-dependent endocytosis and a PAK1 dependent phagocytosis-like mechanism. The capacity of polyplexes to transfect cells was, however, primarily dependent on a flotillin-1-dependent endocytosis pathway.

1. Introduction

Efficient delivery of therapeutic nucleic acids into designated cells and subsequent availability at the intracellular site of action are crucial requirements for successful gene therapy. It is generally accepted that gene carriers are internalized through endocytic vesicles which are then trafficked to other regions of the cell. Thus, the mechanisms that direct cell attachment, endocytosis, intracellular trafficking and release of the nucleic acids from the carrier strongly determine transfection efficiency. Most of these processes are generally dictated by the nature of the gene carrier. It is known that for non-viral gene delivery vehicles both cellular entry and intracellular release of therapeutic nucleic acids is significantly less efficient compared with viral vectors, and non-viral gene therapy thus generally suffers from low transfection efficiencies [1]. They are, however, attractive alternatives to viral carriers, because they are safer to use, are less immunogenic, can be more easily chemically modified and are easier to produce at large-scale. In order to design safe and efficient non-viral carriers for gene delivery, we need a better understanding of the mechanisms involved from cell uptake to intracellular fate. In this respect, cell surface targets need to be identified and evaluated to improve cell attachment and vector internalization to deliver the gene through transfection-efficient pathways. This knowledge will allow further improvements in the design and functionalization of the delivery vehicle with the intention of developing target-specific, effective and safe carriers for nucleic acid delivery.

Currently, the mechanisms behind the cellular processing of non-viral gene complexes remain poorly understood since the highly dynamic character of these processes makes these studies very complex. In addition, the interaction between the target cell and the gene complex might be highly cell-type specific for the type of particle being studied. Therefore, little consistency is found in the scientific literature. The situation is further complicated due to the fact that a single cell can harbor a number of different endocytic pathways and because of interconnections and interdependences between these endocytic processes. However, a common endocytosis classification based on recent reviews distinguishes phagocytosis, macropinocytosis, clathrin-dependent endocytosis (CDE) and

☆ The work is done in Ghent, Belgium.

* Corresponding author. Tel.: +32 (0) 9/2648098; fax: +32 (0) 9/2648189.
E-mail address: kevin.braeckmans@UGent.be (K. Braeckmans).

0142-9612/$ – see front matter © 2011 Elsevier Ltd. All rights reserved.
doi:10.1016/j.biomaterials.2010.12.045

clathrin-independent endocytosis (CIE) [2]. Phagocytosis is characterized by the engulfment of large solid particles of at least 1 μm in size, typically restricted to specialized cells such as macrophages. Macropinocytosis is an induced and transient bulk internalization process, that is typically characterized by the formation of membrane ruffles and the engulfment of large volumes of fluid and membrane into large uncoated vacuoles [3,4]. In addition, some cell types like immature dendritic cells and macrophages exhibit constitutive macropinocytosis, constantly surveying their environment for foreign material [4]. Possibly the best-studied endocytic pathway to date is CDE, which is characterized by the formation of clathrin-coated pits [5]. CIE includes several pathways which all share a dependency on cholesterol [6]. Some of the currently known CIE pathways are caveolin mediated endocytosis (Cav-ME) [7], flotillin mediated endocytosis (Flot-ME) [8], and the pathway clathrin-independent carriers - GPI-enriched endocytic compartments (CLIC/GEEC) [9]. It is clear from recent literature that the use of different endocytic routes is strongly dependent on the cell type, gene carrier and nucleic acid [10–12]. It is also becoming apparent that some endocytic pathways will allow a higher transgene delivery and thus efficiency of transfection than others. For example, polyplex uptake is reported to occur via MP, CDE as well as via CIE [13–15]. And although no consensus yet exists on the description of the exact endocytic pathway that would lead preferentially to transfection, some reports seem to agree that CDE is less preferable for polyplex mediated gene transfer [12,16–18].

Studying endocytic pathways is typically done by attempting to selectively inhibit different endocytic pathways and then quantifying the remaining internalized gene complexes. These studies are often carried out with the help of pharmaceutical endocytic inhibitors [19,20]. However, due to problems of low specificity, alternative methods such as RNA interference (RNAi), transfection of cells with mutant proteins and fluorescence colocalization microscopy have been employed as alternative tools [14]. In this work we have combined these approaches to study endocytosis of a polymeric carrier in retinal pigment epithelium (RPE) cells. These cells form *in vivo* a monolayer of highly specialized cells, interposed between the neurosensory retina and the choroid [21]. This light-absorbing epithelium functions as a blood-retina barrier, regulating the transport of nutrition to the retina [21]. RPE cells are attractive targets for ocular gene therapy because they are involved in several ocular genetic defects such as retinitis pigmentosa and choroidal neovascularization (e.g. AMD) which could conceivably be cured by altering the expression profile in these cells [22,23]. The polymeric vector in this study is p(CBA-ABOL), a linear poly(amido amine) with repetitive disulfide linkages in the main chain, prepared by Michael-type polyaddition of 4-aminobutanol (ABOL) to *N,N′*-cystaminebisacrylamide (CBA) [24]. This polymer contains tertiary amines that are partially protonated around physiological pH, which makes the polymer positively charged and suitable to form positively charged polyplexes by electrostatic interaction with anionic nucleic acids. The disulfide bonds in the polymeric backbone are prone to rapid cleavage into sulfhydryl groups once the polymer has arrived in the reductive intracellular environment due to the presence of thioredoxin reductases and high glutathione concentrations. This identifies this polymer as a "bioreducible polymer" that is rapidly degraded in the intracellular milieu, thereby releasing the DNA from the polymer/DNA complex [25].

The purpose of this work was to gain insight into the mechanisms of attachment and internalization of p(CBA-ABOL)/DNA polyplexes in ARPE-19 cells. We initially evaluated the transfection efficacy and uptake kinetics of p(CBA-ABOL) polyplexes in primary RPE cells and ARPE-19 cells and also investigated the attachment of the polyplexes to RPE cells. Secondly, we studied endocytic uptake of p(CBA-ABOL)/DNA polyplexes by using a library of different endocytic inhibitors. Thirdly, as a complementary strategy, we utilized RNAi to downregulate specific proteins that play key roles in endocytic processes to block the corresponding endocytic events. Finally, we performed fluorescence colocalization microscopy studies to confirm association of the polyplexes with endocytic proteins.

2. Materials and methods

2.1. Materials

Heparinase III, trypan blue, Cpz, MβCD, genistein, nocodazole, dynasore, rottlerin, Lucifer Yellow CH dilithium salt (LY), (defatted) bovine serum albumin (BSA) and sodium chlorate were purchased from Sigma–Aldrich (Bornem, Belgium). Dulbecco's modified Eagle's medium (DMEM), OptiMEM, L-glutamine, fetal bovine serum (FBS), penicillin-streptomycin solution (5000 IU/ml penicillin and 5000 μg/ml streptomycin) (P/S), and phosphate-buffered saline (PBS) were supplied by GibcoBRL (Merelbeke, Belgium). CytoD, human Transferrin (hTf)-AlexaFluor488, BSA-complexed BODIPY FL C5-Lactosylceramind (LacCer), Oregon Green labeled 70 kDa dextran and FITC labeled *Escherichia coli* Bioparticles™ (ECs) were purchased from Invitrogen (Merelbeke, Belgium). Sequences of siRNAs and manufacturer are given in Supplementary. Table. 1. Antibodies against heparan sulfate were purchased from Millipore (Brussels, Belgium). Antibodies for Western blotting are listed in Supplementary. Table. 2. JetPEI™ was purchased from Polyplus (Leusden, The Netherlands). Lipofectamin2000™ for gene transfection and LipofectaminRNAiMAX™ for transfection of siRNA were purchased from Invitrogen (Merelbeke, Belgium). All other reagents were purchased from Sigma–Aldrich (Bornem, Belgium) unless otherwise stated.

2.2. Cell culture

ARPE-19 cells (retinal pigment epithelial cell line; ATCC number CRL-2302) were cultured in DMEM:F12 supplemented with 10% FBS, 2 mM L-glutamine, and 2% P/S. All cells were grown at 37 °C in a humidified atmosphere containing 5% CO_2. Primary bovine RPE cells were isolated from fresh bovine eye bulbs and prepared for culture as previously described [81]. Briefly, after cleaning the fresh eyes from fat, muscle and connective tissue, the eye bulb was dissected around the pupil. The lens and vitreous liquid were then removed and the remaining eyecup was washed in PBS with 4% P/S until the retina detached from the underlying RPE and choroid. After removal of the retina, the eyecup was washed twice with 6 ml of 0.25% w/v trypsin and 1 mM EDTA in PBS for 30 min at 37 °C to detach RPE cells from the underlying choroid. The cells were diluted in cell culture media with 20% FBS and after centrifugation they were seeded in 25 cm^2 culture flasks (SPL Life Sciences, Pocheon, Korea). After 24 h of culture, the adherent cells were washed to discard remaining blood cells. Primary bovine RPE cells were used between passages 6 and 10. All cells were grown at 37 °C in a humidified atmosphere containing 5% CO_2.

2.3. Plasmids

The plasmid construct pEGFP-Flot2 was a kind gift from B. Nichols (Cambridge University, UK) and pEGFP-Cav1 was a kind gift from M. Gumbleton (Cardiff University, UK). Plasmids were all transformed in single step (KRX) competent cells (Promega, Leiden, The Netherlands) according to the manufacturer's instructions. The transformed bacteria were then selected for kanamycin resistance and grown to OD of 1.5. The plasmids were isolated with a QIAfilter Plasmid Giga Kit (Qiagen, Venlo, The Netherlands) and concentrations determined by UV absorption at 260 nm. Finally, the plasmids were suspended and stored in 20 mM HEPES, pH 7.4.

For all plasmid uptake studies, pGL4.13 plasmid (Promega, Leiden, The Netherlands), labeled with the nucleic acid stain YOYO-1™ (λ_{ex} = 491 nm, λ_{em} = 509 nm, Molecular Probes, Merelbeke, Belgium) was used. This is a 4641 base pair (bp) construct and contains a luciferase 2 expression cassette under control of the cytomegalovirus (CMV) promoter, next to a sequence for ampicillin resistance. YOYO-1 (1 mM in DMSO) iodide was added to the plasmid at a mixing ratio of 0.15:1 (v:w) ratio of (dye/base pair), resulting in a theoretical labeling density of 1 YOYO-dye molecule per 10 bp. The mixture was incubated at room temperature for 1 h in the dark. To remove the DMSO and free YOYO-1, the complex was precipitated adding 2 volumes of ice-cold ethanol and 0,1 volume of 5 M NaCl. After incubation for 30 min at 4 °C, centrifugation (17.000 g, 10 min) and washing with ice-cold 70% ethanol, fluorescently labeled plasmid was finally resuspended in 25 mM HEPES, pH 7.2. The concentration of the plasmid was again determined by UV absorption at 260 nm. For microscopy colocalization studies with GFP labeled structures, pGL4.13 plasmid was labeled with Cy5 (Label IT Nucleic Acid Labeling Kit, Mirus Bio Corporation, WI, USA), according to the manufacturer's instructions at a 1:2 (v:w) ratio of Label IT Tracker Reagent and plasmid. For all transfection studies, gWiz™-GFP plasmid (Aldevron, Freiburg, Germany) was used, consisting of 5757 bp and containing the GFP expression cassette under control of the CMV promoter, next to CMV introns and kanamycin resistance.

2.4. Polyplexes

p(CBA-ABOL)/DNA complexes were obtained by adding a polymer solution of 0.6 mg/ml to a plasmid solution of 0.05 mg/ml in a final mass ratio of 48/1 in 25 mM HEPES buffer pH 7.2 and vortexing the mixture for 10 s. These gene complexes have an average hydrodynamic diameter of 120 nm and an average zeta potential of +40 mV (See Supplementary. Fig. 3). This was measured in undiluted samples of the polyplexes on a NanoZS zetasizer (Malvern Instruments, Hoeilaart, Belgium). For every transfection, fresh polyplexes were made and used within 30 min after complexation and were diluted 5× in OptiMEM™ during the addition to the cells.

JetPEI polyplexes were prepared according to the manufacturer's instructions. In summary, 4 μg of pDNA and 8 μl of JetPEI were first separately diluted till 100 μl with a 150 mM NaCl solution. The JetPEI dilution was then added to the pDNA solution, shortly vortexed and used within 30 min after the mixing step. Before adding the polyplexes to the cells, the polyplexes were first diluted 10× in OptiMEM™.

2.5. Pretreatments with pharmacological endocytic inhibitors

For all inhibition studies, 2×10^5 cells were seeded in six-well plates to, 24 h later, reach 70% confluency. The cells were subsequently pre-incubated with endocytic inhibitor in OptiMEM™ 15 μg/ml Cpz, 400 μM genistein and 3 mM MβCD for 2 h, 10 μM rottlerin, 5 μg/ml nocodazole and 5 μg/ml CytoD for 1 h or 80 μM dynasore for 30 min. All endocytic inhibitors were freshly used and fresh inhibitor was also added during uptake period with fluorescently labeled endocytic markers or polyplexes. MβCD and chlorpromazine solutions were filter sterilized through a 0.22 μm pore size filter before use.

2.6. siRNA mediated depletion of endocytic proteins

Cells were seeded at 2×10^5 cells per well in six-well plates and 24 h later transfected with 150 pmol siRNA (See Supplementary. Table. 1) and 7 μl LipofectaminRNAiMAX™ per well in serum free OptiMEM™ for 4 h according to the manufacturer's instructions. As a negative control, cells were transfected with Negative Control siRNA (Eurogentec, Seraing, Belgium) (Supplementary. Table. 1). Cells were subsequently left in growth medium for 20 h before detachment with trypsin and seeding them in 75 cm^2 culture flasks. After another 24 h, cells were transfected for a second time in the culture flask with 1.25 nmol siRNA and 58 μl LipofectaminRNAiMAX™ in OptiMEM™ for 4 h. After 20 h, cells were detached again and seeded in six-well plates in full growth medium and incubated for 12 h before performing endocytosis and transfection assays or cell lysis for assessing depletion (below).

2.7. Immunodetection of proteins following siRNA depletion

Following transfection with siRNA, the cells were washed and incubated for 5–10 min with ice-cold lysis buffer (50 mM Tris-base, 150 mM NaCl, pH 8.0, 1% Triton X-100) containing protease inhibitor cocktail (Roche, Vilvoorde, Belgium). The lysate was centrifuged at 13,000g (4 °C) for 10 min and supernatants were collected for protein analysis with the BCA protein assay kit (Pierce, Erembodegem, Belgium). Then, 20 μg protein was resolved by SDS-PAGE and transferred to nitrocellulose membranes, which were then blocked for 45 min at RT with (TBS containing 5% dried skimmed milk) then probed with CHC, Flot1, Cav1, DNM2, GRAF1, ARF6 and PAK1 antibodies (Supplementary. Table. 2), washed and then incubated with horseradish peroxidase-conjugated anti mouse, anti-rabbit or anti-goat antibodies (Pierce, Northumberland, UK). Protein bands were visualized by the enhanced chemiluminescence detection system (Thermo Fisher, Scientific, Leicestershire, UK). Equal protein loading was confirmed using antibodies recognizing α-Tubulin or CHC.

2.8. Flow cytometry

Cell-associated fluorescence was analyzed with a 5-color FACS Calibur (Beckton Dickinson, Erembodegem, Belgium) equipped with an Argon laser (excitation 488 nm) and a red diode laser (excitation 635 nm). For quantification, all experiments were performed in triplicate and for each sample 1×10^4 events were collected by list-mode data that consisted of side scatter, forward scatter and fluorescence intensities in different channels. Fluorescence emission of AF488, Oregon Green, LY, FITC and Bodipy FL was detected with a 530/30 nm bandpass filter (FL1) and emission of trypan blue was detected with a 670 long pass filter (FL4). Cellquest software (Beckton Dickinson, Erembodegem, Belgium) was used for analysis. Appropriate gating was applied to the scatterplot of untreated cells to select for intact cells. FL1 and FL4 signals were measured for all gated cells.

2.9. Quantification of uptake of endocytic markers or polyplexes

Control or inhibitor pre-treated cells, seeded 24 h earlier in six-well plates at 2×10^5 cells per well, were incubated with fluorescently labeled endocytic marker or gene complexes in OptiMEM™. Due to the presence of hTf in OptiMEM, DMEM was used as an alternative hTf free medium. The concentration and incubation time for the different endocytic markers were applied under following conditions: 16.7 μg/ml hTf for 15 min, 0.81 μM LacCer for 15 min, 5 mg/ml LY for 1 h, 0.5 mg/ml 70 kDa dextran for 3 h and 0.2 mg/ml ECs for 3 h. Polyplexes of p(CBA-ABOL) and YOYO-1 labeled pGL4.13 were incubated with the cells for 2 h at an amount corresponding to 4 μg plasmid per well. For quantification of the internalized fraction of endocytic marker or gene complexes with flow cytometry, it is imperative to remove the fraction that was not internalized and is still associated with the plasma membrane. For hTF and LacCer we applied an acid wash and back exchange protocol, respectively, as described previously [19]. The fluorescence of the plasma membrane associated fraction of FITC labeled ECs, Oregon Green labeled dextran, LY or YOYO-1 labeled pDNA was quenched with a 0.2% trypan blue solution in PBS for 5 min at room temperature. After thorough washing steps with PBS, cells were detached with trypsin, centrifuged and resuspended in ice-cold PBS with 0.1% azide and 1% BSA. Mean fluorescence values of triplicates were analyzed with flow cytometry and used as a measure for uptake of the endocytic markers or gene complexes. For inhibition experiments, mean fluorescence values were corrected for a 0% uptake (negative control) and normalized to a 100% uptake (positive control). The 0% uptake was determined from cells which were incubated with the fluorescent endocytic markers or complexes at 4 °C and underwent the same acid wash, back exchange or quenching. Uptake corresponding to 100% was determined from cells which were not treated with any inhibitor or with control siRNA.

2.10. Analysis of transfection efficiency

Cells were seeded into 6-well plates (2×10^5 cells per well) and allowed to attach overnight. Subsequently, the culture medium was removed and gene complexes, composed of gWiz™-GFP pDNA and gene carrier, were added to the well (4 μg of DNA per well). After 2 h, cells were washed with PBS and incubated for 22 h in full cell culture medium, unless stated differently. The average GFP expression of the total gated population of cells and the amount of GFP-positive cells in the same gate were subsequently measured by flow cytometry. As a negative control, cells were transfected with pGL4.13 plasmid since luciferase expression does not produce a detectable signal in the FL1 channel of the flow cytometer. A cell was considered GFP-positive and therefore successfully transfected if the average fluorescence was above the threshold T_r defined as the 99.5 percentile of the negative control sample. For inhibition experiments, GFP values were corrected for negative control (0% transfection) and normalized to the positive control (100% transfection), the latter being cells that were not treated with any inhibitor or with control siRNA.

2.11. Fluorescence colocalization microscopy

ARPE-19 cells were seeded at a concentration of 300.000 cells per well on sterile MatTek coverslips (1.5)-bottom dishes (MatTek Corporation, MA, USA). The next day, cells were transfected with plasmids coding for the EGFP constructs (pEGFP-Flot2 and pEGFP-Cav1) using Lipofectamin2000™ (Invitrogen, Merelbeke, Belgium) according to the manufacturer's description. The staining with pEGFP-Flot1 not satisfactory, and therefore omitted in this study. Briefly, for every Petri dish, 7 μl of Lipofectamin2000™ was mixed with 4 μg plasmid in 500 μl OptiMEM™ and after 30 min, these lipoplexes were added to 1500 μl OptiMEM™ on top of the cells. After 4 h, the lipoplex containing medium was removed and replaced with full cell culture medium. 24 hr later, the cells were incubated with p(CBA-ABOL) polyplexes, 5× diluted in 2 ml OptiMEM™, representing 4 μg Cy5-labeled pGL4.13 plasmid per well. Mixing the polyplexes with OptiMEM™ induces the formation of micrometer sized polyplex aggregates. Therefore, after 15 min, polyplexes were washed away and replaced with cell culture medium to reduce the amount of bright, non-internalized polyplex aggregates that can cause high background intensity in the fluorescence images. Cells were finally placed in a stage top incubation chamber (Tokai Hit, Shizuoka, Japan), on the microscope, set at 37 °C, 5% CO_2 and 100% humidity. GFP transfected cells were chosen for imaging based on a relatively low expression level of GFP-constructs. Cells were imaged on a custom built wide field fluorescence microscope set-up using a TE2000-E inverted microscope equipped with a Plan Apo VC 100× 1.4 NA oil immersion objective lens (Nikon Belux, Brussels, Belgium). GFP was excited with a 491 nm laser line (Cobolt, Stockholm, Sweden), while Cy5 was excited with a 636 nm diode laser (IQ1C, Power Technology, Little Rock, AR). GFP emission was captured in a spectral range between 500 and 600 nm and Cy5 between 655 and 745 nm. GFP and Cy5 fluorescence images were registered simultaneously on separate halves of the chip of an EMCCD camera (Roper Scientific, Nieuwegein, The Netherlands) and the overlay of the two channels was obtained with custom developed software.

3. Results

3.1. In vitro evaluation of p(CBA-ABOL) as a carrier for gene delivery

Linear disulfide-containing poly(amido amine) polymers such as p(CBA-ABOL) are promising carriers for nucleic acid delivery as disulfide-containing polymers have shown to offer higher average transgene expression and lower cytotoxicity, compared to polyethylenimine (PEI) which is typically considered as the standard

reference for polymer based gene delivery [24,26–29]. To evaluate the transfection efficiency of p(CBA-ABOL) in RPE cells, we compared transgene expression of p(CBA-ABOL) polyplexes with commercially available linear PEI vector JetPEI™ and the lipid based transfection agent Lipofectamin2000™. This was done both in ARPE-19 cells, a continuous human cell line of the RPE, as well as in primary bovine RPE cells (BRPE). RPE cells were transfected in serum free OptiMEM™ for 2 h with 4 μg of gWiz™-GFP plasmid, complexed with the different carriers. The percentage of GFP-positive cells and the average GFP expression were determined by flow cytometry, 24 h post-transfection (Fig. 1). This time point was chosen, because analysis of GFP expression for up to 5 days after transfection in ARPE-19 cells with p(CBA-ABOL) polyplexes showed that maximum GFP expression is reached after 24 h (Supplementary. Fig. 1). In the case of ARPE-19 cells, p(CBA-ABOL) polyplexes were able to transfect 80% of the cell population (Fig. 1, black dots), which was similar to Lipofectamin2000™ lipoplexes, but significantly higher than JetPEI™. Similar observations were obtained for average GFP expression (Fig. 1, black bars).

To further assess the transfection capacity of p(CBA-ABOL) complexes, we also performed experiments on primary bovine RPE cells. Similar trends were observed, although the percentage of transfected cells and average GFP expression was consistently less, compared to ARPE-19 cells. In addition, we assessed immediate cytotoxicity in ARPE-19 cells of the p(CBA-ABOL) transfection for different p(CBA-ABOL)/DNA mass ratios (Supplementary. Fig. 2). Higher mass ratios generally resulted in higher transfection efficiencies, but these were also more toxic to the cells [24]. As a trade off, a mass ratio of 48/1 was chosen for all further experiments since this ratio did not cause any significant cytotoxicity after 2 h exposure to the cells (Supplementary. Fig. 2), while still saturating the cellular uptake machinery (Supplementary. Fig. 3) and leading to high transfection efficiencies (Fig. 1). From these experiments we conclude that under defined conditions p(CBA-ABOL) is a safe and highly efficient polymeric carrier for DNA delivery to the RPE.

3.2. Role of anionic cell surface proteoglycans in p(CBA-ABOL) polyplex attachment and internalization

In order to study the interaction of p(CBA-ABOL)/DNA polyplexes with the plasma membrane, we investigated the role of highly anionic cell surface heparan sulfate proteoglycans (HSPGs). Cell surface HSPGs make up a great deal of the extracellular matrix (ECM) of different cell types [30] and it is known that they can function as primary co-receptors for cellular entry of lipoproteins [31], pathogenic bacteria, cell penetrating peptides [32], viruses [33] and also non-viral gene complexes [14,34,35]. For this reason, we investigated the role of HSPGs in attachment and subsequent uptake of p(CBA-ABOL) polyplexes in ARPE-19 cells. First, we attempted to interfere with the charge interaction between the cationic polyplexes and anionic HSPG chains by adding exogenous heparan sulfate analogs [31]. For this, ARPE-19 cells were exposed for 2 h to YOYO-1 labeled p(CBA-ABOL) polyplexes in OptiMEM in the presence of 10 mg/ml heparin. The presence of heparin led to an increase in size of the polyplexes and caused a charge reversal of the polyplexes to −60 mV (See also Supplementary. Fig. 4). After this 2 h exposure, the cells were washed and the fluorescence of the membrane bound fraction of polyplexes was quenched with trypan blue. Interestingly, since trypan blue formed complexes with the non-internalized polyplexes during the quenching step, trypan blue fluorescence could be used as a measure of plasma membrane associated polyplexes, or in other words cellular attachment. Both cellular attachment (Fig. 2, black bars) and endocytosis (Fig. 2, gray bars) of the p(CBA-ABOL) polyplexes were quantified by flow cytometry. The presence of heparin and consequent charge reversal of the polyplexes completely blocked cellular adhesion and uptake of the polyplexes (Fig. 2). This highlights the charge-based nature of the interaction between p(CBA-ABOL) polyplexes and the cell surface. We note that similar effects were observed when incubating the polyplexes in the presence of 10% FBS, probably because of similar binding of the abundant serum protein albumin and other proteins to the polyplexes (data not shown).

In a complementary experiment, we attempted to interfere with cellular sulfation by inhibiting ATP-sulfurylase, the enzyme that maintains the cellular sulfate pool. Here, ARPE-19 cells were pre-treated for 24 h with 80 mM of sodium chlorate as this treatment is reported to result in a strong reduction of the sulfation of the HSPGs (Keller, 1989). Sodium chlorate treated cells were then incubated with YOYO-1 labeled p(CBA-ABOL) polyplexes and their cell attachment and uptake were measured after 2 h. As a control experiment, uptake of hTf and LY after chlorate treatment was also assessed. hTf is specifically internalized via CDE after binding to the transferrin receptor [5] and LY, a small anionic hydrophilic membrane impermeable fluorescent molecule, is internalized via

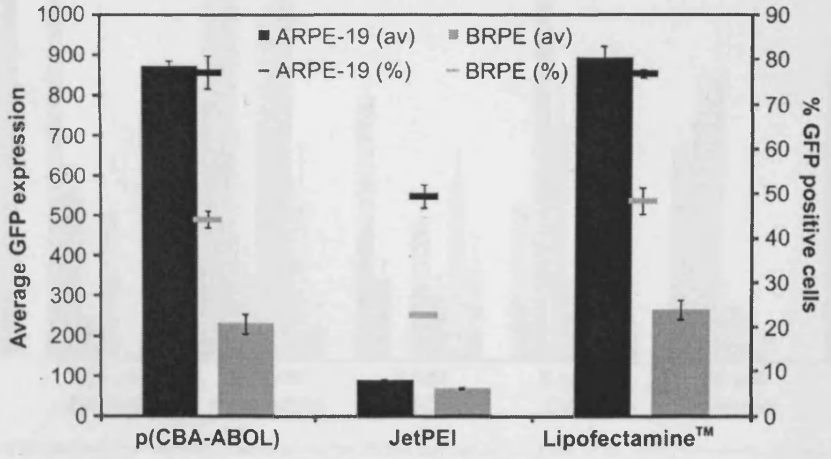

Fig. 1. Comparison of transfection efficacies between different gene carriers p(CBA-ABOL), JetPEI and Lipofectamin2000. Cells were transfected with a GFP reporter plasmid using three different carriers and subsequently washed with cell culture medium. Transfection levels were determined 24 h after transfection using flow cytometry showing the percentage of fluorescent cells (dots) and the average transgene GFP expression (bars). Transfection was assessed on both a continuous cell line (ARPE-19, in black) and primary bovine RPE cells (BRPE, in gray). Experiments were performed in triplicate and error bars represent standard deviations.

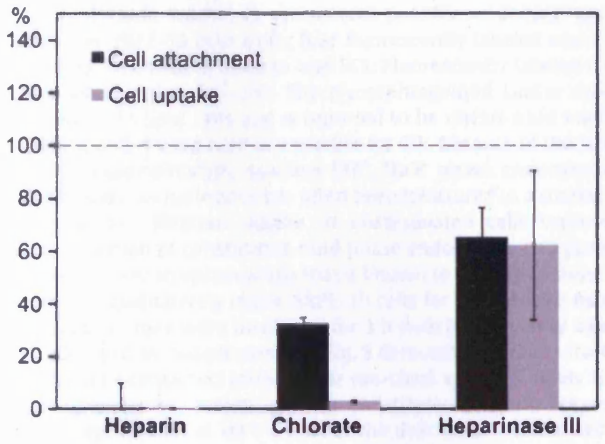

Fig. 2. Cellular attachment and uptake of p(CBA-ABOL)/DNA gene complexes is mediated by cell surface heparan sulfate proteoglycans. Cell attachment (black bars) and internalization (gray bars) of p(CBA-ABOL) polyplexes in ARPE-19 cells are shown. The remaining cell attachment or uptake is expressed as a relative percentage, normalized to untreated cells (represented by the dashed horizontal line). Experiments were performed in triplicate and error bars represent standard deviations.

fluid phase endocytosis [36]. We observed no inhibitory effect of sodium chlorate treatment on fluid phase endocytosis, nor on CDE (data not shown), demonstrating the specificity of this treatment. In contrast, desulfation of HSPGs reduces cell attachment of p(CBA-ABOL) polyplexes by more than 60% (Fig. 2) and consequently, cell uptake of the polyplexes is almost completely inhibited. Overall this indicates the necessity of sulfate groups on the cell surface for polyplex attachment and subsequent internalization.

Finally, as a third complementary strategy, the effect of heparan sulfate hydrolysis on polyplex attachment and endocytosis was examined through treatment with Heparinase III, a heparan sulfate lyase that exclusively cleaves heparan sulfate [37]. ARPE-19 cells were pretreated with this enzyme for 2 h in OptiMEM. p(CBA-ABOL) polyplexes were then added for 2 h in OptiMEM containing fresh Heparinase III. As shown in Fig. 2, this treatment significantly reduced polyplex attachment and to a comparable extent, polyplex uptake. However, in comparison to sodium chlorate treatment, the effect on polyplex internalization is less pronounced. The effect of Heparinase III treatment, however, confirms the particular involvement of heparan sulfate moieties of HSPGs for cell attachment of a significant fraction of p(CBA-ABOL) polyplexes in serum free conditions. Overall, we find that the electrostatic interaction between the cationic p(CBA-ABOL) polyplexes and the negatively charged HSPGs on the cell surface promotes efficient polyplex attachment and uptake.

3.3. *Unraveling the involvement of endocytic pathways: chemical inhibitors*

To unravel the involvement of known endocytic pathways in the internalization of p(CBA-ABOL) polyplexes, we inhibited endocytic processes using chemical inhibitors: chlorpromazine (Cpz), genistein, nocodazole, methyl-β-cyclodextrin (MβCD), cytochalasin D (CytoD), dynasore and rottlerin (Fig. 3). Drug induced cytotoxicity, the extent of inhibition and specificity of these endocytic inhibitors is cell-type-dependent [19] and we therefore first characterized the

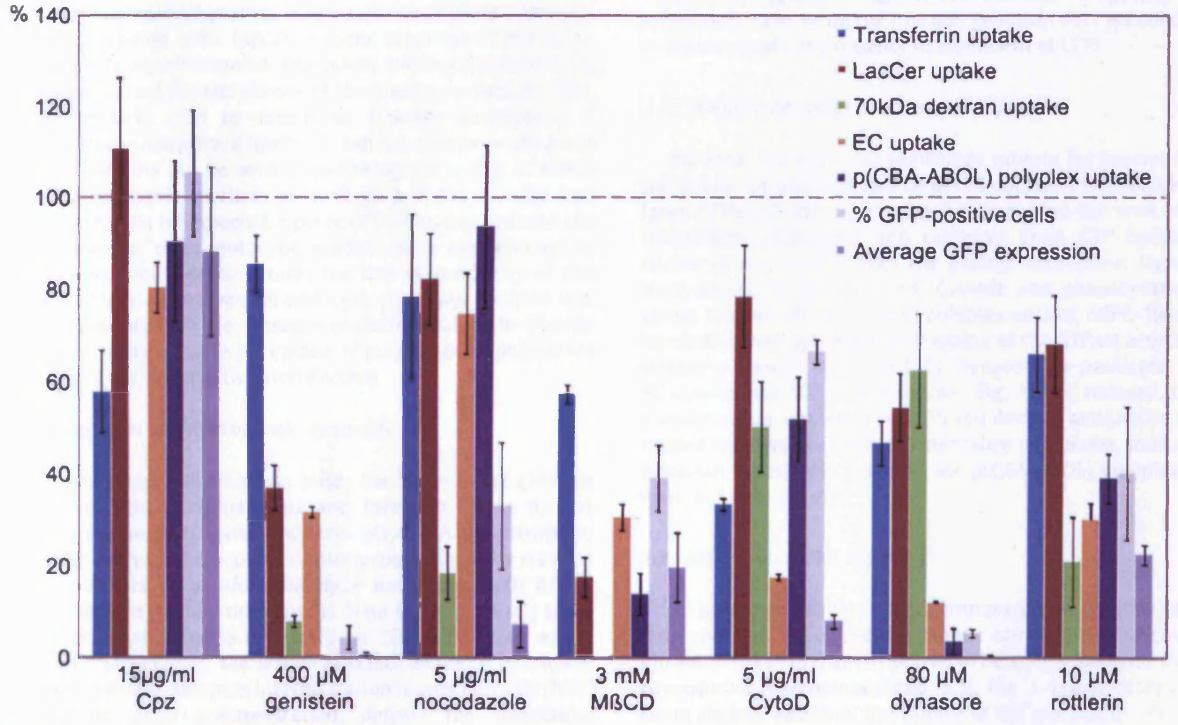

Fig. 3. Internalization of fluorescently labeled endocytic markers (transferrin, LacCer, 70 kDa dextran and ECs) and p(CBA-ABOL) polyplexes, and transfection efficiency following treatment with endocytic inhibitors in ARPE-19 cells. Measurements were performed by flow cytometry. The remaining cell uptake is expressed as a relative percentage, normalized to untreated cells (represented by the dashed horizontal line). Transfection of GFP reporter gene was quantified 24 h later as the average expression per cell and as the percentage of positively transfected cells, again both normalized to the fluorescence of untreated cells (dashed line). Experiments were performed in triplicate and error bars represent standard deviations. (Cpz: chlorpromazine; MβCD: methyl-β-cyclodextrin; CytoD: cytochalasin D).

effect of these inhibitors on several possible endocytic uptake routes in ARPE-19 cells using four fluorescently labeled endocytic markers: hTf, LacCer, dextran and ECs. Fluorescently labeled hTf is used as a marker for CDE. The glycosphingolipid LacCer resides preferably in lipid rafts and is reported to be internalized via Cav-ME [38] and is used here as a marker for CIE. Because of the lack of unique macropinocytic markers [39], fluid phase endocytosis of 70 kDa dextran molecules has often been measured as a marker for this process. Dextran uptake in unstimulated cells represents a combination of constitutive fluid phase endocytosis and possible constitutive macropinocytosis that is known to operate in some cell types. To qualitatively check ARPE-19 cells for constitutive macropinocytosis, they were incubated for 3 h with fluorescently labeled 70 kDa dextran. Supplementary. Fig. 5 demonstrates that a fraction of the cells contained intracellular μm-sized vacuoles, likely to be macropinosomes, resulting from constitutive macropinocytosis. This suggests that at least a part of the dextran is internalized via constitutive macropinocytosis. As a marker for phagocytosis, we used fluorescently labeled *E. coli* Bioparticles™ (ECs). The effects on the endocytic markers after inhibitor treatment in ARPE-19 cells is shown in Fig. 3 (Blue, red, green and orange bars), including the effect of the same inhibitors on polyplex uptake (dark purple bars). To correlate endocytosis route with gene delivery efficiency, we transfected cells with non-fluorescent polyplexes carrying the GFP reporter gene in the presence of endocytic inhibitors. Transfection efficiency is expressed both as percentage of fluorescent cells, and as average fluorescence level per cell (Fig. 3, two last light purple bars). Results from experiments with each type of inhibitor are discussed in turn below.

3.4. Depleting plasma membrane cholesterol

To assess the role of plasma membrane cholesterol, ARPE-19 cells were incubated with MβCD, a cyclic oligomer of glucopyranoside that inhibits cholesterol-dependent endocytic processes by reversibly extracting the steroid out of the plasma membrane [40]. MβCD is regularly used to determine whether endocytosis is dependent on the integrity of lipid rafts but has also been shown to inhibit CDE [40]. As can be seen from the results in Fig. 3, MβCD affected all endocytic markers as well as polyplex uptake and transfection. As can be expected, uptake of LacCer was reduced the most. However, all other endocytic markers were also affected by this treatment, which demonstrates the lack of specificity of this inhibitor for blocking subtypes of endocytic pathways. Despite this, the results indicate that the presence of cholesterol in the plasma membrane is indispensable for uptake of p(CBA-ABOL) polyplexes and their capacity for effective transfection.

3.5. Blocking actin and microtubule dynamics

CytoD is a fungal alkaloid that binds the barbed, fast growing plus ends of actin microfilaments and therefore blocks further polymerization and elongation of actin [41,42]. Actin disruption was visually confirmed on confocal microscopy images by staining the actin network in paraformaldehyde fixed cells with AF488 labeled phalloidin (results not shown). Data in Fig. 3 clearly show that actin polymerization is necessary for CDE, fluid phase endocytosis and phagocytosis; CIE is also affected, although to a lower extent. Interestingly, polyplex internalization is only partially (50%) dependent on actin polymerization, despite the substantial decrease of GFP expression. This suggests that actin polymerization is essential for successful intracellular processing of the internalized polyplexes.

Nocodazole induces depolymerization of the microtubules, which impairs the molecular motor-driven transport of vesicles on these tubular cytoskeletal structures [43]. Nocodazole treatment strongly inhibits the uptake of 70 kDa dextran but has only minor effects on the other endocytic probes including polyplexes (Fig. 3). This drug also had pronounced inhibitory effects on transfection efficiency. According to the proton sponge theory, endosomal acidification is necessary to enable polyplexes, composed of polymers with high buffer capacities around physiological pH, to escape from the endosomes into the cytoplasm and to cause successful gene transfer [44]. It is known that microtubule integrity is necessary for maturation of early/sorting endosomes to late endosomes with the accompanying drop in luminal pH [45,46]. These results suggest that nocodazole probably inhibits endosomal escape of the polyplexes by inhibiting the luminal acidification of the endosomes.

Overall, these results suggest that p(CBA-ABOL) polyplexes are internalized in ARPE-19 cells via an endocytic mechanism that relies on local actin polymerization but not on microtubule integrity.

3.6. Role of CDE

To investigate the involvement of CDE, we applied Cpz, a cationic amphiphilic drug which is believed to inhibit clathrin-coated pit formation by a reversible translocation of clathrin and its adapter proteins from the plasma membrane to intracellular vesicles [47]. As expected, Cpz treatment inhibits hTf uptake, an established CDE marker (See Fig. 3). In contrast, it does not inhibit LacCer uptake, nor polyplex uptake or transfection. This indicates that CDE does not play a significant role in polyplex uptake. This conclusion is corroborated by the genistein data (See Fig. 3). Genistein, a well-characterized inhibitor of tyrosine kinase mediated signal transduction [48], has only a slight effect on CDE, while clearly inhibiting fluid phase uptake, phagocytosis, CIE and completely blocking polyplex uptake. From the Cpz and genistein data we conclude that polyplex uptake is primarily independent of CDE.

3.7. Blocking dynamin function with dynasore

Because dynamin is a regulatory protein for several endocytic pathways, we assessed its role in cell uptake of the polyplexes. This large GTPase forms a helical polymer around the neck of a newly invaginated endosome and catalyzes upon GTP hydrolysis the fission of the vesicle from the plasma membrane. Dynamin has been shown to regulate CDE, Cav-ME and phagocytosis [49]. To assess the role of dynamin in polyplex uptake, ARPE-19 cells were incubated with dynasore, an inhibitor of the GTPase activity of both dynamin-1 and 2 isoforms [50]. Dynasore, as predicted, inhibited EC uptake and 50% of hTf uptake (Fig. 3) and reduced, though to a lower extent, uptake of both 70 kDa dextran and LacCer. Dynasore treated cells were unable to internalize polyplexes, indicating that dynamin function is essential for p(CBA-ABOL) polyplex endocytosis in ARPE-19 cells.

3.8. Inhibition of PKC signaling

To investigate the role of macropinocytosis, we treated the cells with rottlerin, a polycyclic aromatic compound inhibiting protein kinases C (PKC) [51] and reported to be a fairly selective inhibitor of constitutive macropinocytosis [52]. Fig. 3 demonstrates that rottlerin slightly inhibited the uptake of hTf and LacCer and exhibited a pronounced inhibition of polyplexes, ECs and fluid phase uptake of 70 kDa dextran molecules. Since rottlerin seems to affect both fluid phase endocytosis and phagocytosis, it does not provide further information on the possible specific involvement of macropinocytosis on polyplex internalization.

However, the response of the polyplexes and dextran to inhibitors like dynasore and nocodazole was very different. In particular, after nocodazole treatment, complete inhibition of 70 kDa dextran uptake was observed, while uptake of the complexes was similar to untreated cells (**Fig. 3**). In case of dynasore, polyplex uptake was completely inhibited, while 70 kDa dextran uptake was reduced by only 40%. This would suggest that fluid phase uptake and constitutive macropinocytosis is not correlating with p(CBA-ABOL) polyplex uptake in ARPE-19 cells. In contrast, the results in **Fig. 3** generally show a strong correlation between EC and polyplex endocytosis in response to these pharmacological inhibitors. This suggests phagocytosis as a potential uptake route for p(CBA-ABOL) polyplexes in ARPE-19 cells.

3.9. *Unraveling the involvement of endocytic pathways: RNAi*

To complement the chemical inhibitor studies, RNAi was implemented in this work to downregulate expression of key endocytic proteins thus inhibiting specific endocytic pathways. The targeted proteins were clathrin heavy chain (CHC), caveolin-1 (Cav1), flotillin-1 (Flot1), GTPase regulator associated with focal adhesion kinase (GRAF1), ADP ribosylation factor 6 (Arf6), dynamin-2 (DNM2) and serine/threonine-protein kinase (PAK1). A list of the corresponding siRNA sequences, used in this work, is given in **Supplementary. Table. 1.** Downregulation was assessed by Western blotting (**Fig. 5**). The same flow cytometry methods were used to evaluate the effects on endocytic uptake and transfection of the GFP reporter gene (**Fig. 4**).

3.10. *Role of heavy chain clathrin*

As expected, depleting the expression of clathrin heavy chain inhibited transferrin uptake by 80% (**Fig. 4**), however we were surprised to observe that the same depletion caused an induction in the uptake of all other endocytic markers, including polyplexes. In any case, this confirms that internalization of p(CBA-ABOL) polyplexes in ARPE-19 cells is independent of CDE. The depletion in expression of CHC was clearly confirmed by Western blotting (**Fig. 5**A).

3.11. *Role of DNM2 function*

To confirm the involvement of dynamin in polyplex uptake, we downregulated DNM2 expression with the help of RNAi **[53]** and Western blotting demonstrated at least a partial reduction in protein expression (**Fig. 5**B). In agreement with the dynasore data, DNM2 downregulation significantly inhibited hTf, EC and polyplex uptake (**Fig. 4**), although LacCer and 70 kda dextran uptake was not inhibited, despite the significant inhibitory effect of dynasore. Indeed, it was previously reported that selective knockdown of DNM2 may still permit CIE of cholera toxin subunit B (CtxB) and fluid phase endocytosis, possibly because DNM1 adopts the role of DNM2 for vesicle fission **[54]**. Finally, **Fig. 4** also shows that DNM2 depletion results in substantial reduction of transgene expression, indicating that the endocytic pathways that lead to successful transfection are dynamin dependent.

3.12. *Role of Cav1 and Flot1*

Combined, the experiments with chemical endocytic inhibitors suggested that CDE is not involved in polyplex uptake. However, the inhibitors did not allow us to distinguish between different subclasses of CIE pathways. To evaluate the specific involvement of Cav-ME and Flot-ME, two known subclasses of CIE, we used RNAi to downregulate the expression respectively of Cav1 and Flot1. Depletion of these two proteins was again confirmed by Western blotting (**Fig. 5**C). As shown in **Fig. 4**, Cav1 downregulation, as predicted, inhibited a fraction of LacCer uptake, but there was no

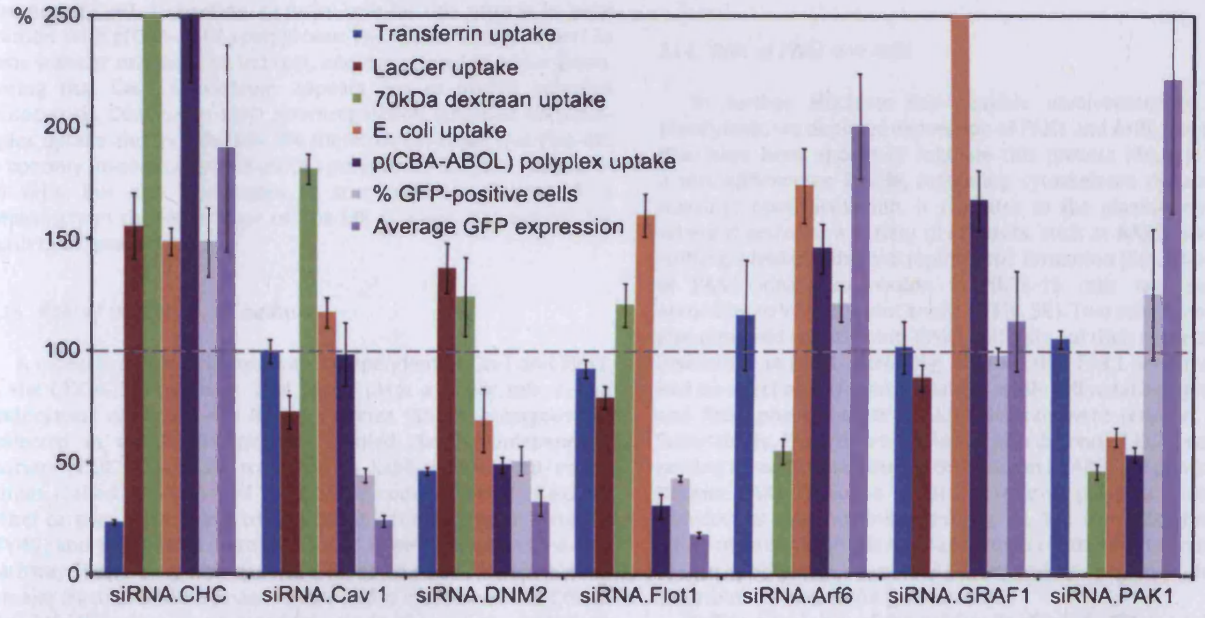

Fig. 4. Internalization of fluorescently labeled endocytic markers (transferrin, LacCer, HMW dextran and ECs), p(CBA-ABOL) polyplexes, and transfection efficiency after siRNA mediated depletion of endocytic proteins in ARPE-19 cells. Measurements were performed by flow cytometry. The remaining cell uptake is expressed as a relative percentage, normalized to cells, treated with NC siRNA (represented by the dashed horizontal line). Transfection of the GFP reporter gene was measured again 24 h later and was both quantified as the average expression per cell and as the percentage of positively transfected cells, again both normalized to the cell population, transfected with negative control siRNA. Experiments were performed in triplicate and error bars represent standard deviations. (CHC: clathrin heavy chain; Cav1: caveolin-1; Flot1: flotillin-1; GRAF1: GTPase Regulator Associated with Focal Adhesion Kinase; Arf6: ADP ribosylation factor 6; DNM2: dynamin-2; PAK1: Serine/threonine-protein kinase).

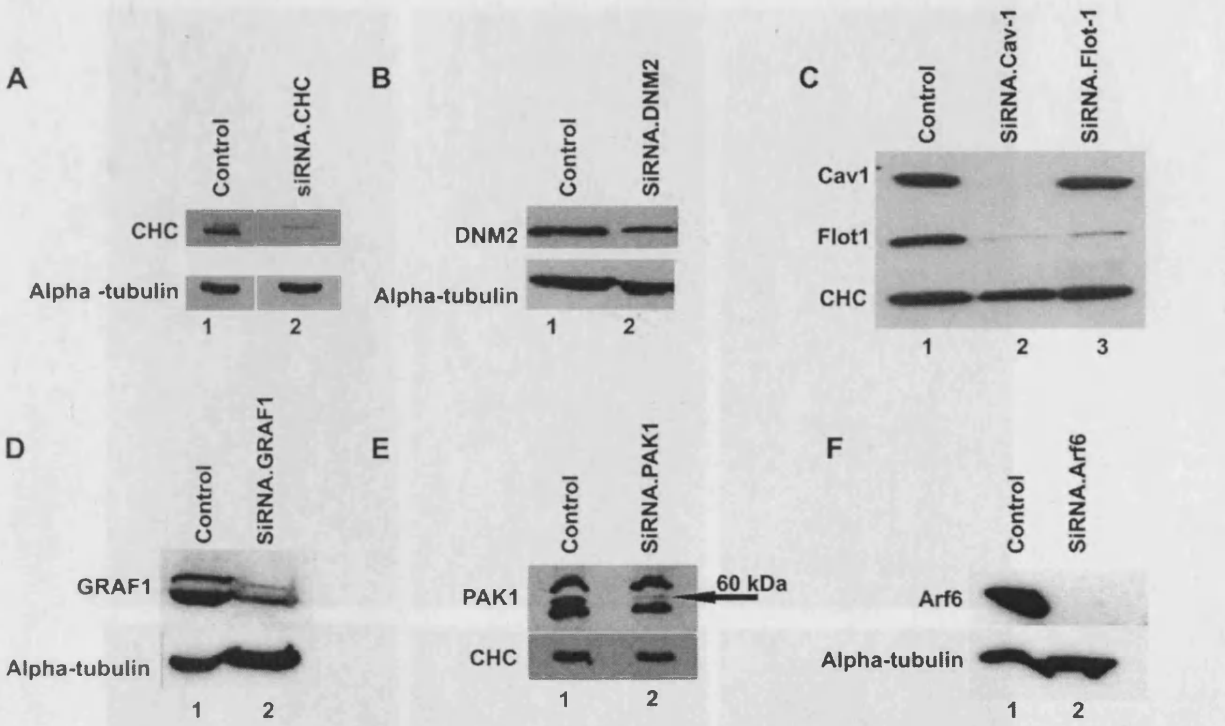

Fig. 5. Protein expression after siRNA downregulation, visualized by Western blotting. In all cases, the control cells were treated with negative control siRNA (Supplementary. Table. 1). For (A), (B), (D) and (F) the expression of α-Tubulin served as an internal control for equal protein loading, while CHC expression levels were used as a reference in (C) and (E). In (E), the PAK1 band of 60 kDa is marked with a black arrow. (CHC: clathrin heavy chain; Cav1: caveolin-1; Flot1: flotillin-1; GRAF1: GTPase regulator associated with focal adhesion kinase; Arf6: ADP ribosylation factor 6; DNM2: dynamin-2; PAK1: Serine/threonine-protein kinase).

effect on uptake of any of the other endocytic markers or polyplexes. Interestingly, transfection was clearly less successful in the absence of Cav1, suggesting a crucial role for this protein in gene transfer with p(CBA-ABOL) polyplexes. The observed role of Cav1 in gene transfer may here be indirect, and not related to endocytosis, noting that Cav1 knockdown appears not to inhibit polyplex endocytosis. Conversely, Flot1 downregulation inhibited both polyplex uptake and transfection. We therefore conclude that Flot-ME is not only involved in p(CBA-ABOL) polyplex endocytosis in ARPE-19 cells, but also contributes to successful transfection. This demonstrates the importance of Flot-ME as a portal to the cell for successful gene transfer.

3.13. Role of the CLIC/GEEC pathway

A recently defined CIE pathway, independent of Cav1 and Flot1, is the CLIC/GEEC pathway. This portal plays a major role in the endocytosis of certain GPI linked proteins [55]. The cargoes are collected in tubular invaginations, called clathrin-independent carriers (CLIC's), and are trafficked to Rab5-independent endosomes, called GPI-enriched endosomal compartments (GEEC's). Other cargoes like Cholera toxin subunit B (CtxB), Simian Virus 40 (SV40) and Shiga toxin were also found to be internalized via this pathway [53]. This pathway is also reported to be responsible for a major fraction of fluid phase uptake and is independent of DNM2 [56]. We therefore investigated its role in entry of the endocytic markers and polyplexes by depleting GRAF1, a protein shown to regulate this pathway [57]. Efficient GRAF1 depletion was confirmed by Western blotting (Fig. 5D). Downregulation of GRAF1 didn't decrease polyplex internalization (Fig. 4), suggesting a lack of involvement of the CLIC/GEEC pathway. Interestingly, we observed that GRAF1 knockdown stimulated both polyplex and phagocytosis uptake, but not transgene GFP expression.

3.14. Role of PAK1 and Arf6

To further elucidate the possible involvement of macropinocytosis, we depleted expression of PAK1 and Arf6, two proteins that have been shown to regulate this process [39,58]. PAK1 is a serine/threonine kinase, regulating cytoskeleton dynamics and motility; upon activation, it relocates to the plasma membrane where it activates a variety of effectors, such as BARS, needed for ruffling, blebbing and macropinosome formation [59]. Knockdown of PAK1 kinase expression in ARPE-19 cells was successful according to Western blot analysis (Fig. 5E). Two other bands were also observed with the anti-PAK1 antibody but their expression was insensitive to PAK1-siRNA. Fig. 4 shows that PAK1 downregulation had no effect on hTf internalization, while cell uptake of polyplexes and fluid phase marker 70 kDa dextran were reduced by 50%. Surprisingly, PAK1 downregulation also decreased EC uptake, suggesting an additional role for this protein in ARPE-19 phagocytosis. Despite PAK1 having a significant role in polyplex endocytosis, transfection was not inhibited (Fig. 4). We conclude that, while either macropinocytosis or phagocytosis contributes to endocytosis of our polyplexes, this PAK1- dependent pathway does not contribute to successful gene transfer.

Arf6 is a member of the Arf family of small GTPases, which are involved in the regulation of membrane structure and transport [60], and is known to be a positive modulator of MP [39]. Successful knockdown of this protein (Fig. 5F) led to a decrease in 70 kDa dextran uptake, while endocytosis of both ECs and p(CBA-ABOL) gene complexes was induced (Fig. 4). This suggests that constitutive

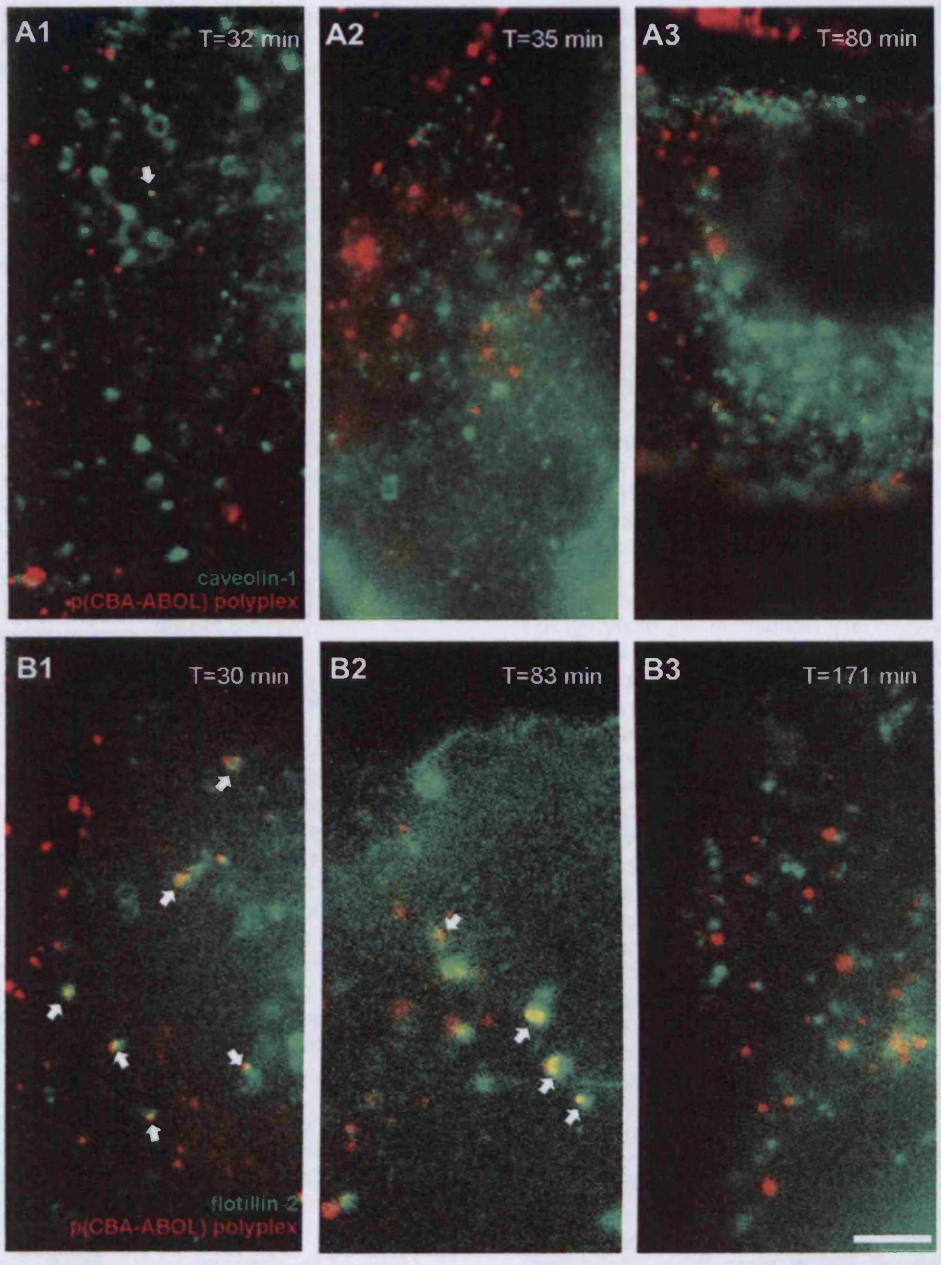

Fig. 6. Colocalization of p(CBA-ABOL) polyplexes with flotillin or caveolin containing vesicles in living ARPE-19 cells. Cells transfected with (A) Cav1-EGFP and (B) Flot2-EGFP were exposed to p(CBA-ABOL) Cy5-pDNA polyplexes for 15 min. After washing, the cells were transferred in a stage top incubator and imaged on a wide field fluorescence microscope in OptiMEM. Fluorescence images, selected from livecell time-lapse movies show colocalization of the polyplexes at early timepoints with Flot2 (B1 and 2), which disappears at later timepoints (B3). The white arrows show colocalizing signals. Very little colocalization is observed between the Cy5-labeled plasmids and Cav1, either at early (A1) or at later timepoints (A2 and 3). Scale bar is 5 μm.

macropinocytosis is not involved in the internalization of p(CBA-ABOL) polyplexes.

3.15. Live cell fluorescence colocalization microscopy

Aside from inhibiting endocytic pathways with chemical inhibitors and siRNA depletion, fluorescence microscopy was utilized to probe further the involvement of Cav-ME or Flot-ME in the initial uptake of p(CBA-ABOL) polyplexes. Cells were transfected with plasmids encoding EGFP-Flot2 or EGFP-Cav1 for visualization of flotillin or caveolin containing endosomes, respectively. It is believed that coassembly of both Flot1 and Flot2 is necessary for Flot-ME to occur [61]. Caveolin containing endosomes are typically termed cavicles and caveosomes [7]. GFP fusion proteins were clearly expressed after 24 h and they were then incubated with p(CBA-ABOL) polyplexes containing Cy5-labeled plasmids. After 15 min of incubation with the polyplexes, cells were washed with OptiMEM and observed as live cells on a stage top incubator by fluorescence microscopy. We clearly observed colocalization within 30 min between polyplexes and flotillin-2 (Fig. 6B1 and 2), which generally disappeared about 150 min after initial incubation with polyplexes (Fig. 6B3). In contrast, virtually no colocalization was

observed between polyplexes and caveolin-1 (Fig. 6A1-3). These observations provide further evidence that p(CBA-ABOL) polyplexes are internalized in flotillin-vesicles rather than caveosomes.

4. Discussion

The RPE is an attractive target for treating diseases such as AMD or retinitis pigmentosa with non-viral nucleic acid carriers following subretinal or intravitreal injection. However the efficiency of subcellular delivery of therapeutic nucleic acids into these cells remains low. The carrier defines the mechanisms that direct cell attachment, subsequent endocytosis and intracellular trafficking and therefore strongly determines transfection efficiency. A better understanding of these mechanisms will help to improve the design of efficient CBA based polymeric carriers since little information is currently available on cellular adhesion, intracellular uptake and intracellular processing of p(CBA-ABOL) polyplexes in RPE cells. Here, we studied cell attachment and endocytosis of polyplexes, composed of the novel bioreducible polymer p(CBA-ABOL) and plasmid DNA. We first focused on cell attachment and proceeded with characterizing the endocytic pathways that are involved in their subsequent uptake by using a combination of pharmacological inhibitors, RNAi knockdown and live cell fluorescence colocalization microscopy.

4.1. In vitro evaluation of p(CBA-ABOL) as a carrier for gene delivery in RPE cells

First, we compared the *in vitro* transfection potential of different carriers on both a continuous RPE cell line and primary bovine cells (BRPE). Overall, the data showed p(CBA-ABOL) to be a promising transfection agent in both cultured and primary cells, outperforming linear PEI and equaling commercial liposome based systems. JetPEI polyplexes transfected only 50% of the cells, which we believe is a consequence of significantly lower cell uptake (4–5 times) during the 2 h exposure time, when compared with the other carrier systems (See Supplementary. Fig. 6). In primary cells, transfection efficiency was lower for all carriers and this is probably due to general lower internalization rates, because we observed that only about half of the amount of p(CBA-ABOL) and Lipofectamin2000™ complexes are internalized in BRPEs cells compared to the RPE cell line (ARPE-19) (See Supplementary. Fig. 6). This is possibly due to their lower metabolic, and therefore lower endocytic activity. In line with this, we observed significant lower cellular growth rates for the primary RPE cells.

4.2. Role of anionic cell surface proteoglycans in p(CBA-ABOL) polyplex attachment and internalization

We identified that the interaction between cationic polyplexes and cell surface HSPGs is essential for efficient internalization. This is in agreement with reports for other types of cationic complexes and can be easily explained by the electrostatic interaction between the positively charged gene carrier and negatively charged heparan sulfate chains [14,34,62,63]. In order to ascertain the rate of polyplex internalization and identify optimal incubation times for cells with the polyplexes, we also evaluated their uptake kinetics in ARPE-19 cells (Supplementary. Fig. 3). Similar to what was found for other gene delivery vehicles, viral and non-viral [1,15], we observed that p(CBA-ABOL) polyplexes are rapidly taken up in ARPE-19 cells and that this internalization is saturated after 2 h. The internalization kinetics follow a sigmoid-like function which is typical for an endocytic uptake pattern because of saturation of the endocytic machinery. These results suggest that general cellular uptake as such is not the bottle neck for efficient transfection, at least in the absence of anionic biopolymers.

4.3. p(CBA-ABOL) polyplex uptake via a PAK1 dependent phagocytosis-like mechanism

As a first strategy to identify the endocytic pathway(s) utilized by p(CBA-ABOL) complexes to enter ARPE-19 cells, we made use of chemical endocytic inhibitors. We have recently shown that chemical endocytic inhibitors should be used with care as their effect is highly cell-type-dependent and not as specific as they are often reported to be [19]. Therefore, alongside our polyplexes, we evaluated the effect of these inhibitors on several types of endocytic markers. These results suggested that polyplex uptake does not involve CDE but is strongly dependent on cholesterol, tyrosine kinase activity and dynamin as well as on actin and PKC activity. Several reports link HSPG mediated endocytosis to macropinocytosis [32,64,65], also in cellular uptake of cationic gene delivery vehicles [15,65–67]. However, Kopatz et al. discovered close similarities between HSPG-dependent phagocytosis in epithelial cells and endocytosis of PEI/DNA polyplexes [62]. Moreover, it has previously been suggested that viruses like HSV-1 can infect both professional and non-professional phagocytes via a phagocytosis-like mechanism after heparan sulfate binding [68]. Despite the difficulties of distinguishing between the involvement of macropinocytosis and phagocytosis in nanomedicine uptake, since there are no chemical inhibitors that are specific for either of them, we were able to come to some conclusions on this matter based on several observations. First, using nocodazole and dynasore, we found marked opposite inhibitory effects for uptake of polyplexes and 70 kDa dextran, the latter often being used as a marker for constitutive macropinocytosis. Interestingly, we found a strong correlation between cellular internalization of the polyplexes and *E. coli* particles, the latter being an established marker for phagocytosis. Second, while actin, tyrosine kinases and PKC, all appear to be required for polyplex uptake in ARPE-19 cells and are known criteria for macropinocytosis [39], these proteins also regulate phagocytosis (Fig. 3) [39] and therefore do not exclude the involvement of a phagocytosis-like mechanism. Third, dynamin is often known to play a redundant role in macropinocytosis [69], though its function is essential for phagocytic cup closure [39]. Using dynasore to block all dynamin isoforms, this study showed a noticeable dependence on dynamin function during polyplex endocytosis, which is again in favor of the involvement of a phagocytosis-like mechanism.

As a second strategy to identify the involvement of endocytic pathway(s) during polyplex endocytosis, we depleted key endocytic proteins with the help of RNAi. By depleting DNM2, we could confirm the involvement of this protein for polyplex uptake. Furthermore, when depleting PAK1 and Arf6 which are both reported to regulate macropinocytosis [39], we observed that Arf6 did not have any inhibitory effect on polyplex uptake, providing further evidence that macropinocytosis is probably not involved in p(CBA-ABOL) polyplex endocytosis. The involvement of PAK1 during polyplex endocytosis could then be attributed to its involvement in phagocytosis in ARPE-19 cells. Indeed, it has been previously reported that PAK1 plays a role in actin rearrangements during phagocytosis [70,71]. The effect of PAK1 knockdown on polyplex uptake could therefore be assigned to the inhibition of phagocytic uptake of the polyplexes.

Finally, it should be noted that our polyplexes have the tendency in physiologic media of high ionic strength to form spherical aggregates with sizes up to 5 μm (Supplementary. Fig. 7). Therefore, the cells were exposed to polyplexes with a wide distribution of sizes. Since the RPE is *in vivo* the most active phagocytic tissue in humans [21], it is unsurprising that these large aggregates were

observed to be internalized in ARPE-19 cells. Taken together, despite the inability to specifically inhibit phagocytosis, our observations suggest that a PAK1 dependent, phagocytosis-like mechanism is involved in the cellular internalization of p(CBA-ABOL) polyplexes in ARPE-19 cells.

4.4. p(CBA-ABOL) polyplex uptake via flotillin-dependent endocytosis

Despite excluding a role for CDE in polyplex uptake, the chemical inhibitors could not differentiate between the various CIE routes. CIE like Cav-ME is often reported to be involved in internalization of non-viral gene delivery vehicles [13]. To discriminate between different CIE pathways, we employed siRNA depletion studies and found no involvement of Cav-ME, the CLIC/GEEC pathway, nor Arf6-dependent endocytosis for polyplex uptake. However, p(CBA-ABOL) polyplex internalization was found to be dependent on DNM2, Flot1 and PAK1. As discussed above, the involvement of PAK1 can be related to phagocytic uptake. Interestingly, however, the strong dependency on Flot1 suggests Flot-ME as an important alternative entry route. To verify this, we investigated the colocalization of flotillin-2 positive vesicles and the polyplexes using livecell dual color fluorescence microscopy. Polyplexes resided within flotillin-2 positive vesicles within 30 min after transfection, but there was no evidence of their association with caveolin and thus caveolae. This is in agreement with a recent study on the uptake of PEI polyplexes and Lipofectamine™ lipoplexes in HeLa cells [14], where a link was found between the attachment of gene complexes to cell surface HSPGs and subsequent Flot-ME of HSPG bound gene complexes. Knowledge of HSPG endocytosis is still quite limited, despite its essential role in the internalization of some viruses, bacteria and cationic peptides [31]. After interacting with heparan sulfate binding ligands, HSPGs are reported to cluster in cholesterol-dependent micro-environments that are internalized in endocytic vesicles deficient of caveolin-1 and clathrin, but positive for flotillin-1. This process requires an intact actin cytoskeleton tyrosine kinase activity, PKC activity, dynamin and activated Rac [72]. This is in strong agreement with our findings here. Whether DNM2 is required for Flot-ME seems to depend on the nature of the internalized cargo. For example, DNM2 is not required for HSPG mediated internalization of eosinophil cationic protein in Beas-2B cells [64], but was shown to be required for HSPG mediated uptake of PEI polyplexes in HeLa cells [14]. This is in good agreement with our findings for p(CBA-ABOL) polyplexes in RPE cells. We conclude that, apart from phagocytosis, the p(CBA-ABOL) polyplexes enter ARPE-19 cells through Flot-ME.

It is accepted that nanoparticle size can have a substantial influence on endocytic uptake of nanomedicines [73], which is attractive in the sense that it would offer possibilities to target for preferred endocytic pathways simply by engineering the size of the nanomedicines. In this study we have found that the p(CBA-ABOL) polyplexes aggregate when suspended in OptiMEM. This could be easily demonstrated using fluorescence single particle tracking (see Supplementary. Fig. 7) [74]. In an attempt to study the influence of size on uptake, we have performed extra experiments in which the polyplexes were first incubated for 30 min in OptiMEM before adding them to the cells. This will increase the extent of aggregation and could give some preliminary insight if the identified endocytosis pathways depend on the size of the complexes. As summarized in Supplementary. Fig. 8, while the polyplex uptake and transfection was increased when pre-incubated in OptiMEM, we could not find a shift in endocytosis pathways, at least as far as the PAK1 and flotillin-1-dependent or Flot-1-dependent routes are concerned. Although this is not a stringent proof, it is a first indication that the results published here, perhaps surprisingly, are not size dependent.

4.5. Correlation between endocytosis and transgene expression

Having established that p(CBA-ABOL) polyplexes are internalized in ARPE-19 cells via a phagocytosis-like mechanism and Flot-ME, it remained to be determined whether they are equally involved in mediating transfection. It is important to evaluate whether certain endocytic pathways preferentially lead to cell transfection, as it would allow one to consider a strategy to target the polyplexes towards the most successful endocytic pathway through ligand coupling. Using siRNA depletion of flotillin-1 we could clearly show that Flot-ME is an important route for transfection. In contrast, despite the significant role of PAK1 in polyplex uptake, PAK1 knockdown did not decrease GFP expression. This suggests that the phagocytosis-like internalization of polyplexes is not as effective for transfection and this could be due to the instant delivery of the polyplexes through phagosomes to degradative lysosomes.

In addition, we observed an intriguingly strong effect of caveolin-1 depletion on reporter gene expression, despite the fact that polyplex uptake was relatively unaffected. Since this protein was not shown to play a major role in early intracellular trafficking of p(CBA-ABOL) polyplexes (Fig. 6), this suggests an indirect effect of Cav1 knockdown. Indeed, Fig. 5C clearly shows that knockdown of caveolin-1 resulted in a comparable downregulation of flotillin-1 expression. Interestingly, a similar though opposite effect has been reported in HeLa cells [75] and in intestinal epithelial cells [76]. To explain the observed effects on uptake and transfection, we propose the following hypothesis. Downregulating caveolin-1 results in a decrease of Flot-ME and thereby decreases polyplex uptake. At the same time caveolin-1 knockdown causes stimulation of phagocytosis (Fig. 4), resulting in a net unaltered uptake of polyplexes. However, because the induced phagocytosis-like internalization pathway of the polyplexes does not contribute to transfection, its overall efficiency drops.

4.6. Inhibiting endocytic pathways: chemical versus molecular inhibition

Chemical inhibitors are frequently used to study endocytosis and results generated from studies using these agents are often insightful. However, without adequate controls their effects are difficult to interpret and could give rise to erroneous conclusions. The experiments with genistein and resulting data highlight this issue. Genistein is frequently used to study Cav-ME functioning as a tyrosine kinase inhibitor that impairs actin recruitment and DNM2 recruitment to the site of endocytosis [48]; both are indispensable for Cav-ME. However, genistein treatment might also affect other endocytosis routes as we observed here and in fact our studies showed that CDE was the only endocytic pathway tested that was insensitive to this drug. Phagocytosis has been also shown to be sensitive for genistein [77,78] and Flot-ME is reported to be tyrosine kinase dependent [79]. Therefore, if genistein inhibits uptake of gene complexes, one cannot necessarily draw the conclusion that they are taken up by Cav-ME. Indeed, while we found that the uptake of p(CBA-ABOL) complexes is inhibited by genistein, RNAi depletion revealed that it is not Cav-ME but rather a combination of phagocytosis and Flot-ME that regulate polyplex uptake. Similar issues and difficulties in interpretation were encountered with rottlerin, a PKC inhibitor reported to inhibit macropinocytosis [52]. Macropinocytosis and phagocytosis have been reported to be PKC dependent [52], thus questioning the specificity of this drug. Indeed, our own results showed rottlerin to inhibit uptake of 70 kDa dextran, but it also inhibited 40% of EC uptake and 30% of hTf and LacCer uptake (Fig. 3).

It is clear that chemical inhibitors by itself are generally not sufficient to fully elucidate endocytosis of gene complexes or

nanoparticles in general. As demonstrated in this work, RNAi downregulation of specific proteins can provide further complementary data. It is however, important to note that not all cells will be evenly affected by siRNA and thus the cell population may be heterogeneous with respect to their level of expression of the target protein. To analyze the cells which were successfully depleted, cotransfection experiments with reporter gene forming a selection marker for knockdown cells are often employed [14]. Alternatively, to increase the probability of downregulating a majority of cells, one can repeatedly transfect the cells with siRNA [14,80]. It is the latter strategy that was applied in this work. Furthermore, siRNA mediated knockdown exhibits generally high specificity. However, in some cases protein downregulation can affect, directly or indirectly, expression of other proteins. These effects were also observed in our studies, where the siRNAs against caveolin-1 seemed to knockdown flotillin-1 expression (Fig. 5C).

5. Conclusion

In this work we performed a detailed study on the attachment and internalization mechanisms of p(CBA-ABOL) gene complexes in a *in vitro* model of the retinal pigment epithelium. To elucidate endocytic mechanisms, we encourage the combination of different methodological approaches, like chemical and RNAi based inhibition, which can be further complemented with dual color fluorescence colocalization microscopy. Here, we show that the polyplexes are internalized via two endocytic portals to the cell, after association with cell surface HSPGs. These portals are flotillin mediated endocytosis and a PAK1 dependent, phagocytosis-like mechanism. Interestingly we found that of both internalization routes, only Flot-ME leads to successful transfection. An elaborate comprehension of both the characteristics of the vectors as well as the mechanisms by which they interact with the targeted cells is required to eventually help us design safe and efficient non-viral gene vectors to transfect the RPE and, by extension, any other type of target cells. This knowledge may help us (1) to evaluate the effects of chemical modifications of the carrier polymer on cell attachment and endocytosis, (2) to identify new specific cell surface targets to improve cell attachment and (3) to aim for specific endocytic pathways that lead to successful transfection.

Acknowledgments

D. Vercauteren is a doctoral fellow of the Institute for the Promotion of Innovation through Science and Technology in Flanders (IWT), Belgium. We gratefully acknowledge the European Commission for funding through the Integrated 6th Framework Programme MediTrans. Monerah al Soraj is supported by a Kuwaity Government sponsored PhD studentship awarded to Cardiff University.

Appendix. Supplementary material

Supplementary data related to this article can be found online at doi:10.1016/j.biomaterials.2010.12.045.

References

[1] Varga CM, Tedford NC, Thomas M, Klibanov AM, Griffith LG, Lauffenburger DA. Quantitative comparison of polyethylenimine formulations and adenoviral vectors in terms of intracellular gene delivery processes. Gene Ther 2005;12:1023–32.
[2] Doherty GJ, McMahon HT. Mechanisms of endocytosis. Annu Rev Biochem 2009;78:31.1–31.46.
[3] Jones AT. Macropinocytosis: searching for an endocytic identity and role in the uptake of cell penetrating peptides. J Cell Mol Med 2007;11:670–84.
[4] Kerr MC, Teasdale RD. Defining macropinocytosis and others. Traffic 2009;10:364–71.
[5] Maxfield FR, Mcgraw TE. Endocytic recycling. Nat Rev Mol Cell Biol 2004;5:121–32.
[6] Mayor S, Pagano RE. Pathways of clathrin-independent endocytosis. Nat Rev Mol Cell Biol 2007;8:603–12.
[7] Pelkmans L, Helenius A. Endocytosis via caveolae. Traffic 2002;3:311–20.
[8] Glebov OO, Bright NA, Nichols BJ. Flotillin-1 defines a clathrin-independent endocytic pathway in mammalian cells. Nat Cell Biol 2006;8:46-U16.
[9] Doherty GJ, Lundmark R. GRAF1-dependent endocytosis. Biochem Soc Trans 2009;37:1061–5.
[10] Douglas KL. Toward development of artificial viruses for gene therapy: a comparative evaluation of viral and non-viral transfection. Biotechnol Prog 2008;24:871–83.
[11] von Gersdorff K, Sanders NN, Vandenbroucke R, De Smedt SC, Wagner E, Ogris M. The internalization route resulting in successful gene expression depends on polyethylenimine both cell line and polyplex type. Mol Ther 2006;14:745–53.
[12] Rejman J, Bragonzi A, Conese M. Role of clathrin- and caveolae-mediated endocytosis in gene transfer mediated by lipo- and polyplexes. Mol Ther 2005;12:468–74.
[13] Midoux P, Breuzard G, Gomez JP, Pichon C. Polymer-based gene delivery: a current review on the uptake and intracellular trafficking of polyplexes. Curr Gene Ther 2008;8:335–52.
[14] Payne CK, Jones SA, Chen C, Zhuang XW. Internalization and trafficking of cell surface proteoglycans and proteoglycan-binding ligands. Traffic 2007; 8:389–401.
[15] Goncalves C, Mennesson E, Fuchs R, Gorvel JP, Midoux P, Pichon C. Macropinocytosis of polyplexes and recycling of plasmid via the clathrin-dependent pathway impair the transfection efficiency of human hepatocarcinoma cells. Mol Ther 2004;10:373–85.
[16] McLendon PM, Fichter KM, Reineke TM. Poly(glycoamidoamine) vehicles promote pDNA uptake through multiple routes and efficient gene expression via caveolae-mediated endocytosis. Mol Pharm; 2010.
[17] Gabrielson NP, Pack DW. Efficient polyethylenimine-mediated gene delivery proceeds via a caveolar pathway in HeLa cells. J Control Release 2009; 136:54–61.
[18] Diaz-Moscoso, Vercauteren D, Rejman J, Benito JM, Ortiz Mellet C, De Smedt SC, et al. Insights in cellular uptake mechanisms of pDNA-polycationic amphiphilic cyclodextrin nanoparticles (CDplexes). J Control Release 2010;143:318–25.
[19] Vercauteren D, Vandenbroucke RE, Jones AT, Rejman J, Demeester J, De Smedt SC, et al. The use of inhibitors to study endocytic pathways of gene carriers: optimization and pitfalls. Mol Ther 2010;18:561–9.
[20] Ivanov Andrei I. Pharmacological inhibition of endocytic pathways: is it specific enough to be useful? Methods Mol Biol 2008;440:15–33.
[21] Strauss O. The retinal pigment epithelium in visual function. Physiol Rev 2005;85:845–81.
[22] Murata T, Cui J, Taba KE, Oh JY, Spee C, Hinton DR, et al. The possibility of gene therapy for the treatment of choroidal neovascularization. Ophthalmology 2000;107:1364–73.
[23] Naik R, Mukhopadhyay A, Ganguli M. Gene delivery to the retina: focus on non-viral approaches. Drug Discov Today 2009;14:306–15.
[24] Lin C, Zhong ZY, Lok MC, Jiang XL, Hennink WE, Feijen J, et al. Novel bioreducible poly(amido amine)s for highly efficient gene delivery. Bioconjug Chem 2007;18:138–45.
[25] Jere D, Arote R, Jiang HL, Kim YK, Cho MH, Cho CS. Bioreducible polymers for efficient gene and siRNA delivery. Biomed Mater 2009;4.
[26] Christensen LV, Chang CW, Kim WJ, Kim SW, Zhong ZY, Lin C, et al. Reducible poly(amido ethylenimine)s designed for triggered intracellular gene delivery. Bioconjug Chem 2006;17:1233–40.
[27] Jeong JH, Kim SH, Christensen LV, Feijen J, Kim SW. Reducible poly(amido ethylenimine)-based gene delivery system for improved nucleus trafficking of plasmid DNA. Bioconjug Chem 2010;21:296–301.
[28] Wang R, Zhou L, Zhou Y, Li G, Zhu X, Gu H, et al. Synthesis and gene delivery of poly(amido amine)s with different branched architecture. Biomacromolecules 2010;11:489–95.
[29] Lin C, Engbersen JFJ. The role of the disulfide group in disulfide-based polymeric gene carriers. Expert Opin Drug Deliv 2009;6:421–39.
[30] Gandhi NS, Mancera RL. The structure of glycosaminoglycans and their interactions with proteins. Chem Biol Drug Des 2008;72:455–82.
[31] Belting M. Heparan sulfate proteoglycan as a plasma membrane carrier. Trends Biochem Sci 2003;28:145–51.
[32] Nakase I, Tadokoro A, Kawabata N, Takeuchi T, Katoh H, Hiramoto K, et al. Interaction of arginine-rich peptides with membrane-associated proteoglycans is crucial for induction of actin organization and macropinocytosis. Biochemistry 2007;46:492–501.
[33] Vives RR, Lortat-Jacob H, Fender P. Heparan sulphate proteoglyeans and viral vectors: ally or foe? Curr Gene Ther 2006;6:35–44.
[34] Mislick KA, Baldeschwieler JD. Evidence for the role of proteoglycans in cation-mediated gene transfer. Proc Natl Acad Sci U S A 1996;93: 12349–54.
[35] Mounkes LC, Zhong W, Cipres-Palacin G, Heath TD, Debs RJ. Proteoglycans mediate cationic Liposome-DNA complex-based gene delivery in vitro and in vivo. J Biol Chem 1998;273:26164–70.

[36] Page E, Goings GE, Upshaw-Earley J, Hanck DA. Endocytosis and uptake of lucifer yellow by cultured atrial myocytes and isolated intact atria from adult rats. Regulation and subcellular-localization. Circ Res 1994;75:335–46.
[37] Ernst S, Langer R, Cooney CL, Sasisekharan R. Enzymatic degradation of glycosaminoglycans. Crit Rev Biochem Mol Biol 1995;30:387–444.
[38] Marks DL, Singh RD, Choudhury A, Wheatley CL, Pagano RE. Use of fluorescent sphingolipid analogs to study lipid transport along thepathway endocytic. Methods 2005;36:186–95.
[39] Mercer J, Helenius A. Virus entry by macropinocytosis. Nat Cell Biol 2009; 11:510–20.
[40] Rodal SK, Skretting G, Garred O, Vilhardt F, van Deurs B, Sandvig K. Extraction of cholesterol with methyl-beta-cyclodextrin perturbs formation of clathrin-coated endocytic vesicles. Mol Biol Cell 1999;10:961–74.
[41] Cooper JA. Effects of cytochalasin and phalloidin on actin. J Cell Biol 1987;105:1473–8.
[42] Sampath P, Pollard TD. Effects of cytochalasin, phalloidin, and pH on the elongation of actin-filaments. Biochemistry 1991;30:1973–80.
[43] Peterson JR, Mitchison TJ. Small molecules, big impact: a history of chemical inhibitors and the cytoskeleton. Chem Biol 2002;9:1275–85.
[44] Akinc A, Thomas M, Klibanov AM, Langer R. Exploring polyethylenimine-mediated DNA transfection and the proton sponge hypothesis. J Gene Med 2005;7:657–63.
[45] Bayer N, Schober D, Prchla E, Murphy RF, Blaas D, Fuchs R. Effect of bafilomycin A1 and nocodazole on endocytic transport in HeLa Cells: implications for viral uncoating and infection. J Virol 1998;72:9645–55.
[46] Baravalle G, Schober D, Huber M, Bayer N, Murphy RF, Fuchs R. Transferrin recycling and dextran transport to lysosomes is differentially affected by bafilomycin, nocodazole, and low temperature. Cell Tissue Res 2005; 320:99–113.
[47] Wang LH, Rothberg KG, Anderson RG. Mis-assembly of clathrin lattices on endosomes reveals a regulatory switch for coated pit formation. J Cell Biol 1993;123:1107–17.
[48] Akiyama T, Ishida J, Nakagawa S, Ogawara H, Watanabe S, Itoh N, et al. Genistein, a specific inhibitor of tyrosine-specific protein-kinases. J Biol Chem 1987;262:5592–5.
[49] Praefcke GJK, McMahon HT. The dynamin superfamily: universal membrane tubulation and fission molecules? Nat Rev Mol Cell Biol 2004;5:133–47.
[50] Macia E, Ehrlich M, Massol R, Boucrot E, Brunner C, Kirchhausen T. Dynasore, a cell-permeable inhibitor of dynamin. Dev Cell 2006;10:839–50.
[51] Gschwendt M, Muller HJ, Kielbassa K, Zang R, Kittstein W, Rincke G, et al. Rottlerin, a novel protein kinase inhibitor. Biochem Biophys Res Commun 1994;199:93–8.
[52] Sarkar K, Kruhlak MJ, Erlandsen SL, Shaw S. Selective inhibition by rottlerin of macropinocytosis in monocyte-derived dendritic cells. Immunology 2005;116:513–24.
[53] Romer W, Berland L, Chambon V, Gaus K, Windschiegl B, Tenza D, et al. Shiga toxin induces tubular membrane invaginations for its uptake into cells. Nature 2007;450:670–5.
[54] Liu YW, Surka MC, Schroeter T, Lukiyanchuk V, Schmid SL. Isoform and splice-variant specific functions of dynamin-2 revealed by analysis of conditional knock-out cells. Mol Biol Cell 2008;19:5347–59.
[55] Lakhan SE, Sabharanjak S, De A. Endocytosis of glycosylphosphatidylinositol-anchored proteins. J Biomed Sci 2009;16.
[56] Gong Q, Huntsman C, Ma D. Clathrin-independent internalization and recycling. J Cell Mol Med 2008;12:126–44.
[57] Lundmark R, Doherty GJ, Howes MT, Cortese K, Vallis Y, Parton RG, et al. The GTPase-activating protein GRAF1 regulates the CLIC/GEEC endocytic pathway. Curr Biol 2008;18:1802–8.
[58] Dharmawardhane S, Schurmann A, Sells MA, Chernoff J, Schmid SL, Bokoch GM. Regulation of macropinocytosis by p21-activated kinase-1. Mol Biol Cell 2000;11:3341–52.
[59] Liberali P, Kakkonen E, Turacchio G, Valente C, Spaar A, Perinetti G, et al. The closure of Pak1-dependent macropinosomes requires the phosphorylation of CtBP1/BARS. EMBO J 2008;27:970–81.
[60] Donaldson JG. Arfs, phosphoinositides and membrane traffic. Biochem Soc Trans 2005;33:1276–8.
[61] Frick M, Bright NA, Riento K, Bray A, Merrified C, Nichols BJ. Coassembly of flotillins induces formation of membrane microdomains, membrane curvature, and vesicle budding. Curr Biol 2007;17:1151–6.
[62] Kopatz I, Remy JS, Behr JP. A model for non-viral gene delivery: through syndecan adhesion molecules and powered by actin. J Gene Med 2004;6:769–76.
[63] Paris S, Burlacu A, Durocher Y. Opposing roles of syndecan-1 and syndecan-2 in polyethylenimine-mediated gene delivery. J Biol Chem; 2008:7697–704.
[64] Fan TC, Chang HT, Chen IW, Wang HY, Chang MDT. A heparan sulfate-facilitated and raft-dependent macropinocytosis of eosinophil cationic protein. Traffic 2007;8:1778–95.
[65] Wittrup A, Sandgren S, Lilja J, Bratt C, Gustavsson N, Mörgelin M, et al. Identification of proteins released by mammalian cells that mediate DNA internalization through proteoglycan-dependent macropinocytosis. J Biol Chem 2007;282:27897–904.
[66] Grosse S, Aron Y, Thevenot G, Francois D, Monsigny M, Fajac I. Potocytosis and cellular exit of complexes as cellular pathways for gene delivery by polycations. J Gene Med 2005;7:1275–86.
[67] Khalil IA, Kogure K, Futaki S, Harashima H. High density of octaarginine stimulates macropinocytosis leading to efficient intracellular trafficking for gene expression. J Biol Chem 2006;281:3544–51.
[68] Clement C, Tiwari V, Scanlan PM, Valyi-Nagy T, Yue BYJT, Shukla D. A novel role for phagocytosis-like uptake in herpes simplex virus entry. J Cell Biol 2006;174:1009–21.
[69] Bonazzi M, Spano S, Turacchio G, Cericola C, Valente C, Colanzi A, et al. CtBP3/BARS drives membrane fission in dynamin-independent transport pathways. Nat Cell Biol 2005;7:570–80.
[70] Castellano F, Chavrier P, Caron E. Actin dynamics during phagocytosis. Semin Immunol 2001;13:347–55.
[71] Zhang J, Zhu J, Bu X, Cushion M, Kinane TB, Avraham H, et al. Cdc42 and RhoB activation are required for mannose receptor-mediated phagocytosis by human alveolar macrophages. Mol Biol Cell 2005;16:824–34.
[72] Lambaerts K, Wilcox-Adelman SA, Zimmermann P. The signaling mechanisms of syndecan heparan sulfate proteoglycans. Curr Opin Cell Biol 2009;21:662–9.
[73] Sahay G, Alakhova DY, Kabanov AV. Endocytosis of nanomedicines. J Control Release 2010;145:182–95.
[74] Braeckmans K, Buyens K, Bouquet W, Vervaet C, Joye P, De Vos F, et al. Sizing nanomatter in biological fluids by fluorescence single particle tracking. Nano Lett 2010;10:4435–42.
[75] Säälik P, Padari K, Niinep A, Lorents A, Hansen M, Jokitalo E, et al. Protein delivery with transportans is mediated by caveolae rather than flotillin-dependent pathways. Bioconjug Chem 2009;20:877–87.
[76] Vassilieva EV, Ivanov AI, Nusrat A. Flotillin-1 stabilizes caveolin-1 in intestinal epithelial cells. Biochem Biophys Res Commun 2009;379:460–5.
[77] Finnemann SC. Focal adhesion kinase signaling promotes phagocytosis of integrin-bound photoreceptors. EMBO J 2003;22:4143–54.
[78] Zhao MW, Jin ML, He S, Spee C, Ryan SJ, Hinton DR. A distinct integrin-mediated phagocytic pathway for extracellular matrix remodeling by RPE Cells. Invest Ophthalmol Vis Sci 1999;40:2713–23.
[79] Riento K, Frick M, Schafer I, Nichols BJ. Endocytosis of flotillin-1 and flotillin-2 is regulated by Fyn kinase. J Cell Sci 2009;122:912–8.
[80] Hybiske K, Stephens RS. Mechanisms of *Chlamydia trachomatis* entry into nonphagocytic cells. Infect Immun 2007;75:3925–34.
[81] Irschick EU, Haaa G, Geiger M, Singer W, Ritsch-Marte M, Konwalinka G, et al. Phagocytosis of human retinal pigment epithelial cells: evidence of a diurnal rhythm, involvement of the cytoskeleton and interference of antiviral drugs. Ophthalmic Res 2006;38:164–74.